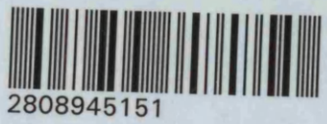

UNIVERSITY OF LONDON THESIS

Degree MD Year 2006 Name of Author AH-SEE, Mei-Lin Wong

EVALUATION OF THE VASCULAR RESPONSE TO NEOADJUVANT CHEMOTHERAPY IN PRIMARY BREAST CANCER

Dr. Mei-Lin W. Ah-See

Marie Curie Research Wing, Mount Vernon Hospital

&

University College London

A thesis to be submitted for the degree of

Doctor of Medicine

to the

University of London

2006

ProQuest LLC
789 East Eisenhower Parkway
P.O. Box 1346
Ann Arbor, MI 48106-1346

Abstract

Neoadjuvant chemotherapy (NAC) is being increasingly used in the treatment of primary breast cancer (PBC). With the primary tumour *in situ*, the neoadjuvant treatment setting allows an *in vivo* assessment of tumour chemo-responsiveness and permits an evaluation of the possible underlying biological mechanisms of response. Angiogenesis is critical for the growth and metastases of breast cancer and with the development of novel agents targeting this process, an understanding of the vascular effects of conventional chemotherapy will enable the rational design of future drug combinations.

Functional magnetic resonance imaging (MRI) provides a non-invasive method for assessing tumour microvasculature. Using this technique, pre-treatment tumour vascularity and changes following two cycles of anthracycline-based NAC were measured in a series of patients with PBC. This demonstrated a significant reduction in the permeability and perfusion-related MRI parameters in tumours responding to treatment. The degree of change in K^{trans} was able to predict for pathological non-response with a positive predictive value of 84%. Further, an evaluation of the pathophysiological correlates of functional MRI demonstrated an association between the permability/perfusion-related parameters and aggressive tumour features.

An evaluation of the effect of anthracycline-based NAC on immunohistochemically-derived measures of tumour angiogenesis was performed on a series of patients treated for PBC. A quantitative and a qualitative measure of tumour angiogenesis was performed (microvessel density [MVD] and pericyte coverage index [PCI] respectively), together with an assessment of VEGF expression. This demonstrated no change in MVD following treatment but a significant increase in PCI reflecting a reduction in the proportion of immature proliferating blood vessels. This was accompanied by a reduction in VEGF expression, which may be mediating this effect.

These observations may have clinical importance as they may help identify patients who could benefit from alternative therapies early in their treatment course and they may assist in the rational design of combination cytotoxic and antiangiogenic treatment regimens.

Acknowledgements

Completion of the work described in this thesis would not have been possible without the contribution of many people at Mount Vernon Hospital, the Paul Strickland Scanner Centre, the Gray Cancer Institute, the John Radcliffe Hospital and the Royal Marsden Hospital.

I would like to thank my supervisors, Andreas Makris and Anwar Padhani, for their constant support, ideas, enthusiasm and endless time.

I am indebted to all in the Paul Strickland Scanner Centre but especially Jane Taylor, James Stirling and Linda Culver with whom I have spent many hours discussing and analysing MRI data.

Many thanks to those in the Marie Curie Research Wing especially Professor Michele Saunders, Helen Cladd, Annette Martin, Jenny Dixon, Jackie Anderson and Margaret Masters. Special thanks also to my predecessor Russell Burcombe for laying the ground work.

Many thanks to Frances Daley at the Gray Cancer Institute for teaching me all about immunohistochemistry and for her constant assistance with the staining. My thanks also to Søren Bentzen, Sonia Noble and Angela.

Thank you to Paul Richman for grading the many pathological specimens.

I would like to thank Professor Adrian Harris at the John Radcliffe Hospital for his enthusiastic advice about the project and to Stephen Fox and Geetha Pillai for their help with vessel counting.

My thanks to the many clinicians who helped recruit patients to the studies - especially Mark Harrison, Peter Ostler, Richard Ashford, Alan Makepeace, Melanie Osbourne, Mike Pittam, Duraisamy Ravichandran, John Nicholls, Murid Chaudhury and Mr. Haque – and the supporting breast care sisters.

My thanks to Martin Leach and James D'Darcy at the Royal Marsden Hospital for providing the MRIW software.

I would like to thank the Breast Cancer Research Trust, the Childwick Trust and the Marie Curie Research Wing for funding this research.

Very special thanks to Jackie Harney, Dawn Carnell and Kate Lankester for your sincere friendship and advice.

To my parents for their infinite time and support.

Thank you to all the women who unselfishly agreed to take part in this research and showed amazing courage in the face of adversity.

Finally, I could not have seen this research through without the unfaltering encouragement, belief and support of my husband, Sam – thank you! – and to our two boys, Sammy and Ralphie, for always having a smile!

Table of Contents

List of Tables

List of Figures

Abbreviations

ABC	Avidin-biotin complex
AC	Doxorubicin, Cyclophosphamide
AC-DOC	Doxorubicin, Cyclophosphamide followed by Docetaxel
ADOC	Doxorubicin, Docetaxel
AI	Apoptotic index
AJCC	American Joint Committee on Cancer
α-SMA	Alpha-smooth muscle actin
AUC	Area under the ROC curve
BOLD	Blood oxygen level dependant
BW	Body weight
CA IX	Carbonic anhydrase IX
CAD	Computed assisted diagnosis
cCR	Clinical complete response
cDNA	Complementary DNA
cNR	Clinically non-responding
CMF	Cyclophosphamide, Methotrexate, 5-Fluorouracil)
cPD	Clinical progressive disease
cPR	Clinical partial response
CR	Complete response
cSD	Clinical stable disease
CT	Computed tomography
CUP	Carcinoma of unknown primary
CVAP	Cyclophosphamide, Doxorubicin, Vincristine, Prednisolone
DAB	Diaminobenzine tetrahydrochloride
DCE-MRI	Dynamic contrast-enhanced magnetic resonance imaging
DFS	Disease-free survival
DCIS	Ductal carcinoma in-situ
DNA	Deoxyribose nucleic acid
DUR	Dose uptake ratio
EBCTCG	Early Breast Cancer Trialist's Collaborative Group

ECP	Endothelial cell proliferation
EES	Extravascular extracellular space
EF	extraction flow
EORTC	European Organisation for Research & Treatment of Cancer
ER	Oestrogen recepector
FAC	5-Fluorouracil, Doxorubicin, Cyclophosphamide
FEC	5-Flourouracil, Epirubicin, Cyclophosphamide
FF	Fibrotic focus
FNAC	Fine-needle aspiration cytology
FVIIIRAg	Anti-factor VIII related antigen
GCR	Good clinical response
G-CSF	Granulocyte-colony stimulating factor
Gd-DTPA	Gadopentetate dimeglumine
[3H]-dT-LI	[3H]-thymidine labelling index
HER-2	Human epidermal growth factor receptor 2
HIF-1	Hypoxia-inducible-factor-1-alpha
HRP	Horseradish peroxidase
IBTR	Ipsilateral breast tumour recurrence
IDC	Invasive ductal carcinomas
ILC	Iinvasive lobular carcinoma
IRS	Immunoreactive score
k_{ep}	Rate constant,
K^{trans}	Transfer constant
KW	Kruskal-Wallis test
LN	Lymph node
MaxAmp	Maximum signal amplitude
Mean Grad	Mean gradient
MI	Mitotic index
MPI	Microvessel pericyte coverage index
MRI	Magnetic Resonance Imaging
MRIW	Magnetic Resonance Imaging Workbench
MTT	Mean transit time
MVD	Microvessel density

MW	Mann-Whitney U-test
NAC	Neoadjuvant chemotherapy
NPI	Nottingham Prognostic Index
NSABP	National Surgical Adjuvant Breast and Bowel Project
OS	Overall survival
P	Paclitaxel
PCI	Pericyte coverage index
pCR	Pathological complete response
PDW	Proton density weighted
PET	Positron emission tomography
PD	Progressive disease
PgR	Progesterone receptor
pINV	Pathological invasive tumour
PPV	Positive predictive value
PR	Partial response
PST	Primary systemic therapy
RCT	randomised controlled clinical trials
rBF	Relative blood flow
rBV	Relative blood volume
RF	Radiofrequency
RFS	relapse-free survival
rMSD	Relative maximum signal drop
ROC	Receiver operating characteristic
ROI	Region of interest
SCF	Supraclavicular fossa
SD	Stable disease
SPF	S-phase fraction
SNR	Signal to noise ratio
T1W	T1-weighted
T2*W	T2*-weighted
TBS	Tris buffer saline
TNM	Tumour, Node, Metastasis
UICC	International Union Against Cancer
v_e	Leakage space

VEGF	Vascular endothelial growth factor
VEGF IRS	Vascular endothelial growth factor immunoreactive score
VEGF-R	Vascular endothelial growth factor receptor
VMI	Vascular maturation index
vWF	Von Willebrand's Factor
WLE	Wide local excision
Wt	Washout

CHAPTER 1: INTRODUCTION

1.1 BREAST CANCER – AN OVERVIEW

1.1.1 EPIDEMIOLOGY

Breast cancer is the most common cancer in women worldwide accounting for 25% of all female malignancies. The incidence of breast cancer is high in western, developed countries and in England and Wales almost 36,000 new cases were diagnosed in the year 2000 with a mortality of 11,500 in 2002 [1]. In the United Kingdom, one in nine women will develop breast cancer at some point in their life. Despite an increasing incidence, mortality rates from breast cancer have fallen, with a reduction of 20% in 1999 compared with the mid-1980s (**figure 1.1**). Earlier detection through the National Health Service mammographic breast screening programme and increased breast awareness, together with advances in systemic therapy have all contributed to this overall improvement in disease specific survival.

1.1.2 TREATMENT

The treatment of breast cancer depends on the stage of disease at presentation. In general, the stages can be grouped into:

1. Early breast cancer
2. Locally advanced breast cancer (operable and inoperable, including inflammatory disease)
3. Metastatic breast cancer

1.1.2.1 Early breast cancer

Early breast cancer can be defined as operable disease confined to the breast, with or without involved mobile ipsilateral axillary lymph nodes. A multimodality approach to treatment is recommended with surgery, systemic therapy and radiation therapy according to both tumour and patient factors. The aim of treatment is to achieve a cure.

In terms of locoregional treatment, it is now well established that wide local excision of the breast cancer followed by adjuvant breast irradiation gives the same outcome in terms of survival as mastectomy and, as such, breast conservation is the treatment of choice for women with breast cancer whenever possible [2]. Following mastectomy, chest wall irradiation is recommended in the presence of risk factors for recurrence (axillary lymph node involvement; incomplete or close resection margins; grade III tumour; lymphovascular invasion) and locoregional nodal irradiation may be recommended according to the axillary surgery received and the extent of nodal involvement. Despite successful locoregional treatment, more than half of women with operable breast cancer will die from metastatic disease if no further treatment is given, indicating the presence of occult micrometastatic disease in these women at the time of initial clinical presentation. In order to reduce the chances of tumour recurrence and improve breast cancer survival, adjuvant (post-surgery) systemic medical therapy is used and can be divided into:

1. cytotoxic chemotherapy
2. endocrine therapy (tamoxifen, aromatase inhibitors)

The benefits of systemic therapy, in term of disease-free and overall survival, have been clearly demonstrated in randomised clinical trials. Most notable have been the meta-analyses performed by the Early Breast Cancer Trialist' Collaborative Group (EBCTCG) on both adjuvant prolonged polychemotherapy [3] and adjuvant tamoxifen therapy [4]. The meta-analysis for polychemotherapy demonstrated that, for women under the age of 50 years, the administration of polychemotherapy conferred an absolute survival benefit at 10 years of 7% and 11% for node-negative and node-positive disease respectively. Further, a comparison of anthracycline-containing regimens with CMF-alone (cyclophosphamide, methotrexate and 5-fluorouracil) demonstrated an additional survival benefit of 3%. These benefits were irrespective of menopausal status, oestrogen-receptor status and the use of adjuvant tamoxifen. The benefits were smaller for women aged 50-69, with an absolute gain of 2% and 3% in 10 year survival rates for node-negative and node-positive disease

respectively. No advantage was found for prolonged treatment beyond 3-6 months.

For adjuvant tamoxifen therapy, the EBCTCG meta-analysis demonstrated a reduction in tumour recurrence at 10 years with tamoxifen therapy in women with oestrogen-recepector (ER) positive or ER-untested tumours. Five years of treatment was shown to be superior to either 1 or 2 years, and this translated into an absolute survival benefit of 5.6% and 10.9% for node-negative and node-positive disease respectively at 10 years, with a 47% reduction in contra-lateral breast cancer. These benefits were irrespective of age, menopausal status and chemotherapy use. These findings and those on polychemotherapy have persisted in the 15 year analysis of disease recurrence and overall survival [5].

Newer systemic agents are currently under investigation in the adjuvant treatment setting with the aim of further improving treatment outcomes following the demonstration of efficacy of these agents in metastatic disease. These include the taxanes (docetaxel and paclitaxel), the aromatase inhibitors (arimidex, letrozole, exemestane) and the biological agent, trastuzumab, a recombinant humanized monoclonal antibody against the human epidermal growth factor receptor, HER-2.

1.1.2.2 Locally advanced breast cancer

Locally advanced breast cancer includes primary tumour extension into the chest wall or skin, inflammatory breast cancer, matted ipsilateral axillary nodal disease and infraclavicular, supraclavicular or internal mammary lymph node involvement. For inoperable locally advanced breast cancer, the recommended first-line treatment modality is neoadjuvant chemotherapy (NAC) or primary systemic therapy (PST) [6]. This is aimed at downstaging the disease with a view to surgery and/or radical radiotherapy while also treating occult micrometastases. Operable locally advanced breast cancer may be treated in a similar fashion to early breast cancer, however, NAC has a role to play when primary surgery would entail a radical mastectomy, as NAC has the potential to downstage disease sufficiently to enable breast-conservation. A full discussion

of neoadjuvant chemotherapy for patients with primary breast cancer is given in **section 1.2.**

1.1.2.3 Metastatic breast cancer

In metastatic breast cancer, treatment is aimed at the palliation of symptoms and may include one or a combination of surgery, systemic therapy and radiotherapy in conjunction with supportive care.

1.1.3 PROGNOSIS

The risk of disease relapse and death from breast cancer depends on both clinical and biological factors. The most powerful clinical prognostic factor is axillary lymph node status, followed by tumour size, as the probability of micrometastases increases with the number of axillary lymph nodes involved and tumour size [7]. Despite this, women with negative axillary lymph nodes still have a 20-30% risk of metastatic relapse while more than 35% of women with positive axillary disease remain disease free despite no adjuvant therapy. Biological prognostic factors include tumour grade, [8, 9], histological tumour type [10] and hormone receptor status [11]. Combination of these prognostic factors can be used to stratify patients according to their risk of relapse and thus guide adjuvant systemic therapy. The Nottingham Prognostic Index (NPI) is one such system for stratifying individual patient risk. The NPI combines tumour grade, tumour size and lymph node status to give an estimate of prognosis that is more discriminating than axillary lymph node status alone (**figure 1.2**) [12, 13]. More recently, a computer program known as "Adjuvant!" has been introduced to help facilitate in adjuvant treatment decision making in primary breast cancer (www.adjuvantonline.com). "Adjuvant!" calculates the individual patient's prognosis according to age, disease stage and tumour grade, and provides an evidence-based estimate of the percentage benefit of different adjuvant systemic therapies for that individual patient.

1.2 BREAST CANCER AND NEOADJUVANT CHEMOTHERAPY

Wide local excision of breast cancer followed by adjuvant breast irradiation is equivalent to mastectomy in terms of survival and is the treatment of choice for women with breast cancer whenever possible [2]. However, for some women breast conservation is not possible due to the size, position or distribution of the primary disease e.g. multifocal or multicentric disease. Neoadjuvant chemotherapy (NAC) (also known as primary systemic therapy (PST) or preoperative chemotherapy) refers to the administration of cytotoxic chemotherapy prior to locoregional treatment with surgery and/or radiotherapy in women with primary breast cancer. It is aimed at both downstaging the primary tumour to increase the chances of breast-conserving surgery where possible and treating potential micrometastatic disease. The neoadjuvant treatment setting has the added advantage of allowing an in vivo assessment of tumour chemo-responsiveness which has been proposed as a surrogate marker of response in micrometastatic disease.

1.2.1 HISTORY OF NEOADJUVANT CHEMOTHERAPY

NAC was first introduced into clinical practise in the 1970s for the treatment of inoperable locally advanced or inflammatory breast cancers and was aimed at both local disease control and the irradication of occult systemic micrometastatic disease. Several non-randomised trials demonstrated high response rates (approximately 70%) and in many, inoperable disease became operable. As a result, NAC has become the standard treatment option for this patient group [6].

At the same time, pre-clinical studies demonstrated that the presence of a primary tumour appeared to inhibit metastatic tumour growth and that removal of the primary tumour lead to both an increase in circulating growth-stimulating factors and an acceleration in metastatic tumour growth as measured by an increase in the labelling index in the residual tumour cells [14, 15]. This acceleration in tumour growth could be prevented, however, by the

administration of cytotoxic chemotherapy prior to surgery [16]. These findings provided a biological rationale for the use of NAC in early operable breast cancers.

In the 1980s, a number of non-randomised phase II studies using various chemotherapy regimens demonstrated that NAC could be used in patients with large but operable breast cancers to downstage the primary tumour and thereby increase the breast-conserving surgery rate [17-22](**Table 1.1**). Clinical complete response (cCR) rates were between 10 and 66% (**appendix 1. UICC clinical response criteria**), with pathological complete response (pCR) rates up to 30%. It was still unknown whether preoperative treatment could result in improved progression-free and overall survival when compared with the same chemotherapy administered postoperatively. Indeed, there was concern that the delay in surgery may, in fact, increase the risk of metastatic spread. This lead to the first generation of NAC randomised controlled clinical trials (RCT) where a direct comparison was made between the same chemotherapeutic regimen administered either pre- or post-operatively.

1.2.2 FIRST GENERATION RCTS OF NAC

The largest of the first generation of RCT of NAC was the National Surgical Adjuvant Breast and Bowel Project (NSABP) B18 trial initially reported by Fisher et al. in 1998 [23]. This study randomised 1523 patients with stage I or II breast cancer to receive four cycles of doxorubicin and cyclophosphamide chemotherapy either pre- or post-operatively. The study demonstrated NAC to be equivalent to adjuvant chemotherapy in terms of disease-free survival (DFS) (66.7% versus 67.3%, $p = 0.99$) and overall survival (79.6% versus 80.0%, $p = 0.83$) at 5 years of follow-up, a finding that persisted at 9-years follow-up [24](**figure 1.3**). The study also found that women receiving NAC were more likely to have breast-conserving surgery (67.8% in the pre-operative group versus 59.8% in the post-operative group). These findings were similar to those from other randomised studies of NAC [25-29] including the EORTC 10902 trial [30] (**table 1.2**).

Of importance, the NSABP-B18 study also demonstrated that the clinical and pathological response to NAC was a powerful predictor of outcome. At the 9-year follow-up analysis [24], there was a significant association between clinical response and DFS, relapse-free survival (RFS) and overall survival (OS). OS at 9 years was 78% in patients with a cCR, 67% in patients with a clinical partial response (cPR) and 65% in clinically non-responding patients (cNR i.e. those patients with stable or progressive disease) ($p = 0.005$; $p = 0.04$ when adjusted for tumour size, clinical lymph node status and age at randomisation). Pathological response was also significantly associated with DFS, RFS and OS. For those patients in whom a pCR was achieved, OS was 85% compared with 73% in patients achieving a cCR but having residual invasive cancer on pathologic examination (pINV). Overall primary tumour response graded as pCR, pINV, cPR or cNR was strongly associated with all outcome measures, and this association persisted after adjustment for tumour size, clinical lymph node status and age at randomisation (OS: $p = 0.006$; DFS: $p = 0.00005$; RFS: $p = 0.0002$) (**figure 1.4**).

The prognostic importance of pathologic lymph node status was also evaluated in the NSABP-B18. For both the preoperative and postoperative chemotherapy group, pathologic lymph node status was a strong predictor of outcome ($p < 0.0001$ for OS, DFS and RFS in both groups). In addition, in the preoperative chemotherapy group, there was a significant correlation between primary tumour response and the number of involved lymph nodes ($p<0.0001$). When primary tumour response was stratified according to pathologic lymph node status, it remained a significant predictor of DFS ($p = 0.006$) and RFS ($p = 0.04$), with a trend to significance for OS ($p = 0.06$). These finding, therefore, suggested that the primary tumour response may represent a true surrogate for micrometastatic disease chemosensitivity.

One issue that did arise from the NSABP-B18 was that of ipsilateral breast tumour recurrence (IBTR). There was a strong correlation between age and rate of IBTR ($p = 0.00003$), with a 13.3% recurrence rate in women aged 50 years or younger at randomisation compared with 5.2% in those older than 50 years. This was felt to reflect the study design, however, which had dictated that

woman under 50 years of age did not received adjuvant tamoxifen therapy. Ipsilateral breast tumour recurrence (IBTR) in patients who had received preoperative chemotherapy was similar to those patients receiving adjuvant chemotherapy (10.7% versus 7.6% respectively, p = 0.12). There was a higher IBTR in those women in whom a mastectomy would have been necessary at presentation but who were subsequently downstaged by NAC to permit lumpectomy when compared with those women in whom breast-conservation would have been possible prior to preoperative chemotherapy (15.9% versus 9.9%). When adjusted for age and clinical tumour size at diagnosis, however, this difference was not statistically significant and may have simply reflected the younger age of the surgically down-staged subgroup.

Thus, the 1st generation trials demonstrated that survival was equivalent for preoperative and postoperative chemotherapy administration and that primary tumour response was a strong predictor of outcome. These findings together with the development the taxane chemotherapy agents (paclitaxel and docetaxel) lead to the development of the second generation of neoadjuvant trials.

1.2.3 SECOND GENERATION NEOADJUVANT TRIALS

The second generation of neoadjuvant trials were aimed at assessing whether pathological complete response rates could be improved upon with newer chemotherapy drugs and/or schedules, and whether an increase in pCR rate would result in improved overall survival. In particular, docetaxel and paclitaxel were evaluated as they had demonstrated response rates of 30-60% in the first-line metastatic setting [31-33], including in patients with anthracycline-resistant disease [34, 35].

1.2.3.1 Docetaxel-containing trials

The Aberdeen TAX 3001study was a landmark study [36]. Although a small study with only 162 patients, it compared eight cycles of the anthracycline-based chemotherapy regimen CVAP (cyclophosphamide, doxorubicin, vincristine and prednisolone) with four cycles of CVAP followed by four cycles of docetaxel.

All patients were assigned to receive four cycles of CVAP and were then clinically reassessed. Those clinically responding patients (cCR or cPR) were randomised to either continue with CVAP for a further 4 cycles or to change to docetaxel for 4 cycles. All clinically non-responding patients (cSD or cPD) were changed to 4 cycles of docetaxel. In the responding randomised group, the study demonstrated a higher pCR rate with the addition of docetaxel (31% vs 15%; p = 0.06 on intent-to-treat analysis). This has subsequently translated into a significant improvement in 5-year DFS (90% versus 72%, p = 0.04) [37] demonstrating for the first time that a change in therapy that increases response rates may improve long-term survival. In addition, the study found that in those patients who failed to clinically respond to 4 cycles of CVAP, a change to docetaxel resulted in an overall clinical response rate of 55% with a pCR rate of 2%.

The NSABP-B27 study is the largest neoadjuvant study to date [38]. The study recruited 2411 patients and was aimed at determining the effect of adding docetaxel to doxorubicin and cyclophosphamide (AC) chemotherapy, both in terms of clinicopathological response and survival in women with operable breast cancer. Patients were randomised into one of three arms: 4 cycles of preoperative AC followed by surgery (group 1); 4 cycles of preoperative AC followed by 4 cycles of docetaxel followed by surgery (group 2); or 4 cycles of preoperative AC followed by surgery followed by 4 cycles of docetaxel (group 3). This randomisation would allow an assessment of the effect of adding docetaxel preoperatively on response in the breast and axilla (comparison of groups 1 and 2) while also permitting an assessment of whether the addition of docetaxel postoperatively was beneficial in certain patient subgroups e.g. those with residual tumour in the breast or axilla following AC (comparison of groups 1 and 3). The preliminary results from the preoperative comparison have shown an increase in cCR and pCR rates with the addition of preoperative docetaxel to AC (from 40.1% to 63.6% [p<0.001] and from 13.7% to 26.1% [p <0.001] respectively). Further, the addition of docetaxel significantly increased the rate of pathologically negative lymph nodes (from 50.8% to 58.2%, p<0.001). The early follow-up data (median follow-up of nearly 70 months) has not yet shown any difference in terms of DFS or OS [39].

1.2.3.2 Paclitaxel-containing trials

Paclitaxel was assessed in a phase III study conducted at the MD Anderson [40]. 174 patients were randomised to receive preoperatively either 4 cycles of paclitaxel (P) or 4 cycles of 5-fluorouracil, doxorubicin and cyclophosphamide (FAC). This was followed by surgery and a further 4 cycles of FAC plus tamoxifen in those women aged 50 years and older with oestrogen receptor positive disease. The cCR rate were comparable in both groups (27% P versus 24% FAC; $p = 0.85$ for all clinical response data) however, there was a higher pCR rate in the FAC group of 17%, with only 8% with P (no p-value given but $p = 0.17$ for all pathological response data). This difference has not translated into a survival difference (4 year DFS 81% for FAC and 85% for PAC-FAC, $p = 0.2$).

The European Cooperative Trial in Operable Breast Cancer assessed P in combination with other agents [41]. This trial randomised 892 patients to one of 3 treatment arms: adjuvant doxorubicin followed by cyclophosphamide, methotrexate and 5-fluorouracil (CMF); adjuvant doxorubicin and paclitaxel (AP) followed by CMF; or preoperative AP followed by CMF. 23% of the patients achieved a pCR following NAC with a significantly higher pathological LN negative rate compared with the adjuvant regimens (61% versus 38%). The beneficial effect of the addition of P to doxorubicin and CMF on long-term outcome remains to be seen.

1.2.3.3 Dose-dense scheduling

Dose density refers to the administration of chemotherapy with a shortened time interval between each cycle. The effect of dose-dense scheduling on response to preoperative chemotherapy has been assessed, however the effects on long-term outcome are as yet unknown.

A randomised trial at the MD Anderson assessed three P treatment schedules [42]. 258 patients were randomised to either receive 4 cycles of P ($225mg/m^2$)

once every 3 weeks; 12 cycles of weekly P (80mg/m^2/week) if clinically lymph node (LN) negative; or 4 cycles of P (150mg/m^2/week given for 3 weeks followed by one week off every cycle) if clinically LN positive. Following surgery all patients received 4 cycles of FAC. The trial showed that the dose-dense schedules achieved significantly higher pCR rates when compared to the standard 3-week regimen (29% 14%, $p<0.01$).

The GERPAR*DUO* study aimed to compare dose-dense doxorubicin and docetaxel (ADOC) given every 2 weeks, with granulocyte-colony stimulating factor (G-CSF) support, against conventional 3-weekly doxorubicin and cyclophosphamide followed by docetaxel (AC-DOC) [43]. The study aimed to recruit 1000 patients but was closed early by the Data Monitoring Committee following the second interim analysis which analysed the results from 395 patients. This revealed higher cCR and pCR rates with the conventional 3-weekly AC-DOC schedule compared with the dose-dense regimen (57% versus 32% and 22% versus 11%, respectively) with a similar rate of pathologically negative LNs (61%) for AC-DOC to that seen with this regimen in the NSABP-B27 study. These two trials tell us that, while paclitaxel is schedule-dependant, docetaxel is not. This information is important in planning future large adjuvant trials.

1.2.3.4 Biological agents

Following the demonstration of efficacy in the metastatic breast cancer, new biological agents are also being assessed in the neoadjuvant setting. In particular, trastuzumab, a recombinant humanized monoclonal antibody against the human epidermal growth factor receptor, HER-2, has been evaluated in combination with cytotoxic chemotherapy in with HER-2 positive disease. In a study of 42 women with operable breast cancer, Buzdar et al. randomised patients to receive 4 cycles of P followed by 4 cycles of 5-flourouracil, epirubicin and cyclophosphamide (FEC) with or without weekly trastuzumab [44]. The planned sample size was 164 patients, however, the study was terminated by the Data Monitoring Committee after the completion of treatment in only 34 patients due to a staggering 42% difference in pCR rate between the 2

treatment arms (25% and 67% for chemotherapy alone and chemotherapy plus trastuzumab respectively, p=0.02). The long-term DFS and OS data from this trial is eagerly awaited in light of such a high pCR rate.

1.2.4 THIRD GENERATION NEOADJUVANT TRIALS

With the advances in molecular biology and imaging technology, a new generation of clinical trials have evolved aimed at determining whether it is possible to predict response to NAC on an individual patient level and thus tailor therapy appropriately. Prognostic factors, such as tumour size and nodal involvement at presentation, have not been shown to predict for response to NAC, although clinical response after 2 cycles of treatment with docetaxel, doxorubicin and cyclophosphamide chemotherapy was recently shown to be a predictor for pCR [45]. In the adjuvant setting, overexpression of the proto-oncogene c-*erb*B-2 (HER-2) has been associated with a decreased response to cyclophosphamide, methotrexate and 5-fluorouracil (CMF) chemotherapy [46] and an increased response rate to doxorubicin [47, 48]. The expression of the hormone receptors (oestrogen receptor, ER, and progesterone receptor, PgR) is known to predict for response to endocrine therapy [4, 49-51] although in the metastatic setting, there have been mixed results regarding their role [52-55].

With the primary tumour in situ, the neoadjuvant treatment setting provides an ideal discovery platform for new potential markers of response to treatment. As already noted, clinical, radiological and pathological primary tumour response act as intermediate surrogates of long-term outcome while access to the primary tumour during treatment allows for in vivo testing for changes in molecular or functional biomarkers that may predict for response. Three approaches are currently under investigation:

1. Assessment of biologic markers
2. Genomic expression profiling
3. Functional imaging

1.2.4.1 Biologic markers

With the advances in molecular biology has come the search for biological markers of tumour treatment response. Biomarkers commonly measured in routine clinical practise, such as ER, PgR and HER-2, have been evaluated, as well as more sophisticated markers, in particular, those reflecting upon apoptosis (e.g. apoptotic index (AI), *bcl*-2) and proliferation (e.g. S-phase fraction (SFP), Ki67 antigen, mitotic index (MI), [3H]-thymidine labelling index ([3H]-dT-LI)).

Makris et al. assessed ER, PgR, HER-2 (c-erbB-2), p53, Ki-67, bcl-2, SPF and ploidy on fine-needle aspiration cytology (FNAC) samples taken prior to treatment, at day 10 and at day 21 after the first treatment cycle in 90 women receiving neoadjuvant mitozantrone, methotrexate +/- mitomycin C chemotherapy plus tamoxifen [56]. They found a significantly higher clinical response rate in tumours negative for HER-2 compared with HER-2 positive tumours (93% versus 57% respectively) but no significant difference for the other baseline markers or any of the treatment-induced changes. With a larger patient number (n=158), however, they were able to demonstrate that positive ER status and a decrease in Ki-67 on day 10 or day 21 could also predict for good clinical response (GCR, defined as cCR plus minimal residual disease [a residual nodularity after a good response which is insufficient to be measured]) [57]. A recent analysis of their 10-year follow-up data found superior DFS and OS in those patients achieving a GCR compared with those achieving only a cPR, cSD or cPD, strengthening the possible role of these biomarkers as surrogates of long-term outcome following NAC [58]. Data from other patient series have failed to confirm the findings observed for tumour response according to ER and HER-2 status [17, 59-63], however, change in Ki-67 as a predictor of response has been demonstrated in other studies.

In a study of 106 patients treated with either primary tamoxifen (n=33), chemotherapy (n=33) or chemoendocrine treatment (n=40), Assersohn et al. found that the percentage change in Ki-67 in the first 21 days of treatment was significantly different between responders and non-responders receiving either tamoxifen or chemotherapy alone but not the combination [64]. In addition,

using FNAC samples from a reproducibility cohort of 37 untreated patients, they found that a decrease in Ki-67 from baseline of 36% or more was required for that change to be deemed significant on an individual patient level. Using this cut-off, they were able to predict for response to chemotherapy and chemoendocrine therapy in 85% and 88% of patients respectively. Burcombe et al. showed similar results, with tumours displaying a greater than 75% reduction in Ki-67 following NAC being more likely to have a pathological response ($p=0.004$) [61]. Bottini et al. also found that Ki-67 expression was significantly reduced following NAC and that the reduction correlated with tumour response. However, although clinical response was a significant independent predictor of disease recurrence ($p<0.03$), reduction in Ki-67 was not [65]. A number of groups have assessed the baseline tumour proliferation rate and have demonstrated that a high rate may predict for response to treatment [60, 61, 63, 66-69].

The results from studies assessing apoptotic markers have also given mixed results. In a small study of 28 patients, Chang et al. found an increase in AI could predict for response [70]. In a larger study of 65 patients, however, Archer et al. found that although there was a significant rise in AI 24 hours post-NAC in core biopsy samples, this increase failed to correlate with either clinical response or survival [69]. Using bcl-2 as a marker of apoptosis, others have also failed to demonstrate a relationship between apoptosis and response to NAC in PBC [56, 63, 67, 71].

Thus, although some studies have shown promising results, the role of biological markers as predictors of response to NAC requires further evaluation. A summary of some of the studies of biologic markers to predict response to NAC is shown in **table 1.3**.

1.2.4.2 Genomic expression profiling

The development of high-throughput quantitation of gene expression and complementary DNA (cDNA) technology has now made it possible to study the expression of many genes simultaneously, thus enabling the characterisation of

expression patterns in different breast cancers. This has been termed genomic expression profiling. Using this technology, Perou et al. were the first to demonstrate that individual breast tumours have a distinctive "molecular portrait" [72]. Using complementary DNA microarrarys, they assessed the gene expression patterns in 65 breast tumour samples from 42 patients. They found that the gene expressions from 2 tumour samples from the same patient were almost always more similar to each other than to gene expressions from tumours from other patients. Further, sets of co-expressed genes were identified that could be related to specific physiological variations between individual tumours. These findings have lead to the search for gene expression profiles that might predict for individual response to treatment. These molecular portraits or "signatures" might be able to distinguish molecular phenotypes associated with response to specific chemotherapy agents and hence provide a clinical test for predicting treatment response at an individual tumour level from the outset.

In a prospective study of 24 patients with PBC, Chang et al. assessed gene expression profiling according to response to neoadjuvant docetaxel chemotherapy [73]. They found differential patterns of expression of 92 genes that significantly correlated with clinical response to docetaxel, with sensitive tumours displaying higher expression of genes involved in the cell cycle, cytoskeleton, adhesion, protein transport, protein modification, transcription and apoptosis. These findings have been taken forward into a randomised multicentre trial to prospectively validate the docetaxel gene expression profile and to determine if the gene expression profile for response to doxorubicin and cyclophosphamide chemotherapy is different.

1.2.4.3 Functional imaging

The optimum method for assessing response to NAC is unclear. Clinical response at the end of treatment has traditionally been used as a surrogate marker of outcome. It has been shown to correlate with DFS and/or OS in a number of studies [58, 74, 75], including the largest neoadjuvant trial (NSABP-B18) at 9 years follow-up [24]. Not all studies have found this association, however [25, 26, 30, 76]. This may be because clinical assessment of the local

response is a crude measure, dependant on several variables including primary tumour size, oedema, necrosis and subjective variation in tumour measurements. Indeed, clinical evaluation has been shown to frequently overestimate tumour size [77-81].

Radiological assessment by mammography and/or ultrasonography has been used as a more objective measurement of response, but neither has been shown to be superior to clinical assessment for predicting pathological tumour size following neoadjuvant chemotherapy [79, 82]. In addition, correlation between radiological response, as assessed by mammography or ultrasonography, and outcome has not been widely studied. Complete pathological response has been shown to be associated with improved outcome [24, 30], however, in most trials with anthracycline-based chemotherapy only a minority of patients display complete tumour regression (4-13%)[24, 29, 30, 83], thereby reducing the usefulness of pCR as a surrogate marker of outcome.

As a result, newer functional imaging technique are currently under evaluation for a potential role in the assessment of response to NAC. The standard radiological criterion for monitoring the response of breast tumours to treatment has been based on measurements of tumour size changes, however, this approach does not inform upon the mechanisms of tumour response. Functional changes within the tumour are likely to precede anatomical changes and therefore, the ability to monitor functional changes may inform upon tumour response earlier on in treatment. Advances in radiological technology have lead to the development of functional imaging techniques that provide a non-invasive method for assessing both tumour function and morphology. Theses techniques include dynamic contrast-enhanced magnetic resonance imaging (DCE-MRI), spiral computed tomography (spiral CT), colour Doppler ultrasound and positron emission tomography (PET). These techniques provide non-invasive methods for assessing the tumour microvasculature and have an increasing role in the evaluation of the effects of the novel antiangiogenic and vascular targeting agents. Additionally, PET is also able to inform upon other tumour properties such as cellular vitality (using [18F]-fluorodeoxy-D-Glucose) and cellular proliferation (using [18F]-fluorothymidine).

PET and DCE-MRI have both been studied in the neoadjuvant chemotherapy setting in breast cancer. Smith et al. assessed [18F]-fluorodeoxy-D-Glucose ([18F]-FDG) PET to predict pathological response to NAC in 30 patients [84]. They found that the mean reduction in the dose uptake ratio (DUR) after one cycle of chemotherapy was significantly greater in primary breast cancers that subsequently demonstrated a pathological response to treatment (pPR or pCR) compared with those tumours that failed to respond. Further, after a single cycle of chemotherapy, PET was able to predict pCR with a sensitivity of 90% and specificity of 74%. They concluded that PET may have a role in identifying treatment non-responders early on in therapy thus enabling a therapy change and possible improve outcome.

DCE-MRI has been widely used in the assessment of residual disease following NAC in primary breast cancer and can assist in the planning of subsequent surgery [85-90]. More recently, functional DCE-MRI for predicting response to NAC has been assessed. Martincich et al. found a reduction in the early enhancement ratio after 2 cycles of NAC was associated with a major histological response to treatment, however, tumour volume reduction after 2 cycles of NAC had the strongest predictive value for pathological response [91].

The role of multi-parameter functional MRI in predicting response to NAC early on in therapy is examined in the prospective study described in chapter 2. DCE-MRI and breast cancer is discussed in detail in **section 1.4**.

1.2.5 IN SUMMARY

In summary, neoadjuvant chemotherapy has a well-established role in the management of both operable and inoperable breast cancer. Clinical and pathological response to NAC have been shown to be predictors of long-term outcome and hence current trials are aimed at assessing whether an improvement in response rates might translate into improved survival. Strategies for increasing response rates include new chemotherapy regimens and schedules, as

well as the use of new molecular biological techniques and functional imaging technology for identifying early response predictors.

1.3 BREAST CANCER AND ANGIOGENESIS

In solid tumours, growth beyond two millimetres cannot occur without vascular support [92]. Angiogensis is the formation of new blood vessels from the existing microvasculature and is known to be a prerequisite for solid tumour growth and metastasis [93]. Angiogenesis is regulated by multiple stimulatory and inhibitory angiogenic factors or chemokines (**table 1.4**). In normal physiological angiogenesis there is a balance between these factors but in tumours an "angiogenic switch" leads to an imbalance of chemokines favouring angiogenesis.

1.3.1 VASCULAR ENDOTHELIAL GROWTH FACTOR

The most potent pro-angiogenic factor in breast tumours is vascular endothelial growth factor-A (VEGF), initially termed vascular permeability factor due to its hyperpermeable effect on vessels [94]. VEGF is produced by both tumour cells and host cells in response to hypoxia and inflammation. Hypoxia-inducible-factor-1-alpha (HIF-1) is upregulated in response to hypoxia and leads to VEGF transcription and overexpression [95]. VEGF overexpression can also occur in normoxic conditions, suggesting alternative regulatory mechanisms that are independent of hypoxia, such as alterations in the genes involved in the control of VEGF expression [96].

VEGF induces endothelial cell migration, proliferation and hence neovascularisation within tumours [97]. The tumour vessels created lack the normal hierarchical structure, however, and are disorganised, chaotic and hyperpermeable [98]. It also acts as an endothelial cell survival factor [99]. Elevated levels of VEGF within breast tumours has been associated with a poorer overall prognosis when measured from the tumour cytosol [100, 101] or by immunohistochemistry [102, 103]. Levels of circulating VEGF have also

been shown to be elevated in breast cancer patients compared with normal controls [104]. In one study, a decline in serum VEGF was shown to correlate with a partial response or stable disease following docetaxel chemotherapy in metastatic disease [105]. No correlation has been found between circulating VEGF levels and tumour VEGF expression [104, 106] although a correlation has been noted between serum VEGF levels and primary tumour bulk and intratumoural microvessel density [104].

In light of its central role in tumour angiogenesis, VEGF and its receptors (VEGF-R) have become potential therapeutic targets in cancer treatment. The VEGF-targeting agents currently under investigation include anti-VEGF monoclonal antibodies (e.g. bevacizumab[107]), the VEGF trap (a synthetic VEGF-R which binds circulating VEGF)[108], anti-VEGF-R monoclonal antibodies (e.g.DC101 [109]) and VEGF-R tyrosine kinase inhibitors (e.g. ZD6474[110], PTK/ZK [111]). Bevacizumab has obtained FDA approval for use with combination chemotherapy in first-line metastatic colorectal cancer. In metastatic breast cancer, a randomised phase III trial of capecitabine versus capecitabine/bevacizumab in women previously treated with an anthracycline and a taxane, has demonstrated a higher response rate with the combination therapy but no improvement in progression-free survival [112]. An on-going large randomised phase III trial of paclitaxel versus paclitaxel/bevacizumab in first-line metastatic breast cancer (ECOG E2100) is being conducted to determine whether there is a greater benefit from the addition of bevacizumab when patients have not been heavily pre-treated.

1.3.2 IMMUNOHISTOCHEMICAL QUANTIFICATION OF ANGIOGENESIS

1.3.2.1 Microvessel density

Quantification of the angiogenic status of tumours is currently performed by counting the number of microvessels in immunostained tissue sections. This gives an intratumoural microvessel density (MVD) which is a measure of the net effect of tumour angiogenesis and angioregression. A monoclonal antibody

against one of the panendothelial cell antigens is used to highlight the tumour vasculature. Commonly used antibodies for assessing MVD in breast cancer are anti-factor VIII related antigen (FVIIIRAg or von Willebrand's Factor, vWF), anti-CD34 and anti-CD31 [113]. However, these antibodies have different sensitivities and immunostaining characteristics. Anti-CD31 is also known to stain plasma cells, macrophages and occasional carcinoma cells [114], while anti-CD34 stains normal perilobular and periductal stroma within the breast preventing the assesssment of vessels around carcinoma in situ using this antibody [115]. The individual antibody used may influence the results for a tumour's MVD. Comparisons have been made between the different antibodies. Lee et al. performed a comparison of these antibodies in seven breast cancers specimens [114]. They found anti-vWF staining to be the most reproducible, but that it stained fewer vessels than anti-CD31, although consistent staining with anti-CD31 was not possible. Anti-CD34 produced less intense staining compared with anti-vWF but was easily assessable. In a much larger study, Martin et al. evaluated the three antibodies in 174 primary breast cancer specimens [116]. They demonstrated that the use of antibodies to CD31 and CD34 identified more vessels than antibodies to vWF. Furthermore, they also found staining with anti-CD31 to be the least reliable method, staining only 87% of the sections compared with 98% with anti-CD34 and 99% with anti-vWF. Thus, the antibody employed for determining MVD is an important factor to be considered. The anti-CD34 mouse monoclonal antibody, antibody QBEnd/10 (Novocastra Labs Ltd, UK, NCL-L-END™), was employed for determining MVD in the study of the effect of neodjuvant FEC chemotherapy on tumour angiogenesis in primary breast cancers described in chapter 3.

The most commonly used technique for quantifying MVD was first described by Weidner et al. [117]. They counted the total number of vessels within a 200x magnification field from selected areas with the highest vascularity (termed "vascular hotspots"). They included any staining endothelial cell or endothelial-cell cluster that was clearly separate from adjacent microvessels, tumour cells and other connective-tissues elements in their count. Vessel lumens were not

required for a structure to be defined as a microvessel. Using the anti-vWF antibody, they found MVD was an independent predictor of metastastic disease in women with breast cancer - mean MVD count of 101 per 200x field was observed in patients with metastases compared with only 45 per 200x field in those patients who were free of metastases ($p = 0.003$).

In a subsequent study using the same technique, Weidner et al. also found MVD to be a significant independant predictor for overall survival (OS) in women with early stage breast cancer [118]. They found all patients with >100 microvessels per 200x field experienced tumour recurrence within 33 months from diagnosis, compared with <5% of patients with 33 or less microvessels per 200x field and for those women with node-negative disease, MVD was the only significant predictor of overall survival ($p<0.001$).

A pathological hypothesis for these associations, and the rationale for counting vessels within the "vascular hotspot", is the presence of both angiogenic and non-angiogenic cells within a tumour. Those cells with the angiogenic phenotype are more likely to produce a detectable metastasis if shed for the primary tumour than the non-angiogenic cells, and those cells with the highest angiogenic potential should be present within the vascular hotspot. Thus, MVD counted from the vascular hotspots should be an indicator of the proportion of these highly angiogenic cells and hence be a predictor of metastases and survival. An alternative hypothesis, however, is that an increased MVD may simply represent a larger vascular surface area across which tumour cells can escape and metastasise [119].

1.3.2.2 Chalkley point counting

More recently, Chalkley point counting has been evaluated as a method for quantifying angiogenesis in vascular hotspots. This technique employs a 25-point eyepiece graticule which is applied over the vascular hotspot at 250x field. The graticule is orientated such that the maximum number of points hit on, or within, the areas of immunohistochemically highlighted microvessels. The Chalkley count is the number of grid points that hit stained microvessels and

gives a relative area estimate rather than a true vessel count. The advantage of this method is a reduction in bias that may occur in the observer-dependent step of deciding whether two adjacent immunostained structures represent one or two separate blood vessels. Using this method and the anti-CD31 antibody, Fox et al. found tumour microvessel density, as quantified by Chalkley point counting, was a significant predictor of RFS (p=0.01) and OS (p=0.028) in 109 patients with node-negative breast cancer [120]. In a larger study of 836 patients with a median follow-up of over 11 years, Hansen et al. confirmed that tumour angiogenesis, as assessed by Chalkley counting using the anti-CD34 antibody, was an independent prognostic factor for DFS and OS in both lymph node negative and lymph node positive breast cancer patient groups [121].

1.3.3 CLINICAL AND THERAPEUTIC RELEVANCE OF TUMOUR ANGIOGENESIS

1.3.3.1 Angiogenesis and prognosis in breast cancer

As mentioned in **sections 1.3.2.1 and 1.3.2.2**, a number of studies have shown tumour angiogenesis, as quantified by MVD or Chalkley count, to be an independent prognostic factor for both relapse-free and overall survival in breast cancer [117, 118, 120, 121]. Indeed, more than 40 retrospective studies have been published with the majority reporting a positive association between MVD and outcome. As such, MVD may be useful in guiding, for example, adjuvant treatment decisions in those patients considered to be otherwise low-risk for recurrent disease e.g. negative lymph node status. However, not all investigators have confirmed the prognostic value of MVD (data reviewed in Fox 1997 and Hasan 2002 [122, 123]). Possible explanations for the conflicting results regarding the prognostic value of MVD include: type of endothelial antibody employed; counting technique used; region of tumour assessed; and cut-offs defined for "increased vascularity" [122]. In light of this, the College of American Pathologists, in its consensus statement in 1999 on prognostic factors in breast cancer, ranked MVD in category III, which encompasses "all factors which are not sufficiently studied to demonstrate their prognostic significance" [124].

In order to reduce the methodological variabilities of angiogenesis quantification in tumour tissue sections, the "International Consensus on the methodology and criteria of evaluation of angiogenesis quantification in solid human tumours" was published in 1996 [113] and updated in 2002[125]. It currently recommends Chalkley counting, using the anti-CD34 antibody, as the standard method for the quantification of angiogenesis and suggests the introduction of quality control through reference slide sets by international collaborative groups. In addition, it suggests large prognostic and predictive studies comparing manual with automated hotspot selection. The consensus also suggests a comparison of MVD assessment with candidate surrogate markers of angiogenesis, for example, the fibrotic focus (FF), a scar-like area replacing necrosis in the centre of an invasive ductal carcinoma thought to result from previous and on-going intra-tumoural hypoxia [126].

The predictive value of MVD with regards to treatment response, whether that be to conventional chemotherapy or novel antiangiogenic agents, is currently under assessment, as is the interpretation of changes in MVD during and following therapy. In a series of 577 node-positive breast cancers treated with adjuvant chemotherapy as part of the Cancer and Leukemia Group B protocol 8541, Guidi et al. found no association between MVD and either RFS or OS. Further, MVD failed to predict outcome to treatment with dose intensification or tamoxifen [127].

In a neoadjuvant chemotherapy study, Makris et al. found that, despite a lower Chalkley count in patients who had received NAC for primary breast cancer prior to surgery, compared with patients who had undergone primary surgery, the Chalkley count did not correlate with the clinical response to NAC [128]. Similarly, Bottini et al. found that despite a reduction in MVD following NAC, neither baseline nor the change in MVD predicted for tumour response [129]. In the metastatic setting, Tynninen et al. have also demonstrated a failure of MVD to predict for treatment response [130]. These results suggest MVD does not predict for therapeutic efficacy, certainly in response to conventional cytotoxic chemotherapy, and that changes in MVD do not appear to be related to the

treatment response. Interestingly, a study of neoadjuvant tamoxifen therapy in locally advanced breast cancer did demonstrate a significant association between clinical tumour response and change in MVD, as assessed by Chalkley count, with reduction in MVD in responding tumours and an increase in non-responding tumours [131]. This positive finding may relate to the longer duration of treatment compared with the chemotherapy studies, however, it is worth noting that no correlation was observed between tumour proliferation and MVD in this study.

Thus, MVD alone appears to be unhelpful as a predictor of treatment response to NAC. This may be related to the failure of MVD to inform upon the qualitative, or functional, aspect of tumour neovascularisation. Alternative measures that reflect the functional status of the tumour microvasculature may be more useful and this forms the basis of the study described in chapter 3 examining the effect of neodjuvant FEC chemotherapy on tumour angiogenesis in primary breast cancers, as assessed quantitatively using MVD and qualitatively using pericyte coverage index. Qualititative measures of angiogenesis are discussed in more detail in **section 1.3.3.2**.

In relation to antiangiogenic therapy, Hlatky et al. have also proposed that MVD cannot be used as a predictor of treatment efficacy, nor can a reduction in MVD be used to reflect a response to antiangiogenic treatment [132]. They argue that MVD does not provide a direct measure of the angiogenic activity or angiogenic dependence of a tumour, but simply reflects the intercapillary distance within a tumour which is determined by both angiogenic and non-angiogenic factors. For example, lower MVD counts have been observed in some tumours compared with their corresponding normal tissue despite active angiogenesis within the tumours and probably reflects the lower oxygen consumption of tumour cells and their increased tolerance of tissue hypoxia [133]. Further, tumours with low MVD counts have been shown to respond to antitangiogenic therapy [134] and therefore MVD alone cannot be used to predict for treatment efficacy. In addition, in terms of assessing treatment efficacy, change in MVD in itself cannot be used as a measure of vascular inhibition as it is the result of the combined effect of vascular dropout and tumour-cell dropout. Thus, following

antiangiogneic therapy, initial capillary inhibition and elimination leads to a decrease in MVD, followed by a slowing in the decrease in MVD or even an increase in MVD as the tumour cells die in response to the loss of their supporting vasculature. The tightness of the coupling between the vascular and cellular dropout determines both the extent to which the MVD fluctuates during treatment and the time it takes to return to the pre-treatment MVD level following drug elimination, the so-called "restoration time". These factors are likely to vary between different tumour types and if the restoration time is less than the time between tumour biopsies then the change in MVD will provide little information (**figure 1.5**). Thus, bearing these problems in mind, attention has focussed on more qualitative, or functional, measures of tumour angiogenesis and whether they might be more able to predict for treatment response.

1.3.3.2 Qualitative measures of angiogenesis

Qualitative measures of angiogenesis aim to assess vascular differentiation and functionality. These aspects of tumour angiogenesis are currently being evaluated using new parameters that measure endothelial cell phenotypic characteristics, such as activation and differentiation. These new parameters include: biochemical markers known to be upregulated in vascular endothelial proliferation (e.g. CD105 (also known as endoglin), Kdr); differentiation markers present on mature vessels (e.g. LH39); the endothelial cell proliferation index (ECP index); and pericyte coverage index (PCI). These new qualitative measures of tumour angiogenesis may be more informative than more simply obtained MVD alone in terms of determining prognosis or predicting response to therapy.

Eberhard et al. assessed the functional angiogenic status of six different tumour types (glioblastomas [n=30], renal cell carcinomas [n=22], colon carcinomas [n=18], breast carcinomas [n=24], lung carcinomas [n=15] and prostate carcinomas [n=19]) and compared it with the physiological angiogenesis of the cyclic bovine corpus luteum [133]. They evaluated: MVD count (using anti-CD34, lectin BS-I or anti-vWF); proliferating capillary index, also known as

endothelial cell proliferation, ECP, (using double immunostaining with a marker of proliferation [anti-PCNA or anti-Ki67] and a panendothelial marker [anti-CD34 or lectin BS-I]); proliferating tumour versus endothelial cell index (the ratio of proliferating tumour cells to proliferating endothelial cells); and microvessel pericyte coverage index (using double immunostaining with a panendothelial marker [anti-CD34 or anti-vQWF] and a mural cell marker [anti-alpha-smooth muscle actin (anti-α-SMA]). They found all tumour types to have high MVD counts, with significantly higher counts in glioblastomas and renal cell carcinomas (**figure 1.6**). Interestingly, they observed the tumour MVD counts to be lower compared with those of the corresponding normal tissues except for prostate cancers. Using endothelial cell proliferation as the marker of the angiogenesis, they found active angiogenesis in all tumours but with significant differences between and within tumour types (**figure 1.6 and 1.7**). Further, the rate of angiogenesis was higher in the physiological angiogenesis in the ovarian corpus luteum.

The functional status of the tumour bed was assessed using microvessel pericyte coverage index (MPI), as pericyte recruitment to microvessels is thought to reflects vessel maturation [135-137]. Again varying degrees of vascular maturation was observed both between and within tumour types, with breast carcinomas exhibiting the highest MPI values, and glioblastomas and renal cell carcinomas the lowest. Thus, tumours differ in their degree of angiogenesis and the functional status of their vascular bed. This variation occurs both between and within tumour types and, as such, may result in a differential response to new antiangiogenic therapies. Determining the quality of the tumour vascular bed may be important, therefore, in the design and selection of antiangiogenic therapies for individual tumours.

Kakolyris et al. evaluated vascular differentiation and remodelling in 12 normal breast samples and 50 breast cancer specimens using the monoclonal antibody LH39 [138, 139]. LH39 has been shown to recognise a basement membrane epitope present in the lamina lucida of mature vessels but not in newly formed vessels [140, 141]. By defining mature vessels as those staining with both anti-

CD31 and LH39 antibodies, and immature (remodelling) vessels as those staining only with anti-CD31, a vascular maturation index (VMI) was derived (the percentage fraction of mature vessels over the total number of vessels). The VMI was found to be higher in the normal breast samples compared with the breast cancers (median VMI 66.5% and 8.8% respectively). Further, a significant inverse correlation was found between VMI and nodal status and thymidine phosphorylase expression. No association was found between VMI and a quantitative measure of angiogenesis (Chalkley count using anti-CD31) or VEGF expression. These findings again suggest that the quality of the tumour microvasculature may provide additional information regarding the tumour vascular efficiency compared with vessel count alone. In particular, the degree of vascular maturation and remodelling may provide valuable mechanistic and prognostic information about individual tumours, while also providing a potential therapeutic target that is able to exploit the difference between normal tissues and cancer.

Kumar et al. assessed the prognostic value of the Transforming Growth Factor β receptor, CD105, in a series of 106 breast cancers and compared it with CD34 [142]. Anti-CD105 antibodies have been shown to preferentially bind "activated" endothelial cells *in vitro* and in tissues undergoing active angiogenesis. Further, it has been shown that CD105 is strongly expressed in tumour blood vessels but only weakly expressed, or not at all, in the blood vessels of normal tissues [143]. CD105 staining allows a distinction to be made between vessels created by active tumour angiogenesis and normal blood vessels entrapped, or co-opted, by the tumour. They found MVD using anti-CD105 was an independent prognostic factor in breast cancer whereas MVD using anti-CD34 was not. Thus, MVD using anti-CD105 antibody may give a more accurate reflection of active tumour angiogenesis and hence explain its greater prognostic value.

More recently, real-time assessment of tumour microvasculature functionality has been made possible through functional imaging techniques, such as DCE-MRI, PET and functional multi-detector CT. These techniques are being used to

assess both baseline tumour vascular characteristics and the changes that occur following treatment with both conventional and novel anticancer agents. Functional imaging has become particularly important in the assessment of antiangiogenic and vascular targeting agents, where conventional response assessments according to changes in tumour size may not occur or may be delayed. The pathophysiological correlates of these functional imaging parameters remain to be fully assessed and an evaluation of the pathophysiological correlates of multi-parameter functional MRI is discussed in the study described in chapter 4.

The effect of neodjuvant FEC chemotherapy on tumour angiogenesis in primary breast cancers, as assessed quantitatively using MVD and qualitatively using pericyte coverage index, is examined in the prospective study described in chapter 3.

Thus, to summarise, the assessment of qualitative measures of tumour angiogenesis may give a more accurate assessment of the angiogenic activity and angiogeneic dependence of a tumour, and inform upon specific individual tumour features. This will improve our understanding of tumour biology and help explain some of the differential treatment responses that can be seen both between and within tumour types to the same treatment. They may also assist in the design and use of targeted novel therapies, for example, the use of an antiangiogenic agent directed at mature vasculature in those tumours with a high pericyte coverage index. In addition, these qualitative parameters they may act as useful predictive markers for treatment response or provide additional prognostic information.

1.4 MULTI-PARAMETER FUNCTIONAL MRI AND BREAST CANCER

1.4.1 INTRODUCTION

With the advent of antiangiogenic and vascular targeting agents in the treatment of cancer, the importance of functional imaging techniques and their role in assessing tumour response to treatment has increased dramatically. Multi-parameter functional vascular MRI provides a non-invasive imaging method for assessing tumour microvasulature and exploits the differences in tissue vascularity between benign and malignant processes to enable diagnosis and monitor response. Multi-parameter functional vascular MRI can be divided into non-enhanced and contrast media-enhanced methods (dynamic contrast-enhanced MRI [DCE-MRI]). The role of functional MRI in the evaluation, treatment and follow-up of patients with known or suspected breast cancer is now well established, but continues to expand with the developments in MRI software, processing and contrast media. The current role of functional MRI in breast cancer is discussed, with particular emphasis on DCE-MRI.

1.4.2 OVERVIEW OF MRI PRINCIPLES

Water molecules make up 60-70% of the constituents of body tissues. The ^{1}H nuclei that are contained in water molecules have a positive charge and are constantly spinning. As they spin, the moving positive charge produces an electric current and an associated magnetic field (they behave like little magnets). When placed in an external magnetic field, such as in an MRI machine, the protons align themselves either north or south to this field. More protons are aligned north to the external magnetic field, producing a net longitudinal magnetic moment in this direction. They continue to spin, like a spinning top, and this motion known as precession. The precession frequency, ω_0 (Lamor frequency) is determined by the magnetic field strength, B_0 , by the equation:

$$\omega_0 = \gamma B_0$$

where γ is a constant, the gyromagnetic ratio. By the use of radiofrequency (RF) wave pulses, the proton alignment can be temporarily altered, changing the longitudinal magnetisation and the protons become aligned and so precess in phase, producing a magnetic moment in a transverse plane. Once the pulse stops, the protons relax back to their original position, and gradually precess out of phase due to interactions with locally fluctuating magnetic fields produced by the protons themselves (spin-spin interaction). As they relax, they emit a RF signal that can be detected in an external receiver or coil, in which an electrical current is induced. The RF signal intensity depends on the type of RF pulse initially used to perturb their natural alignment and on the structure and water content of the tissues. The relaxivity of a tissue can be described in terms of spin-lattice (longitudinal relaxation rate [T1]), which reflects the rate that the spinning protons are able to achieve their original longitudinal orientation by energy transfer to the surrounding environment, and spin-spin (transverse relaxation rate [T2]) which reflects the rate that the spinning go out-of-phase due to local magnetic field inhomogeneities.

The use of static magnetic field gradients in orthogonal planes allow encoding of spatial information of the emitted RF signals and subsequent construction of 2D or 3D images of the signal intensity. The RF pulses and field gradients can be adjusted in multiple ways to give different signal intensities for a given tissue – for example on a T1 weighted image fat appears bright, but intermediate on a T2 weighted image. This gives MRI an advantage over CT examination of excellent soft tissue contrast, without the use of ionising radiation, and the ability to image in any plane.

1.4.3 DYNAMIC CONTRAST-ENHANCED MRI (DCE-MRI)

DCE-MRI uses extrinsic paramagnetic contrast media to increase the distinction between benign and malignant disease. Paramagnetic substances have small local magnetic fields which induce a shortening of the relaxation times of the protons in the surrounding tissues, so-called proton relaxation enhancement. This results in a change in the signal intensity of the tissues. The most

commonly used contrast medium is gadopentetate dimeglumine (Gd-DTPA) which is a low molecular weight agent (<1000Daltons) that rapidly diffuses from the intravascular space to the extravascular extracellular space (EES). The rate of diffusion into the EES is determined by the permeability of the capillaries, the surface area of the capillaries and the blood perfusion to the tissue.

DCE-MRI exploits the intrinsic differences that affect contrast medium behaviour in a variety of tissue types to aid in the diagnosis of benign versus malignant disease processes, and, as such, has emerged as a powerful imaging tool in the management of patients with breast cancer. Early breast MRI studies showed that breast cancers enhanced following contrast-agent administration [144, 145], however benign breast diseases, such as fibroadenoma, fibrocystic disease, radial scar and mastitis, were also found to enhance [90, 145-148]. Thus, the presence of enhancement alone should not be used to distinguish malignant from benign disease. The optimal interpretation of DCE-MRI in the breast employs a combination of the morphological and functional characteristics of a lesion.

1.4.4 DCE-MRI AND BREAST CANCER

DCE-MRI studies can be performed to be sensitive to the presence of contrast medium in the EES which reflect on microvessel permeability, extracellular leakage space and perfusion. Such sequences are called T1-weighted (or relaxavity) DCE-MRI. Similarly, sequences can be performed that are sensitive to the vascular phase of contrast medium delivery and reflect on tissue perfusion and blood volume. Such sequences are called T2* (or susceptibility) DCE-MRI [149].

1.4.4.1 T1-weighted DCE-MRI of breast cancer

T1-weighted DCE-MRI sequences are sensitive to the presence of contrast medium in the EES. The presence of diluted contrast medium in the EES leads to shortening of the T1 relaxation rate of the tissue and thus causes tissue

enhancement. A large body of literature has shown that breast cancers enhance earlier and to a greater extent than benign breast diseases on T1-weighted DCE-MRI. This difference is most marked in the early period (1-3 minutes) after bolus contrast medium administration [144, 150-152]. There is, however, an overlap in the enhancement rates of benign and malignant lesions [145-147] and therefore any kinetic parameter used for tissue characterisation has to take into consideration the relative contrast medium behaviour in different tissues.

1.4.4.1.1 Data acquisition, analysis and processing

Most T1 DCE-MRI studies employ gradient-echo sequences to monitor the tissue enhancing effects of contrast media. The commonest contrast medium used is gadopentetate dimeglumine (Gd-DTPA) at a dose of 0.1 mmol/kg body weight (b.w.). Gradient-echo sequences have good contrast medium sensitivity, yield images with high signal to noise ratio and enable data acquisition to be performed rapidly. The degree of signal enhancement seen on T1-weighted images is dependent on both physiological and physical factors and these include tissue perfusion, capillary-permeability to contrast agent, volume of the extracellular leakage space, native T1-relaxation rate of the tissue, contrast agent dose, imaging sequence, parameters utilised and on-machine scaling factors [153].

1.4.4.1.2 Pulse sequence timing

The optimal timing for breast MRI sequences is dependent on the goal of imaging. High-resolution and short imaging-time represent competing examination strategies on currently available equipment. If high sensitivity is required, then a single high sensitivity, high resolution, fat suppression 3D technique (with voxel sizes less than 1 mm) can be used. This can be performed in 2-4 minutes which is within the time window where the differential enhancement between malignant and benign lesions is greatest. Using this technique, however, image interpretation has to be based on morphological characteristics alone.

If the goal is to maximise specificity, then repeated data acquisitions are recommended. On current MRI system's, higher temporal resolution necessitates reduced spatial resolution and/or decreased coverage. The highest specificity MRI breast studies have used 2D dynamic techniques with data acquisition rates of 1-12 seconds. Higher temporal resolution techniques appear to improve the specificity of examinations because of better characterisation of the signal intensity-time curve. One study has suggested the optimal data acquisition rate to be 1-2 seconds [150]. Unfortunately, the temporal requirements of fast dynamic imaging limits the spatial resolution and coverage, and thus multi-focal disease may be overlooked. If multi-focality is a concern, volume coverage at the slower data acquisition rates are preferable.

A combination of both kinetic and morphologic information is best at achieving optimal discrimination between benign and malignant lesions. Therefore, as a compromise, a dynamic high resolution 3D technique (slower dynamic 3D technique) is used by many where each time point is acquired every 45-90 seconds. This approach does not require prior knowledge of lesion location. Both Kuhl et al [154] and Liu et al. [155] have reported on the value of such techniques where an integration of contrast agent kinetics and architecture evaluation (morphology) is performed. An important factor, however, is concordance between the kinetic information and the morphologic features. This is because some malignant lesions, including invasive ductal and lobular carcinomas and certain ductal carcinoma in-situ lesions, do not enhance rapidly but morphology can suggest the presence of malignancy e.g. architectural distortion or mass with spiculated borders. Such lesions must be treated as suspicious. However, it should be noted that not all such lesions will be malignant, with fibrocystic disease and sclerosing adenosis being causes of false positive results.

Thus, if the goal is to determine the likelihood that a previously identified lesion is malignant, then the best strategy is to use the minimal number of slices necessary to cover the lesion and to obtain a series of acquisitions with high temporal resolution. However, if the goal is to detect multicentric or multi-focal disease, search for a primary tumour or demonstrate the extent of a known

cancer, then good spatial resolution and whole breast coverage are essential and is best achieved with a 3D MR technique.

1.4.4.1.3 Post-processing of data

A breast MRI study can yield many hundreds of images, the analysis of which can be very time consuming. This can be eased with dedicated workstations and specialist software. Specialist software is available which incorporates functions such as simple subtraction, multiplanar imaging capability, maximum intensity projections (MIP) and signal-intensity time analysis. These are the minimum tools required for the analysis of breast MRI. More sophisticated tools that are not widely available include tumour segmentation with volume estimation, image fusion, automated detection and classification of abnormalities (computed assisted diagnosis or CAD) and 3D image registration.

In practice, subtraction images are performed first. Early subtraction studies are obtained by subtraction of the images obtained at approximately 90-120 seconds from the pre-contrast images; late subtraction studies comprise images obtained after 5 minutes minus the pre-contrast images. The subtraction images will display any significant patient motion which can generate pseudolesions. If significant motion is present, then the images can be realigned using 3D registration software [156] or the appropriate individual non-subtracted images of the dynamic series can be reviewed for morphological and kinetic analysis.

Both early and late subtraction images are inspected for the presence of enhancing lesions. The morphological and kinetic descriptions of any lesions should follow the MRI lexicon adapted from the American College of Radiology Breast Imaging and Data Reporting System terminology for breast MRI [157]. Morphological features that suggest the possibility of malignancy include: a mass with irregular or spiculated borders; a mass with peripheral enhancement; and ductal enhancement. Features suggesting benign disease include: a mass with smooth or lobulated borders; a mass demonstrating no contrast enhancement; a mass with non-enhancing internal septations; and patchy parenchymal enhancement.

Kinetic analysis in everyday practise uses the region of interest (ROI) method. The early subtraction images are used to determine the position for ROI placement. If enhancement is low or minimal, then the late subtraction data set can be used. If no enhancement is seen, the baseline data (non-enhanced) is used for ROI placement. When lesion enhancement is homogenous the entire outline of the lesion is used. The outer limit of the lesion acts as a boundary of the ROI to minimise partial volume effects. When lesion enhancement is heterogeneous on the early subtraction images, the maximally enhancing area of the lesion is used excluding areas of necrosis, artefacts and adjacent blood vessels. The ROI is chosen in order to be constant in position and size for each image in the series under analysis. The ROI must be small enough (at least 3-5 pixels) but not too small, because a ROI of 1-2 pixels may include a vessel and is likely to have increased pixel noise. In small lesions it is essential to check that the ROI is placed without partial volume averaging which may occur in the through-plane direction. An ROI is also placed on background (air surrounding breasts) away from phase encoding artefacts and another placed on an area of fat adjacent to or parallel with the enhancing region within the breast if possible. These additional ROIs help to scale the y-axis of the signal intensity time curves and aid interpretation.

The simplest way of assigning pathological significance to signal intensity-time curves is to provide a description of the initial enhancement period (1-2 minutes) followed by an assignment of the late enhancement pattern. The initial enhancement can be described as fast, medium or slow, and the late pattern as persistant, plateau or wash-out (pattern I-III) (**Figure 1.8**). This scheme has been widely adopted following its initial clinical evaluation by Kuhl et al. [154]. They examined 263 breast lesions and found that the distribution of curve types in 101 malignant lesions was type I, 8.9%; type II, 33.6%; and type III, 57.4% and in 165 benign lesions was type I, 83.0%; type II, 11.5%; and type III, 5.5%. The diagnostic efficacy of pattern evaluation of the signal intensity-time curves were: sensitivity, 91%; specificity, 83%; and diagnostic accuracy, 86%. This compared with enhancement rate: sensitivity, 91%; specificity, 37%; diagnostic accuracy, 58%. It is important to note that heterogeneity of curve shapes within a lesion

are also diagnostically informative. A malignant tumour may well enhance with type I and II shapes but the heterogeneous nature of enhancement and variety of curve shapes in different anatomical areas is strongly suggestive of malignancy.

1.4.4.1.4 Data quantification and limitations

Signal enhancement seen on a dynamic acquisition of T1-weighted images can be measured in two ways:

1. by the analysis of signal intensity changes (semi-quantitative)
2. by quantifying contrast agent concentration change using pharmacokinetic modelling techniques (quantitative).

Semi-quantitative parameters describe tissue signal intensity enhancement using of a number of descriptors. These parameters include onset time (time from injection or appearance in an artery to the arrival of contrast medium in the tissue[150]); gradient of the upslope of enhancement curves; maximum signal intensity; and washout gradient. As the rate of enhancement is important for improving the specificity of examinations, parameters that include an additional time element are also used (e.g. maximum intensity time ratio[151]; maximum focal enhancement at one minute [144, 158]). The uptake integral or initial area under the time signal curve (initial AUC) has also been studied[159].

Semi-quantitative parameters have the advantage of being relatively straightforward to calculate but have a number of limitations. These limitations include the fact that they do not accurately reflect contrast medium concentration in the tissue of interest and can be influenced by scanner settings (including gain and scaling factors) which can alter baseline values and therefore can alter calculated semi-quantitative parameter values. Semi-quantitative parameters have a close but complex and undefined link to underlying tissue physiology and contrast agent kinetics. These factors limit the usefulness of semi-quantitative parameters and make comparisons between patients and system difficult.

Quantitative techniques use pharmacokinetic modelling techniques that are usually applied to tissue contrast agent concentration changes. Quantitative analysis requires conversion of the MRI signal intensities to T1-relaxation rates and then Gd-DTPA concentrations[160]. Concentration-time curves are then mathematically fitted using one of a number of recognised pharmacokinetic models, e.g. Tofts'model[161], and quantitative kinetic parameters are derived for tumour regions of interest and on a pixel by pixel basis **(Figure 1.9).** Examples of modelling parameters include the volume transfer constant of the contrast agent, K^{trans}, formally called permeability-surface area product per unit volume of tissue; leakage space as a percentage of unit volume of tissue, v_e; and the rate constant, k_{ep} (also called K_{21}). These standard parameters are related mathematically ($k_{ep} = K^{trans} / v_e$)[162].

The transfer constant (K^{trans}) describes the transendothelial transport of low molecular weight contrast medium by diffusion. If the delivery of the contrast medium to a tissue is insufficient (flow-limited situations or where vascular permeability is greater than inflow) then blood perfusion will be the dominant factor determining contrast agent kinetics and K^{trans} approximates to tissue blood flow per unit volume. The latter situation is commonly found in breast tumours. If tissue perfusion is sufficient and transport out of the vasculature does not deplete intravascular contrast medium concentration (non-flow limited situations, e.g. in areas of breast fibrosis or in the irradiated breast) then transport across the vessel wall is the major factor that determines contrast medium kinetics. K^{trans} then approximates to permeability- surface area product. As low molecular weight contrast media do not cross cell membranes, the volume of distribution is effectively the EES (also called leakage space, v_e). The rate constant or k_{ep} describes the rate at which the contrast agent diffuses back into the vasculature from the EES. This tissue compartmental model is shown in **figure 1.10.**

The quantitative parameters discussed above are more complicated to derive compared to those derived semi-quantitatively which deters their use at the workbench. The model chosen may not exactly fit the data obtained, and each model makes a number of assumptions that may not be valid for every tissue or

tumour type[162, 163]. Nonetheless, if contrast agent concentration can be measured accurately and the type, volume and method of administration are consistent, then it may possible to directly compare pharmacokinetic parameters acquired serially in a given patient and in different patients imaged at the same or different scanning sites [164, 165].

1.4.4.2 Clinical validation of T1W DCE-MRI

A number of studies have attempted to correlate the morphological findings on breast T1W DCE-MRI with key histological features [166-168]. Early rim enhancement appears to correlate with high MVD (periphery more than centre), increased expression of VEGF, relatively small amounts of fibrosis and small cancer cell nests. Delayed peripheral (rim) enhancement appears to correlate with larger amounts of fibrosis and exuberant inflammatory infiltrate while delayed central enhancement appears to correlate with the presence of internal fibrosis and necrosis. Vascular density in malignant tissue is higher than normal parenchyma but there is an overlap with some benign lesions including fibroadenomas and inflammatory and proliferative processes [169, 170]. A number of studies have assessed whether there is a correlation between the kinetic DCE-MRI parameters and immunohistochemical staining in breast cancer. Broad correlations between T1 kinetic parameters estimates and MVD have been shown by some studies [170, 171] while others have found no correlation [172, 173]. It appears that factors other than MVD are important in determining the degree of tissue enhancement, such as VEGF expression [166] although some have found no correlation between VEGF expression and the degree of enhancement [174]. The issue of visible tumour vascularity (as assessed by immunohistochemistry) versus functional tumour vascularity (as assessed by DCE-MRI) remains to be addressed.

1.4.4.3 Clinical experience with T1W DCE-MRI

1.4.4.3.1 Screening

It is estimated that 5-10% of all breast cancers have a dominantly inherited component depending on the population studied. Two high penetrance genes have been identified that predispose to breast cancer, BRCA1 and BRCA2, and germline mutations in these genes are responsible for the majority of these inherited breast cancers and are associated with breast cancer at a younger age. For women carrying either of these two genes, there is a cumulative lifetime risk of developing breast cancer of 40-85% depending on the type of mutation and population being studied. In addition, there are many familial breast cancers not attributed to either BRCA1 or BRCA2. Currently, approaches to reducing the risk of developing breast cancer in these patients includes prophylactic mastectomy [175, 176], ovarian ablation [177] and chemoprevention [178, 179]. In addition to their toxicity and, in the case of prophylactic mastectomy, disfigurement, none of these methods can eliminate the risk entirely and hence screening is now under investigation. Although some studies have demonstrated screening mammography can be efficacious for women as young as 40 years old [180, 181], the value of screening young women at high genetic risk with mammography remains to be confirmed. It has been suggested that mammography has low sensitivity when screening women with BRCA1/2 carriers due to young age and hence increased breast density, a higher tumour growth rate and atypical mammographic and histopathological characteristics [182]. Additionally, there is concern regarding the radiation exposure from mammography in youung women with inherited abnormalities in DNA repair, as in BRCA-1 and BCRA-2 mutations. In light of this, T1W DCE-MRI has been evaluated as a screening test for women at high genetic risk of developing breast cancer.

Many studies of breast MRI in women at high genetic risk have reported while some studies are still ongoing. Details of the sensitivities and specificities of MRI screening in the literature to date, and the comparisons with conventional screening methods, are shown in **Table 1.5**. Most studies have found high sensitivity for detecting early cancers but lower specificity. Breast MRI does have a number of limitations as a screening tool, however, due to both technical (e.g. the requirement of intravenous of contrast medium; long examination and analysis times; variable specificity (53-97%) and biological reasons (e.g.

limitations when characterising some lobular and medullary carcinomas; limited ability to detect ductal carcinoma *in-situ* and small invasive cancers [**see sections 1.4.4.3.3 and 1.4.4.3.4**). Further, to date there is no evidence that early diagnosis of breast cancer in high risk women results in a decrease in breast cancer-specific mortality. As such, recommendation of breast screening in this patient group with DCE-MRI cannot be made with certainty. It is worth mentioning, however, that DCE-MRI screening may benefit other young women with increased risk of breast cancer from other causes, such as childhood or young adult cancer survivors previously treatment with thoracic irradiation e.g. mantle irradiation in the treatment of Hodgkin's disease [183].

1.4.4.3.2 Axillary lymphadenopathy and the unknown primary tumour

Less than 1% of patients with breast cancer present with palpable axillary lymphadenopathy with no clinically or mammographically detectable breast lesion (carcinoma of unknown primary (CUP) syndrome) [184]. Following the histological confirmation of adenocarcinoma from the axillary disease, treatment usually involves either ipsilateral mastectomy or breast irradiation with axillary node dissection followed by systemic therapy as appropriate (chemotherapy with/without endocrine therapy). However, a third of patients undergoing mastectomy have no primary tumour identified on pathology [185, 186], while radiotherapy alone to the breast has been associated with an increased risk of local recurrence [187]. In light of this, a number of studies have assessed the role of DCE-MRI for detecting occult primary breast cancers to aid in the treatment decision process.

Orel et al. reported on 22 women presenting with malignant axillary lymph nodes and negative clinical and mammographic examinations [188]. MRI identified a primary breast cancer in 19 of the 22 patients (86%) with the lesion sizes measuring between 4 and 30mm. Two patients with invasive ductal carcinoma (2mm; 17- and 20- mm) had false negative MRI results. Olsen et al. assessed 40 patients with isolated axillary adenocarcinoma from an unknown primary, again with no detectable breast lesion either clinically or mammographically [189]. MRI identified a primary breast lesion in 28 of the 40

women. Of the 12 patients with a negative MRI study, 5 underwent mastectomy but tumour was found in only one of the specimens. A number of smaller studies have revealed similar results [190, 191]. Thus, contrast-enhanced MRI can detect occult breast cancer in patients presenting with malignant axillary disease from an unknown primary source where clinically breast examination and mammography are normal (**Figure 1.11**). Given the poor performance of mammography in this situation [187, 192], MRI of the breast should now be considered the investigation of choice in this clinical situation (**Table 1.6**).

1.4.4.3.3 Lobular cancer

Lobular carcinoma of the breast is characterised pathologically by infiltration of the carcinoma cells in a "single-file" ("Indian-files") fashion. This induces a less prominent desmoplastic reaction and, as a result, mammography and ultrasound tend to have a low sensitivity for invasive lobular carcinoma (ILC). In addition, lobular carcinomas are associated with an increased incidence of multifocality (additional tumour within the same quadrant as the index lesion) and multicentricity (additional tumour within a separate quadrant to the index lesion) and disease extent can often be underestimated resulting in incomplete excision with breast-conserving surgery [193].

DCE-MRI for both diagnosis and assessment of disease extent of ILC has been evaluated and demonstrated diagnostic superiority over the conventional imaging modalities. In one series of 17 patients with ILC, MRI detected 30 lesions compared with 21 on conventional imaging, while also identifying multiple lesions in 7 cases and contralateral disease in 1 patient [194]. Qayyam et al. [195] compared the DCE-MRI characteristics of ILC with the histopathological finding in 13 patients. They described 3 patterns for ILC and the histopathological correlates: a solitary mass with irregular margins (n=4) which corresponded with the same morphology on pathological assessment; multiple lesions either connected by enhancing strands (n=6) or separated by non-enhancing intervening tissues (n=2) which correlated with non-contiguous tumour foci with malignant cells streaming in single-file fashion in the breast stroma or small tumour aggregates separated by normal tissue; and enhancing

septa only (n=1) corresponding with streaming of tumour cells in the breast stroma.

Yeh et al. [196] assessed the morphological and functional DCE-MRI features in a series of 15 cases of ILC presenting with a palpable mass or an unknown primary. The functional parameter measured was the extraction flow (EF) product, a quantitative measure of contrast medium uptake. They found the range of EF product to be 25 to 120 with the majority of cases within the 30s (level for normal breast is 25 or less). In 2 tumours, however, a substantial part of the tumour demonstrated an EF product within the normal range. A focal mass was found in 8 cases (7 irregular and 1 round; six ill-defined and 2 spiculated margins) but a mixture of enhancement patterns was seen. Multi-focal disease was demonstrated in 4 cases and an unsuspected contralateral tumour in 1 case. They concluded that the combination of morphology and functional characteristics on DCE-MRI is able to detect the majority of cases of ILC despite the variability seen. Caution is still required, however, as some lesions display features similar to normal breast.

1.4.4.3.4 Ductal Carcinoma *in-situ* (DCIS)

DCE-MRI has been used for the detection of ductal carcinoma *in-situ* (DCIS). DCIS is usually diagnosed by x-ray mammography due to the presence of microcalcification and currently accounts for approximately 20% of screening-detected cancers. DCIS can be successfully treated with either mastectomy alone or wide local excision followed by adjuvant breast irradiation but relies on complete excision of disease. Often this is only achievable with mastectomy due to the high rate of multifocal and multicentric disease [197-200]. Several investigators have described the morphological and kinetic features of DCIS on MRI although most of these studies have had small patient numbers. In a relatively large study, Neubauer et al. retrospectively evaluated the DCE-MRI features of 39 consecutive patients with pure DCIS [201]. They defined categories for signal increase (C1 = normal, C2 = slow, continuous, C3 = strong initial and slow further increase, C4 = strong initial increase followed by a plateau phenomenon, and C5 = strong initial increase followed by a washout

phenomenon) and morphological patterns (M0 = no pattern observed, M1 = linear or linear-branched, M2 = segmental dotted or granular, M3 = segmental homogeneous, and M4 = focal spot-like). C4 and C5 signal intensity-time patterns were considered suspicious of malignancy and 62% of DCIS demonstrated this pattern. In terms of enhancement, segmental enhancement was seen in 82% and segmental dotted or granular patterns (M2) were seen in 73%. When signal increase and morphology were taken together, 70% of non-high grade and 92% of high grade DCIS were correctly identified as being suspicious for malignancy. They concluded that segmental enhancement is a hallmark of DCIS (with hormone effects as the main differential diagnosis) and that the combination of morphology and signal intensity enhancement considerably improves the rate of detection. Gilles et al, have reported similar findings and also noted that early enhancement on DCE-MRI in patients with DCIS is associated with angiogenesis in the stroma that surrounds ducts involved by DCIS [202]. However, it should be remembered that not all ductal enhancement on breast MRI is due to DCIS. Liberman reported that ductal enhancement can also be caused by atypical ductal hyperplasia, lobular carcinoma *in-situ*, fibrocystic change, ductal hyperplasia, and fibrosis [203]. Therefore, the clinical utility of MRI in the evaluation of DCIS remains uncertain.

1.4.4.3.5 Tumour staging: Tumour volume determination, multicentricity and multifocality

An accurate assessment of the primary tumour extent is crucial for deciding the best management for breast cancer patients. It is particularly important when considering the feasibility of breast-conserving surgery. An inaccurate assessment can lead to incomplete tumour excision thus resulting in either the need for a second surgical procedure or a high rate of recurrence following "apparent" curative surgery. Unfortunately, clinical examination, mammography and breast ultrasonography are poor at accurately defining the primary tumour extent and are capable of both overestimating and underestimating the histologically defined tumour size [77, 80, 204, 205]. As a result, the role of T1W DCE-MRI in this setting has been examined and a number of studies have shown MRI to be superior to both mammography and ultrasonography [89, 206-

208]. When comparing the largest pathological cancer diameter with the tumour size defined by each technique, Davies et al. found MRI to have the highest correlation coefficient (r=0.98) when compared with ultrasonography (r=0.45) and mammography (r=0.46). MRI also had the smallest standard error of 0.34 compared with 0.78 and 1.04 for ultrasonography and mammography respectively [206]. Esserman et al. has also demonstrated MRI to be superior to mammography with a 98% accuracy for defining anatomic tumour extent compared to only 55% for mammography [89]. In addition, MRI can identify synchronously contralateral occult primary tumours in between 3% and 24% of women presenting with breast cancer [209-212].

The presence or absence of tumour multifocality and/or multicentricity is critical when planning the optimal surgical management of breast cancer. It now well established that MRI can identify additional sites of tumour, not detected using conventional imaging, in between 6 and 34% of women with known breast cancer. MRI identifies multifocal disease in 1-20% of women and muticentric disease in 2-20% [90, 209, 213-217]. Kramer et al. demonstrated MRI to have a sensitivity for the diagnosis of multicentricity of 89% compared with 79% for ultrasonography, 66% for mammography and only 47% for clinical examination [218]. Thus, more accurate depiction of tumour size and prediction of the distribution of tumour by MRI may help to achieve definitive surgery in one procedure [219, 220]. This benefit can be expected to be greater in cases where mammography and ultrasound have difficulties, for example, in patients with dense breasts or invasive lobular carcinoma. It should be remember, however, that there is the potential to increase the number of mastectomies and so specificity for individual lesions must be high [221]. If doubt exists, a biopsy to document additional disease is recommended prior to definitive surgery.

1.4.4.3.6 DCE-MRI and Neoadjuvant chemotherapy

As discussed in **section 1.2.2**, neoadjuvant chemotherapy delivered prior to definitive surgery in primary breast cancer provides equal survival to primary

surgery followed by adjuvant chemotherapy, while increasing breast-conservation rates due to tumour down-staging.

A proportion (2-30%) of patients receiving NAC will fail to response to treatment and will have a worse outcome [23, 29, 75]. The ability to identify non-responders early during treatment would enable the use of alternative therapies which may be more beneficial [36]. Currently, measurement of breast tumour size is used to monitor response to treatment and assess the volume of residual disease after treatment. Recently, von Minckwitz et al. demonstrated that clinical response after two cycles of NAC could predict for pCR [45], however, many studies evaluating NAC in patients with breast cancer have shown that clinical examination frequently overestimates tumour size [77-81]. Further, change in tumour size often becomes apparent only after several cycles of chemotherapy. Conventional imaging with X-ray mammography & ultrasonography are also imperfect techniques and neither has been shown to be superior to clinical assessment for predicting pathological tumour size [82]. Therefore, DCE-MRI has two potential roles to play in the assessment of patients receiving NAC. Firstly, DCE-MRI may help in the early identification of non-responding patients thus allowing treatment intervention that may be more beneficial. Secondly, DCE-MRI may provide a more accurate assessment of residual tumour at the end of NAC and thus aid in the decision regarding surgery.

1.4.4.3.7 Monitoring Tumour Response

DCE-MRI evaluates response on the basis of both change in tumour size and on the amount and speed of enhancement. The value of DCE-MRI as an early predictor of the efficacy of NAC in patients with breast cancer has not been fully evaluated and is the subject of the prospective study discussed in chapter 2. Both Knopp and Hayes et al. have, however, shown that successful treatment causes decreases in the rate and magnitude of enhancement and that poor response results in persistent abnormal enhancement [222, 223]. Esserman et al. have suggested that the morphological MRI appearances of breast cancer prior to

therapy can predict likelihood of response but this has not been verified by other workers [224].

1.4.4.3.8 Evaluating Residual Disease

Currently, tumour size is used to assess the volume of residual disease after NAC by clinical examination, x-ray mammography and/or ultrasound. Each of these techniques, however, overestimates the extent of residual disease at the end of treatment [225-229]. Clinical palpation is an imperfect evaluation method because of intervening skin and soft tissue and is unable to distinguish active disease from post-chemotherapy fibrosis. Assessments by x-ray mammography are hampered by radiographic magnification and it may be difficult to distinguish residual tumour from post-chemotherapy fibrosis [227, 228]. It is also well-recognised that some tumours are simply not visualized in patients with radiographically dense breasts. In some patients, ultrasound appears better in assessing tumour response and Doppler ultrasound of residual disease is being evaluated [229].

Feldman et al. made the observation that there was a significant difference between the clinical and pathological evaluation of residual disease, such that the improved patient survival achieved in those with complete pathological response ($p=0.002$) would not be appreciated if patients had been judged clinically ($p=0.09$) [226]. Women with normal examinations may well have residual active disease requiring further treatment. Further, in some cases, small volumes of residual disease after NAC can be difficult to target at operation. In a study of 80 women, Sever et al. assessed the value of insertion of an intra-tumoural coil prior to NAC in order to guide surgery, particularly in those obtaining a cCR [230]. Of the 80 women treated, 47 achieved a cCR (59%), with 19 women (24%) also achieving a radiological CR on mammography and breast ultrasound. In these 19 patients, localisation was possible exclusively by use of the coil and in 11 patients, residual disease was found. Further, in 3 of the 11 patients, widespread microscopic disease was found and these subsequently required mastectomy. This study demonstrates that clinical and conventional radiological assessment of disease following NAC may not accurately reflect the

true pathological extent and thus, more accurate methods of assessing residual disease would improve the selection and precision of subsequent treatment methods.

Several studies have shown that contrast enhanced MRI is the most accurate technique for evaluating pathological response and volume of residual active disease at the end of treatment [231-238]. Non-dynamic fat suppressed breast MRI assesses the presence of residual disease better than mammography when the presence of residual abnormal enhancement on post-contrast images is used [233]. Interestingly, many have observed that the fibrosis observed after chemotherapy is hylanised and does not arise from granulation tissue (seen post-operatively) [239] and this enables residual active disease to be depicted as an area of persistent abnormal enhancement [240, 241]. Microscopic disease can of course not be detected, but MRI can indicate the extent of remaining tumour tissue on which to plan breast conserving surgery.

1.4.4.3.9 Detecting relapse

The surgical management of primary breast cancer depends on a number of factors including tumour size, position, multicentricity, patient choice and contraindications to radiotherapy. Breast-conserving surgery with radiotherapy is now known to be equivalent to mastectomy in terms of survival and is generally the treatment of choice for early stage breast cancer [2, 242, 243]. In some studies, however, breast-conservation has been associated with a higher rate of local recurrence compared to mastectomy although, despite this, overall survival has remained equivalent. [242, 243]. Early detection of local recurrence is important as many patients can be successfully treated by salvage mastectomy [244, 245].

The recommended follow-up for local recurrence is involves routine clinical examination and mammography [246, 247]. Ultrasonography and core biopsy are used to confirm the diagnosis of recurrence. In the first six months after surgery, mammograms show a general increased density, architectural

distortion, skin thickening, asymmetric densities, dystrophic calcification and features of fat necrosis [248-250]. Mammographic changes are most helpful in suggesting recurrence six months to one year later after surgery. It is well recognised that features of scar tissue can mimic those of recurrent cancer on mammography [251] and, therefore, any increase in the extent of the post surgical abnormality or the development of a mass within the area of distortion must be regarded as suspicious. The overall positive predictive value of cancer detection in the treated breast using mammography is thought to be around 72% [252] with a false negative rate of 5-15% [253].

As a result, the role of DCE-MRI in detecting tumour recurrence in the surgically operated breast has been assessed. Some studies previously reported that non-enhanced T2 weighted sequences alone could be used to differentiate tumour from scar tissue as recurrent tumour demonstrated a higher signal intensity than dysplastic tissue and fibrosis [254, 255]. However, other groups failed have to show this [148, 152, 256, 257] and therefore un-enhanced MRI scans must be considered unreliable.

In contrast, a number of studies have now shown the benefit of DCE-MRI for detecting recurrent tumour in the previously treated breast and relies on the different enhancement pattern of malignant disease compared with benign post-treatment changes such as scarring and fat necrosis. On T1 weighted sequences following Gd-DTPA contrast medium rapid, early (within 3 minutes) and avid enhancement is seen in recurrent tumour compared with slower enhancement of lower magnitude in benign disease [152, 256-259] [260, 261]. Gilles et al. also noted nodular enhancement to be associated with invasive carcinoma while linear enhancement was seen with ductal carcinoma in-situ [152]. Mussurakis et al. reported significant differences between benign and malignant lesions for enhancement index, maximum uptake, amplitude of uptake, wash-in rate, wash-out rate and the reciprocal of half the time to maximum. The respective sensitivity and specificity for each parameter was: enhancement index, 1.00 and 0.96; maximum uptake, 1.00 and 0.96; amplitude of uptake, 0.91 and 0.94; wash-in rate, 0.82 and 0.47; wash-out rate, 0.91 and 0.59; and the reciprocal of half the time to maximum, 1.00 and 0.51 [260].

The timing of DCE-MRI following surgery is an important factor in the accuracy of the technique, however, as benign proliferative disease and recent fat necrosis may mimic malignant recurrence within 6 months of surgery and 9 months of breast irradiation [258, 262]. Indeed, in some patients post-operative scarring may continue to enhance up to 18 months post-treatment although beyond that time no significant enhancement is seen [263]. The absence of focal enhancement, even in the first year post-treatment, is thought to be able to exclude recurrent malignancy with a negative predictive value of 100% [264].

When compared with other techniques for detecting local recurrence, DCE-MRI has a consistently high sensitivity (91%-100%) with an associated high specificity (88%-93%) [218, 265-267]. This compares with sensitivities for other techniques as follows: clinical examination alone, 51%-89%; mammography alone 50%-67%; ultrasound 85%; and cytology 79% [218, 265, 267]. Of note, Drew et al. showed clinical examination combined with mammography to have 100% sensitivity but a poor specificity at 67% [265].

MRI may reveal other lesions in the post surgical breast, which can confound evaluation by clinical examination, mammography or ultrasound. These include seromas, haematomas, oil cysts, fat necrosis and areas of residual or recurrent DCIS. Many of these have characteristic appearances on MRI and hence definitive diagnoses can be made.

1.4.4.4 T2*-weighted DCE-MRI of breast cancer

1.4.4.4.1 Data acquisition

T2*-weighted (susceptibility) DCE-MRI sequences are sensitive to the vascular phase of contrast medium delivery and reflect on tissue perfusion and blood volume. Such perfusion-weighted images of the breast can be obtained using "bolus-tracking techniques". These monitor the passage of contrast material through a capillary bed as it produces magnetic field (Bo) inhomogeneities

which result in a decrease in signal intensity of surrounding tissues [268, 269]. The decrease in signal intensity of tissues can be observed with susceptibility-weighted sequences. The degree of signal loss observed is dependent on the vascular concentration of the contrast agent together with the microvessel size [270] and density. The signal to noise ratio (SNR) of such images can be improved by using high doses of contrast medium (i.e., ≥ 0.2-mmol/kg body weight) [271]. High specification MR systems are ideally suited to this task and allow multi-slice acquisitions. Such studies are also possible on conventional MRI systems using standard gradient-echo techniques but the need to acquire data at a 1-2 second resolution requires that the matrix size is relatively coarse and often limited to 1-2 slices.

1.4.4.4.2 Data quantification and limitations

Tracer kinetic principles can be used to provide estimates of relative blood volume (rBV), relative blood flow (rBF) and mean transit time (MTT) derived from the first-pass of contrast agent through the microcirculation [268, 269, 272] (**Figure 1.12**). These variables are related by the central volume theorem equation

$$BF = BV/MTT.$$

The most robust parameter which can be extracted reliably from first pass techniques is rBV, which is obtained from the integral of the time series data during the first pass of the contrast agent [273]. This cannot readily be done for the breast because of the loss of compartmentalization of the contrast medium. Solutions to counter T1 enhancing effects of gadolinium chelates include pre-dosing with contrast medium to saturate the leakage space, and idealized model fitting where the time series data is fitted to a gamma-variate function from which the parameters rBV, rBF and MTT are derived (**Figure 1.13**). From a practical perspective, it is not always necessary to quantify T2*-weighted DCE-MRI data to obtain insights of the spatial distribution of tissue perfusion. Simple subtraction images can demonstrate the maximal signal attenuation (also termed

relative maximum signal drop, rMSD), which has been strongly correlated with relative blood flow and volume in tumors [274, 275]. Subtraction analysis should only be done, however, if there is a linear relationship between rBV and rBF, that is when MTT is in a narrow range. This is often the case in non-necrotic breast tumours (**Figure 1.14**).

1.4.4.5 Clinical experience with T2*W DCE-MRI

To date, clinical experience with T2*W DCE-MRI is limited. Both Kuhl et al. and Kvistad et al. have evaluated the value of T2*W DCE-MRI for characterising breast lesions using visual assessments [276, 277]. Both studies showed strong decreases in signal intensity in malignant tissues whereas susceptibility effects in fibroadenomas were minor. Thus, it was possible to differentiate carcinomas from fibroadenomas with high specificity using T2*W characteristics despite significant overlap in T1 enhancement patterns. The pathophysiological explanation probably relates to differences in the microvessel arrangements, density and size between malignant tumours and fibroadenomas. Weind et al. conducted a histopathological study comparing microvessel distributions in invasive breast cancer and fibroadenomas that shed light on these observations [278]. They showed that there was complete overlap in MVD counts between the breast cancers and the fibroadenomas but the distribution of microvessels was distinctive. Microvessel distribution in the breast carcinomas showed marked regional variations with fewer vessels seen within the centre of tumours compared to the periphery whereas the microvessel distribution in fibroadenomas was more evenly spread within the stroma. Other investigators have also shown microvessel density "hot spots" in breast cancers [167, 279]. Both Kuhl et al. and Kvistad et al. comment that the T2* effects occurred in focal areas which may correspond to the "hot spot" MVD counts in tumours.

The role of T2*W DCE-MRI for evaluating response to neoadjuvant chemotherapy in primary breast cancer is examined in chapter 2.

1.4.5 NON-ENHANCED MRI METHODS – BOLD MRI

Non-enhanced MRI techniques use intrinsic paramagnetic substances to provide the contrast between tissues. Blood oxygen level dependant (BOLD) MRI is an example of a non-enhanced MRI method. This technique uses deoxyhaemoglobin as an "intrinsic" contrast medium. Deoxyhaemoglobin is a paramagnetic substance under normal circumstances and thus its presence affects the signal intensity of the surrounding tissues. BOLD MRI can therefore provide a potential method for assessing the level of tissue oxygenation. Gradient-echo T_2* weighted images that are sensitive to changes in blood volume, blood flow and blood oxygenation are used.

Vascular function can be evaluated by analysis of BOLD contrast changes in response to hyperoxia and hypercapnia [280]. Clinical application of this technique has revealed high signal enhancements in response to carbogen (5% $C0_2$: 95%0_2) inhalation in human tumours [281]. The primary advantage of BOLD MRI is that there is no need to administer contrast material. Further, BOLD contrast is not sensitive to fluctuation in permeability. A major reservation for intrinsic contrast imaging is the low contrast to noise ratio in the images obtained.

The role of BOLD MRI for evaluating response to neoadjuvant chemotherapy in primary breast cancer is examined in chapter 2 and an assessment of the pathophysiological correlates of the BOLD MRI parameter, R2* is discussed in chapter 4.

1.5 SUMMARY AND AIMS OF THESIS

The neoadjuvant treatment setting in primary breast cancer provides a platform for the in vivo assessment of tumour chemo-responsiveness and the underlying response mechanisms. In addition, response in the primary tumour may act as a surrogate marker of response in occult micrometastatic disease. With the advent of novel therapies that target the tumour vasculature, it is important to

understand of the effects of conventional cytotoxic chemotherapy on the tumour vasculature. This will help in the rational design of future treatment regimens combining conventional and novel anticancer agents.

Thus, the aims of the research in this thesis are:

1. To assess the vascular effects of neoadjuvant conventional cytotoxic chemotherapy in primary breast cancer using multi-parameter functional MRI (DCE-MRI and BOLD-MRI) performed prior to and during chemotherapy treatment and to determine whether the baseline parameter values or treatment changes predict for clinicopathological response.

2. To evaluate the effect of neoadjuvant chemotherapy on the quantitative and qualitative measures of tumour angiogenesis, as assessed using immunohistochemical staining techniques, and to determine whether the baseline parameter values or treatment changes predict for clinicopathological response.

3. To assess the pathophysiological correlates of the DCE-MRI and BOLD MRI kinetic parameters in primary breast cancers.

Table 1.1. Non-randomized studies of neoadjuvant chemotherapy

Study	No.	Chemotherapy	cCR (%)	pCR (%)
Bonadonna et al.[17]	161	CMF x 3-4, FAC x 3-4, FEC x 3	17	4
Hortobagyi et al.[18]	174	FAC x 3	17	NK
Gardin et al.[19]	125	FAC x 3	10	4
Smith et al. [20]	50	EcisF x 8	66	NK
Chollet et al.[21]	50	ACVF	51	30
Kuerer et al. [22]	156	FAC x 4	NK	19

Abbreviations: CMF, cyclophosphamide, methotrexate, 5-fluorouracil; FAC, 5-fluorouracil, doxorubicin, cyclophosphamide; FEC, 5-fluorouracil, epirubicin, cyclophosphamide; EcisF, epirubicin, cisplatin, 5-fluorouracil; ACVF, doxorubicin, cyclophosphamide, vinorelbine, 5-fluorouracil.

Table 1.2. First generation randomised controlled trials of neoadjuvant chemotherapy

Study	No.	Group	Schedule	Time of follow-up	OS	P value
Fisher et al. [23] (Wolmark et al. [24])	1523	Preop	AC-S	5 years (10 years)	80% (69%)	0.83 (0.80)
		Postop	S-AC		80% (70%)	
Mauriac et al. [25]	272	Preop	EVM – MTV –S&/or RT	10 years	55%	NS
		Postop	S – EMV-MTV		55%	
Semiglazov et al. [26]	271	Preop	TMF-RT-S-TMF	5 years	86%	>0.05
		Postop	RT-S-TMF		78%	
Scholl et al. [27]	414	Preop	FAC-S-RT	54 months	86%	0.04
		Postop	RT-S-FAC		78%	
Powles et al.[28] & Makris et al. [29]	309	Preop	MMMT-S-MMMT	48 months		NS
		Postop	S-MMMT			
van der Hage et al. [30]	698	Preop	FEC-S	4 years	82%	0.4
		Postop	S-FEC		84%	

Abbreviations: OS, overall survival; AC, doxorubicin & cyclophosphamide; S, surgery; EVM, epirubicin, vincristine, methotrexate; MTV, mitomycin, thiotepa, vindesine; RT, radiotherapy; TMF, thiotepa, methotrexate, 5-fluorouracil; FAC, 5-fluorouracil, doxorubicin, cyclophosphamide; MMMT, methotrexate, mitoxantrone, mitomycin, tamoxifen; FEC, 5-fluorouracil, epirubicin, cyclophosphamide.

Table 1.3. Studies of biologic markers to predict response to NAC in primary breast cancer

	Patient no.	Treatment	Markers assessed	Biologic markers predicting response	Other markers predicting response
Makris et al. 1997[56]	90	2M/3M + tamoxifen	ER, PgR, c-*erb*B-2, p53, Ki-67, bcl-2, SPF, ploidy	None	c-*erb*B-2 negative
Chang et al. 1999 [57]	158	2M/3M + tamoxifen	Tumour size, nodal disease, ER, PgR, c-erbB-2, p53, bcl-2, Ki67, SPF, ploidy	Decrease Ki67 on d10 or d21	ER positive; c-*erb*B-2 negative
Assersohn et al. 2003[64]	106	Anthracycline or anthracenedione-based chemotherapy +/- tamoxifen; tamoxifen alone	Ki-67	Change Ki-67 on d21	-
Burcombe et al. 2005[61]	118	Anthracycline or anthracenedione-based chemotherapy	ER, PgR, HER-2, Ki-67	>75% reduction Ki-67 at end of treatment	None
Bottini et al 2001[65]	157	CMF+tamoxifen; epirubicin	Ki67, p53, bcl2, c-erbB2, ER, PgR	Change Ki-67at end of treatment	None
Chang et al. 2000[70]	28	2M	AI, Ki67, SPF, ploidy	Increase AI; decrease Ki67 on d21	-
Archer et al. 2003 [69]	65	Antracycline-based	AI, Ki-67, HER-2	High Ki-67, high GI (Ki-67/AI ratio)	None
Collecchi et al. 1998[67]	70	FEC	[3H]-dT-LI, bcl-2	High [3H]-dT-LI	-
Faneyte et al. 2003[63]	97	Antracycline-based	Tumour size, *bcl-2*, ER, p53, HER-2, Ki67	High Ki67; positive p53	Large tumour size; ER negative
Penault-Llorca et al. 2003[59]	115	Antracycline-based	Grade, ER, PgR, HER-2, Ki67, p53	None	HER-2 positive
Vincent-Salomon et al. 2004[66]	55	CAF	ER, PgR, SPF, MI, Ki67	High MI; high SPF; high Ki67	ER negative, PgR negative
Kallab et al 2004 [71]	26	DT	ER, PgR, HER-2, Ki67, bcl-2, p53,p21, EGFR, p-glycoprotein	None	None

2M= mitoxantrone, methotrexate; 3M= 2M + mitomycin C;ER= oestrogen receptor; PgR=progesterone receptor; SPF=S-phase fraction; CMF= cyclophosphamide, methotrexate, 5-fluorouracil; FEC=5-fluorouracil, epirubicin, cyclophosphamide; [3H]-dT-LI = [3H]-thymidine labelling index; CAF = cyclophosphamide, 5-fluorouracil, doxorubicin; MI=mitotic index; DT = doxorubicin, docetaxel; EGFR=epidermal growth factor receptor

Table 1.4. Examples of endogenous proangiogenic and antiangiogenic factors that regulate angiogenesis

PROANGIOGENIC FACTORS	ANTIANGIOGENIC FACTORS
Vascular endothelial growth factor	Thrombospondin
Acidic & basic fibroblast growth factors	Angiostatin
Platelet-derived growth factor	Endostatin
Transforming growth factors α, β	Vasostatin
Prostaglandins E1, E2	Interferon-α, β, γ
Epidermal growth factor	Interleukin-12
Tumour necrosis factor-α	Platelet factor 4
Interleukin-8	Tissue inhibitors of metalloproteinase
Vascular integrin $\alpha_v\beta_3$	
Matrix metalloproteinases	

Table 1.5. Comparison of MRI screening for breast cancer in high-risk groups with clinical examination, mammography and ultrasonography

Country (City)	Study	No. women reported	No. BRCA1 or BRCA2 carriers	No. cancers detected	MRI Results		Other modalities tested					
							Clinical examination		Mammography		Ultrasound	
					Sensitivity	Specificity	Sensitivity	Specificity	Sensitivity	Specificity	Sensitivity	Specificity
Canada (Toronto)	WARNER et al. (2001)[282]	196	96	6	100%	91%	33%	99.5%	33%	99.5%	60%	93
Germany (Bonn)	KUHL et al. (2000)[283]	192	-	15	100%	95%	-	-	33%	93%	33%	80%
Italy (Rome)	PODO et al. (2002) [284]	105	-	8	100%	99%	Not Stated	-	Not stated	-	-	-
Netherlands (Nijmegen)	STOUTJESDIJK et al. (2001) [285]	179	-	13	100%	93%	-	-	42%	96%	-	-
Netherlands (Rotterdam)	TILANUS-LINTHORST et al. (2000)[286]	109	-	3	100%	-	Not stated	-	Not stated	-	-	-
Netherlands (Rotterdam)	KRIEGE et al. (2004)[287]	1909	358	51	80%	90%	18%	98%	33%	95%	-	-

Table 1.6. Current and potential new indications for breast MRI

Indication	Comments
Problematic mammogram	Mammographic and ultrasound evaluation should be done first and MRI in selected patients with equivocal or suspicious findings.
Staging breast cancer when multiple or bilateral tumours are suspected	MRI improves accuracy of staging, detecting multicentricity and multifocality particularly for large tumours in the radiographically dense breast and lobular cancers. MRI has a high negative predictive rate. Unsuspected contralateral malignancy can be detected in 5-10% of lobular cancer cases.
High risk screening: breast cancer gene carriers and history of mantle irradiation for lymphoma at young age	MRI may be a valuable adjunct in these high risk patients but MRI is NOT appropriate for general breast cancer screening.
Lobular cancer	Tumour extent can be difficult to detect with mammography, is commonly multifocal/multicentric or bilateral (approximately 10%) and is a frequent cause of positive surgical margins.
Metastatic cancer in axillary lymph-nodes without detectable lesion on conventional imaging	MRI can locate a primary breast tumour in the majority, enabling breast conservation surgery
Monitoring response to neoadjuvant chemotherapy	Helpful for identifying the extent of residual active disease following completion of chemotherapy for locally advanced breast cancer. Monitoring response to treatment during therapy is experimental.
Positive surgical margins following breast conservation surgery	MRI can identify the extent of residual disease
Distinguishing tumour recurrence from surgical scar and other causes of a mass following breast surgery	Recommended 6 months or more after surgery
Suspected implant rupture or suspected cancer in patients with history of liquid silicone injection	

Figure 1.1. Age-standardised incidence of and mortality from female breast cancer in England and Wales (Rate per 100,000). (*Taken from National Statistics, www.statistics.gov.uk*)[1]

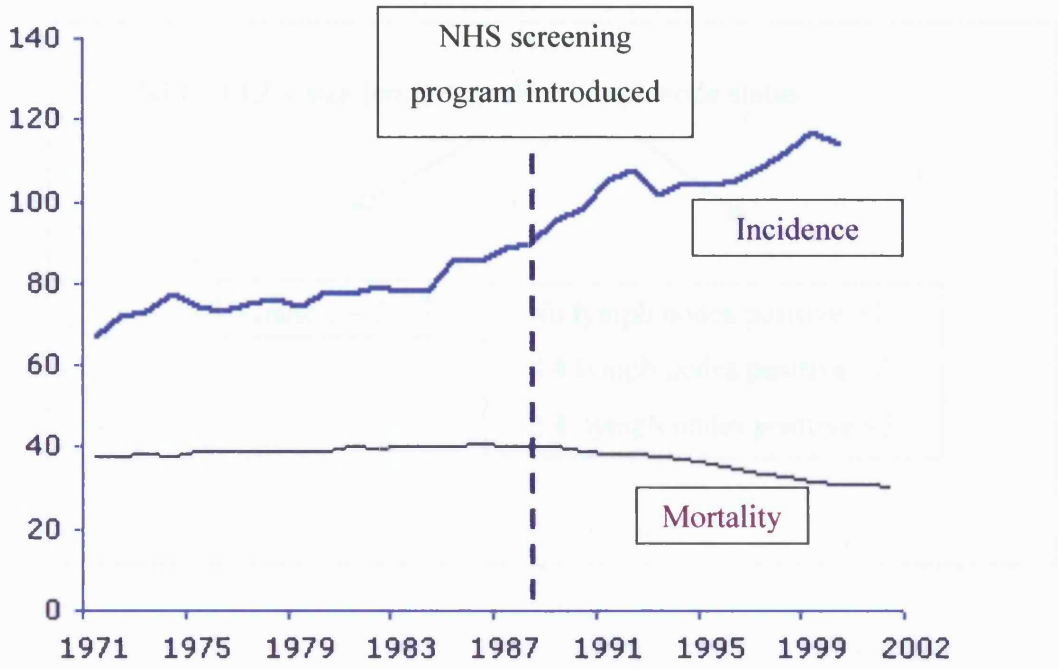

Figure 1.2. The Nottingham Prognostic Index (NPI)

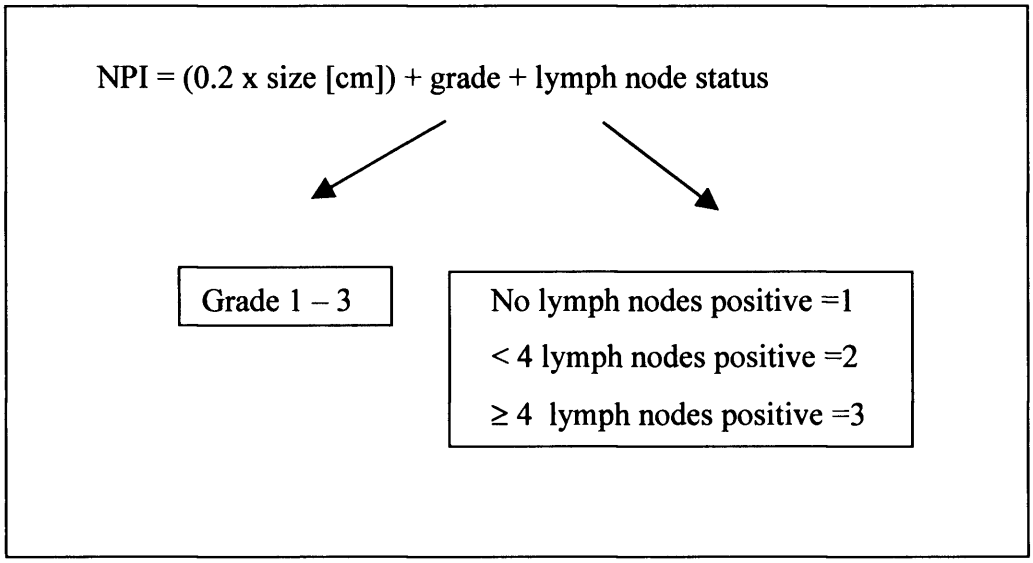

NPI	Prognosis	10 year overall survival
≤ 2.4	Excellent	94%
≤ 3.4	Good	83%
≤ 4.4	Moderate	70%
< 5.4	Moderate II	51%
≥ 5.4	Poor	19%

Figure 1.3. Overall survival and disease-free survival according to treatment through 9 years of follow-up from the NSABP-B18 trial (Postop = postoperative chemotherapy; Preop = preoperative chemotherapy). ***Taken from Wolmark et al, 2001.[24]***

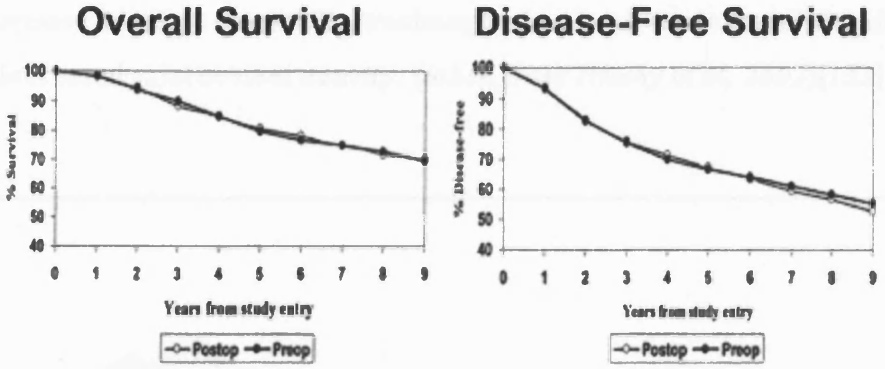

Figure 1.4. Comparison of outcome of patients treated with preoperative chemotherapy according to primary breast tumour response through 9 years of follow-up from the NSABP-B18 trial. ***Taken from Wolmark et al, 2001.[24]***

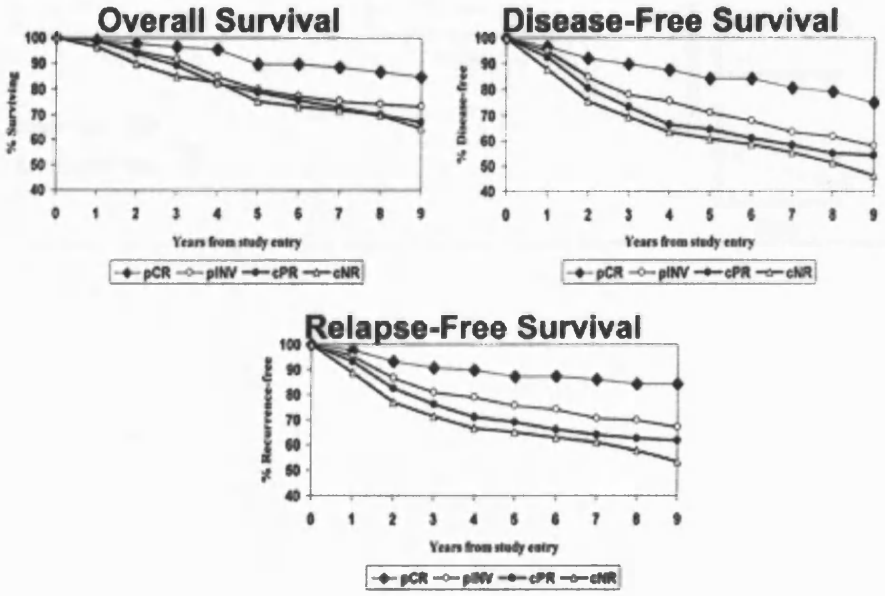

Figure 1.5. Microvessel density in a shrinking tumor is determined by the combined effects of capillary dropout and tumor cell dropout. The time-dependent coupling of these two forms of cell dropout is reflected by the intercapillary distance and, in turn, by microvessel density. Thus, following antiangiogenic therapy a regressing tumor may exhibit decreased microvessel density, essentially unchanged levels of microvessel density, or even increased microvessel density. (*taken from Hlatky et al, 2002*)[132]

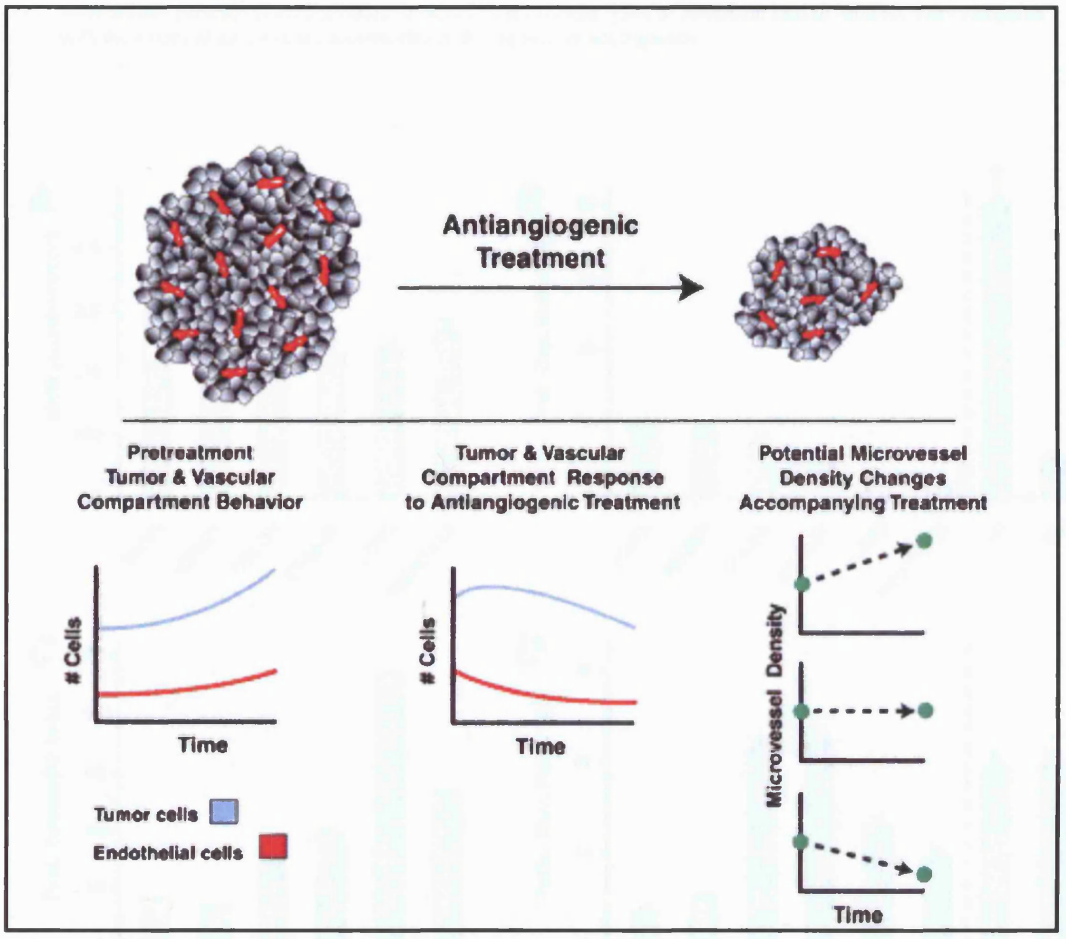

Figure 1.6. Quantitative analysis of endothelial cell proliferation and pericyte recruitment during pathological tumour angiogenesis and physiological ovarian angiogenesis. All data are expressed as mean ± SE. (*taken from Eberhard et al, 2000*)[133]

A. **MVD count:** colon carcinomas, mammary carcinomas, lung carcinomas, and prostate carcinomas have similarly high MVD counts. Glioblastomas and renal cell carcinomas have higher average MVD counts ($P < 0.005$).
B. **Proliferating. Capillary Index.** A ranked order of the intensity of angiogenesis in the different types of tumors was determined as follows: glioblastomas > renal cell carcinomas > colon carcinomas > mammary carcinomas > lung carcinomas > prostate carcinomas. Proliferating. Capillary Index values in malignant human tumours were compared with the intensity of angiogenesis in the cyclic bovine corpus luteum [*CR*; early corpus rubrum (angiogenesis)], midstage corpus luteum (*CL*; maturation), and regressing corpus luteum (*REG-CL*; regression).
C. **Proliferating tumour versus endothelial cell index**: A quantitative ratio of the total number of proliferating tumour cells in all tumours: the total number of endothelial cells : provides a relative parameter that reflects the per tumour cell angiogenic capacity of the tumours.
D. **Microvessel pericyte coverage index**: indices of the different types of malignant human tumours were compared with the values of the transient neovasculature during ovarian angiogenesis.

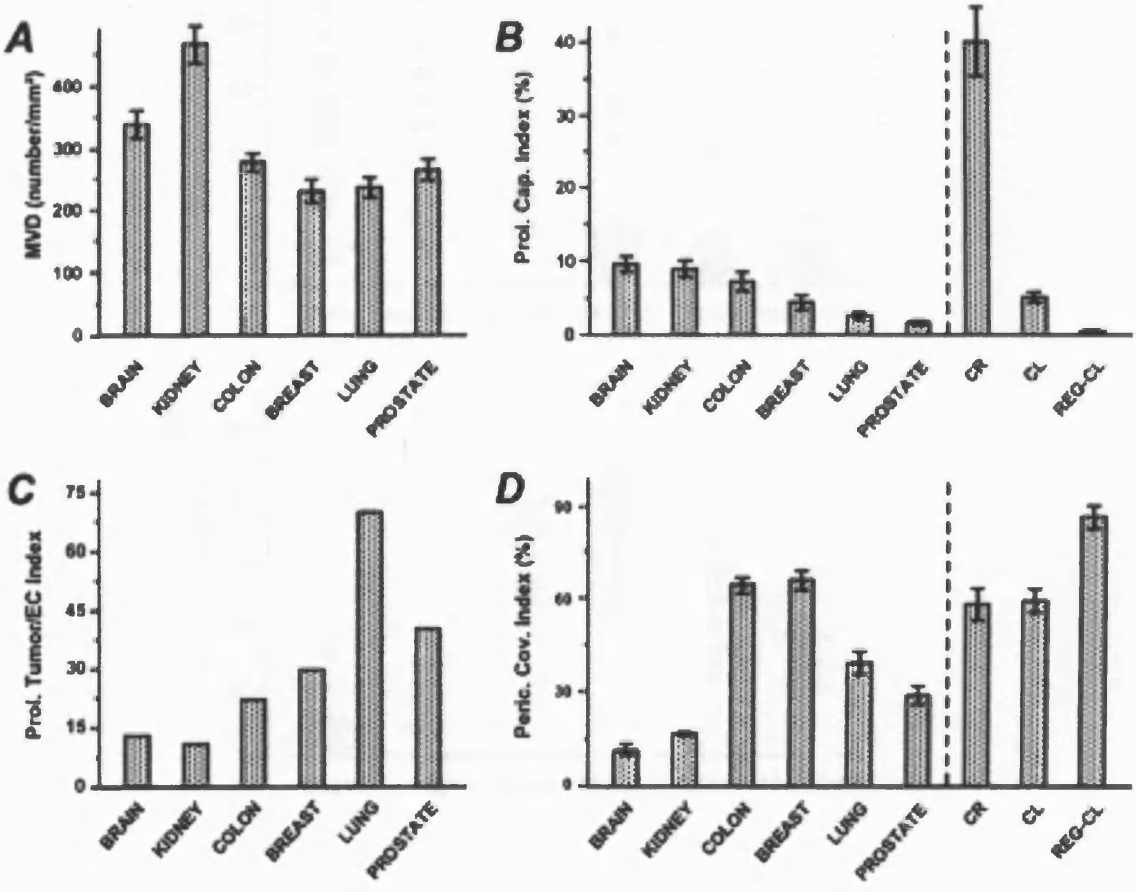

Figure 1.7. Endothelial cell proliferation and pericyte recruitment in individual malignant human tumours (*taken from Eberhard et al, 2000*)[133]

A. **Proliferating Capillary Index** (Prol. Cap. Index) in six different tumour types. Prol. Cap. Index in glioblastomas, renal cell carcinomas, and colon carcinomas vary over a wide range. In contrast, with few exceptions, mammary carcinomas, lung carcinomas, and prostate carcinomas have uniformly low Prol. Cap. Index values.

B. **Microvessel pericyte coverage index** (Peric. Cov. Index) in six different tumour types. These varied over a much smaller range than the Prol. Cap. Index

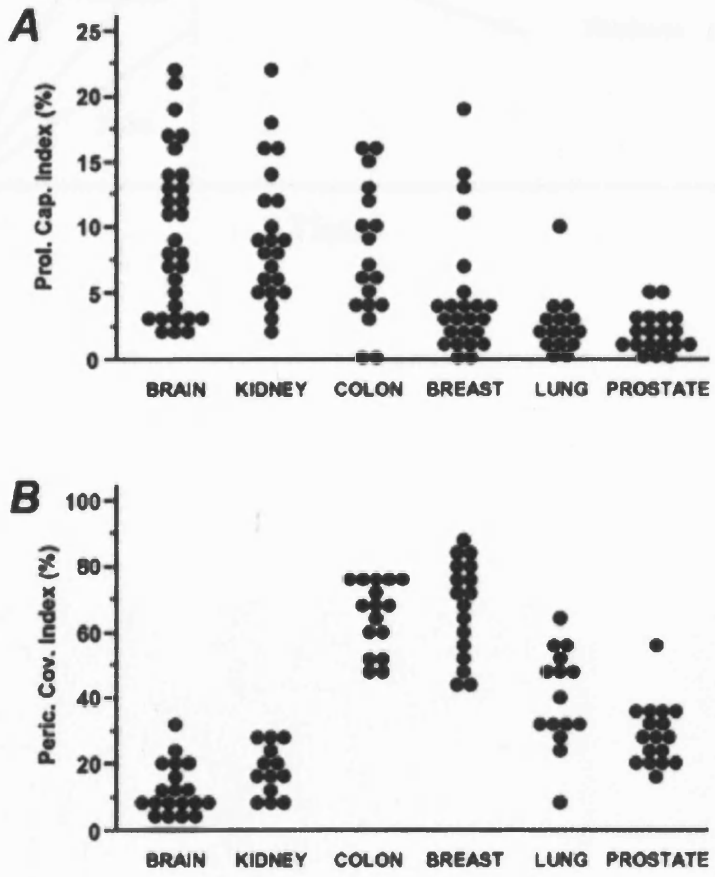

Figure 1.8. Stylized diagram illustrating classification of signal-intensity time curves in breast MRI. ***Modified from Schnall MD and Ikeda DM (1999)[288]***

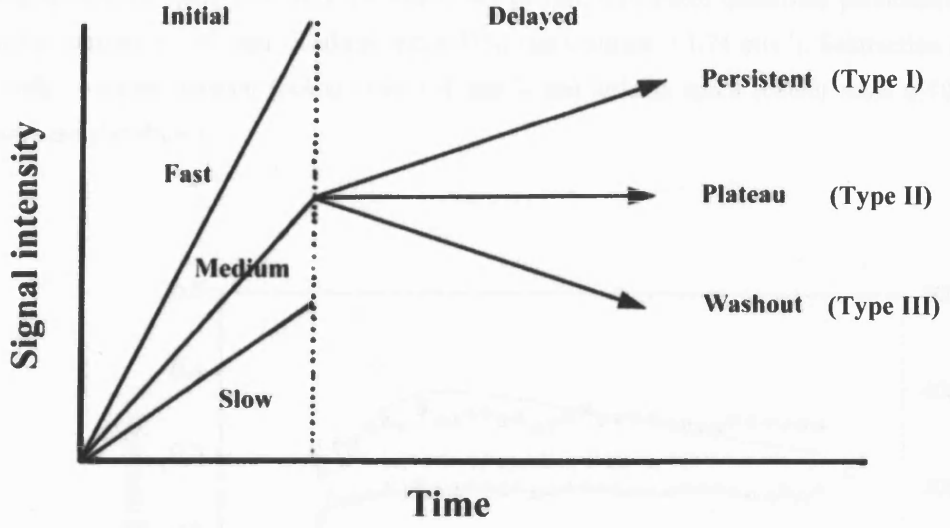

Figure 1.9. Converting signal intensity into contrast concentration & model fitting. Contrast medium injection (11 ml of Gd-DTPA) took place after the third data point. Quantification of time signal intensity data (Δ) from a ROI within the tumour into contrast agent concentration (•) is performed first according to the method described by Parker et al.[160]. The model fitting procedure (continuous line) is done using the Tofts' model [164]. Note that model fitting to contrast agent concentration data is not perfect. Calculated quantified parameters are transfer constant = 0.82 min^{-1}, leakage space 47%, rate constant = 1.74 min^{-1}). Subtraction (100 seconds), transfer constant (colour scale 0-1 min^{-1}) and leakage space (colour scale 0-100%) images are also shown.

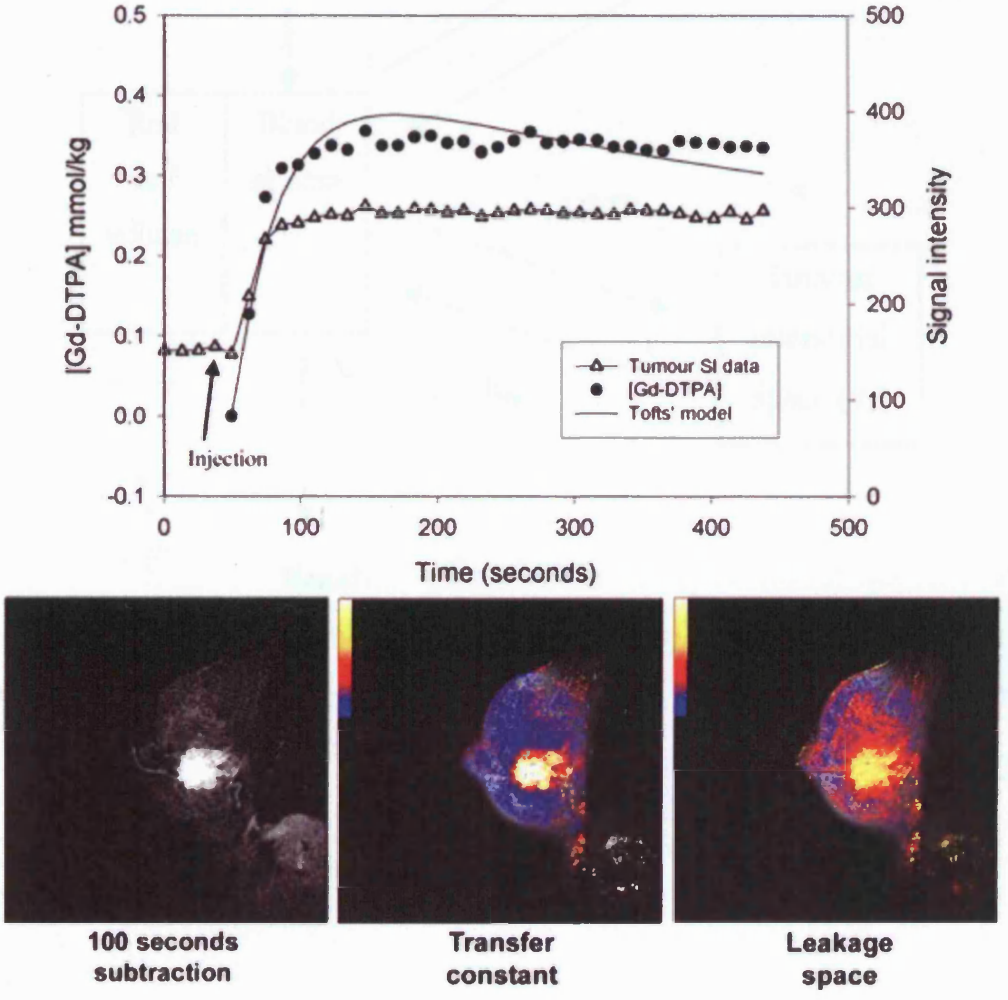

Figure 1.10. Tissue compartmental model of low molecular weight contrast medium kinetics

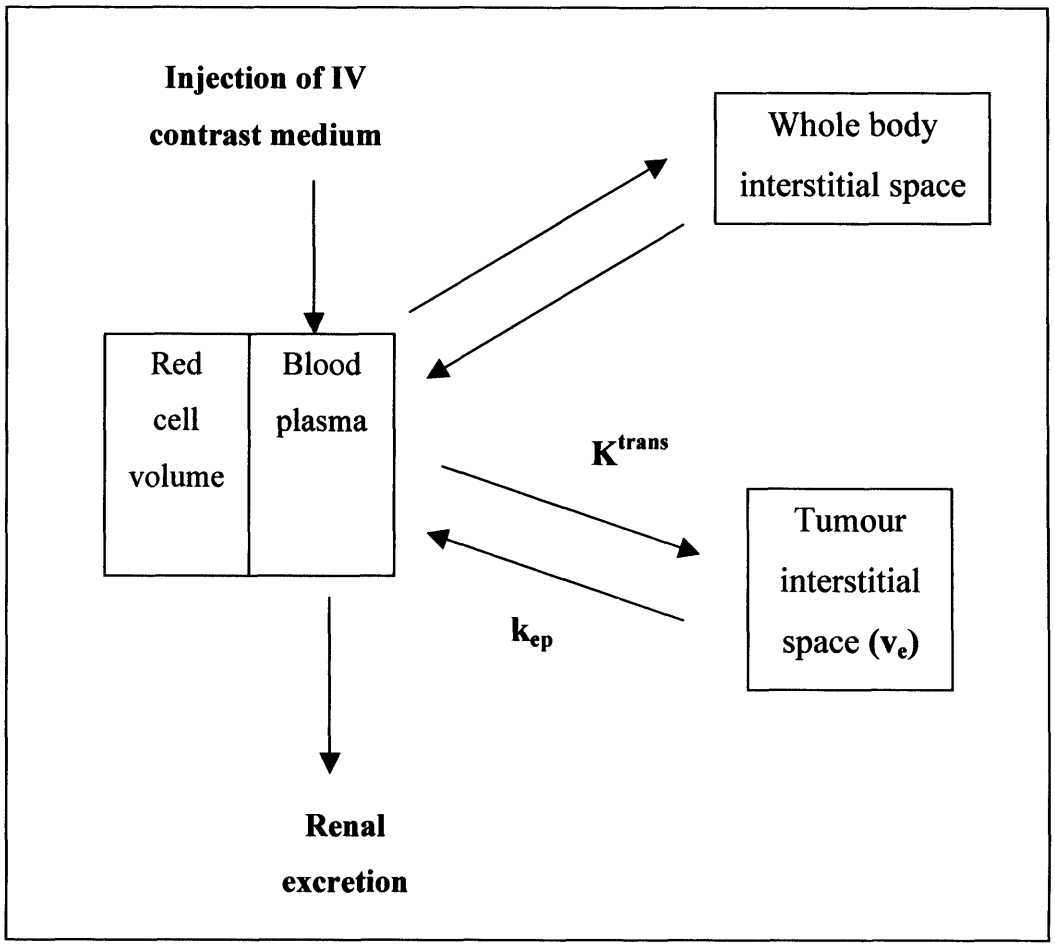

Figure 1.11. Carcinoma of unknown primary origin. 70 year old woman presenting with metastatic disease in right axillary lymph nodes consistent with breast origin and a normal mammogram (not shown). (A) Axial T_2-weighted image shows no significant abnormality. (B and C) T_1-weighted coronal images of the right breast before and after 0.2 mmol/kg Gd-DTPA given intravenously shows 3 focal areas of enhancement (arrows). (D) Subtraction image shows the enhancing lesions well. (E) Signal intensity time curves from regions of interest at the 9 o'clock (ROI-1) and 1 o'clock (ROI-2) show fast early enhancement and plateau and well as wash-out in the delayed phase. (F and G) follow-up examination (3 months later) following unsuccessful chemotherapy shows deterioration of appearances with widespread areas of abnormal enhancement.

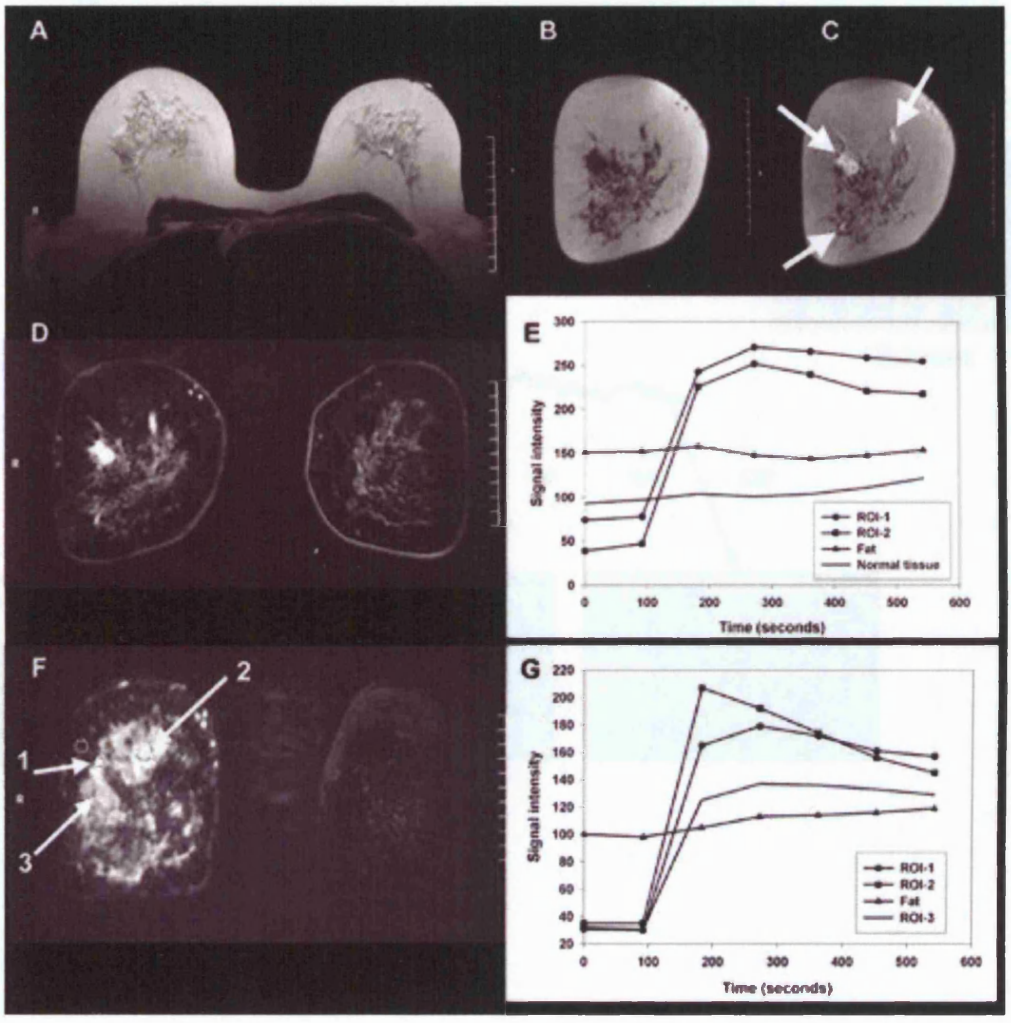

Figure 1.12. Typical T_2*-weighted DCE-MRI study. 30-year old woman with a grade 3 invasive ductal cancer of the right breast. 22 ml of IV contrast Gd-DTPA was given after the 10th data point (arrow). First pass T_2* susceptibility effects cause darkening of the tumour (arrows) (subtle but the effect is better appreciated in the subtraction image (insert)). No darkening of the breast parenchyma is seen. The first pass and recirculation phases are indicated. Signal intensity changes for 2 regions of interest are shown on the subtraction image of the nadir point for ROI corresponding to the tumour.

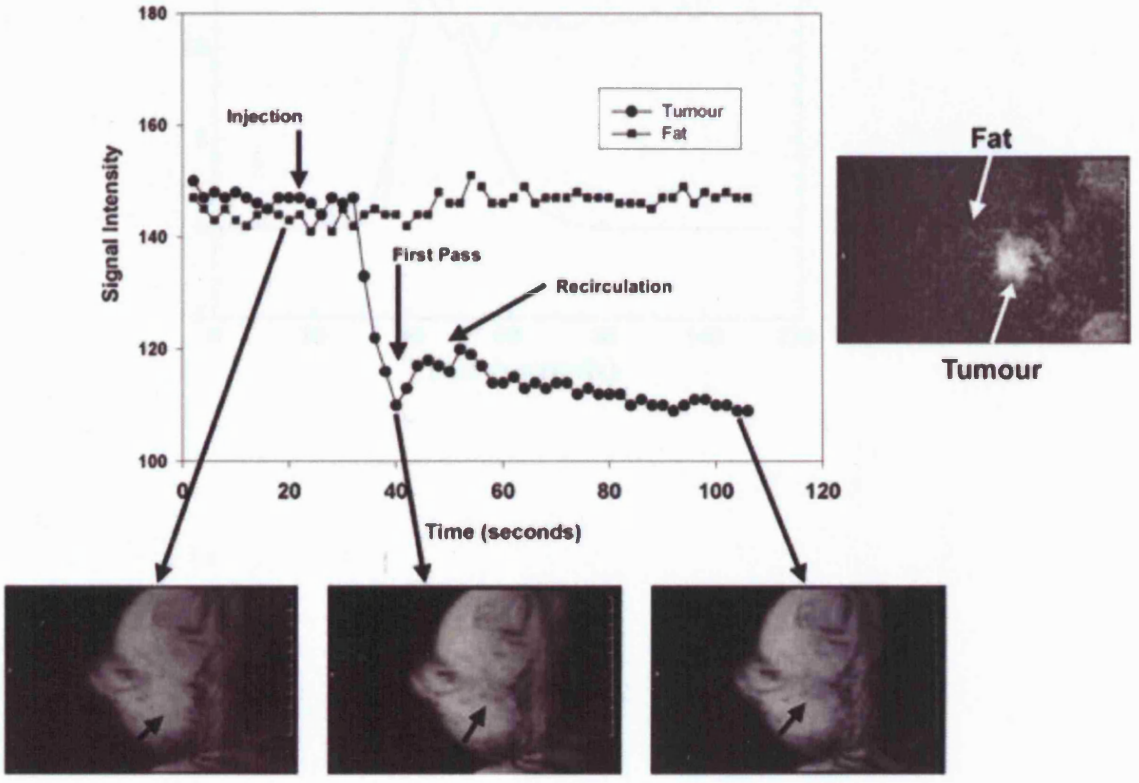

Figure 1.13. Model fitting of T2*-weighted data. T2* signal intensity data from the tumour ROI are converted into R_2* (1/T2*) and then fitted with a gamma variate function. The computed values of rBV, rBF and MTT for this region of interest are 265, 10.6 arbitrary units and 25.1 seconds. Parametric maps representing blood flow kinetics are shown in **figure 1.14.**

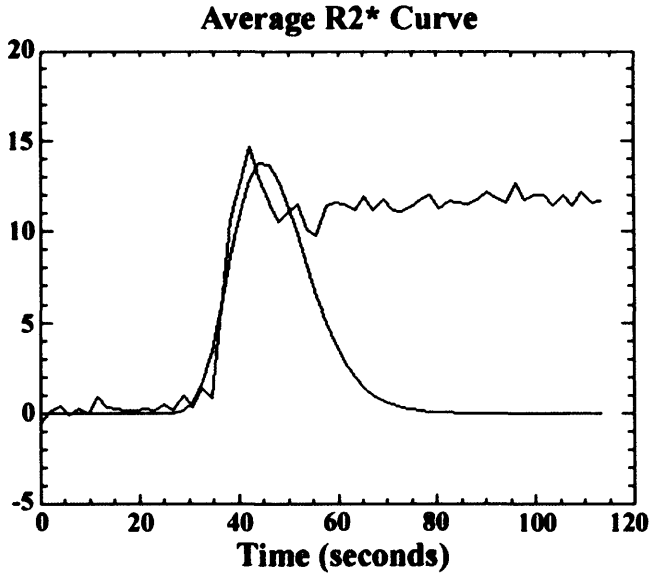

Figure 1.14. Parametric T_2*-weighted DCE-MRI images. Parametric images of relative blood volume (rBV), relative blood flow (rBF) and mean transit time (MTT) are derived on a pixel-by-pixel basis using gamma variate fitting as shown in **figure 1.13**. Also shown is the T2*-weighted DCE-MRI subtraction image. The graphs show how relative maximum signal drop (rMSD) is calculated and that there is a linear correlation between relative blood volume and flow at a pixel level within the tumour ROI.

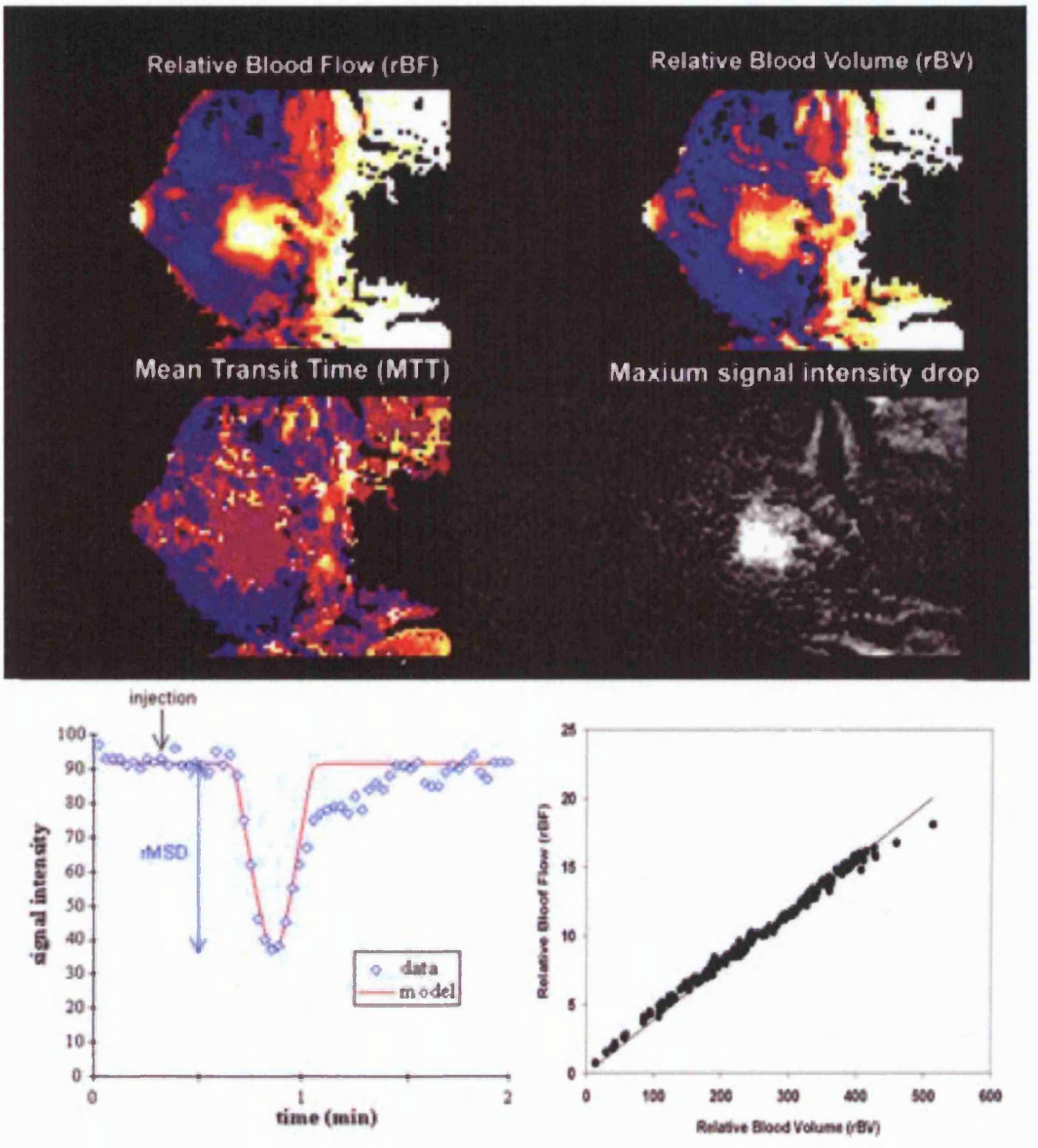

CHAPTER 2: EVALUATION OF THE EFFECT OF NEOADJUVANT CHEMOTHERAPY IN PRIMARY BREAST CANCER USING MULTI-PARAMETER FUNCTIONAL MRI

2.1 INTRODUCTION

The ability to identify early during treatment those women with primary breast cancer who will fail to respond to neoadjuvant chemotherapy would enable the use of alternative therapies that may be more effective [36]. Dynamic contrast medium-enhanced MRI (DCE-MRI) using gadolinium chelates provides a method for assessing and characterizing tumour microvasculature and provides both semi-quantitative and quantitative data which reflect tumour microvessel permeability and perfusion [149, 162]. Blood oxygen-level dependant (BOLD) MRI potentially provides a means of measuring tumour oxygenation by exploiting the different magnetic properties of oxyhaemoglobin and deoxyhaemoglobin [280].

This chapter describes the findings from a prospective study assessing multi-parameter functional MRI (DCE-MRI and BOLD-MRI) of the breasts in women receiving neoadjuvant chemotherapy for primary breast cancer (PBC) and addresses whether changes in the MRI-derived tumour microvascular characteristics and oxygenation, when measured early on in treatment, can predict for the final clinical and pathological response.

Thus, the aims of this study were:

- To assess the baseline functional MRI parameters in women with PBC and determine whether they correlate with the final clinical and pathological response to six cycles of FEC chemotherapy.

- To assess the changes in the functional MRI parameters in women with PBC following two cycles of neoadjuvant FEC chemotherapy and determine whether these changes correlate with the final clinical and pathological response to six cycles of FEC chemotherapy.

- To determine which functional MRI parameters are best able to predict

pathological non-responsive to treatment

- To determine the reproducibility of each functional MRI parameter and determine how much of a change would be statistically significant for an individual patient following 2 cycles of chemotherapy

- To consider how DCE-MRI could be used in a neoadjuvant chemotherapy paradigm with the aim of improving response rates

2.2 PATIENTS AND METHODS

2.2.1 PATIENTS AND TREATMENT

The study entitled " Evaluation of MRI during neoadjuvant chemotherapy in primary breast cancer" commenced at Mount Vernon Hospital, Northwood, Middlesex. U.K., in October 2001 following approval by the local research ethics committee (Mount Vernon and Watford Hospitals, protocol number EC2001-26). This was a prospective study aimed at evaluating the nature of the functional angiogenic response, as determined by Magnetic Reasonance Imaging, observed in women receiving neoadjuvant chemotherapy for primary breast cancer. Women with newly diagnosed non-metastatic histologically-proven breast cancer who were due to receive six cycles of neoadjuvant FEC chemotherapy (5-fluorouracil 600mg/m^2 intravenously [IV], epirubicin 60mg/m^2 IV and cyclophosphamide 600mg/m^2 IV every 21 days) were eligible for the study.

Between October 2001 and June 2003, 37 patients with primary breast cancer (T2-4bN0-3cM0 according to the tumour, node metastasis staging system 2002) were enrolled onto the study. Inclusion criteria were: (1) Histologically-proven primary breast cancer, (2) Age 18-70 years old (3) World Health Organisation (WHO) perfomance status 0 or 1 (appendix 2) [289], (4) Not lactating or pregnant, (5) No pre-exisiting condition which would deter the delivery of FEC chemotherapy (angina, congestive cardiac failure or recent myocardial

infarction), (6) Absolute neutrophil count >1.5 x 10^9/l and platelets >100 x 10^9/l, (7) written informed consent. Exclusion criteria were: (1) MRI scan contra-indicated (**appendix 3**) (2) known allergy to gadopentetate dimeglumine (Gd-DTPA).

Pre-treatment assessment included full clinical history and physical examination (with UICC 2002 TMN staging of the disease [**appendix 4**]); full blood count; urea and electrolytes; liver function tests; bilateral mammography; breast ultrasound; core biopsy +/- fine needle aspiration cytology of the primary breast tumour.

Prior to commencing FEC NAC, each patient underwent a baseline pre-treatment multi-parameter functional MRI scan (see section 2.23). Each patient then received two cycles of chemotherapy followed by a second MRI investigation prior to the third cycle of chemotherapy (estimated 6 weeks apart). Patients were assessed clinically prior to each cycle of chemotherapy and continued to a total of 6 cycles of FEC chemotherapy provided there was no evidence of clinically progressive disease (cPD) as defined by standard International Union Against Cancer criteria (see appendix 1). At completion of chemotherapy, patients were reassessed clinically and radiologically (mammography +/- ultrasound) and further treatment recommended according to the response to chemotherapy, the clinician's discretion and patient choice. Further treatment involved surgery to the breast (mastectomy or breast-conserving surgery) with or without axillary lymph node surgery, or, in some cases where a complete clinical and radiological response had been achieved, radiotherapy alone to the breast and ipsilateral axillary and supraclavicular fossa (SCF) lymph nodes. In those patients who received surgery, post-operative radiotherapy to the breast or chest wall with or without regional nodal irradiation was delivered according to the clinical oncologist's discretion and local protocol. Adjuvant hormonal therapy with tamoxifen (20mg daily for five years) was recommended for patients with oestrogen or progesterone receptor positive breast cancer. A summary of the treatment plan is shown in **table 2.1**. The patient information sheet and consent form are shown in **appendices 5 and 6.**

2.2.2 RESPONSE CRITERIA

2.2.2.1 Clinical response

Clinical response was evaluated from the bidimensional clinical measurements of the primary breast tumour prior to and following 6 cycles of FEC chemotherapy and was defined according to the UICC/WHO criteria [290, 291] as follows:

Complete Response (cCR)	Disappearance of all known disease
Partial Response (cPR)	Decrease by at least 50% of the sum of the products of the largest perpendicular diameters of measurable lesions
Stable disease (cSD)	Less than 50% decrease and less than 25% increase in the sum of the products of the largest perpendicular diameters of measurable lesions
Progressive disease (cPD)	Increase of more than 25% in the size of a measurable lesion or appearance of a new lesion

For the study analysis, clinical responders were defined as those patients with cCR or cPR. Clinical non-responders were defined as those patients with cSD or cPD. This classification was in accordance with other clinical studies [24, 36]. Those patients who progressed during neoadjuvant chemotherapy, such that a therapy change was instituted before completing six cycles of FEC chemotherapy, were defined as clinical non-responders (n=2).

2.2.2.2 Pathological response

Pathological response was evaluated by a single consultant pathologist (PIR) from a comparison of the pre-treatment core biopsy and the post-chemotherapy surgical resected specimen. Response was graded in accordance with previously described criteria [292-294]:

Pathological response	Description
Grade 1	No residual invasive cancer or DCIS (pathological CR)
Grade 2	Residual DCIS but no invasive cancer
Grade 3	Microscopic residual cancer
Grade 4	Macroscopic residual cancer with chemotherapy-induced changes and/or histological tumour response
Grade 5	Macroscopic invasive cancer with no response features

Chemotherapy-induced changes included (1) enlarged cells, (2) finely vacuolated "bubbly" voluminous cytoplasm, (3) enlarged vesicular nucleus with prominent single eosinophilic nucleolus, (4) occasionally enlarged hyperchromatic dense nucleus with an irregular outline, (5) compact hyalinized fibrous tissue at the site of good tumour response. Histological tumour response was an apparent reduction in tumour cell to stroma ratio. Examples of each grade of pathological response are shown in **figure 2.1**.

For the study analysis, pathological responders were defined as those patients with a grade 1, 2, 3 or 4 response. Pathological non-responders were defined as those patients with a grade 5 response. Those patients with a clinical & radiological CR who did not receive surgery but received radiotherapy alone were classified as pathological responders. Those patients with cSD or cPD who subsequently received alternative chemotherapy without surgery were classified as pathological non-responders.

2.2.3 MULTI-PARAMETER FUNCTIONAL MRI PROTOCOL

All MRI scans were performed at the Paul Strickland Scanner Centre, Mount Vernon Hospital, Northwood, Middlesex, UK. All patients were examined on a 1.5T Siemens Symphony scanner (Siemens AG, Munich, Germany) using a dedicated breast coil (**figure 2.2**). Quality assurance (QA) was performed daily on the MRI scanner with recalibration of the breast coil on T1W DCE-MRI

using the T1 phantom after every change in the system and every machine service (breast coil code determined). For the reproducibility cohort, each patient was imaged twice within 7 days thus ensuring the same breast coil code and minimal magnet changes.

Initial T1 and T2 weighted anatomical scans were performed in the sagittal plane to select an imaging plane through the centre of the tumour. For the BOLD-MRI, eight spoiled gradient-echo images of the central slice position were acquired with a range of different echo times (TE 5-75ms, TR 100ms, flip angle 40°, slice thickness 8mm, sagittal plane) and the rate of signal decay (R_2*=1/T2*) was calculated. A proton density weighted (PDW) image was acquired (TR 350 ms, TE 4.7 ms, flip angle 6°, central slice position, slice thickness 8mm). Dynamic T1-weighted images were acquired at a time resolution of 12 seconds for 40 measurements (TR 11 ms, TE 4.7 ms, flip angle 35°, slice thickness 8mm, sagittal plane, total imaging time 8 minutes 5 seconds) from 4 slices (3 through the tumour [middle slice corresponding to central slice position] and 1 through the contralateral normal breast). Gadopentetate dimeglumine (Gd-DTPA) was injected IV using a power injector (dose 0.1mmol/kg b.w.) at 4 ml/s during the fifth acquisition. Following this, a T2*-weighted DCE-MRI sequence was used to acquire data every 2 seconds over 2 minutes (TE=20ms, TR=30ms, flip angle=40°, single central slice position, slice thickness 8mm, sagittal plane, same slice position) with 0.2mmol/kg b.w. Gd-DTPA at 4ml/s after 20s (**figure 2.3**).

2.2.4 MRI IMAGE ANALYSIS

All calculations were performed pixel-by-pixel using custom analysis software called Magnetic Resonance Imaging Workbench (MRIW) which was developed at the Institute of Cancer Research, Royal Marsden Hospital, London, UK [295]. Analysis of the MRI data for each patient (both scans) was performed at the same sitting. For each scan, the tumour region of interest (ROI), defined as the contrast-enhancing region on early T1-weighted subtraction images (100 seconds), was drawn by one investigator (ARP) who was unaware of the patient's clinical and pathological details (figure 2.4). The spoiled gradient-echo

[FLASH] sequences were used to calculate the R_2* measurement using an IDL® least-squares fitting routine (**figure 2.5**).

Signal intensity on the T1-weighted images was converted to T1 relaxation rate values using the PDW image, in conjunction with a calibration experiment involving phantoms with known T1 relaxation rate values. Gd-DTPA concentration was calculated for each pixel during the dynamic acquisition from the equation:

$$C_t(t) = (1/T_1(t) - 1/T_1(0))/R_1$$

where $C_t(t)$ is the tissue Gd-DTPA concentration at time t after injection, $T_1(0)$ is the baseline tissue T_1, $T_1(t)$ is the T_1 at time t and R_1 is the longitudinal relaxivity of protons *in vivo* due to Gd-DTPA. The Gd-DTPA concentration-time curve was fitted to the Tofts and Kermode model [161] using methods previously described [296]. Semi-quantitative (mean gradient [MeanGrad], maximum signal amplitude [MaxAmp] and washout [Wt]) and quantitative (transfer constant [K^{trans}], leakage space [v_e], rate constant [k_{ep}], and maximum Gd-DTPA concentration [MaxGd]) kinetic parameters were calculated on the central slice through the tumour (figure 2.6). Using the same technique, data from all three slices through the tumour were analyzed and the quantitative T1-weighted kinetic parameters for the combined three-slice data (K^{trans}, v_e, k_{ep} and MaxGd) kinetic parameters were calculated.

The data from the T2* DCE-MRI (single central slice) were used to calculate relative blood volume (rBV), relative blood flow (rBF) and mean transit time (MTT) by fitting the time varying R_2* data to a gamma-variate function where, by the central volume theorem equation (figure 2.7):

$$BF = BV/MTT.$$

Using the single centre-slice data, the median and 5^{th}-95^{th} centile values for each parameter were derived from the whole tumour ROI for the pre-treatment and post-two cycles of FEC chemotherapy MRI scans, and the treatment changes

calculated. Using the three-slice data, the median value for the T1W quantitative kinetic parameters were derived from the combined whole tumour ROIs for the pre-treatment and post-two cycles of FEC chemotherapy MRI scans, and the treatment changes calculated.

All calculations were performed pixel-by-pixel within the tumour ROI with the exclusion of modelling failures. Modelling failures were either non-enhancing or enhancing. Non-enhancing modelling failures were defined as those pixels where MaxGad equalled zero. Enhancing modelling failures were defined as those pixels where K^{trans} was less than $0.01min^{-1}$ or greater than $5min^{-1}$, or when the MRIW's fitting alogorithm was unable to find a solution to the model for the data observed.

2.2.5 REPRODUCIBILITY COHORT

The study entitled " Evaluation of MRI during neoadjuvant chemotherapy in primary breast cancer" included a reproducibility arm where patients with primary breast cancer were imaged, as described above, twice within one week prior to commencing any therapy (either neoadjuvant chemotherapy or primary surgery). The data from this cohort were used to calculate the repeatability statistic for each parameter using the Bland & Altman methods [297]. 17 patients in total were recruited to this arm of the study.

2.2.6 NORMAL BREAST DATA

Single-slice dynamic T1W images were acquired from a random slice taken through the normal contralateral breast during each MRI scan. Using the methods described above, quantitative T1W kinetic parameters (K^{trans}, v_e, k_{ep} and MaxGd) were calculated for the pre-treatment and post-two cycles of FEC chemotherapy MRI scans from a randomly placed ROI. The treatment changes between the two scans were calculated.

2.3 STATISTICS

Statistical analysis was performed using the StatsDirect statistical software package (StatsDirect, Cheshire, UK). Pre-treatment MRI parameter values and MRI-derived tumour size were correlated using Spearman's rank correlation coefficient, Rho.

Pre-treatment parameter values and treatment changes were correlated with clinical and pathological response following 6 cycles of chemotherapy using the Mann-Whitney U-test (MW). The statistical significance was the 2-tailed p-value for rejecting the hypothesis of zero correlation.

The repeatability range for each parameter was calculated from the reproducibility cohort data using the methods of Bland and Altman [297]. The 95% confidence interval is the key statistical parameter that is be used to determine whether a change in a kinetic parameter following treatment is statistically significant or not for one or several patients. For each patient in the reproducibility cohort, the difference (d) between the two pre-treatment measurements of a parameter was calculated. Data was transformed using natural logarithmns if the variability of d was found to depend on its mean value (a significant two-tailed Kendall's tau test). The square root of the mean squared difference, dsd, ($=\sqrt{[(\Sigma d^{2})/n]}$ where n is the number of patients) was then calculated. The 95% confidence interval for change for a group of n patients is then equal to $\pm(1.96 \times dsd)/\sqrt{n}$). For an individual patient, n=1, so the 95% confidence interval for change is equal to $\pm(1.96 \times dsd)$. This is known as the repeatability statistic, r, and is expressed as a percentage of the group mean pre-treatment value for each parameter. It provides a range within which the difference between pre and post-treatment values would be expected to lie for 95% of observations, assuming that no difference exists between the pre-treatment and the post-treatment values. Thus, following the application of the repeatability statistic to an individual patient's data, if the difference (d) falls outside this range then a significant change is deemed to have occurred. The

repeatability range for each parameter was calculated to determine how much of a change would be statistically significant for a single patient (n=1).

Receiver operating characteristic (ROC) curve analysis was used to determine which parameters best predicted for pathological non-response. Area under the ROC curve (AUC), sensitivity and specificity for each parameter was calculated.

Spearman's rank correlation coefficient, Rho, was used to compare the parameter values derived using single centre-slice data and three-slice data. MedCalc Software (MedCalc, Mariakerke, Belgium) was used to compare ROC analysis using single centre-slice data and three-slice data.

2.4 RESULTS

2.4.1 PATIENT CHARACTERISTICS AND TUMOUR RESPONSE

37 patients were recruited into the study. Nine patients were not evaluable. This was a result of either failure to undergo both MRI scans (four patients were unable to tolerate the first MRI scan due to discomfort, nausea or claustrophobia; one was unable to fit in the scanner due to body habitus) or failure to have the second MRI at the specified time point (one patient declined the second scan due to a previous experience of nausea and vomiting; one was unable to undergo the second scan due to exacerbation of unrelated back pain; two patients underwent the second MRI scan following 3 cycles of chemotherapy).

Thus there were 28 evaluable patients in total. The 28 evaluable patients underwent a multi-parameter functional MRI scan prior to and following two cycles of neoadjuvant FEC chemotherapy. The median time between scans was 42 days (range 34 – 49 days) and the median time from first MRI scan to first cycle of FEC chemotherapy was 2 days (range 0–10 days).

The median age of the 28 evaluable patients was 46 years old (range 29–70 years). The median number of cycles of neoadjuvant FEC chemotherapy received was 6 (range 2-7). Seventeen patients were pre-menopausal and 11 were postmenopausal. Details of the clinical stage of disease at diagnosis, tumour pathology, treatment administered and response to treatment (clinical and pathological) are shown in **table 2.2**. In two patients (patient numbers 6 and 16), chemotherapy was changed prior to surgical assessment and these patients were therefore classified as pathological non-responders. Of note, patient number 16 was found to have metastatic liver disease following the first MRI scan but was included in the analysis. Two patients (patient numbers 28 and 29) achieved a clinical and radiological (on mammography and ultrasound) CR and received radical radiotherapy to the breast and nodal areas alone (axilla and SCF) without surgery. These patients were classified as pathological responders.

One patient (patient number 11) obtained a clinical CR with a radiological PR and received radical radiotherapy to the breast and nodal areas alone. Prior to radiotherapy, this patient underwent a post-chemotherapy biopsy of the residual radiological abnormality which revealed a grade 3 pathological response. This patient was therefore classified as a pathological responder.

Thus, of the 28 evaluable patients, there were 19 clinical responders and 9 clinical non-responders, giving an overall clinical response rate of 68%. There were 11 pathological responders and 17 pathological non-responders giving an overall pathological response rate of 39%. Twenty-two patients completed all six cycles of FEC chemotherapy and proceeded to surgery. Of these 22, only one patient achieved a pathological CR, giving a pCR rate of 4.5%.

2.4.2 SINGLE CENTRE-SLICE DATA

The median values for each MRI-derived kinetic parameter was calculated using Microsoft Excel. The 5^{th}-95^{th} centile range was calculated for the T1W semiquantitative and quantitative parameters and the T2*W quantitative parameters. The parameters evaluated were:

1. T1W semi-quantitative parameters:

(i) Mean gradient (MeanGrad)(AU)

(ii) Maximum signal amplitude (MaxAmp)(%)

(iii) Washout (Wt)(AU)

2. T1W quantitative parameters:

(i) Transfer constant (K^{trans})(min^{-1})

(ii) Leakage space (v_e)(%)

(iii) Rate constant (k_{ep})(min^{-1})

(iv) Maximum Gd-DTPA concentration (MaxGd)(mmol/kg)

3. T2*W quantitative parameters:

(i) Relative blood volume (rBV)

(ii) Relative blood flow (rBF)

(iii) Mean transit time (MTT)(sec)

4. BOLD-MRI quantitative parameter, R_2* (sec^{-1}).

The parameter values from the pre-treatment and post-two cycles of FEC chemotherapy MRI scans were derived and the treatment changes in the median and 5^{th}-95^{th} centile range were calculated. The 5^{th}-95^{th} centile range was the 5^{th} centile parameter value subtracted from the 95^{th} centile parameter value. The MRI-defined tumour size (product of the bi-dimensional mesurements of the contrast-enhancing ROI on early T1W subtraction images [100seconds] in the sagittal plane) was also determined at each scan and the change in size following 2 cycles FEC chemotherapy was calculated.

2.4.2.1 Pre-treatment parameter data

No correlation was found between the pre-treatment MRI-defined tumour size and the pre-treatment median values for any of the functional MRI parameters: MeanGrad, Rho=-0.07, p=0.74; MaxAmp, Rho=0, p=1.00; Wt, Rho=0.24, p=0.22; K^{trans}, Rho=-0.3, p=0.12; v_e, Rho=0.02, p=0.94; k_{ep}, Rho=-0.22, p=0.27; MaxGd, Rho=0.01, p=0.98; rBV, Rho=-0.06, p=0.76; rBF, Rho=0.01, p=0.97; MTT, Rho=-0.09, p=0.65; and R_2*, Rho=-0.08, p=0.71.

Primary breast tumours that demonstrated an overall clinical response after chemotherapy had the following median pre-treatment parameter values: MRI-defined tumour size, 13.2cm^2; MeanGrad, 40.7AU; MaxAmp, 81%; Wt, -0.24AU; K^{trans}, 0.61min^{-1}; v_e, 54%; k_{ep}, 1.08min^{-1}; MaxGd, 0.41mmol/kg; rBV, 150; rBF 5.3; MTT, 24.1sec; and R_2*, 33.1sec^{-1}. These values were not significantly different to those for tumours that did not demonstrate a clinical response: MRI-defined tumour size, 17.9cm^2; MeanGrad, 29.2AU; MaxAmp, 92%; Wt, –0.20AU; K^{trans}, 0.57min^{-1}; v_e, 52%; k_{ep}, 1.04min^{-1}; MaxGd, 0.43mmol/kg; rBV, 191; rBF 8.2; MTT, 23.4sec; and R_2*, 31.9sec^{-1} (MW, p>0.05 for all groups). These values are shown in **table 2.3**.

The median pre-treatment parameter values from primary breast tumours that demonstrated an overall pathological response were: MRI-defined tumour size, 13.2cm^2; MeanGrad, 40.7AU; MaxAmp, 95%; Wt, –0.24AU; K^{trans}, 0.66min^{-1}; v_e, 57%; k_{ep}, 1.19min^{-1}; MaxGd, 0.45mmol/kg; rBV, 177; rBF 6.89; MTT, 24.5sec; and R_2*, 32.7sec^{-1}. These values did not differ significantly to those seen in tumours that failed to demonstrate a pathological response: MRI-defined tumour size, 13.1 cm^2; MeanGrad, 38.2AU; MaxAmp, 87%; Wt, –0.23AU; K^{trans}, 0.57min^{-1}; v_e, 52%; k_{ep}, 1.04min^{-1}; MaxGd, 0.39mmol/kg; rBV, 150; rBF 5.3; MTT, 23.4sec; and R_2*, 33.7sec^{-1} (MW, $p>0.05$ for all groups). These results are shown in **table 2.4.**

Analysis of the 5th-95th centile range data revealed no significant difference in pre-treatment values for clinical or pathological responders and non-responders (MW, $p>0.05$ for all groups). These results are shown in **table 2.5 and table 2.6.**

Thus, pre-treatment median parameter values, 5th-95th centile range and tumour size failed to predict for final clinical or pathological response to neoadjuvant FEC chemotherapy.

2.4.2.2 Parameter changes compared with tumour response

In general, a reduction in the semi-quantitative and quantitative kinetic parameters reflecting tumour vessel permeability and perfusion was seen following 2 cycles of NAC in primary breast tumours that subsequently demonstrated a clinical or pathological response following completion of NAC. **Figure 2.8** shows an example of the pre-treatment and post 2 cycles of FEC chemotherapy MRI images (anatomical and functional parametric maps) from patient number 29 who had a responding tumour.

In general, no significant change or an increase in tumour vessel permeability and perfusion kinetic parameters was observed in those tumours that subsequently failed to demonstrate a clinical or pathological response to NAC. **Figure 2.9** shows an example of the pre-treatment and post 2 cycles of FEC

chemotherapy MRI images (anatomical and functional parametric maps) from patient number 20 who had a non-responding tumour.

No trend was seen in the BOLD MRI parameter, R_2*, that predicted for response.

Statistical analysis of the 28 patient data revealed that change in median MeanGrad, MaxAmp, K^{trans}, k_{ep}, rBV and rBF significantly correlated with **clinical response** to NAC (MW, $p<0.05$ for all groups). In responding tumours, there was a **reduction** in the median kinetic parameter values as follows: MeanGrad, 47.7%; MaxAmp, 11.5%; K^{trans}, 29.6%; k_{ep}, 31.2%; rBV, 59.3%; and rBF, 56.4%. In non-responding tumours there was an **increase** in the median kinetic parameter values as follows: MeanGrad, 4.9%; MaxAmp, 7.1%; K^{trans}, 16.8%; k_{ep}, 5.5%; rBV, 73.4%; and rBF, 70.6%. These results are shown in **table 2.7** and **figure 2.10**.

Statistical analysis of the 28 patient data demonstrated that change in median MeanGrad, MaxAmp, K^{trans}, k_{ep}, MaxGd, rBV and rBF also significantly correlated with final **pathological response** to NAC (MW, $p<0.05$ for all groups). In those tumours that demonstrated a pathological response, there was a **reduction** in the median kinetic parameter values as follows: MeanGrad, 67.0%; MaxAmp, 25.2%; K^{trans}, 49.5%; k_{ep}, 45.4%; MaxGd, 17.0%; rBV, 61.1%; and rBF, 63.4%. In the pathologically non-responding tumours there was **a minor reduction or an increase** in the median kinetic parameter values as follows: MeanGrad, –2.4%; MaxAmp, 11.9%; K^{trans}, 3.5%; k_{ep}, -4.8%; MaxGd, 7.8; rBV, -2.4%; and rBF, -3.5%. These results are shown in **table 2.8** and **figure 2.11**.

Change in the 5-95th centile range for MeanGrad, Max Amp, K^{trans}, k_{ep}, MaxGad, rBV and rBF significantly correlated with both clinical and pathological response to treatment (MW, $p<0.05$ for all groups). In addition, change in the 5-95th centile range for MTT was significant for final pathological response to NAC (MW, $p<0.05$). In the clinically responding tumours, there

was a **reduction** in the 5^{th}-95^{th} centile range of the kinetic parameters as follows: MeanGrad, 58.1%; MaxAmp, 13.1%; K^{trans}, 31.4%; k_{ep}, 37.0%; MaxGd, 7.3%; rBV, 40.5%; and rBF, 36.7%. In clinically non-responding tumours, there was an **increase** in the 5^{th}-95^{th} centile range of the kinetic parameters as follows: MeanGrad, 14.3%; MaxAmp, 14.1%; K^{trans}, 19.7%; k_{ep}, 12.9%; MaxGd, 13.2%; rBV, 53.2%; and rBF, 53.9%. These results are shown in **table 2.9** and **figure 2.12**. In the pathologically responding tumours, there was a **reduction** in the 5^{th}-95^{th} centile range of the kinetic parameters as follows: MeanGrad, 61.2%; MaxAmp, 15.2%; K^{trans}, 58.9%; k_{ep}, 45.3%; MaxGd, 11.1%; rBV, 62.1%; and rBF, 57.9%. This was associated with an increase in the 5^{th}-95^{th} centile range of MTT of 18.5%. In the pathologically non-responding tumours, there was a **minor reduction or an increase** in the 5^{th}-95^{th} centile range of the kinetic parameters as follows: MeanGrad, -7.1%; MaxAmp, 11.9%; K^{trans}, 18.7%; k_{ep}, 12.4%; MaxGd, 13.2%; rBV, -0.7%; and rBF, 3.6%. This was associated with a **reduction** in the 5^{th}-95^{th} centile range of MTT of 19.3%. These results are shown in **table 2.10** and **figure 2.13**.

Assessment of the change in MRI-derived tumour size following 2 cycles of NAC demonstrated a reduction in tumour size in all response groups. In clinically responding tumours, there was a reduction of 32.8% compared to a reduction of 13% in clinically non-responding tumours. This difference was statistically significant (MW, $p<0.05$). In the tumours than demonstrated a final pathological response, there was a reduction in MRI-derived tumours size of 35.5% compared with 14.8% in pathological non-responders. This difference was not statistically significant (MW, $p=0.11$). These results are shown in **table 2.7 & 2.8** and **figures 2.10 & 2.11.**

Change in the median Wt, v_e, MaxGd and MTT, and change in 5^{th}-95^{th} centile range for Wt, v_e and MTT did not correlate with final clinical response. Change in the median Wt, v_e and MTT, and change in 5^{th}-95^{th} centile range for Wt and v_e did not correlate with final pathological response (**table 2.9 & 2.10** and **figures 2.13 & 2.13**).

For the BOLD MRI parameter, R_2*, a 12.9% increase in the median R_2* was observed in clinical responders compared to an increase of 0.7% in clinical non-responders. This difference was not statistically significant (MW, p=0.2). For pathological responders, median R_2* increased by 16.3% compared with a reduction of 1.5% in pathological non-responders. This difference was not statistically significant (MW, p=0.1) (**table 2.7 & 2.8** and **figures 2.10 & 2.11**).

2.4.2.3 Receiver operating characteristic (ROC) curve analysis

ROC curve analysis was used to determine which parameters best predicted for pathological non-response. This revealed the best parameters to be: K^{trans}, AUC=0.83 (sensitivity 100%, specificity 73%); k_{ep}, AUC=0.82 (sensitivity 88%, specificity 73%); rBF, AUC=0.83 (sensitivity 81%, specificity 80%); and MaxAmp, AUC=0.87 (sensitivity 100%, specificity 82%). The results of the ROC curve analysis according to the MRI sequence are shown in **table 2.11** and **figure 2.14**.

2.4.3 THREE-SLICE T1W QUANTITATIVE DATA

The median values for each parameter from the three-slice analysis was calculated using Microsoft Excel. The parameters evaluated were:

(i) Transfer constant (K^{trans})(min^{-1})
(ii) Leakage space (v_e)(%)
(iii) Rate constant (k_{ep})(min^{-1})
(iv) Maximum Gd-DTPA concentration (MaxGd)(mmol/kg)

The parameter values from the pre-treatment and post-two cycles of FEC chemotherapy MRI scans were derived and the treatment changes in the median were calculated.

2.4.3.1 Pre-treatment parameter data

No correlation existed between the pre-treatment MRI-defined tumour size and the pre-treatment median values for any of the MRI parameters: K^{trans}, Rho=-0.16, p=0.41; v_e, Rho=0.03, p=0.87; k_{ep}, Rho=-0.21, p=0.29; MaxGd, Rho=0.02, p=0.93.

Primary breast tumours that demonstrated an overall clinical response after chemotherapy had the following median pre-treatment parameter values: K^{trans}, 0.56min^{-1}; v_e, 51%; k_{ep}, 1.05min^{-1}; MaxGd, 0.41mmol/kg. These values were not significantly different to those for tumours that did not demonstrate a clinical response: K^{trans}, 0.58min^{-1}; v_e, 49%; k_{ep}, 1.03min^{-1}; MaxGd, 0.40mmol/kg (MW, p>0.05 for all groups). These values are shown in **table 2.12**.

The median pre-treatment parameter values in primary breast tumours that demonstrated an overall pathological response were: K^{trans}, 0.57min^{-1}; v_e, 54%; k_{ep}, 1.25min^{-1}; MaxGd, 0.45mmol/kg. These values did not differ significantly to those seen in tumours that failed to demonstrate a pathological response: K^{trans}, 0.55min^{-1}; v_e, 49%; k_{ep}, 1.03min^{-1}; MaxGd, 0.37mmol/kg (MW, p>0.05 for all groups). These results are shown in **table 2.13**.

2.4.3.2 Parameter changes compared with tumour response

Analysis of the 28 patient data revealed that change in median K^{trans}, k_{ep} and MaxGd significantly correlated with clinical response to NAC (MW, p<0.05 for all groups). In responding tumours, there was a **reduction** in the median kinetic parameter values as follows: K^{trans}, 39.8%; k_{ep}, 33.3%; and MaxGd, 0.8%. In non-responding tumours there was an **increase** in the median kinetic parameter values as follows: K^{trans}, 18.1%; k_{ep}, 7.4%; and MaxGd, 8.3%. These results are shown in **table 2.14** and **figure 2.15**.

Change in median K^{trans}, k_{ep} and MaxGd significantly correlated with final pathological response to NAC (MW, p<0.005 for all groups). In those tumours that demonstrated a pathological response, there was a **reduction** in the median kinetic parameter values as follows: K^{trans}, 52.3%; k_{ep}, 50.3%; and MaxGad, 13.0%. In the pathologically non-responding tumours there was **a minor**

reduction or an increase in the median kinetic parameter values as follows: K^{trans}, 16.9%; k_{ep}, -8.5%; and MaxGd, 6.3%. Change in median v_e did not correlate with responsiveness when assessed using 3-slice data. These results are shown in **table 2.15** and **figure 2.16**.

2.4.4 COMPARISON OF SINGLE CENTRE-SLICE VERSUS THREE-SLICE DATA

The relative utility of multi-slice (three-slice) versus single centre-slice T1W DCE-MRI for predicting final pathological response to NAC in patients with primary breast cancer was assessed.

Median quantitative parameter values (K^{trans}, v_e, k_{ep} and MaxGd) before and after 2 cycles of treatment were compared for the single centre-slice and 3-slice analysis using Spearman's rank correlation coefficient. This revealed a good correlation between the values for single centre-slice and 3-slice evaluations for all parameters (Rho>0.8, p<0.001 for all groups). The correlation for pre-treatment median K^{trans} is shown in **figure 2.17**. Median percentage change after 2 cycles of NAC for single centre-slice and 3-slice evaluations for all parameters also demonstrated a good correlation (Rho>0.8, p<0.001 for all groups). The correlation for percentage change in median K^{trans} is shown in **figure 2.18**.

Using ROC curve analysis, the predictive performance of the different kinetic parameters for determining pathological response from the 3-slice data was assessed (**figure 2.19**). This demonstrated change in median K^{trans} to be the best parameter for predicting response with an AUC=0.93 (sensitivity 94%, specificity 80%). The 3-slice K^{trans} demonstrated significantly better test performance compared to single centre-slice only evaluation: AUC 0.93 (sensitivity 88%, specificity 82%) versus AUC 0.83 (sensitivity 100%, specificity 73%), p=0.02) (**table 2.16**).

2.4.5 REPRODUCIBILITY DATA

The clinical utility of centre-slice versus 3-slice evaluations was further assessed by the application of the repeatability range for each parameter to predict pathological non-response on an individual basis.

2.4.5.1 Reproducibility cohort

Seventeen patients were recruited into the reproducibility arm of the MRI study. Two patients were unable to tolerate the first scan; two patients did not undergo the second scan (one declined and one underwent a repeat breast biopsy prior to the second scan and was therefore excluded); and one patient had metastatic axillary lymph nodes with no primary breast lesion and was therefore excluded. Thus, twelve patients with primary breast cancer were imaged twice within one week (median 1 day, range 1-7 days) prior to commencement of therapy. Of these 12 patients, 9 subsequently received NAC and 3 underwent primary surgery. The median age of the reproducibility cohort was 53 years old (range 37-62 years). The patient characteristics are shown in **table 2.17**. Histograms demonstrating the median values obtained for each parameter for each patient on the two reproducibility MRI examinations are shown in **figure 2.20**.

2.4.5.2 Repeatability Statistics

Using the Bland and Altman methods [297], the repeatability statistics were calculated for each parameter for single centre-slice and three-slice analysis (**table 2.18**). The repeatability range represents the range outside which a change would be required following an intervention, in this study two cycles of NAC, for that change to be deemed a 'true' or statistically significant change due to the intervention. The repeatability range for each parameter was calculated to determine how much of a change would be statistically significant for a single patient (n=1).

For the single centre-slice analysis, the repeatability range for each parameter, expressed as percentage change of the mean, was as follows: MeanGrad, -62.3 to 165.0%; MaxAmp, +/- 28.0%; K^{trans}, -51.3 to 105.3%; ve, +/- 17.5%; k_{ep}, -47.8 to 91.7%; MaxGd, +/- 18.7%; rBV, +/- 74.9%; rBF, +/- 63.9%; MTT, +/-

22.1%; and R2*, +/- 17.5%. The repeatability range for MRI-derived tumour size expressed as percentage change of the mean was –26.5 to 36.1% (**table 2.18**).

For the three-slice analysis, the repeatability range for each parameter, expressed as percentage change of the mean, was as follows: K^{trans}, -42.4 to 73.6%; ve, +/- 29.9%; k_{ep}, -57.8 to 136.8%; and MaxGd, +/- 18.8% (**table 2.18**).

Application of the repeatability range to the clinical data revealed change in K^{trans} as evaluated on the three-slice data was the best predictor of pathological response correctly predicting pathological non-response in 16 of 17 patients (94%) (figure 2.21) and response in 8 of 11 patients (73%) (**figure 2.22**). **Table 2.18** shows patient pathological response classification according to functional MRI parameters and MRI-derived tumour size.

2.4.6 NORMAL BREAST DATA

For the 28 evaluable patients, the median value for each parameter from the single-slice analysis of the normal contralateral breast was calculated using Microsoft Excel. The parameters evaluated were:

(i) Transfer constant (K^{trans})(min^{-1})
(ii) Leakage space (v_e)(%)
(iii) Rate constant (k_{ep})(min^{-1})
(iv) Maximum Gd-DTPA concentration (MaxGd)(mmol/kg)

The parameter values from the pre-treatment and post-two cycles of FEC chemotherapy MRI scans were derived and the treatment changes in the median were calculated.

The pre-treatment median parameter values were lower in the normal breast tissue compared with the tumour ROI (**figure 2.23**) and there was no correlation between the values from the normal breast tissue and the tumour ROI (**table 2.19**).

Neither the pre-treatment parameter values nor the change in median parameter values in the normal breast following two cycles of NAC predicted for clinical or pathological response to NAC for any of the quantitative parameters assessed (**tables 2.20, 2.21, 2.22** and **2.23**).

2.5 DISCUSSION

The ability to identify early during treatment those women with primary breast cancer who will fail to respond to neoadjuvant chemotherapy would enable the use of alternative therapies that may be more effective [36]. In the clinic, response to NAC is currently assessed using the combination of clinical examination and conventional imaging techniques, such as mammography and breast ultrasound. These methods rely on a change in tumour size for assessing response which often becomes apparent only after several cycles of chemotherapy. Further, these methods can fail to accurately assess the pathological extent of residual tumour [230]. As a result, newer functional imaging techniques are being evaluated for their ability to classify tumour response earlier on in treatment and hence facilitate the tailoring of treatment to individual response. These techniques include PET and multi-parameter functional MRI. Other approaches currently under evalution have evolved from the recent advances in molecular biology and focus on the identification of predictive markers of response. These include the use of immunohistochemistry to assess, for example, markers of proliferation, and microarray technology to identify chemotherapy response genes.

In this study, we evaluated the role of multi-parameter functional MRI during NAC for PBC, using the techniques of:

(1) T1W and T2*W dynamic-contrast enhanced MRI (DCE-MRI), employing the low molecular weight contrast agent, Gd-DTPA, and

(2) Blood Oxygen Level Dependant MRI (BOLD MRI), which employs dexoyhaemoglobin as an intrinsic contrast agent.

DCE-MRI provides a non-invasive imaging method for assessing the tumour microvasculature and in particular, informs upon microvessel permeability and perfusion. BOLD-MRI has been shown to inform upon tumour oxygenation by

exploiting the different magnetic properties of oxyhaemoglobin and deoxyhaemoglobin.

The baseline pre-treatment kinetic parameter values did not correlate with the pre-treatment MRI-derived tumour size and were therefore not dependent on the presenting tumour size. Analysis according to clinical and pathological response also demonstrated no relationship between the baseline parameter values and tumour response to NAC. Thus, the pre-treatment MRI-derived functional vascular characteristics of primary breast cancer are not influenced by tumour size and do not inform upon clinico-pathological response to anthracycline-based neoadjuvant chemotherapy.

The changes seen in the kinetic parameter values from baseline following 2 cycles of neoadjuvant FEC chemotherapy did, however, inform upon final clinico-pathological response to treatment. Group analysis of the 28 evaluable patients demonstrated that the changes seen in the T1W and T2*W DCE-MRI parameters reflecting tumour microvessel permeability and perfusion (Mean Grad, MaxAmp, K^{trans}, k_{ep}, rBV and rBF) were significantly different between both the clinically and pathologically responding tumours and the non-responding tumours. In the responding groups, an overall reduction in these kinetic parameter values was seen, both in terms of the median values and the 5^{th} to 95^{th} centile range, compared with only a minor reduction or an increase the non-responding groups.

In terms of tumour size, the early change in MRI-derived tumour size was found to correlate with final clinical response but not with final pathological response. This is of particular note as the conventional imaging methods currently employed for assessing tumour response (mammography and ultrasonography) rely on changes in tumour size. Von Minckwitz et al. recently found that clinical response after 2 cycles of NAC could predict for pCR [45]. Unfortunately, we were unable to assess this finding in our patient cohort due to incomplete clinical data following 2 cycles of chemotherapy, however, we did find an appreciable discordance between final clinical and final pathological response, with almost a third of patients (8/28) failing to obtain a pathological response despite achieving a clinical response at the end of treatment. This would suggest that

clinical response alone does not reliably inform upon final pathological response.

Complete pathological response to NAC has been shown to predict for improved overall survival [24, 30, 83], however, in most trials with anthracycline-based chemotherapy only 5-10% of patients achieve a pCR, thereby reducing its clinical usefulness as a surrogate marker of outcome. Indeed, in our study, only one of the 22 patients who completed the intended 6 cycles of FEC NAC achieved a pCR, giving a pCR rate of 4.5%. Therefore, an assessment of pathological response, where patients are classified as responders (complete and partial pathological response) and non-responders might be a more useful surrogate for outcome. The prognostic significance of a partial pathological response, however, is largely unknown. In one study of 176 patients with large or locally advanced breast cancers receiving NAC, Ogston et al. evaluated lesser degrees of pathological response using a new five-point pathological grading system where the fundamental feature was a reduction in tumour cellularity (Miller/Payne grading system) [294]. They found a significant correlation between the new grading system and both DFS and OS at 5 years. Further, in a multivariate analysis of prognostic factors, the Miller/Payne grading system was shown to be an independent predictor of overall survival. In addition to changes in tumour:stromal cellular ratio, other histological features reflecting pathological response to NAC have been described [292, 293]. We therefore derived a grading system for pathological response, in accordance with the Miller/Payne grading system and the other previously described criteria, and defined our patients as either pathological responders or non-responders. We, thus, used final pathological response as our endpoint measure of the clinical effectiveness of NAC and evaluated the MRI data in relation to this measure.

ROC curve analysis was used to compare the predictive performance of the different kinetic parameters from the single centre-slice analysis to determine pathological response. ROC curves provide a method to compare diagnostic examination accuracy and are designed to illustrate the overall information yielded by an imaging examination, regardless of the criteria used to interpret the images. The curve is a plot of sensitivity (probability of a positive test if the

condition is present, also known as true-positive fraction) versus [1-specificity](probability of a positive test if the condition is absent, also known as false-positive fraction). ROC curve analysis provides a cut-off value for the diagnostic test where sensitivity and specificity are at an optimum and yields a measure of the area under the ROC curve (AUC) where, in general, the larger the AUC, the better the diagnostic examination. Thus, ROC curve analysis revealed the best parameters to be change in MaxAmp, K^{trans} and rBF (table 2.11). Although change in MaxAmp appeared the best parameter with an AUC 0.87, sensitivity 100% and specificity 82%, as a semi-quantitative parameter it is less reliable compared with the quantitative parameters. This is because the semi-quantitative parameters can be affected by a number of factors including machine settings and manufacturer, field strength and contrast dose. Further, the signal intensity and the dose of contrast agent were not linearly related in the sequence used in this study. The quantitative parameters K^{trans} and rBF were further evaluated by applying the repeatability range derived from the repeatability cohort data, to determine which was the better predictor of pathological response on a patient-by-patient basis. The repeatability, derived using the Bland and Altman method, determines the range in parameter value outside which a change deemed to be significant. K^{trans} was found to be the better predictor, correctly classifying 100% of pathological non-responders and 36% of pathological responders. This compared with rBF, which correctly classified 88% of pathological non-responders and 20% of pathological responders.

Data from the T1W DCE-MRI single-slice (centre-slice) and the multi-slice (three-slice) analysis were then compared in order to assess their relative utility in predicting final pathological response to NAC. Only the quantitative kinetic parameters were assessed. A good correlation was observed between the pre-treatment and post 2 cycles NAC median values, as well as for the median percentage change after 2 cycles of NAC, for the single centre-slice and three-slice evaluations for all parameters ($r>0.8$, $p<0.001$ for all groups). As with the single-slice analysis, the three-slice group analysis demonstrated failure of the pre-treatment values to predict for final pathological response to NAC. Change in median K^{trans}, k_{ep} and MaxGd, however, significantly correlated with final

pathological response. ROC curve analysis revealed change in median K^{trans} to be the best predictor of response (AUC 0.93, sensitivity 94% and specificity 82%), with a significantly improved test performance compared to single-slice evaluation (p=0.02). Further, application of the 3-slice reproducibility range, confirmed change in median K^{trans} as the best predictor of pathological response, correctly classifying 94% of pathological non-responders (**figure 2.21**) and 73% of pathological responders (**figure 2.22** and **table 2.18**).

The changes observed in the BOLD-MRI parameter, R_2*, did not correlate with either the final clinical or pathological response to treatment. This would suggest that changes in the oxygenation of breast tumours do not predict for response. The effect of scarring and fibrosis on the R_2* within breast tumours remains unclear, however, and whether R_2* solely reflects oxygenation or whether it is a more complex parameter is remains under investigation. This is discussed further in **section 4.5**.

In summary, the early changes observed in the kinetic MRI parameters reflecting tumour microvessel permeability and perfusion can predict for final pathological response to neoadjuvant anthracycline-based chemotherapy, with change in median K^{trans} on multi-slice DCE-MRI examinations being the best predictor of response. In light of these findings, multi-slice T1W DCE-MRI could assist in tailoring treatment to each individual patient, using change in median K^{trans} after two cycles of NAC to guide therapy. An example of how multi-slice T1W DCE-MRI could be used in the management of patients receiving NAC is illustrated in **figure 2.24**. If the initial NAC regimen is six cycles of FEC then women receiving this treatment would undergo a T1W multi-slice DCE-MRI of the breasts prior to commencing treatment and then again following 2 cycles of chemotherapy. In those women where there was a significant reduction in median K^{trans} (outside the repeatability range), pathological response could be predicted with a positive predictive value (PPV) of 89% and continued treatment with FEC would be recommended. In those women where there was a non-significant reduction (within the reproducibility range), or a significant increase in median K^{trans}, then pathological non-response could be predicted with a PPV of 84%, and treatment would be altered to a non-cross resistant agent, such as

docetaxel. The aim of such an intervention would be to improve the pathological response rate and the individual patient's long-term outcome in non-responding patients, while avoiding the added toxicity and cost of taxane chemotherapy in the anthracycline-responding patients.

Table 2.1. MRI study treatment plan

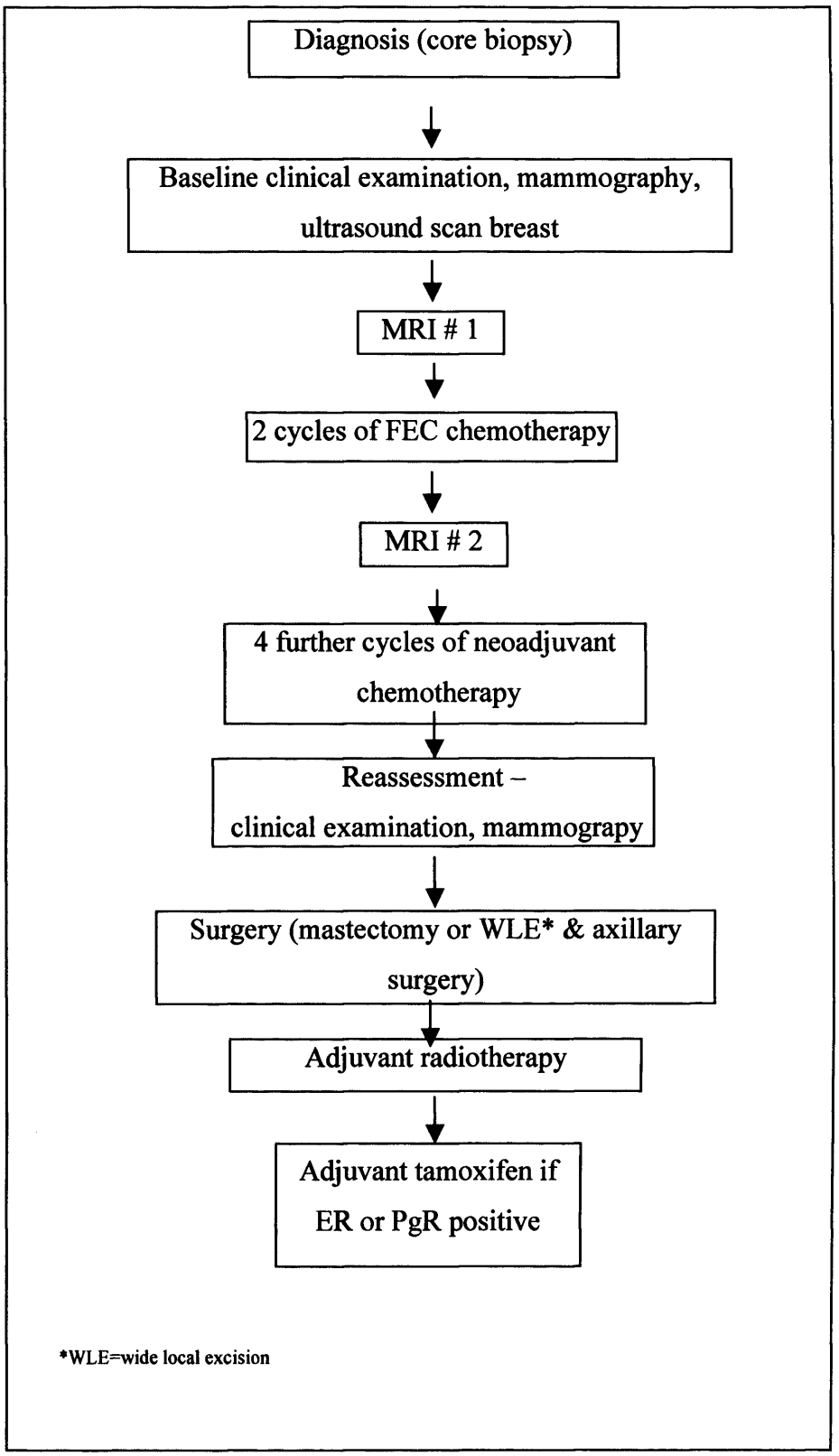

Table 2.2. MRI study population

Patient No.	Age	Menopausal Status	TNM Stage	Tumour grade & type	No. FEC cycles	Clinical Response to FEC	Pathological Response (grade)
2	43	Pre	T2N1M0	G3 IDC	6	PR	R (3)
3	56	Post	T2N1M0	G2 IDC	6	CR	R (3)
4	34	Pre	T3N0M0	G3 IDC	6	PR	R (4)
5	34	Pre	T3N2M0	G3 IDC	6	SD	NR (5)
6	46	Post	T4dN1M0	NOS	5 (changed to docetaxel)	SD	NR*
7	38	Pre	T2N0M0	G2 IDC	6	PR	R (4)
10	33	Pre	T2N1M0	G2 IDC	6	PR	NR (5)
11	45	Pre	T4dN3cM0	IDC	6	CR	R (3 on bx)
12	59	Post	T2N0M0	G2 IDC	6	PR	NR (5)
14	47	Pre	T2N0M0	G2 IDC	6	CR	R (3)
15	51	Post	T3N0M0	G3 IDC	6	PR	NR (5)
16	41	Pre	T4dN1M1	NOS	7 (changed to paclitaxel/trastuzumab)	PD	NR*
18	43	Pre	T4aN0M0	IDC	4 (proceeded to surgery)	PD	NR (5)
20	39	Pre	T2N1M0	IDC	6	SD	NR (5)
21	39	Pre	T2N0M0	G2 IDC	6	PR	NR (5)
22	51	Post	T2N3cM0	Mucinous	6	SD	NR (5)
24	29	Pre	T2N1M0	G2 IDC	2 (proceeded to surgery)	PD	NR (5)
25	53	Pre	T3N0M0	G2 lobular	6	PR	NR (5)
27	46	Pre	T2N0M0	G2 IDC	6	PR	NR (5)
28	50	Post	T2N0M0	G3 IDC	6	CR	R*
29	52	Post	T3N0M0	G3IDC	6	CR	R*
31	53	Post	T2N0M0	G2 IDC	5 (due to side-effects)	PR	R (4)
32	40	Pre	T3N1M0	G2 IDC	6	PR	R (2)
34	70	Post	T4bN0M0	G2 lobular	4 (proceeded to surgery)	PD	NR (5)
36	60	Post	T4dN0M0	G3 IDC	6	PR	NR (5)
39	56	Post	T4dN1M0	G1 lobular	6	SD	NR (5)
40	43	Pre	T2N0M0	G2 NOS	6	PR	NR (5)
41	47	Pre	T3N0M0	G3 IDC	6	CR	R (3)

IDC= invasive ductal carcinoma; NOS = breast cancer not otherwise specified; *did not receive surgery

Table 2.3. Pre-treatment median parameter values according to final clinical response

	n	Size (cm^2)	T1W semiquantitative			T1W quantitative				T2*W quantitative			BOLD quantitative
			Mean Grad (AU)	MaxAmp (%)	Wt (AU)	K^{trans} (min^{-1})	v_e (%)	k_{ep} (min^{-1})	MaxGad (mmol/kg)	rBV	rBF	MTT (sec)	R_2* (sec^{-1})
Clinical Responders	19	13.2	40.7	81	-0.24	0.61	54	1.08	0.41	150	5.30	24.1	33.1
Clinical Non-Responders	9	17.9	29.2	92	-0.20	0.57	52	1.04	0.43	191	8.20	23.4	31.9
Mann-Whitney U-test		p=0.09	p=0.31	p=0.21	p=0.66	p=0.44	p=0.74	p=0.31	p=0.80	p=0.81	p=0.57	p=0.13	p=0.99

Table 2.4. Pre-treatment median parameter values according to final pathological response

	n	Size (cm^2)	T1W semiquantitative			T1W quantitative				T2*W quantitative			BOLD quantitative
			Mean Grad (AU)	MaxAmp (%)	Wt (AU)	K^{trans} (min^{-1})	v_e (%)	k_{ep} (min^{-1})	MaxGad (mmol/kg)	rBV	rBF	MTT (sec)	R_2* (sec^{-1})
Pathological Responders	11	13.2	40.7	95	-0.24	0.66	57	1.19	0.45	177	6.89	24.5	32.7
Pathological Non-Responders	17	17.1	38.2	87	-0.23	0.57	52	1.04	0.39	150	5.30	23.4	33.7
Mann-Whitney U-test		p=0.68	p=0.31	p=0.89	p>0.99	p=0.16	p=0.46	p=0.16	p=0.10	p=0.48	P=0.36	p=0.24	P=0.79

Table 2.5. Pre-treatment parameter 5th-95th centile range according to final clinical response

	n	T1W semiquantitative			T1W quantitative				T2*W quantitative		
		Mean Grad	MaxAmp	Wt	k^{trans}	v_e	k_{ep}	MaxGad	rBV	rBF	MTT
Clinical Responders	19	156	102	1.25	1.11	45	1.95	0.33	383	11.23	11.64
Clinical Non-Responders	9	126	110	1.19	1.48	40	3.05	0.36	282	11.18	7.75
Mann-Whitney U-test		p=0.92	p=0.99	p=0.48	p=0.84	p=0.93	p=0.80	p=0.60	p=0.37	p=0.99	p=0.22

Table 2.6. Pre-treatment parameter 5th-95th centile range according to final pathological response

	n	T1W semiquantitative			T1W quantitative				T2*W quantitative		
		Mean Grad	MaxAmp	Wt	k^{trans}	v_e	k_{ep}	MaxGad	rBV	rBF	MTT
Pathological Responders	11	161	110	1.21	1.72	47	3.63	0.36	446	14.81	11.65
Pathological Non-Responders	17	114	95	1.34	1.08	40	1.95	0.31	326	9.87	7.75
Mann-Whitney U-test		p=0.33	p=0.60	p=0.52	p=0.14	p=0.21	p=0.29	p=0.06	p=0.12	p=0.28	p=0.54

Table 2.7. Median percentage change in median kinetic parameter values according to clinical response

MRI sequence	Parameter	Clinical Responders (% change)	Clinical Non-responders (% change)	p-value (MW test)
T1W semi-quantitative	MeanGrad	-47.7	4.9	**<0.05**
	MaxAmp	-11.5	7.1	**<0.05**
	Wt	0.9	16.9	0.81
T1W quantitative	K^{trans}	-29.6	16.8	**<0.01**
	v_e	0	5.2	0.31
	k_{ep}	-31.2	5.5	**<0.005**
	MaxGd	-3.0	7.8	0.14
T2*W quantitative	rBV	-59.3	73.4	**<0.001**
	rBF	-56.4	70.6	**=0.001**
	MTT	-4.8	1.15	0.29
BOLD	R_2*	12.9	0.7	0.72
	Tumour size	-32.8	-13.0	**<0.05**

Table 2.8. Median percentage change in median kinetic parameter values according to pathological response

MRI sequence	Parameter	Pathological Responders (% change)	Pathological Non-responders (% change)	p-value (MW test)
T1W semi-quantitative	MeanGrad	-67.0	-2.4	**<0.05**
	MaxAmp	-25.2	5.4	**<0.001**
	Wt	20.2	5.3	0.64
T1W quantitative	K^{trans}	-49.5	3.5	**<0.005**
	v_e	-2.0	3.7	0.23
	k_{ep}	-45.4	-4.8	**<0.005**
	MaxGd	-17.0	7.8	**<0.05**
T2*W quantitative	rBV	-61.1	-2.4	**<0.01**
	rBF	-63.4	-3.5	**=0.005**
	MTT	-4.2	0.5	0.87
BOLD	R2*	16.3	-1.5	0.10
	Tumour size	-35.5	-14.8	0.11

Table 2.9. Median percentage change in 5^{th}-95^{th} centile range for kinetic parameter values according to clinical response

MRI sequence	Parameter 5^{th}-95^{th} centile range	Clinical Responders (% change)	Clinical Non-responders (% change)	p-value (MW test)
T1W semi-quantitative	MeanGrad	-58.1	14.3	**<0.01**
	MaxAmp	-13.1	14.1	**<0.001**
	Wt	7.7	9.2	>0.99
T1W quantitative	K^{trans}	-31.4	19.7	**<0.05**
	v_e	-4.2	13.2	0.17
	k_{ep}	-37.0	12.9	**<0.05**
	MaxGd	-7.3	13.2	**<0.05**
T2*W quantitative	rBV	-40.5	53.2	**<0.0005**
	rBF	-36.7	53.9	**<0.005**
	MTT	4.8	-16.6	0.54

Table 2.10. Median percentage change in 5^{th}-95^{th} centile range for kinetic parameter values according to pathological response

MRI sequence	Parameter 5^{th}-95^{th} centile range	Pathological Responders (% change)	Pathological Non-responders (% change)	p-value (MW test)
T1W semi-quantitative	MeanGrad	-61.2	-7.1	**<0.05**
	MaxAmp	-15.2	11.9	**<0.05**
	Wt	16.9	4.6	0.34
T1W quantitative	K^{trans}	-58.9	18.7	**<0.005**
	v_e	-2.1	9.1	0.67
	k_{ep}	-45.3	12.4	**<0.01**
	MaxGd	-11.1	13.2	**<0.001**
T2*W quantitative	rBV	-62.0	-0.7	**<0.05**
	rBF	-57.9	3.6	**<0.01**
	MTT	18.5	-19.3	**<0.05**

Table 2.11. ROC curve analysis on change in median parameter values for predicting pathological non-response (single-slice analysis)

Test	Parameter	Optimal cut-off (% change)	AUC	Sensitivity (%)	Specificity (%)
Morphology	**Size**	-30.9	0.68	71	72
T1W semi-quantitative	**MeanGrad**	-47.6	0.76	88	73
	MaxAmp	-12.5	0.87	100	82
	Wt	83.1	0.56	94	27
T1W quantitative	**K^{trans}**	-45.1	0.83	100	73
	v_e	-1.9	0.64	82	55
	k_{ep}	-24.7	0.82	88	73
	MaxGad	-6.6	0.73	94	63
T2*W quantitative	**rBV**	-34.5	0.81	69	90
	rBF	-55.6	0.83	81	80
	MTT	-24.4	0.48	13	100
BOLD	**R_2***	11.6	0.70	75	70

Table 2.12. Three-slice analysis pre-treatment median parameter values according to final clinical response

	n	T1W quantitative			
		K^{trans} (min^{-1})	v_e (%)	k_{ep} (min^{-1})	MaxGad (mmol/kg)
Clinical Responders	19	0.56	51	1.05	0.41
Clinical Non-Responders	9	0.58	49	1.03	0.40
p-value (Mann-Whitney U-test)		p=0.74	p=0.88	p=0.40	p=0.92

Table 2.13. Three-slice analysis pre-treatment median parameter values according to final pathological response

	n	T1W quantitative			
		K^{trans} (min^{-1})	v_e (%)	k_{ep} (min^{-1})	MaxGad (mmol/kg)
Pathological Responders	11	0.57	54	1.25	0.45
Pathological Non-Responders	17	0.55	49	1.03	0.37
p-value (Mann-Whitney U-test)		p=0.19	p=0.61	p=0.18	p=0.13

Table 2.14. Three-slice analysis of median percentage change in median T1W quantitative kinetic parameter values according to clinical response

MRI sequence	Parameter	Clinical Responders (% change)	Clinical Non-responders (% change)	p-value (MW test)
T1W quantitative	K^{trans}	-39.8	18.1	=0.002
	v_e	2.0	9.6	0.16
	k_{ep}	-33.3	7.4	=0.0005
	MaxGd	-0.81	8.3	<0.05

Table 2.15. Three-slice analysis of median percentage change in median T1W quantitative kinetic parameter values according to pathological response

MRI sequence	Parameter	Pathological Responders (% change)	Pathological Non-responders (% change)	p-value (MW test)
T1W quantitative	K^{trans}	-52.9	16.9	<0.0001
	v_e	2.3	7.0	0.16
	k_{ep}	-50.3	-8.5	<0.005
	MaxGd	-13.0	6.3	<0.005

Table 2.16. ROC curve analysis on change in median T1W quantitative parameter values to predict pathological response comparing single-slice and three-slice analysis

Test	Parameter	Optimal cut-off (% change)	AUC	Sensitivity (%)	Specificity (%)
Morphology	Size	-30.9	0.68	71	72
T1W quantitative: SINGLE - SLICE	K^{trans}	-45.1	0.83	100	73
	v_e	-1.9	0.64	82	55
	k_{ep}	-24.7	0.82	88	73
	MaxGd	-6.6	0.73	94	63
T1W quantitative: THREE-SLICE	K^{trans}	-32.5	0.93	94	82
	v_e	-4.3	0.66	94	45
	k_{ep}	-19.7	0.85	82	91
	MaxGd	-1.9	0.81	94	64

Table 2.17. MRI reproducibility cohort characteristics

Patient No.	Age	Menopausal Status	TNM Stage	Tumour grade & type	Treatment received
Rp 1	52	Post	T3N0M0	G3IDC	NAC
Rp 2	58	Post	T2N0M0	G2 IDC	NAC
Rp 4	38	Pre	T2N0M0	G1 IDC	NAC
Rp 6	58	Post	T1N0M0	G1 IDC	BCS
Rp 7	47	Pre	T3N0M0	G3 IDC	NAC
Rp 9	56	Post	T2N0M0	Lobular	NAC
Rp 10	56	Post	T1N0M0	G1 IDC	BCS
Rp 11	41	Pre	T1N0M0	G2 IDC	BCS
Rp 12	54	Post	T2N0M0	G2 IDC	NAC
Rp 15	37	Pre	T4dN0M0	G2 IDC	NAC
Rp 16	48	Pre	T3N0M0	G3 IDC	NAC
Rp 17	62	Post	T2N1M0	G2 IDC	NAC

NAC = neoadjuvant chemotherapy
BCS = primary breast conserving surgery

Table 2.18. Patient pathological response as classified by functional MRI parameters (single-slice and three-slice) and repeatability range

MRI Sequence	Parameter	Non-responders correctly classified (patient numbers)	Responders correctly classified (patient numbers)	Repeatability range (% change in individual patient median required for significance at 95% confidence)
T1W semiquantitative	MeanGrad	100% (17/17)	55% (6/11)	-62.3 to +165.0
	MaxAmp	100% (17/17)	45% (5/11)	-28.0 to +28.0
T1W quantitative (single-slice)	K^{trans}	100% (17/17)	36% (4/11)	-51.3 to +105.3
	v_e	100% (17/17)	27% (3/11)	-17.5 to +17.5
	k_{ep}	94% (16/17)	45% (5/11)	-47.8 to +91.7
	MaxGd	94% (16/17)	45% (5/11)	-18.7 to +18.7
T2*W quantitative	rBV	88% (14/16)	20% (2/10)	-74.9 to +74.9
	rBF	88% (14/16)	20% (2/10)	-63.9 to +63.9
	MTT	88% (14/16)	0% (0/10)	-22.1 to +22.1
BOLD	R_2*	81% (13/16)	40% (4/10)	-17.5 to +17.5
T1W quantitative (3-slice)	K^{trans}	94% (16/17)	73% (8/11)	-42.4 to +73.6
	v_e	100% (17/17)	9% (1/11)	-29.9 to +29.9
	k_{ep}	88% (15/17)	36% (4/11)	-57.8 to + 136.8
	MaxGd	100% (17/17)	36% (4/11)	-18.8 to +18.8
	Tumour size	59% (10/17)	73% (8/11)	-26.5 to 36.1

Table 2.19. Correlation between pre-treatment T1W quantitative kinetic parameter values from the tumour ROI and the normal contralateral breast tissue

MRI sequence	MRI parameter	Tumour ROI vs. normal contralateral breast tissue
		Spearman's Rank Correlation Coefficient, Rho (p-value)
T1W Quantitative (single-slice)	K^{trans}	0.08 (0.70)
	v_e	-0.01 (0.96)
	k_{ep}	-0.002 (0.94)
	MaxGd	-0.19 (0.32)

Table 2.20. Pre-treatment median kinetic parameter values according to clinical response in the normal contralateral breast tissue

MRI sequence	Parameter (median)	Clinical Responders	Clinical Non-responders	p-value (MW test)
T1W quantitative	K^{trans}	0.06	0.05	0.56
	v_e	0.18	0.18	0.38
	k_{ep}	0.36	0.30	0.88
	MaxGd	0.12	0.11	0.77

Table 2.21. Pre-treatment median kinetic parameter values according to pathological response in the normal contralateral breast tissue

MRI sequence	Parameter (median)	Pathological Responders	Pathological Non-responders	p-value (MW test)
T1W quantitative	K^{trans} (min^{-1})	0.06	0.05	0.49
	v_e (%)	0.22	0.18	0.15
	k_{ep} (min^{-1})	0.29	0.35	0.85
	MaxGd (mmol/kg)	0.12	0.11	0.96

Table 2.22. Median percentage change in median kinetic parameter values according to clinical response in the normal contralateral breast tissue

MRI sequence	Parameter (median)	Clinical Responders (% change)	Clinical Non-responders (% change)	p-value (MW test)
T1W quantitative	K^{trans}	-16.6	-0.4	0.85
	v_e	-4.9	-16.0	0.53
	k_{ep}	-1.9	-11.2	0.77
	MaxGd	-10.9	-17.1	0.47

Table 2.23. Median percentage change in median kinetic parameter values according to pathological response in the normal contralateral breast tissue

MRI sequence	Parameter (median)	Pathological Responders (% change)	Pathological Non-responders (% change)	p-value (MW test)
T1W quantitative	K^{trans}	-24.0	1.4	0.38
	v_e	-22.9	-0.11	0.15
	k_{ep}	-1.88	-11.15	0.96
	MaxGd	-21.2	0	0.19

Figure 2.1.1. Example of pathological response grade 1

(i) pre-treatment core biopsy histology (invasive ductal carcinoma, not graded)

(ii) post-chemotherapy histology (pathological complete response)

(i)

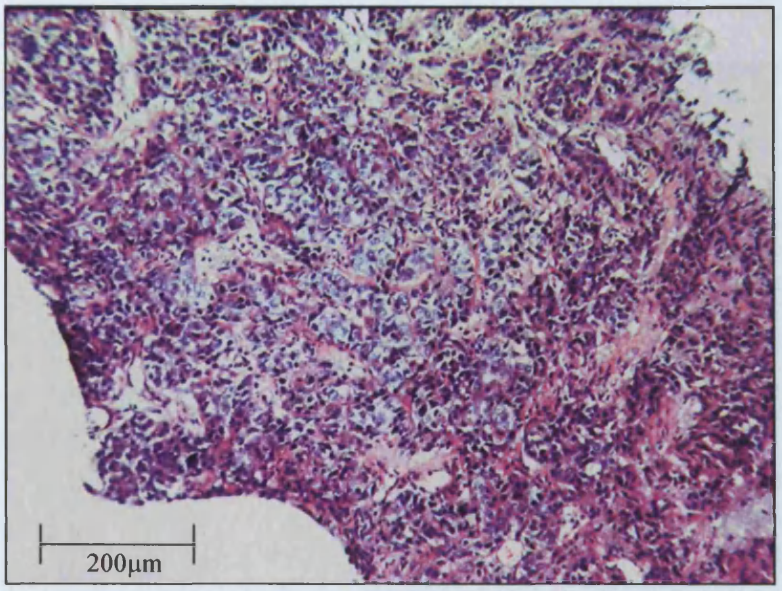

(ii)

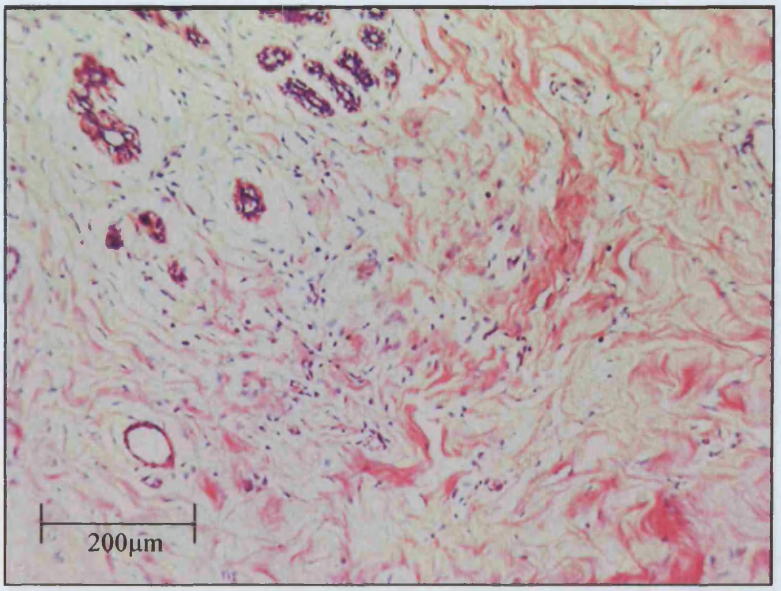

Figure 2.1.2. Example of pathological response grade 2

(i) pre-treatment core biopsy histology (grade 2 invasive ductal carcinoma)

(ii) post-chemotherapy histology (residual DCIS, no tumour cells)

(i)

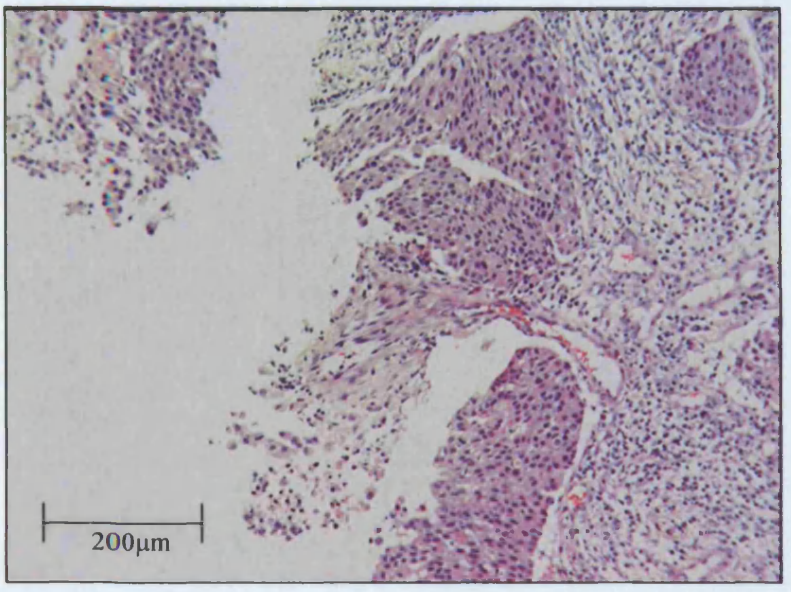

(ii)

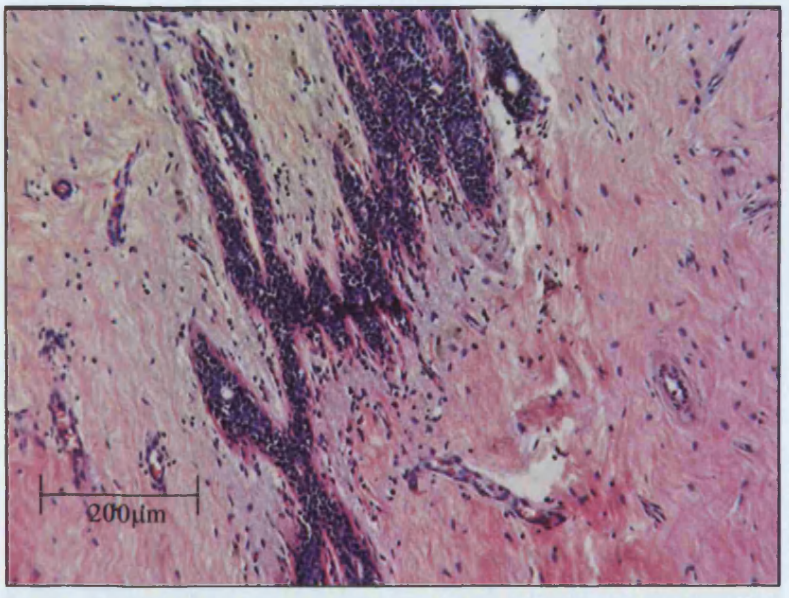

Figure 2.1.3. Example of pathological response grade 3

(i) pre-treatment core biopsy histology (grade 3 invasive ductal carcinoma)

(ii) post-chemotherapy histology (microscopic residual cancer cells)

(i)

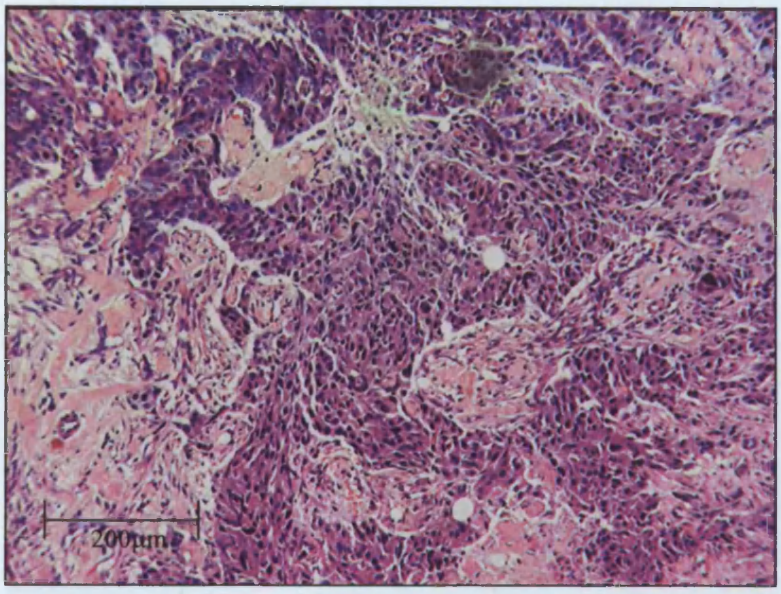

(ii)

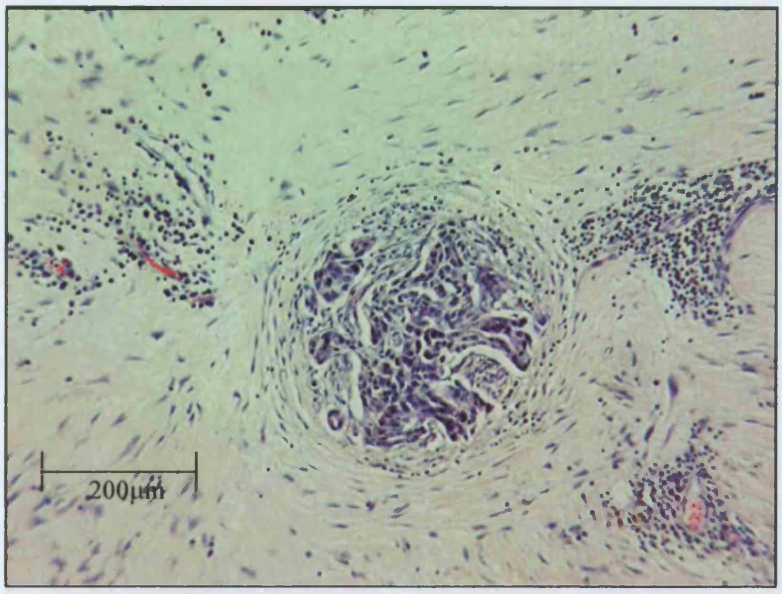

Figure 2.1.4. Example of pathological response grade 4

(i) pre-treatment core biopsy histology (grade 3 invasive ductal carcinoma)

(ii) post-chemotherapy histology (macroscopic residual cancer with chemotherapy-induced changes &/or histological tumour response)

(i)

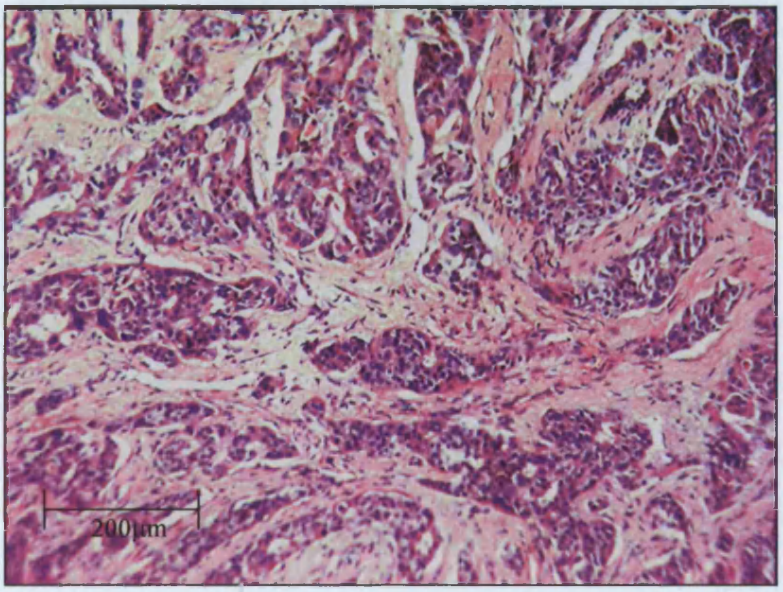

(ii)

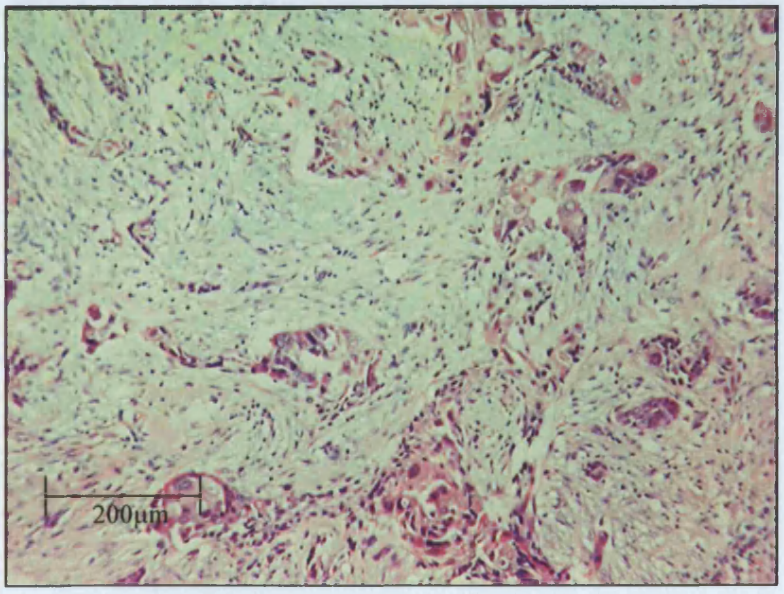

Figure 2.1.5. Example of pathological response grade 5

(i) pre-treatment core biopsy histology (grade 3 invasive ductal carcinoma)

(ii) post-chemotherapy histology (macroscopic invasive cancer with no response features)

(i)

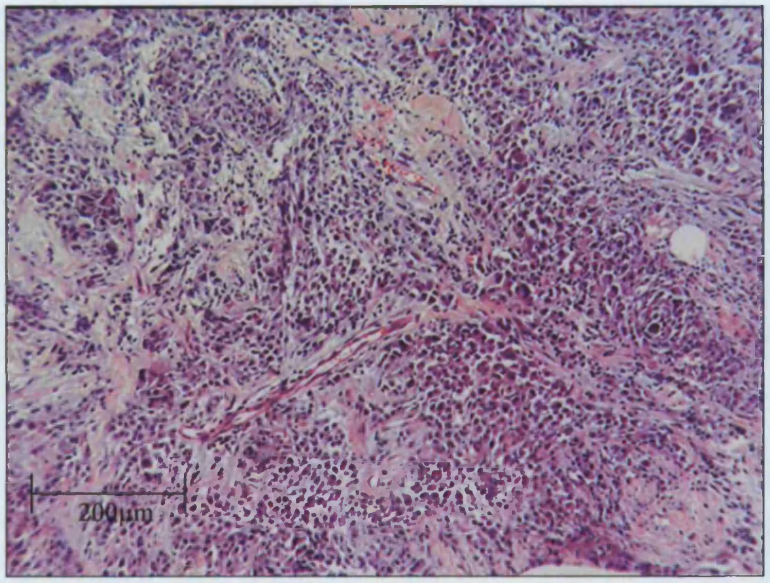

(ii)

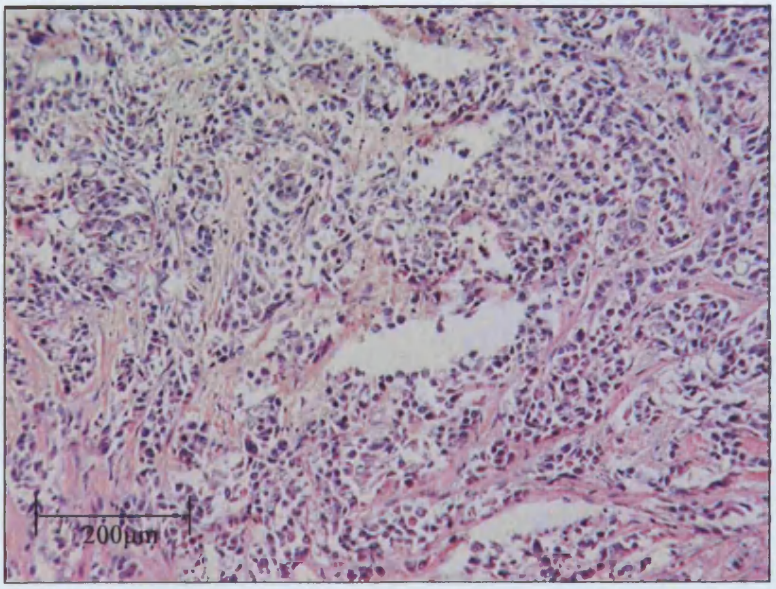

Figure 2.2. 1.5T Siemens symphony scanner

(i) with patient in position for MRI scan of breasts

(ii) breast coil with phantom in place for calibration

(i)

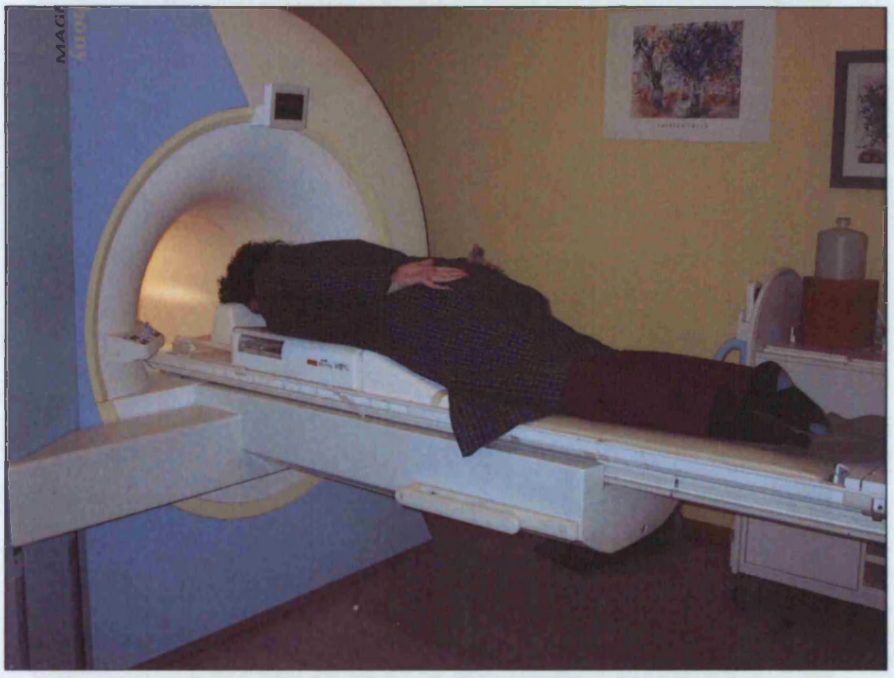

(ii)

Figure 2.3. MRI study patient example of

(a) T1W image pre-contrast (b) T1W image post contrast (subtraction image)

(c) T2*W image pre-contrast (d) T2*W image post contrast (subtraction image)

(e) Proton density image (f) R2* decay image

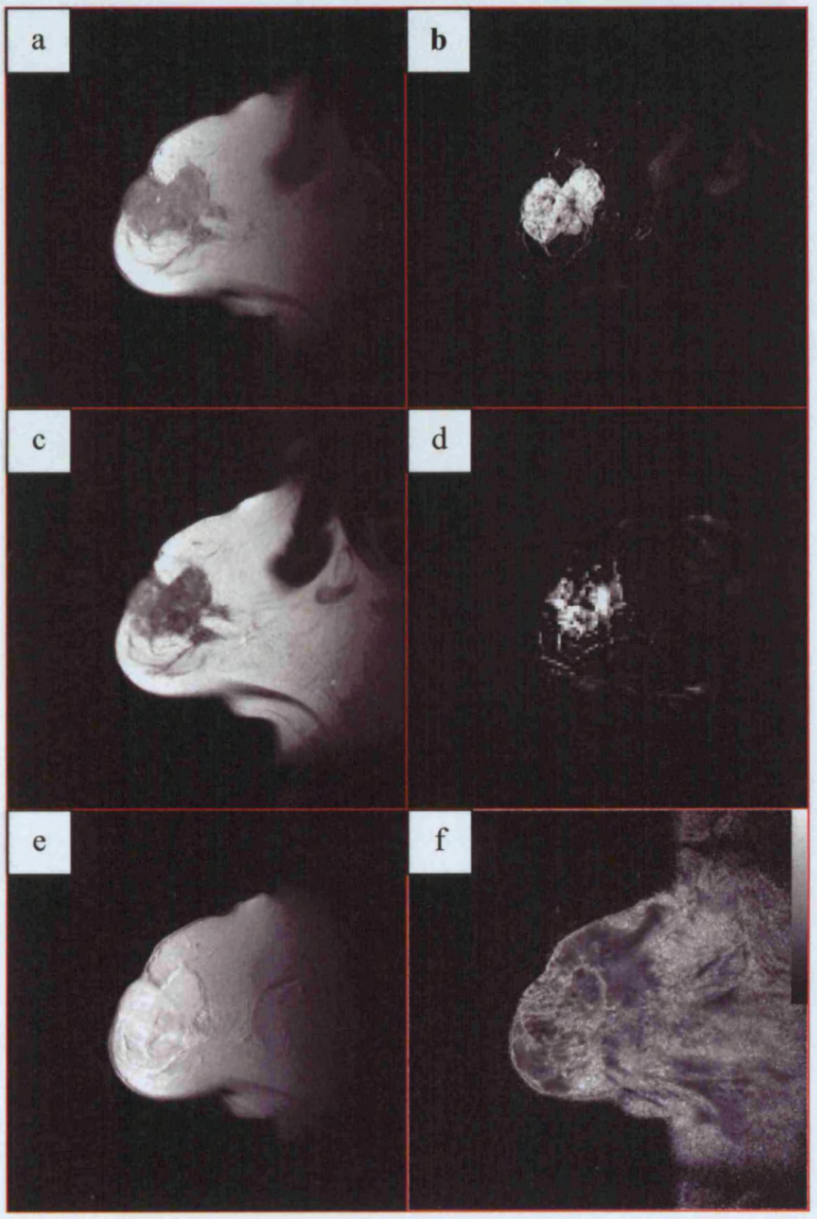

Figure 2.4. Example of tumour ROI

Figure 2.5. R2* signal intensity time decay curve

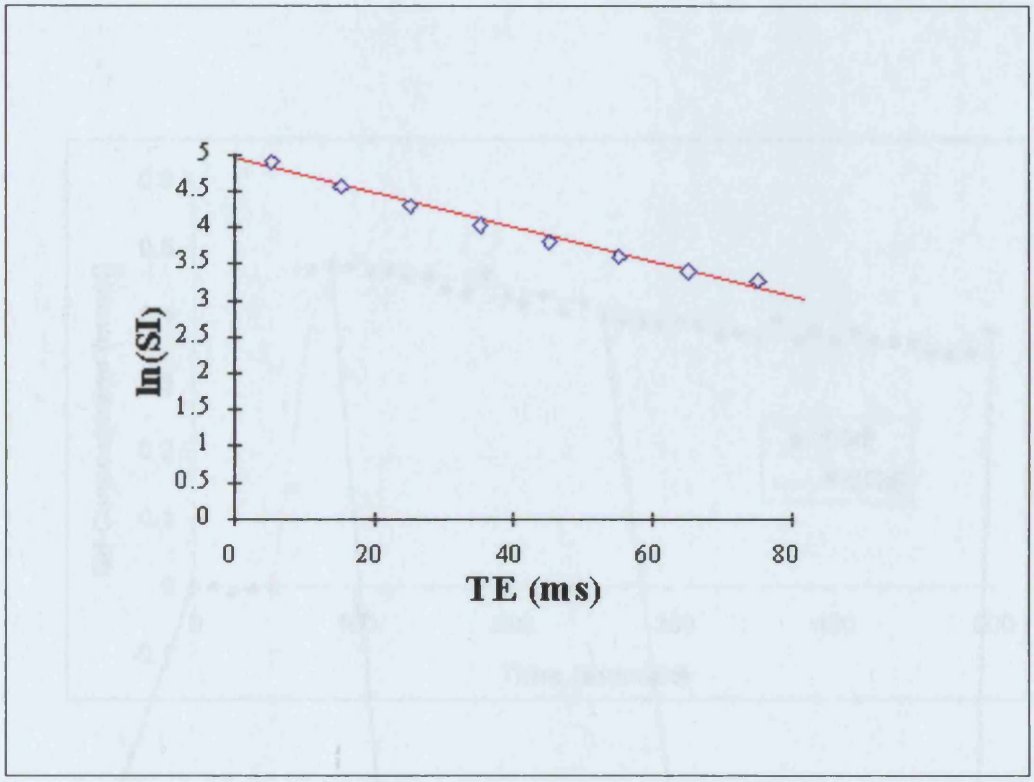

Figure 2.6. Gd-DTPA concentration-time curve data fitted to Tofts and Kermode model – data from patient showing change in Gd-DTPA uptake within tumour ROI over time and overlying model fit. T1W images from the central slice are shown at four time points and the associated K^{trans} parametric map.

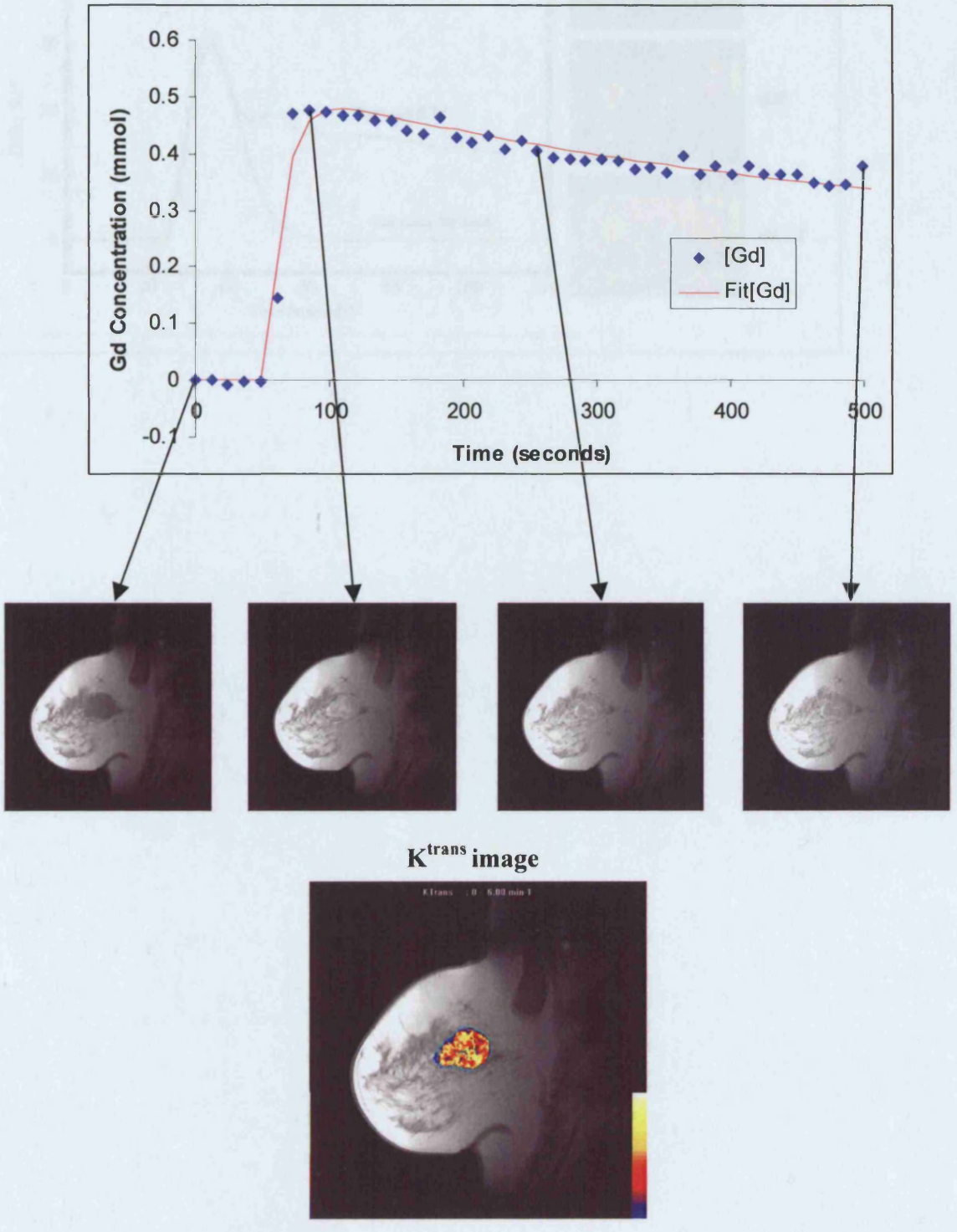

Figure 2.7. Fitting of T2* time series data to a gamma variate function

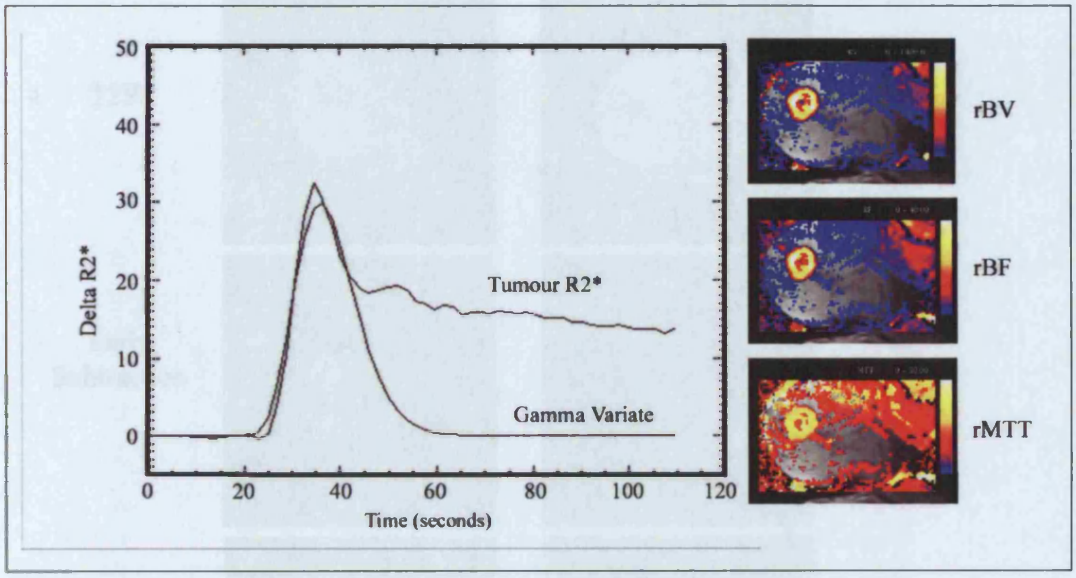

Figure 2.8. Pre-treatment and post-2 cycles of neoadjuvant FEC chemotherapy DCE-MRI images in a responding patient (patient number 29)

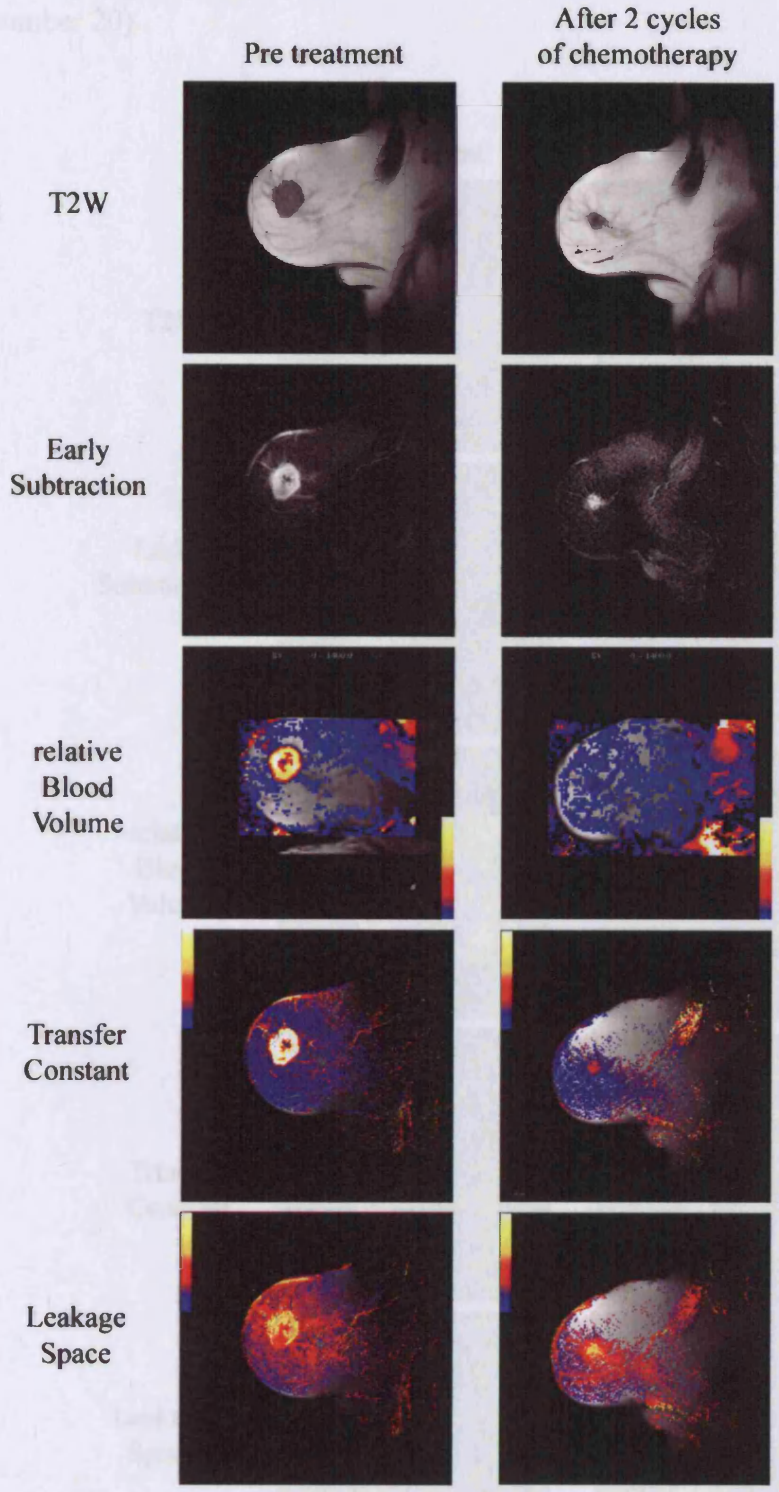

Figure 2.9. Pre-treatment and post-2 cycles of neoadjuvant FEC chemotherapy DCE-MRI images in a non-responding patient (patient number 20)

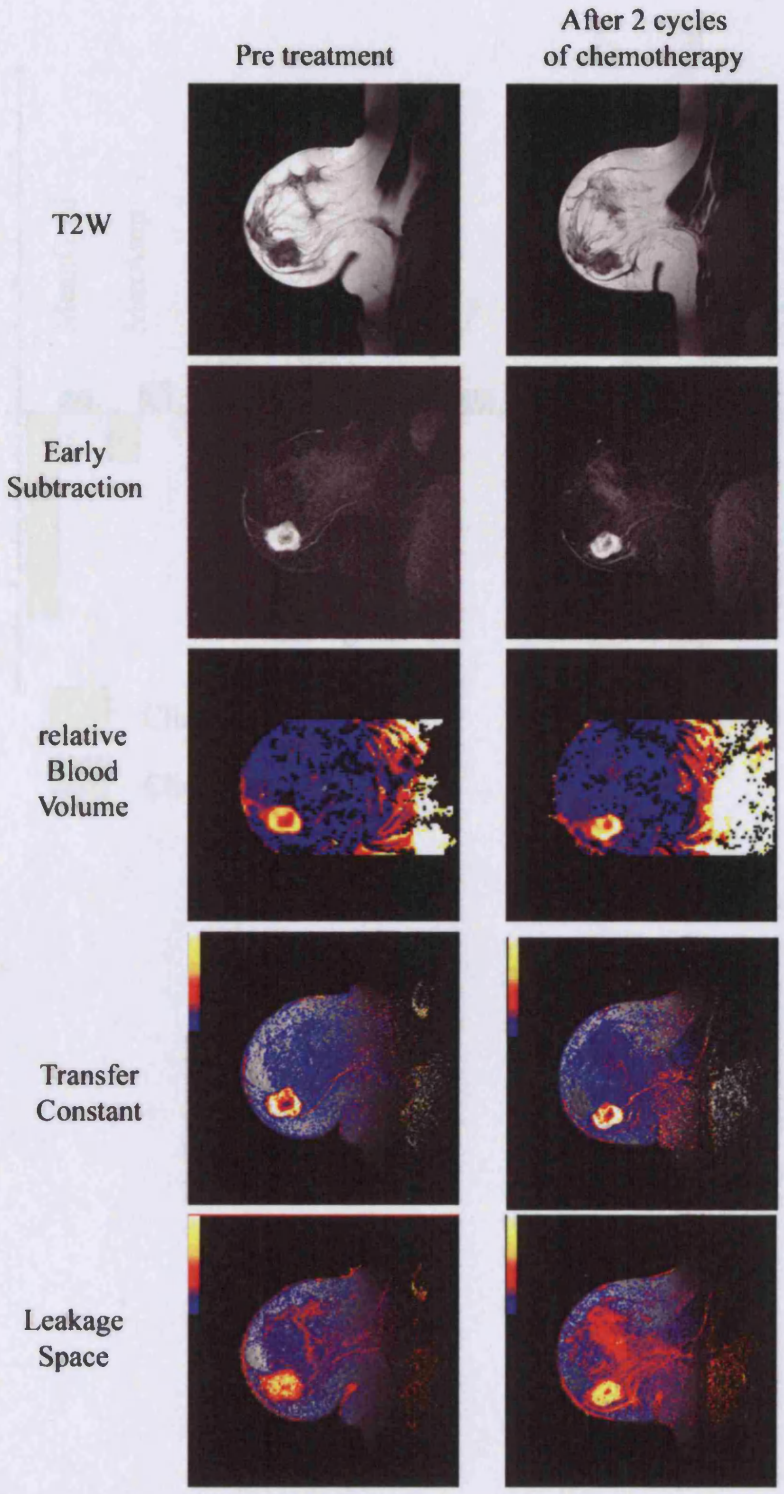

Figure 2.10. Median percentage change in median kinetic parameter values according to clinical response

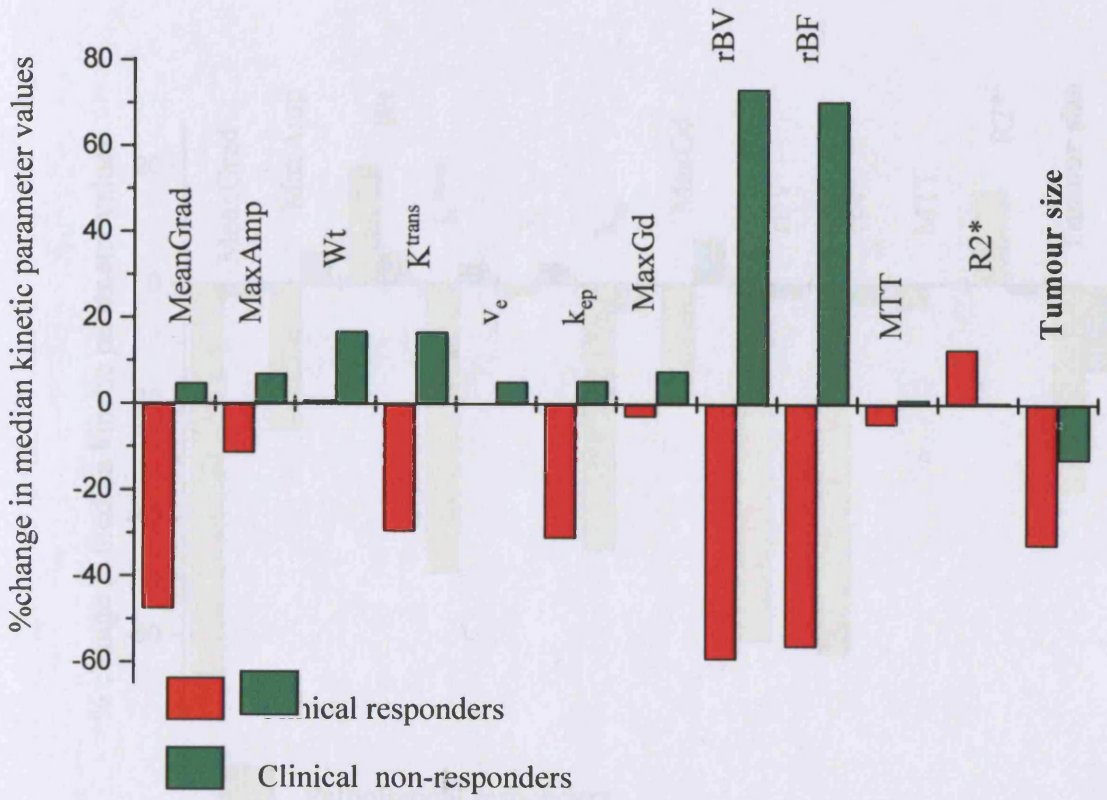

Figure 2.11. Median percentage change in median kinetic parameter values according to pathological response

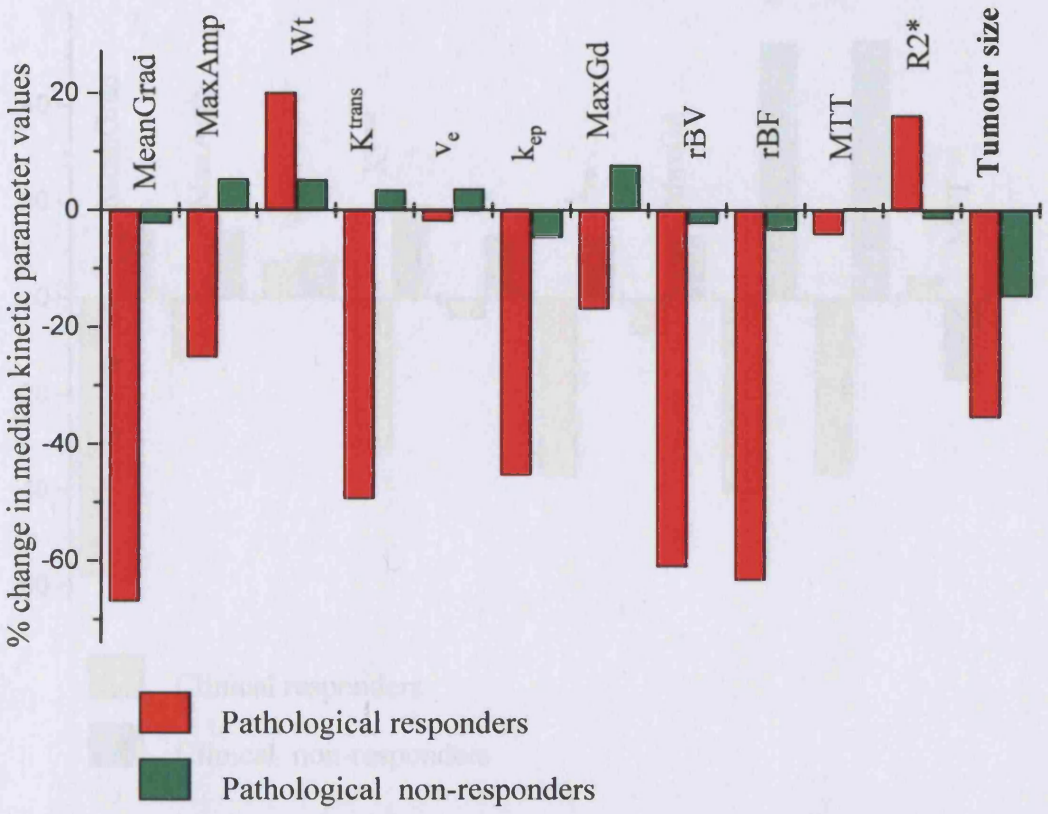

Figure 2.12. Median percentage change in 5th –95th centile range for kinetic parameters according to clinical response

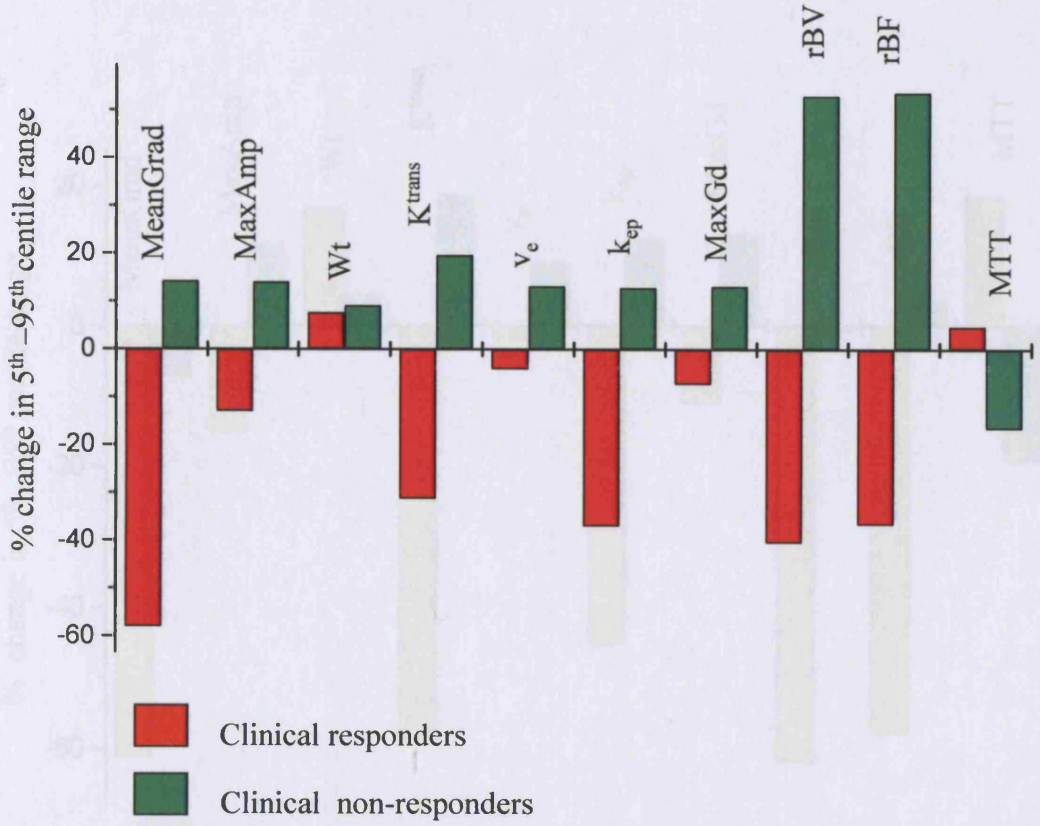

Figure 2.13. Median percentage change in 5th –95th centile range for kinetic parameters according to final pathological response

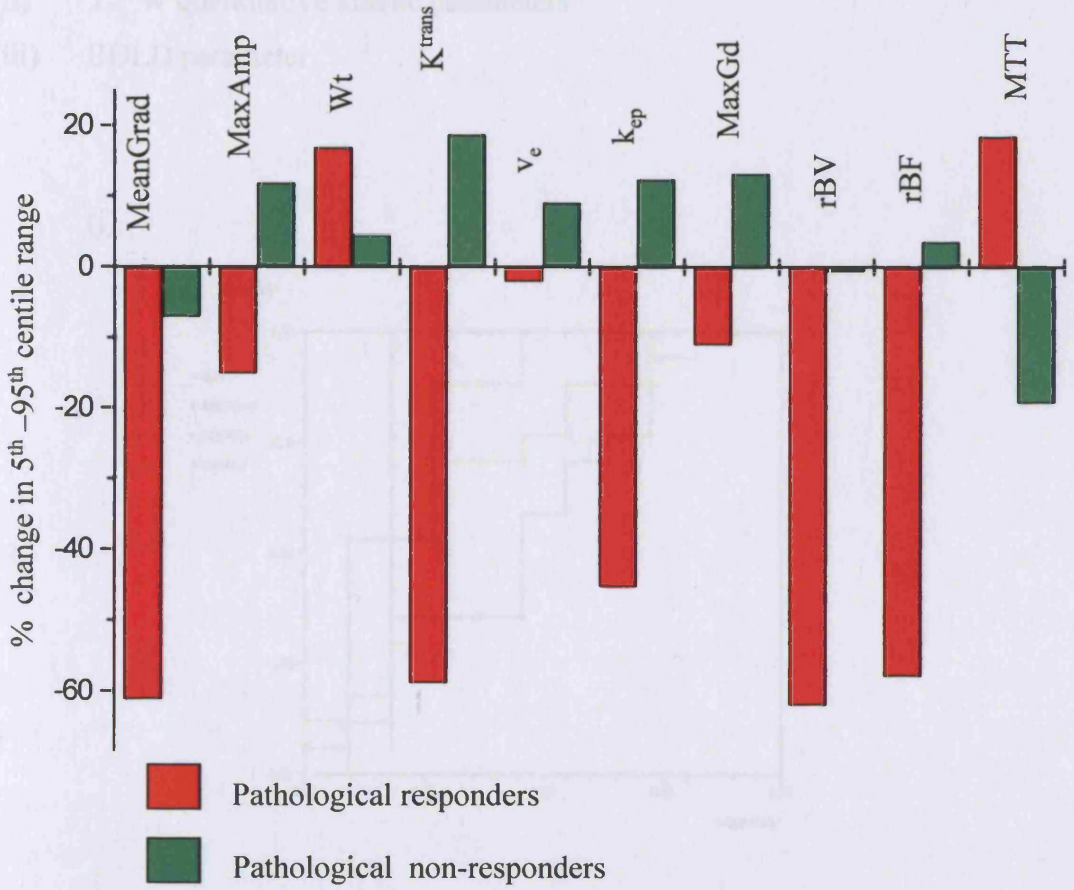

Figure 2.14. ROC curve analysis of MRI-derived tumour size change and percentage change in median for predicting pathological non-response (single-slice analysis)

(i) T1W semiquantitative kinetic parameters

(i) T1W quantitative kinetic parameters

(ii) T2*W quantitative kinetic parameters

(iii) BOLD parameter

(i)

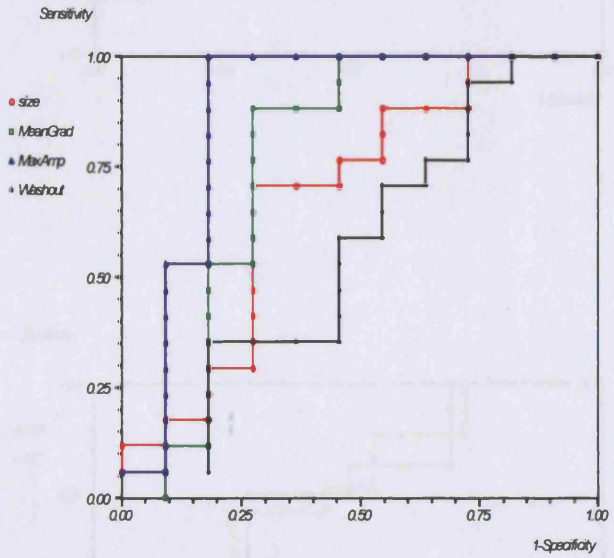

(ii)

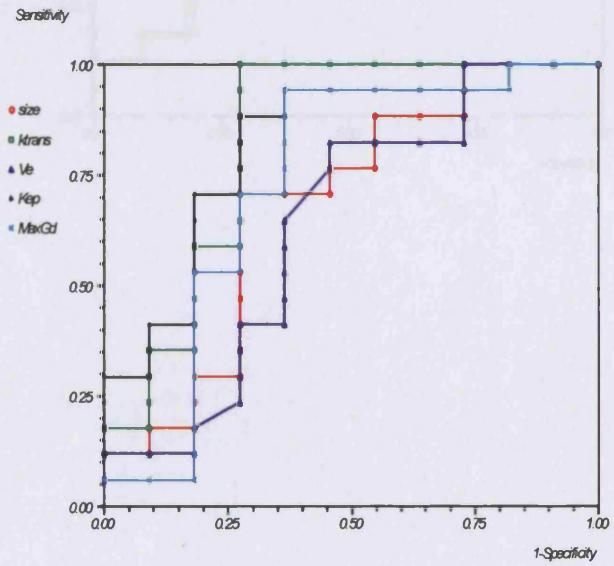

(iii)

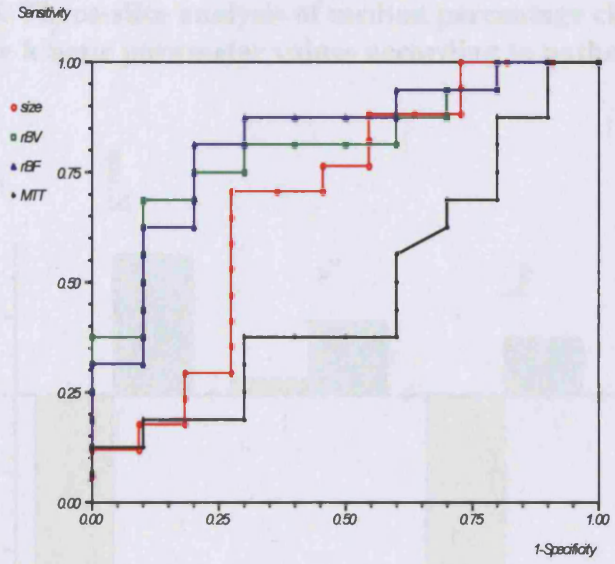
Sensitivity
size
rBV
rBF
MTT
1.00
0.75
0.50
0.25
0.00
0.00
0.25
0.50
0.75
1.00
1-Specificity

(iv)

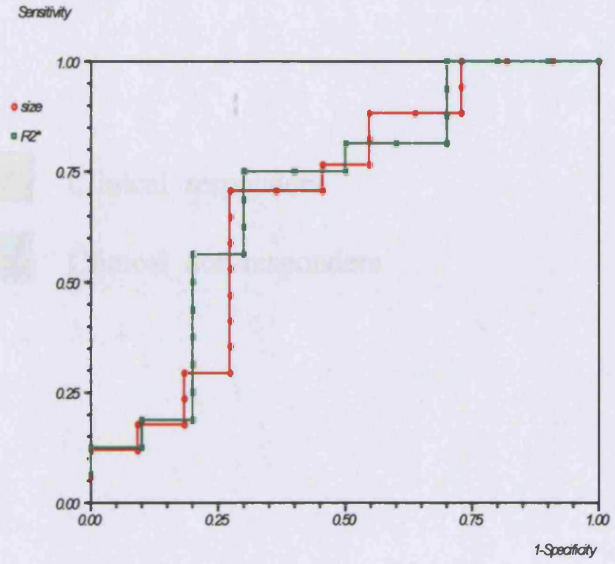
Sensitivity
size
RZ*
1.00
0.75
0.50
0.25
0.00
0.00
0.25
0.50
0.75
1.00
1-Specificity

Figure 2.15. Three-slice analysis of median percentage change in median T1W quantitative kinetic parameter values according to pathological response

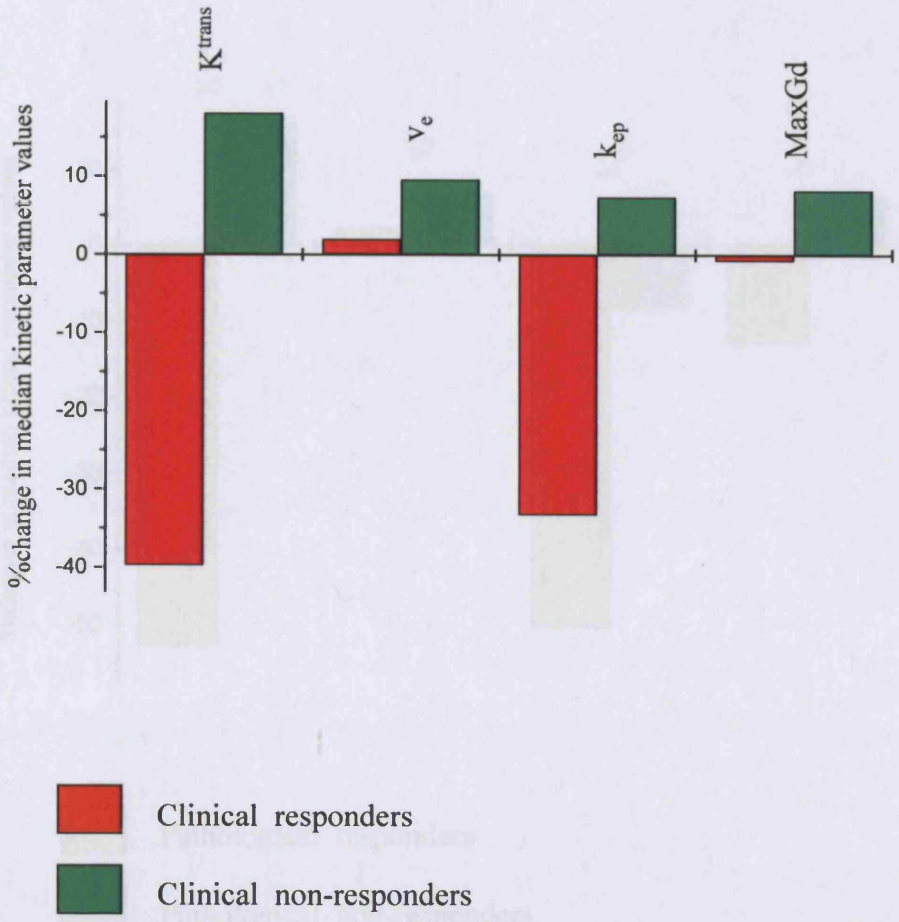

Figure 2.16. Three-slice analysis of median percentage change in median T1W quantitative kinetic parameter values according to pathological response

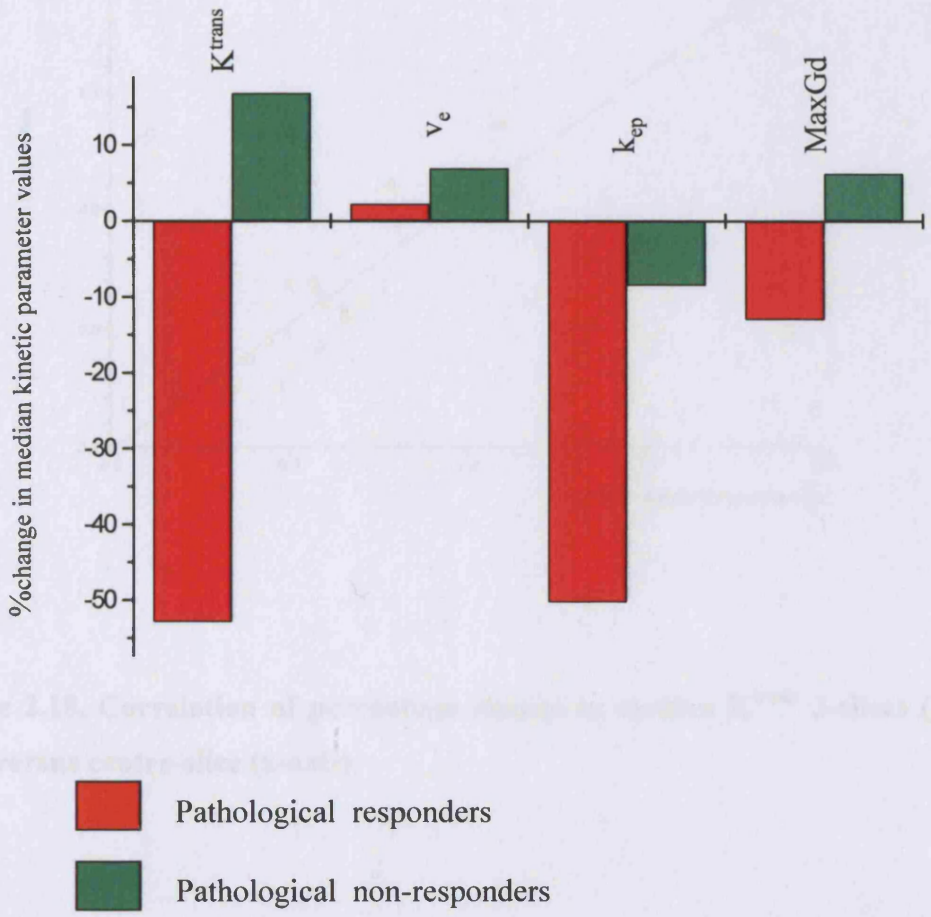

Figure 2.17. Correlation of pre-treatment median K^{trans} 3-slices (y-axis) versus single centre-slice (x-axis)

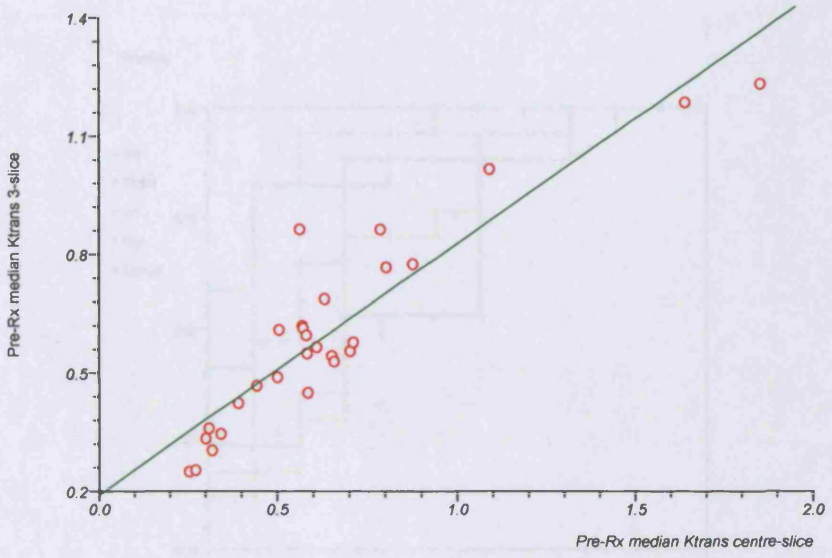

Figure 2.18. Correlation of percentage change in median K^{trans} 3-slices (y-axis) versus centre-slice (x-axis)

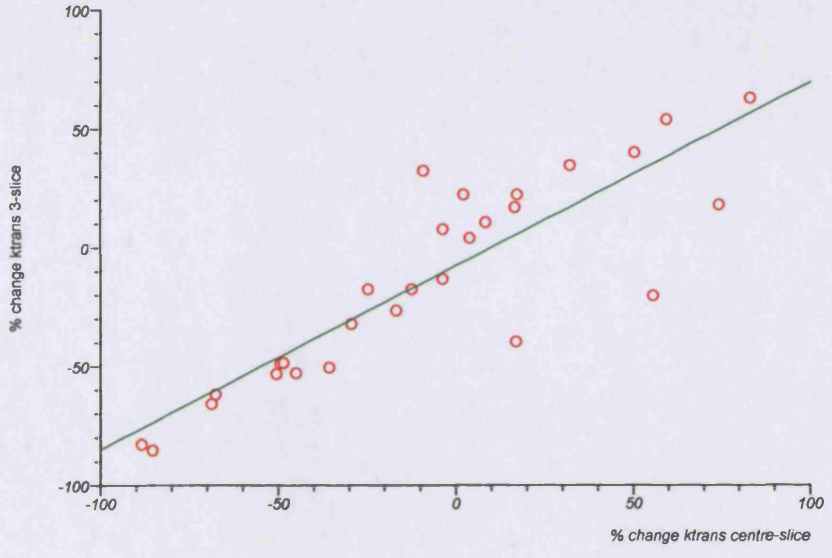

Figure 2.19 ROC curve analysis (3-slice data) comparing diagnostic performance of T1W quantitative kinetic parameter values and lesion size changes to predict pathological response

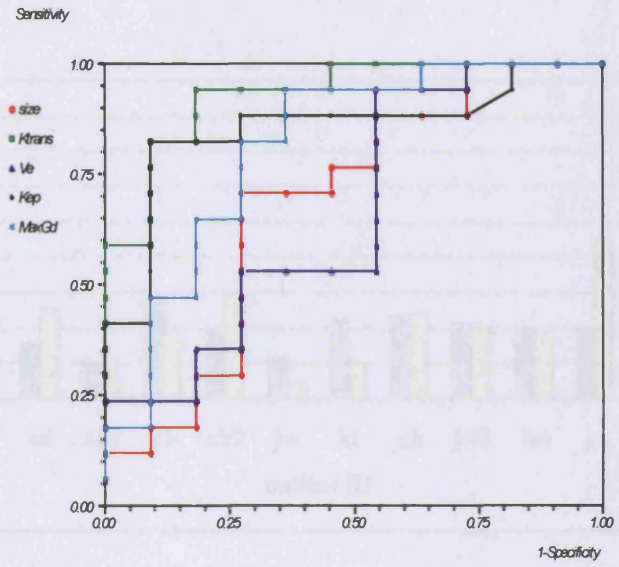

Figure 2.20. Median parameter values obtained for each patient on the two reproducibility MRI examinations (Spearman's rank correlation coefficient, Rho, and p-value shown in table at end)

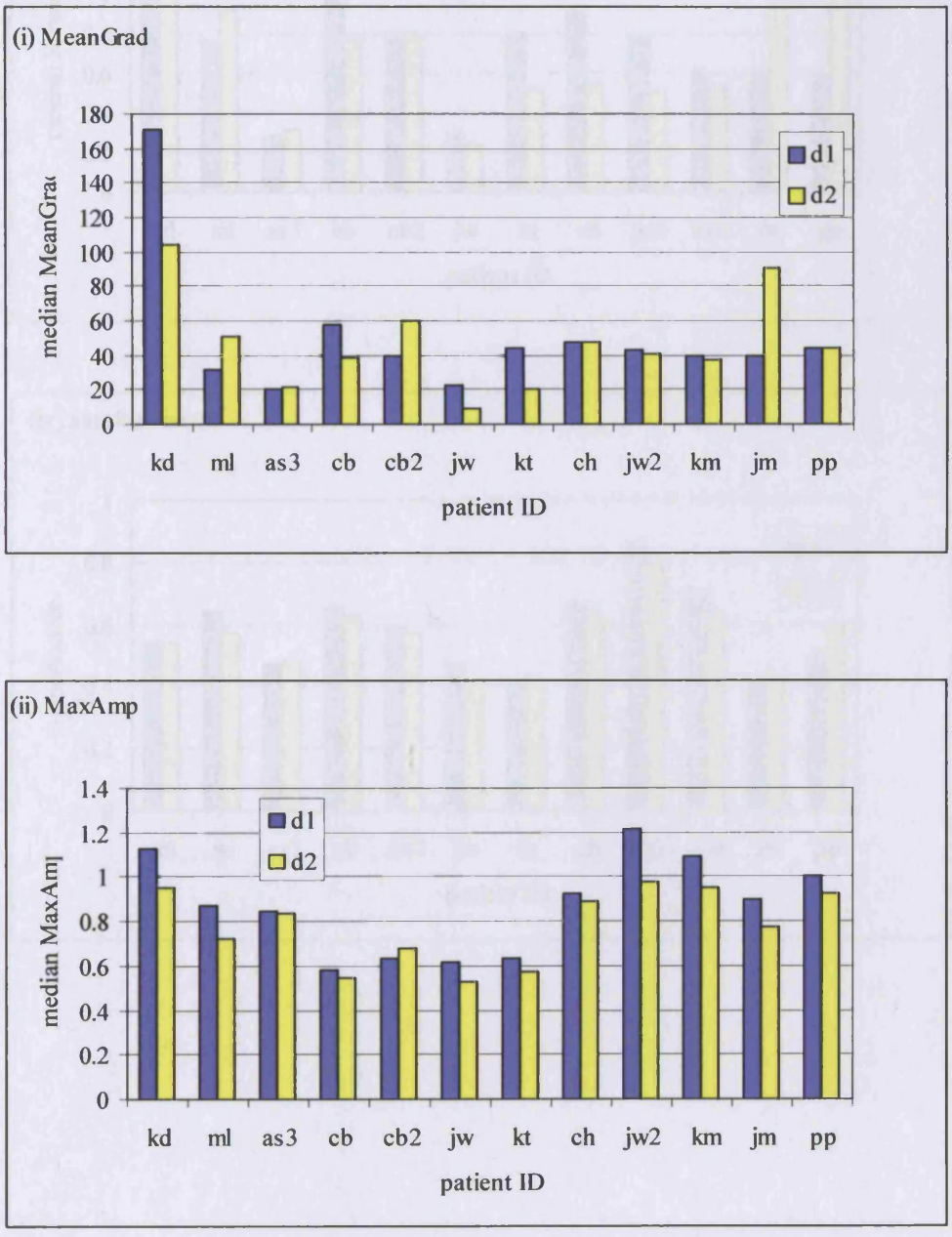

(iii) single-slice Ktrans

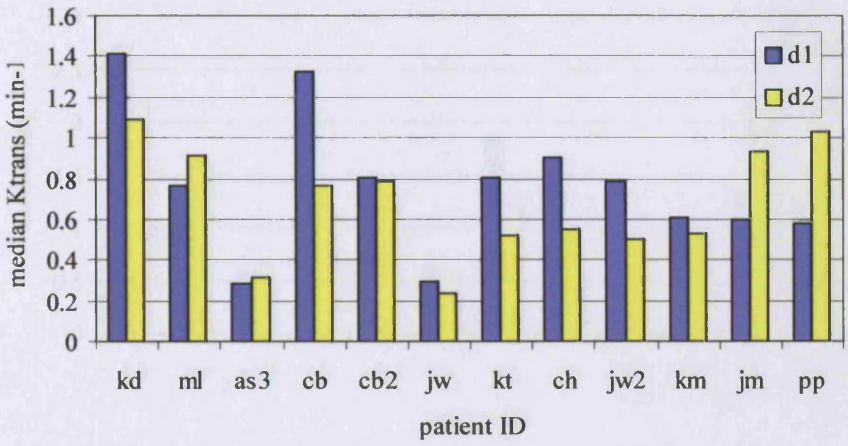

(iv) single-slice ve

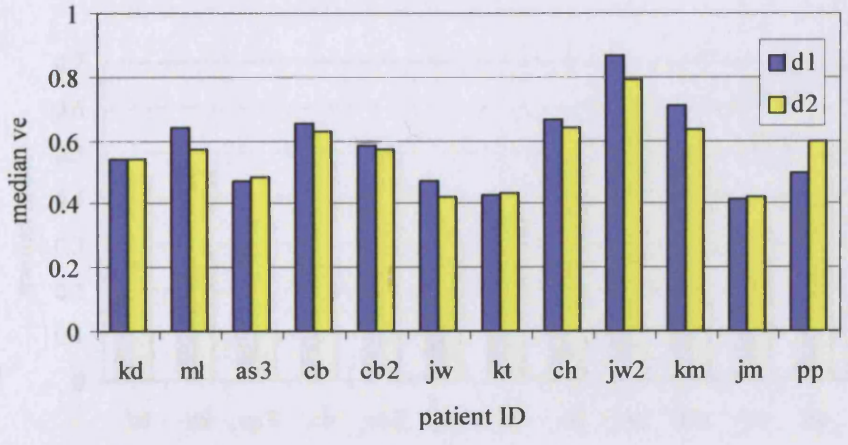

(v) single-slice kep

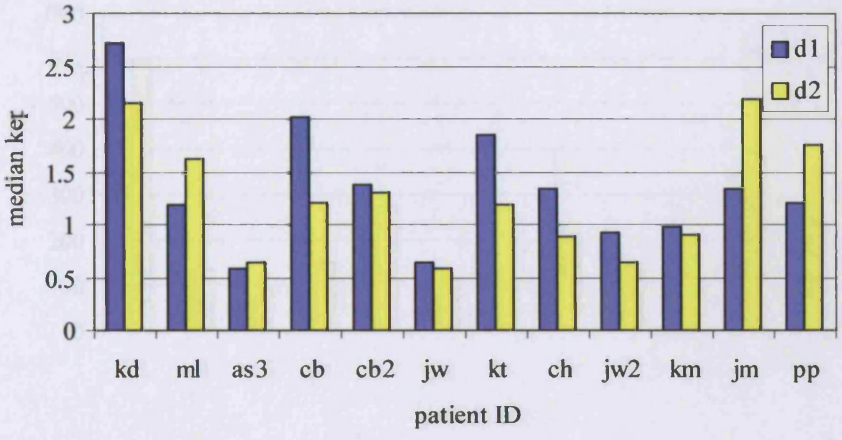

(vi) single-slice MaxGd

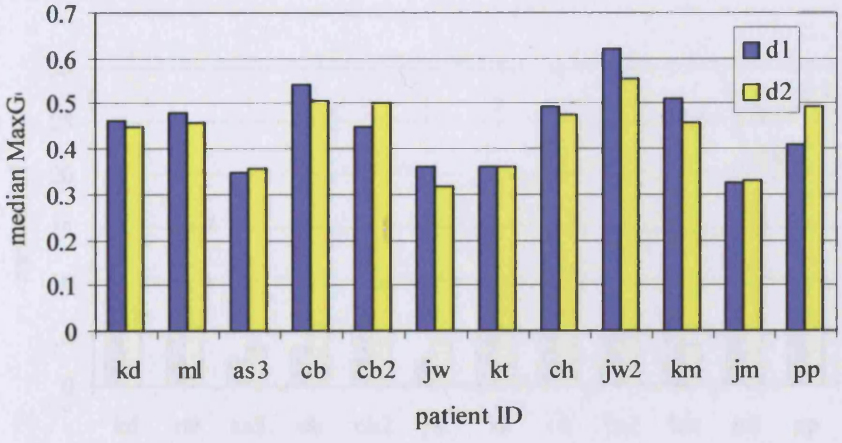

(vii) rBV

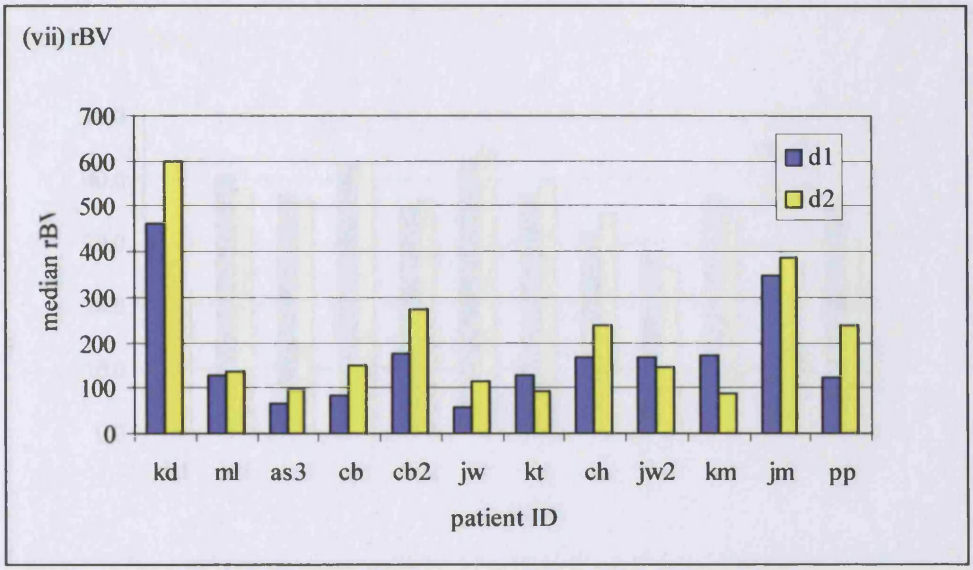

(viii) rBF

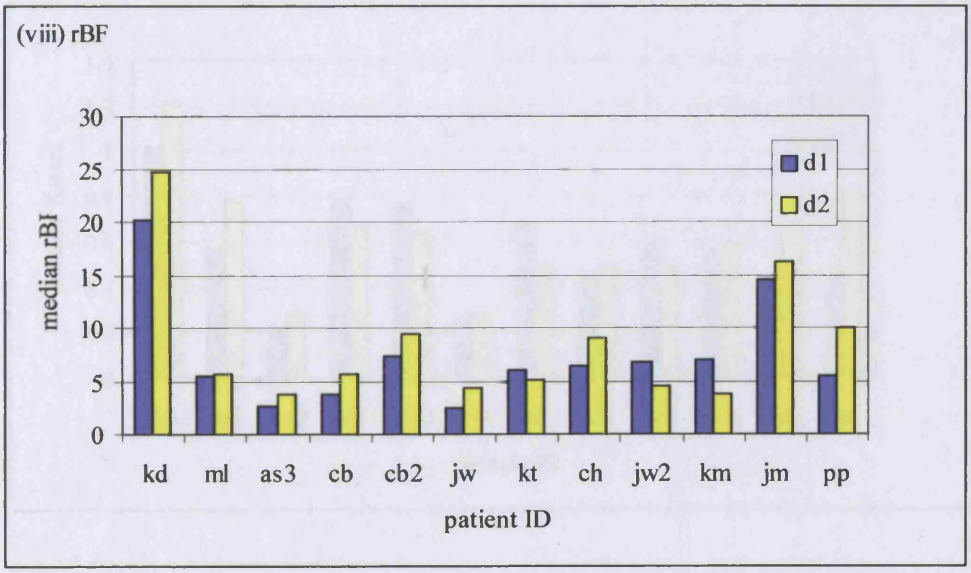

(ix) R2*

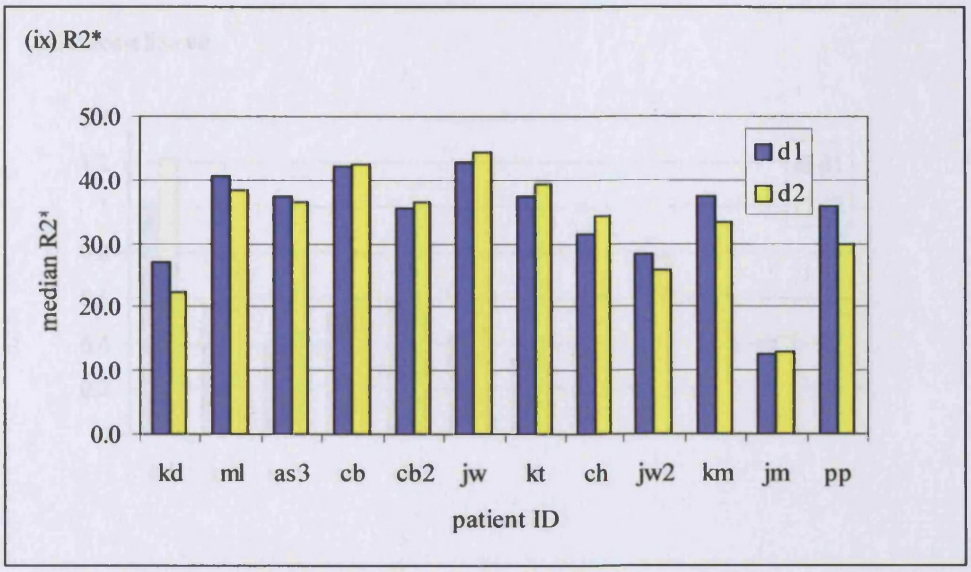

(x) three-slice Ktrans

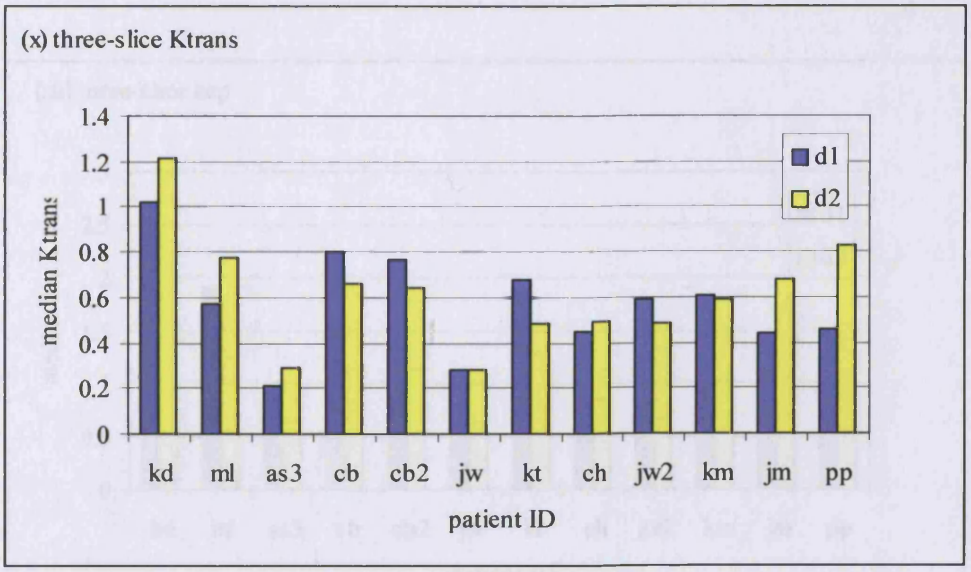

(xi) three-slice ve

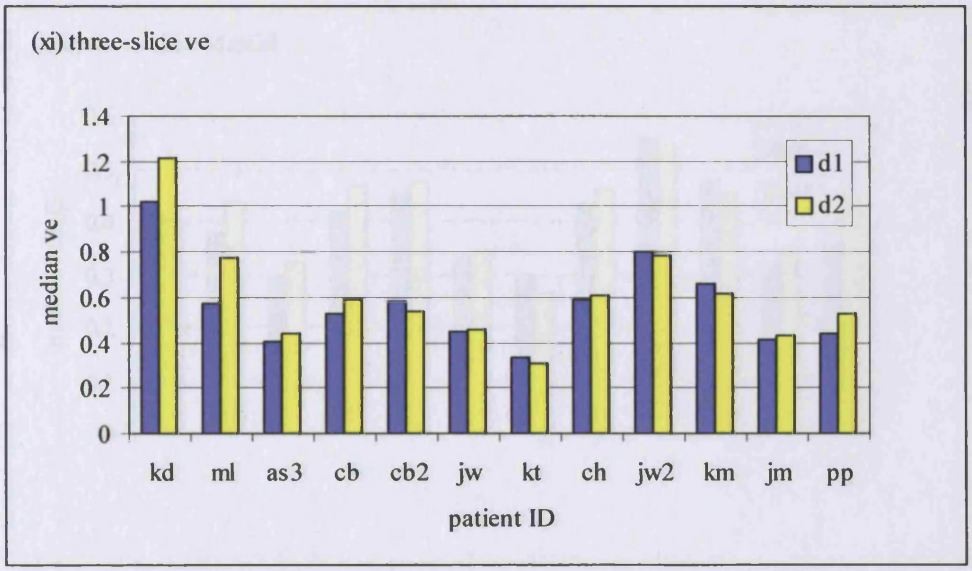

(xii) three-slice kep

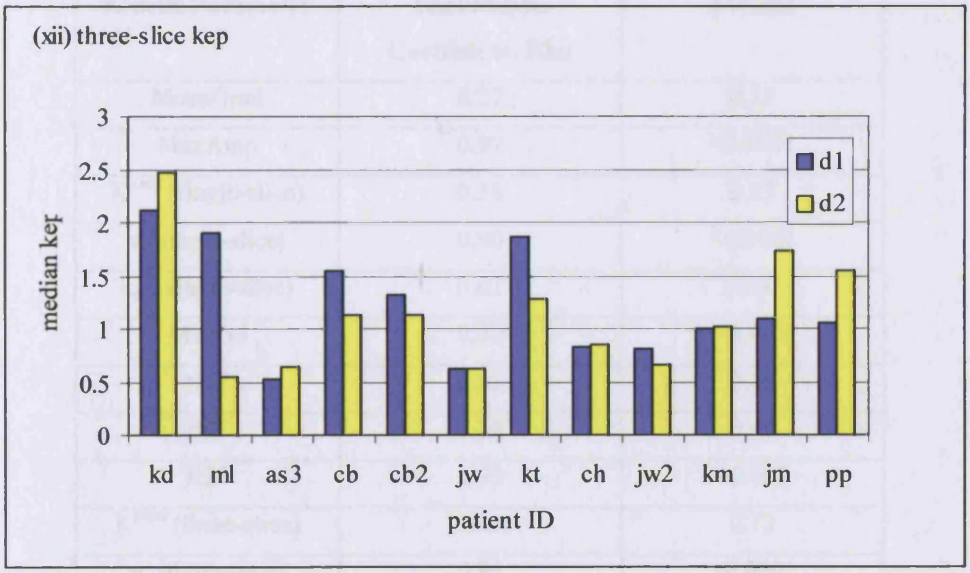

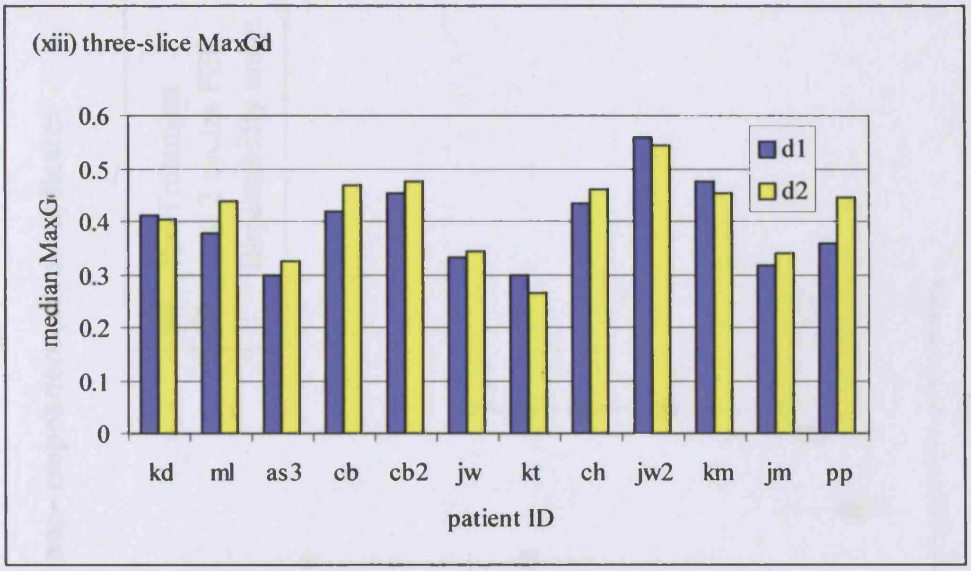

Kinetic Parameter	Spearman's Rank Correlation Coefficient, Rho	p-value
MeanGrad	0.27	0.38
MaxAmp	0.97	<0.0001
K^{trans} (single-slice)	0.36	0.25
v_e(single-slice)	0.90	<0.0001
k_{ep} (single-slice)	0.62	=0.03
MaxGd	0.80	=0.002
rBV	0.23	0.46
rBF	0.26	0.40
R2*	0.79	=0.003
K^{trans} (three-slice)	0.46	0.13
v_e (three-slice)	0.93	<0.0001
k_{ep} (three-slice)	0.50	0.09
MaxGd (three-slice)	0.92	<0.0001

Figure 2.21. Three-slice K^{trans} repeatability range applied to pathological non- responders (arrow indicates single incorrectly classified patient)

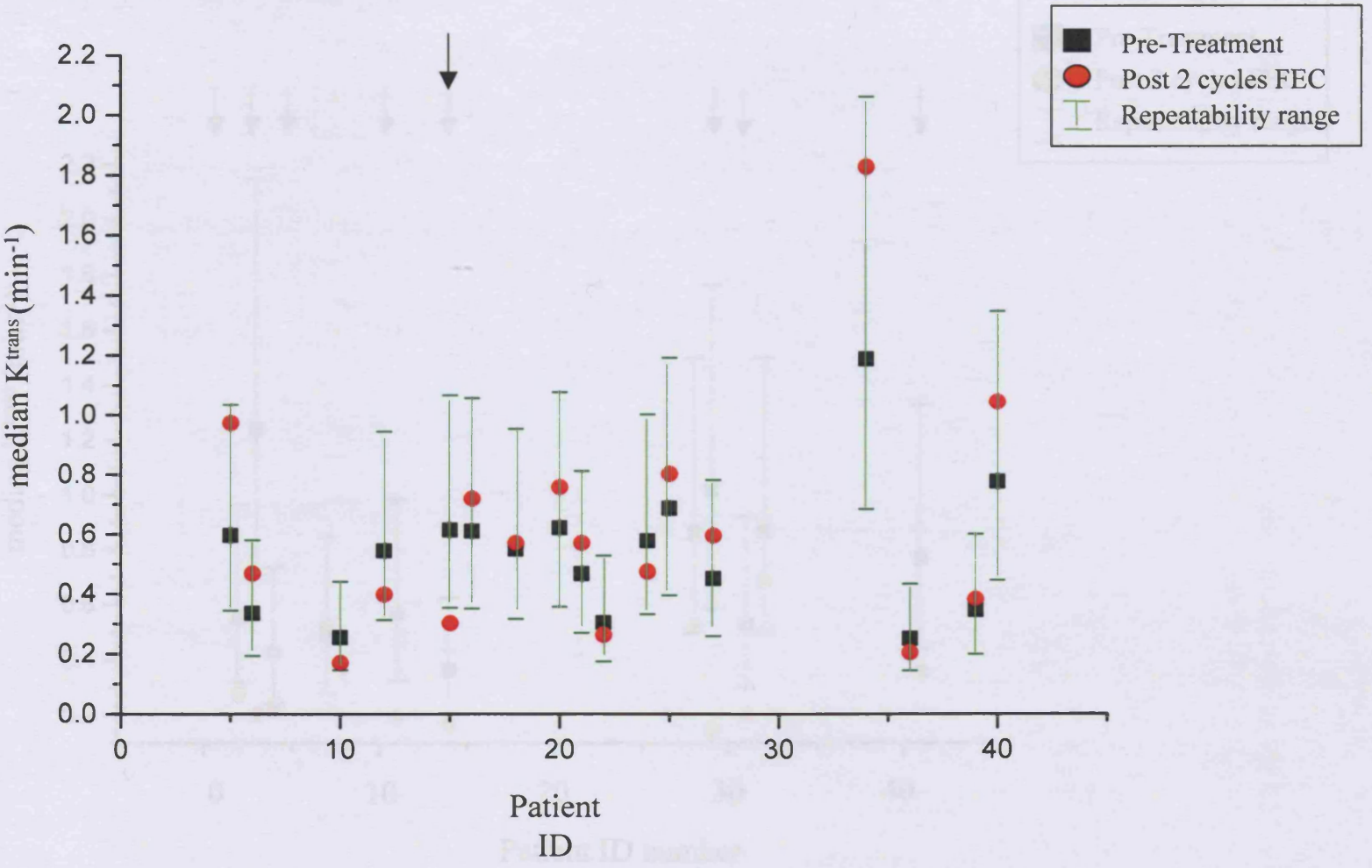

Figure 2.22. Three-slice K^{trans} repeatability range applied to pathological responders (arrows indicate correctly classified patients)

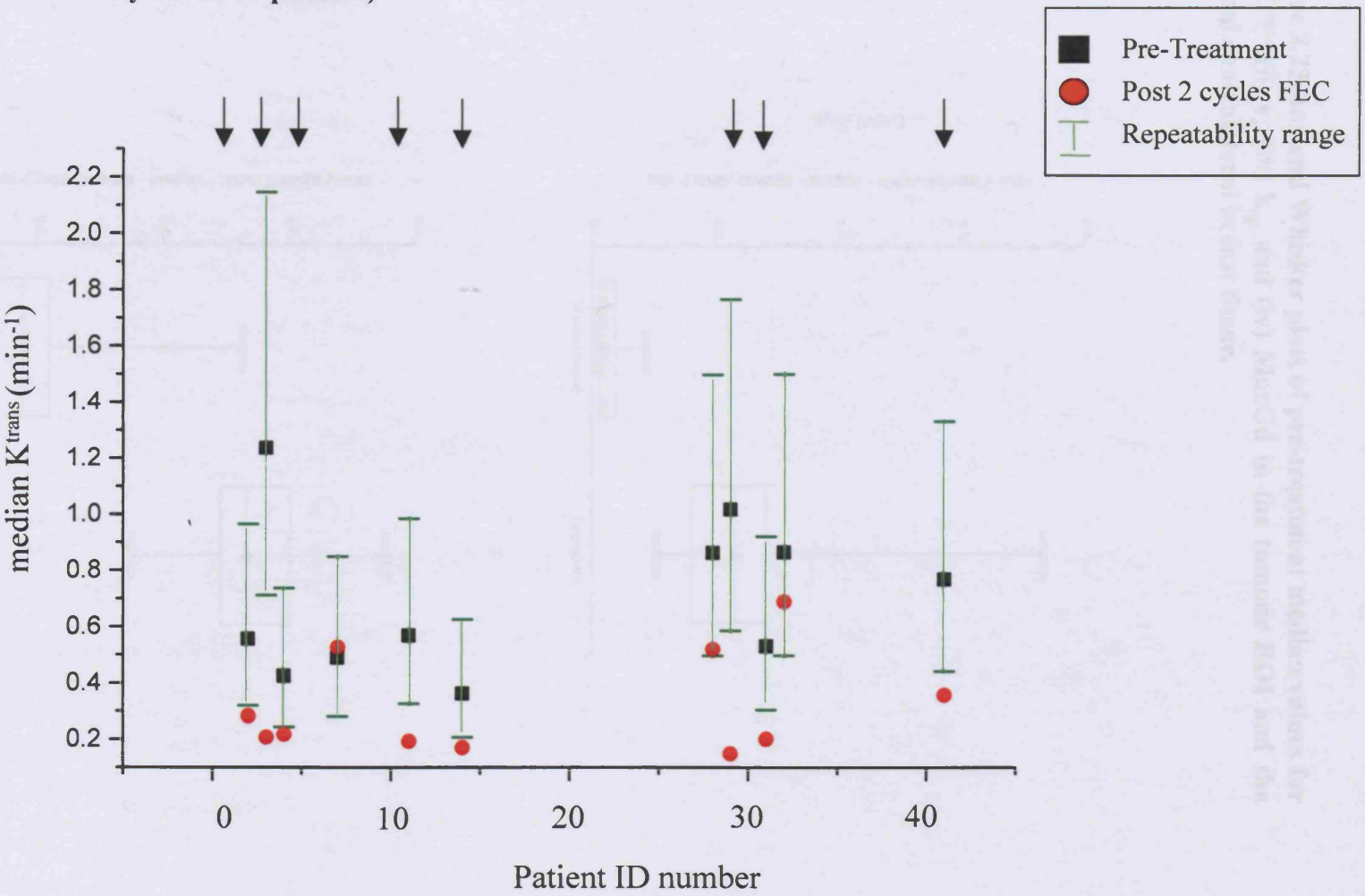

Figure 2.23 Box and Whisker plots of pre-treatment median values for (i) K^{trans} (ii) v_e (iii) k_{ep} and (iv) MaxGd in the tumour ROI and the normal contralateral breast tissue.

(i)

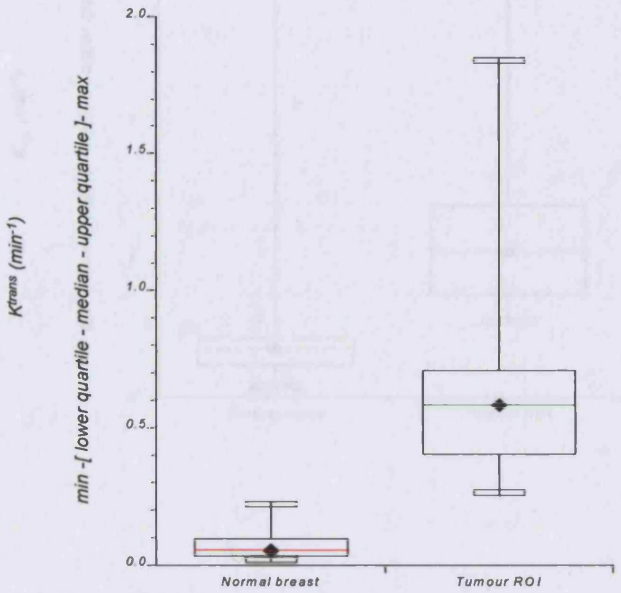

(ii)

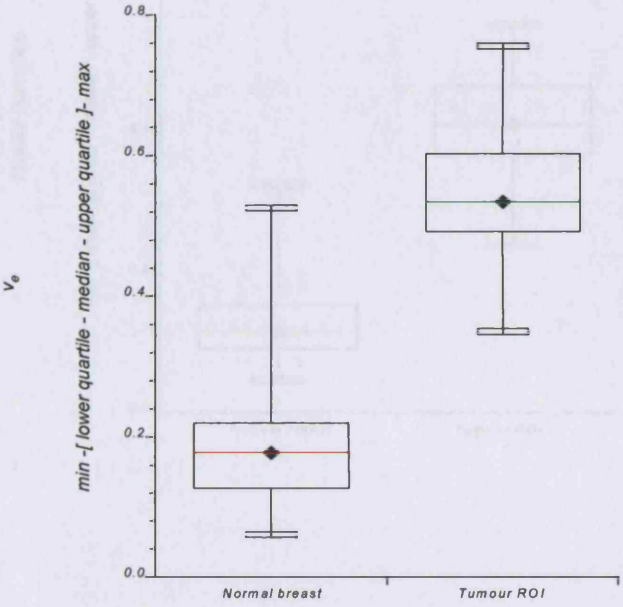

(iii)

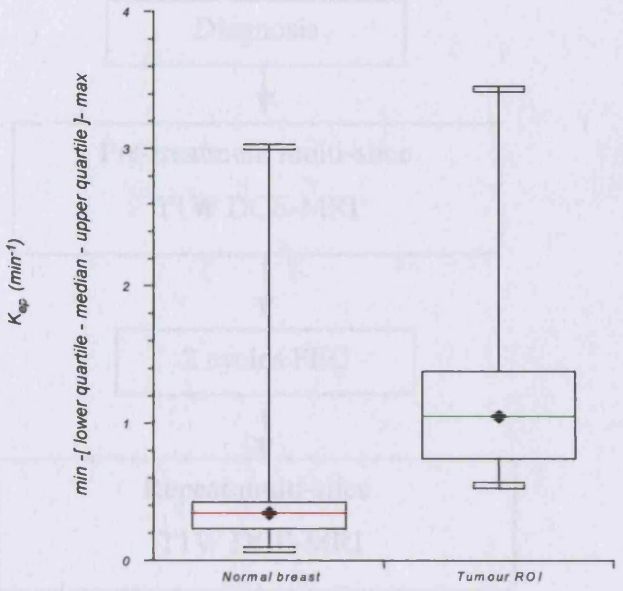
K_{ep} (min^{-1})
min -[lower quartile - median - upper quartile]- max
0
1
2
3
4
Normal breast
Tumour ROI

(iv)

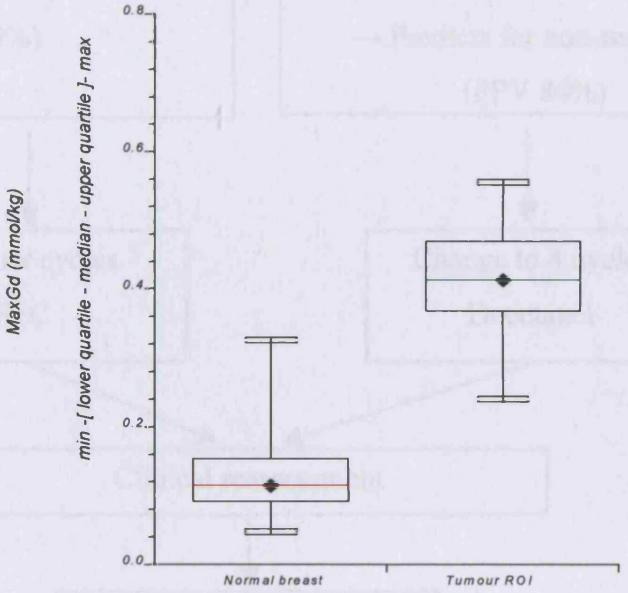
MaxGd (mmol/kg)
min -[lower quartile - median - upper quartile]- max
0.0
0.2
0.4
0.6
0.8
Normal breast
Tumour ROI

Figure 2.24. Multi-slice T1W DCE-MRI treatment intervention pathway

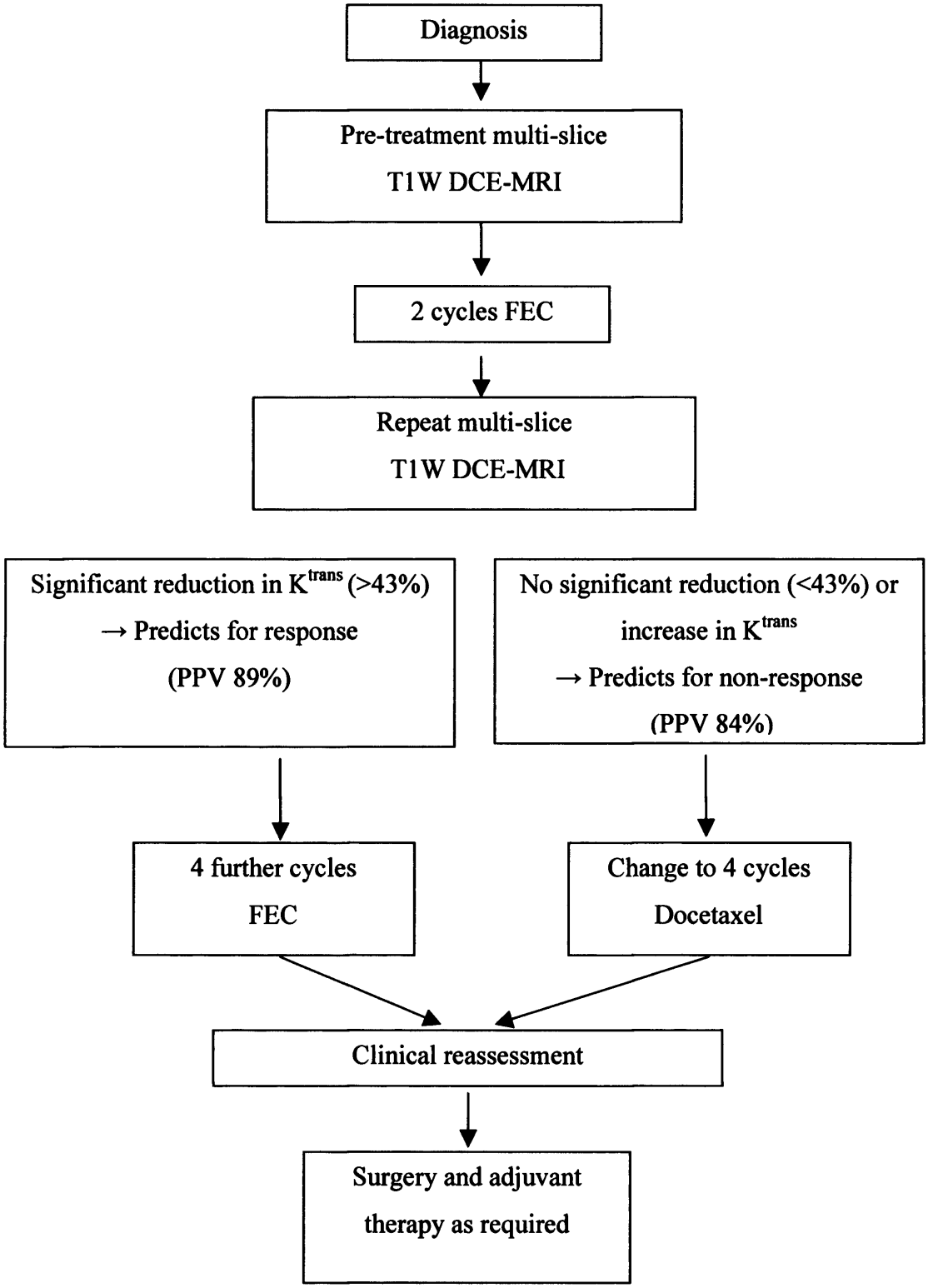

CHAPTER 3: IMMUNOHISTOCHEMICAL ASSESSMENT OF THE EFFECTS OF NEOADJUVANT CHEMOTHERAPY ON TUMOUR ANGIOGENESIS IN PRIMARY BREAST CANCER

3.1 INTRODUCTION

Angiogenesis is known to be a prerequiste for both tumour growth and metastases [93]. Angiogenesis is regulated by multiple stimulatory (pro-angiogenic) and inhibitory angiogenic factors or chemokines. In normal physiological angiogenesis there is a balance between these factors, however, in tumours it is postulated that an "angiogenic switch" leads to an imbalance of chemokines favouring angiogenesis. In breast tumours, the most potent pro-angiogenic factor is VEGF and tumour expression of VEGF has been shown to be of prognostic value [97, 100, 101, 103].

Microvessel density (MVD) is currently the best recognised method for assessing the intensity of tumour angiogenesis and the majority of studies with MVD have shown it to be an independent prognostic factor for both relapse-free and overall survival in patients with breast cancer [117, 120, 298]. A smaller number of studies have failed to demonstrate this association and possible explanations for this include type of endothelial antibody employed, the counting technique used and the region of tumour assessed [122]. A further explanation, however, may be that MVD provides only a static measure of the tumour vascular status rather than a measure of functional vascularity. Eberhard et al. addressed this issue of the "functional" status of tumour vessels and demonstrated that pericyte recruitment, as assessed by alpha-smooth muscle actin (α-SMA, indicates a difference in the functional status of the tumour vasculature which may reflect varying degrees of maturation of the tumour vascular bed [133].

This chapter describes a study evaluating the effect of neoadjuvant anthracycline-based chemotherapy on tumour angiogenesis through the assessment of tumour MVD, microvessel pericyte recruitment (pericyte coverage index, PCI) and the expression of VEGF in primary breast tumours.

The aims of the study were:

- To determine whether the angiogenesis-related parameters of tumour MVD, PCI and VEGF expression in diagnostic breast cancer core-biopsy specimens predict for clinical or pathological response to neoadjuvant 5-fluorouracil, epirubicin and cyclophosphamide (FEC) chemotherapy.

- To determine the changes in tumour MVD, PCI and VEGF expression following neoadjuvant FEC chemotherapy as assessed on surgical excision specimens and whether any changes relate to final clinical or pathological response.

- To assess the interrelationships between tumour MVD, PCI and VEGF expression in primary breast cancer before and after neoadjuvant FEC chemotherapy.

3.2 PATIENTS

Eligible patients for this study were those who had presented with primary breast cancer and had received neoadjuvant FEC chemotherapy prior to definitive surgery. Samples of the formalin-fixed paraffin-embedded pre-treatment diagnostic core biopsy and the post-chemotherapy resected tumour specimen were required for analysis. The study included patients recruited to the "Evaluation of MRI during neoadjuvant chemotherapy in primary breast cancer" study.

Pre-treatment diagnostic core biopsy specimens were available from 90 patients for CD34/α-SMA analysis. Of these patients, 62 also had samples available for VEGF analysis. The patient demographics are shown in **table 3.1.** Pre-treatment samples from an additional 9 patients who had received non-FEC neoadjuvant chemotherapy (n=6) or who had undergone primary surgery (n=3) were included in the comparison of pre-treatment VEGF with pre-treatment MVD and PCI.

Eighty paired pre- and post-neoadjuvant FEC chemotherapy breast specimens (diagnostic core biopsy and definitive surgical specimen respectively) were available for the assessment of MVD and PCI using CD34/α-SMA immunohistochemical doublestaining. The patient demographics are shown in **table 3.2.** Of these, 48 paired samples were available for VEGF assessment.

3.2.1 RESPONSE CRITERIA

3.2.1.1 Clinical response

Clinical response was evaluated from the bidimensional clinical measurements of the primary breast tumour prior to and following 6 cycles of FEC chemotherapy and was defined according to the UICC/WHO criteria (**appendix 1**) [290, 291] as follows:

Complete Response (cCR)	Disappearance of all known disease
Partial Response (cPR)	Decrease by at least 50% of the sum of the products of the largest perpendicular diameters of measurable lesions
Stable disease (cSD)	Less than 50% decrease and less than 25% increase in the sum of the products of the largest perpendicular diameters of measurable lesions
Progressive disease (cPD)	Increase of more than 25% in the size of a measurable lesion or appearance of a new lesion

For the study analysis, clinical responders were defined as those patients with cCR or cPR. Clinical non-responders were defined as those patients with cSD or cPD. This classification was in accordance with other clinical studies [24, 36]. Those patients who progressed during neoadjuvant chemotherapy, such that a

therapy change was instituted before completing six cycles of FEC chemotherapy, were defined as clinical non-responders (n=1).

3.2.1.2 Pathological response

Pathological response was evaluated by a single consultant pathologist (PIR) from a comparison of the pre-treatment core biopsy and the post-chemotherapy surgical resected specimen. Response was graded in accordance with previously described criteria [292-294]:

Pathological response	Description
Grade 1	No residual invasive cancer or DCIS (pathological CR)
Grade 2	Residual DCIS but no invasive cancer
Grade 3	Microscopic residual cancer
Grade 4	Macroscopic residual cancer with chemotherapy-induced changes and/or histological tumour response
Grade 5	Macroscopic invasive cancer with no response features

Chemotherapy-induced changes included (1) enlarged cells, (2) finely vacuolated "bubbly" voluminous cytoplasm, (3) enlarged vesicular nucleus with prominent single eosinophilic nucleolus, (4) occasionally enlarged hyperchromatic dense nucleus with an irregular outline, (5) compact hyalinized fibrous tissue at the site of good tumour response. Histological tumour response was an apparent reduction in tumour cell to stroma ratio. Examples of each grade of pathological response are shown in **figure 2.1**.

For the study analysis, pathological responders were defined as those patients with a grade 1, 2, 3 or 4 response. Pathological non-responders were defined as those patients with a grade 5 response.

3.3 MATERIALS AND METHODS

3.3.1 IMMUNOHISTOCHEMISTRY

3.3.1.1 Principle of the Avidin-Biotin Complex (ABC) method

Immunohistochemical staining was performed using the avidin-biotin complex (ABC) method. This method depends on the high affinity of avidin (streptavadin) for biotin via four binding site (dissociation constant 10^{-19}M). A biotinylated immunoglobulin is used as a link antibody. Biotinylation is a mild process where biotin molecules are covalently bound to the constant regions of

the heavy chain. Open sites on avidin on a separate pre-formed avidin-biotin enzyme complex bind to the biotin on the link antibody. Horseradish peroxidase (HRP) and alkaline phosphatase are commonly used as the enzyme labels within the pre-formed avidin-biotin enzyme complex. The sequence of reagent application is: primary antibody followed by biotinylated secondary antibody followed by pre-formed avidin-biotin enzyme complex.

3.3.1.2 Horseradish peroxidase (HRP)

In the presence of an electron donor, HRP activity results in the formation of an enzyme-substrate complex followed by oxidation of the electron donor. The electron donor provides the driving force in continuing catalysis of peroxidase, while its absence stops the reaction. There are several electron donors that become coloured insoluble products upon oxidation and these are known as chromogens. Diaminobenzine tetrahydrochloride (DAB) is a commonly used chromogen in peroxidase based immunohistochemistry and produces a brown insoluble end product on oxidation. When using HRP, endogenous cellular peroxidases must be blocked to ensure the stain is specific to bound antibody. This is done by bathing the samples in hydrogen peroxide before adding the primary antibody. HRP was used for CD34 staining in the CD34/α-SMA doublestaining technique and for the VEGF immunohistochemical staining.

3.3.1.3 Alkaline phosphatase

In the alkaline phosphatase immunostaining method, alkaline phosphatase hydrolyses naphthol phosphate esters (substrate) to phenolic compounds and phosphates. The phenols couple to colourless diazonium salts (chromogen) to product insoluble, coloured azo dyes. The Fast Red substrate-chromogen solution was used for α-SMA staining in the CD34/α-SMA doublestaining technique.

3.3.1.4 Doublestain immunohistochemistry for CD34 and α-SMA

The pre- and post-treatment pathological specimens for each patient were stained simultaneously. Paraffin-embedded sections, 4μm thick, were cut from tumour blocks and mounted onto microscope slides (Surgipath Europe Ltd, X-tra slides™). Slides were dewaxed in xylene for 5 minutes prior to rehydration through graded alcohols (100, 90, 70%) to water and then washed in tris buffer saline (50mmol tris-HCL)(TBS). Each section was encircled with a resin pen. The DAKO EnVision™ doublestain system (DakoCytochromation Ltd, UK, K1395) was used to perform the staining. The slides were incubated with 0.03% hydrogen peroxidase for 5 minutes to block endogenous peroxidase activity, then washed in water followed by TBS. Anti-CD34 mouse monoclonal antibody, QBend/10 (Novocastra Labs Ltd, UK, NCL-L-END™) diluted 1/50 in antibody diluent (DakoCytochromation Ltd, UK, S3022) was applied and the slides incubated for 30 minutes. The slides were washed with TBS and then labelled polymer, horseradish peroxidase (secondary antibody [mixed anti-mouse Ig and anti-rabbit Ig]) was applied for 30minutes. The slides were washed with TBS and then substrate-chromogen solution, liquid diaminobenzidine (DAB+), was applied for 3 minutes. The slides were washed with TBS and then incubated with a doublestain blocking reagent. Following washing with TBS, mouse monoclonal anti-actin, α- smooth muscle antibody (Sigma-Aldrich, UK, A 2547™) (anti-α-sm-1 or α-SMA) diluted 1/20 000 in antibody diluent (DakoCytochromation Ltd, UK, S3022) was applied for 60 minutes. The slides were washed in TBS and then incubated with labelled polymer, alkaline phosphatase (secondary antibody [mixed anti-mouse Ig and anti-rabbit Ig]) for 30 minutes. The slides were washed with TBS and then substrate-chromogen solution, Fast Red, was applied for 5 minutes. The slides were rinsed with water, counterstained with Gills haematoxylin (Surgipath Europe Ltd, 01500E) and coverslips were mounted using aqueous mounting medium (DakoCytomation Ltd, UK, Faramount Mounting Medium, S3025™). This process is demonstrated in **figure 3.1.a.** All immunohistochemical runs included a positive control slide (breast carcinoma).

3.3.1.5 Quantification of MVD and PCI

Vessel counting was performed at x 200 magnification. For each specimen, random fields were counted with a median number of 10 fields (range 4-30) in the core biopsy specimens and 8 fields (range 2-16) in the post-treatment tumour specimens. In the case of small core biopsies (n=20), vessel counting was performed on all fields (median 6.5; range 1-21). Five post-treatment specimens had minimal residual tumour and only a single field was assessable. Post-treatment specimens with a pathological CR (grade 1 pathological response) or only residual DCIS (grade 2 pathological response) were not included in the analysis as MVD and PCI were only assessed in areas with tumour cells.

For MVD, the number of microvessels (CD34 positive) per field were counted & expressed per mm^2 (1 field = $0.18mm^2$). Single endothelial cells, endothelial cell clusters and microvessels within the tumour, clearly separated from adjacent microvessels, were counted. Areas adjacent to DCIS were not counted. For PCI, the number of CD34 & α-SMA positive vessels (or endothelial cell(s)) were counted per field and expressed as a percentage of all CD34 positive vessels within that field. The median MVD and PCI for each specimen was used in the analysis. Examples of CD34/α-SMA doublestaining of breast tumour specimens are shown in **figure 3.1**.

3.3.1.6 Immunohistochemistry for VEGF

The pre- and post-treatment pathological specimens for each patient were stained simultaneously. Formalin-fixed paraffin-embedded sections, 4μm thick, were cut from tumour blocks and mounted onto microscope slides (Surgipath Europe Ltd, X-tra slides™). Slides were dewaxed in xylene for 5 minutes prior to rehydration through graded alcohols (100, 90, 70%) to water. Each section was encircled with a resin pen. Antigen retrieval was performed on the slides by placing them in a bath of TBS and boiling for 12 minutes in a 800W microwave oven (2450 MHz Panasonic NN-6453BBPQ). The volume of fluid was topped up to its original level and the slides were then left to stand for 10 minutes at

room temperature before being washed well in running tap water. Slides were then transferred to the Dako Autostaining machine (DakoCytochromation Ltd, UK) containing peroxidase block (DakoCytochromation Ltd, UK, S2023), the detection reagents (ChemMate™ HRP, DakoCytochromation Ltd, UK, K5001) and anti-human VEGF mouse monoclonal antibody (VEGF AB-7, NeoMarkers Inc., Fremont, USA) diluted 1/100 in antibody diluent (DakoCytochromation Ltd, UK, S3022). The autostainer programme included 5 minutes in peroxidase block, 1 hour incubation in primary antibody (anti-VEGF antibody), 30 minutes incubation in ChemMate™ secondary and tertiary reagents and 5 minutes in DAB substrate. When the programme was completed, stained slides were removed from the machine, washed with water and counterstained with Gills haematoxylin (Surgipath Europe Ltd, 01500E). The slides were then washed in water, dehydrated in graded alcohols (70, 90, 100%) and mounted in DPX (Surgipath Europe Ltd, 08600E). All immunohistochemical runs included a positive control slide (breast carcinoma).

3.3.1.7 Quantification of VEGF staining

Quantification of VEGF staining was performed by two observers at one sitting. A VEGF immunoreactive score (IRS) was devised to quantify the degree of VEGF staining in a similar manner to described elsewhere[174]. The VEGF IRS was calculated as the product of the intensity of VEGF scoring and the percentage of cells staining. The intensity of VEGF staining was scored as: negative=0, weak=1, moderate=2, strong=3. The percentage of cells staining was scored as: 0% = 0, <5% = 1, 5-20% = 2, 20-50% = 3, >50% = 4. Thus the possible range of VEGF IRS was from 0 to 12 (**figure 3.2**). Examples of tumour specimens with different VEGF IRS are shown in **figure 3.3**.

3.4 STATISTICAL ANALYSIS

Statistical analysis was performed using the StatsDirect statistical package (StatsDirect, Cheshire, UK). The relationship between MVD count, PCI and VEGF expression was quantified using Spearman's rank correlation coefficient, Rho. Pre-treatment and change in MVD, PCI and VEGF according to clinical & pathological response to 6 cycles of neoadjuvant FEC was assessed using the Mann-Whitney U-test (MW). Change in MVD, PCI and VEGF following chemotherapy in the whole group was evaluated using the Wilcoxon's signed ranks test. Pre-treatment MVD, PCI and VEGF according to clinical and pathological subgroups was evaluated using the Kruskal-Wallis test (KW). A p-value <0.05 was required for statistical significance.

3.5 RESULTS

3.5.1 PRE-TREATMENT ANGIOGENESIS-RELATED PARAMETERS TO PREDICT RESPONSE

3.5.1.1 Pre-treatment microvessel density and pericyte coverage index

Ninety pre-treatment (diagnostic) core-biopsy breast tumour samples taken from patients prior to receiving neoadjuvant FEC chemotherapy were available for intratumoural MVD and PCI assessment. The median MVD was 76.9/mm^2 (range 6.25 – 493.8/mm$^{2;}$ interquartile range 47.8 – 107.6/mm^2) and the median PCI was 18.7% (range 0 - 66.7%; interquartile range 6.7 – 31.3%). No correlation was found between the pre-treatment MVD and pre-treatment PCI (Rho = -0.12, p = 0.27).

3.5.1.2 Pre-treatment MVD and PCI according to clinical response

Of the 90 patients, there were 71 clinical responders and 19 clinical non-responders. The median MVD in the clinically responding patient group (n = 71)

was 75/mm^2 (range 9.26 – 493.8/mm^2; interquartile range 44.4 – 108.3/mm^2) and in the clinically non-responding group (n = 19) was 86.1/mm^2 (range 6.3 – 242.6/mm^2; interquartile range 58.3 – 116.7/mm^2). This difference was not statistically significant (MW, p = 0.49). The median PCI in the clinically responding group (n = 71) was 18.3% (range 0 – 66.7%; interquartile range 6.7 – 31.7%) and in the clinically non-responding group (n = 19) was 21.5% (range 0 – 40%; interquartile range 3.2 – 33.3%). This difference was not statistically significant (MW, p = 0.98). These results are shown in **table 3.3** and illustrated using Box and Whisker plots in **figure 3.4**. No association was found between the pre-treatment MVD or PCI and the clinical response subgroups CR, PR, PD or SD (KW, p=0.45 and p= 0.61 respectively) (**figure 3.5**).

3.5.1.3 Pre-treatment MVD and PCI according to pathological response

Of the 90 patients, 86 underwent surgery following neoadjuvant chemotherapy. There were 27 pathological responders and 59 pathological non-responders. The median MVD in the pathologically responding patient group (n = 27) was 77.8/mm^2 (range 9.26 – 242.6/mm^2; interquartile range 41.7 – 122.8/mm^2) and in the pathologically non-responding group (n = 59) was 75/mm^2 (range 6.3 – 493.8/mm^2; interquartile range 50 – 105.6/mm^2). This difference was not statistically significant (MW, p = 0.87). The median PCI in the pathologically responding group (n = 27) was 13.6% (range 0 – 66.7%; interquartile range 7.8 – 29.8%) and in the pathologically non-responding group (n = 59) was 21.4% (range 0 – 54.5%; interquartile range 3.2 – 33.3%). Again, this difference was not statistically significant (MW, p = 0.84). These results are shown in **table 3.4** and illustrated using Box and Whisker plots in **figure 3.6**. No association was found between the pre-treatment MVD or PCI and the pathological response subgroups 1 to 5 (KW, p=0.36 and p=0.92 respectively) (**figure 3.7**).

3.5.1.4 Pre-treatment Tissue Vascular Endothelial Growth Factor

Sixty-two pre-treatment (diagnostic) core-biopsy breast tumour samples taken from patients prior to receiving neoadjuvant FEC chemotherapy were available for vascular endothelial growth factor (VEGF) assessment. Tissue VEGF was scored using the VEGF immunoreactive score (IRS) as described in section 3.3.1.7 and illustrated in **figure 3.2**. The median VEGF IRS was 6 (range 0 – 12; interquartile range 4 - 9).

3.5.1.5 Pre-treatment tissue VEGF according to clinical response

Of the 62 patients, there were 50 clinical responders and 12 clinical non-responders. The median VEGF IRS in the clinically responding patient group (n = 50) was 6 (range 0 – 12; interquartile range 4 - 9) and in the clinically non-responding group (n = 12) was also 6 (range 3 – 12; interquartile range 4 - 9). There was no significant difference between the clinical responders and non-responders (MW, p = 0.87) (**table 3.5** and **figure 3.8**). No association was found between the pre-treatment VEGF and the clinical response subgroups CR, PR, PD or SD (KW, p=0.78) (**figure 3.9**).

3.5.1.6 Pre-treatment tissue VEGF according to pathological response

Of the 62 patients, 59 underwent surgery following neoadjuvant chemotherapy. There were 19 pathological responders and 40 pathological non-responders. The median VEGF IRS in the pathologically responding patient group (n = 19) was 8 (range 2 – 12; interquartile range 4 - 12) and in the pathologically non-responding group (n = 40) was 4 (range 0 – 12; interquartile range 4 - 8). This difference was not statistically significant (MW, p = 0.32). These results are shown in **table 3.6** and illustrated using Box and Whisker plots in **figure 3.10**. No association was found between the pre-treatment VEGF and the pathological response subgroups 1 to 5 (KW, p=0.73) (**figure 3.9**).

3.5.1.7 Correlation of pre-treatment tissue VEGF, MVD and PCI

Seventy-one pre-treatment core-biopsy breast tumour samples taken from patients prior to receiving either NAC (n = 68) or primary surgery (n = 3), were assessed for the relationship between tumour VEGF and both MVD and PCI. The median values (range; interquartile range) were: VEGF IRS, 8 (0 – 12; 4 - 12); MVD, 75/mm^2 (6.3 – 400/mm^2; 45.4 – 105.2/mm^2); and PCI, 18.3% (0 – 66.7%; 6.7 – 31.6%). There was a trend towards a positive correlation between VEGF and MVD (Rho= 0.22, p = 0.06) (**figure 3.11**). No correlation was seen between VEGF and PCI (Rho= -0.09, p = 0.45) (**figure 3.12**).

3.5.2 CHANGES IN ANGIOGENESIS-RELATED PARAMETERS FOLLOWING NAC

3.5.2.1 Changes in MVD and PCI following NAC

Eighty paired pre- and post-neoadjuvant FEC chemotherapy breast specimens (diagnostic core biopsy with corresponding surgical resection specimen) were available for assessment of MVD and PCI. The median (range; interquartile range) pre-treatment MVD and PCI values were **76.4/mm^2** (6.25 – 493.8/mm^2; 46.5 – 106.6/mm^2) and **17.3%** (0 – 66.7%; 6.6 – 30.4%) respectively. The median (range; interquartile range) post-treatment MVD and PCI values were **72.2/mm^2** (25 – 261.1/mm^2; 50 – 100/mm^2) and **25.5%** (0 – 100%; 18.2 – 43.3%) respectively. There was no significant difference between the pre- and post-treatment MVD values (Wilcoxon's signed rank test, p = 0.48). However, there was a statistically significant difference between the pre- and post-treatment PCI values (Wilcoxon's signed rank test, p<0.0001) with a significant increase in PCI following chemotherapy. These results are shown in **table 3.7** and illustrated using Box and Whisker plots and Ladder plots in **figures 3.13** and **3.14**.

3.5.2.2 Change in MVD and PCI according to response

3.5.2.2.1 Clinical response

Of the 80 patients with pre- and post-treatment evaluations, there were 62 clinical responders and 18 clinical non-responders. The median change in MVD following chemotherapy was 0 (range -393.8 to 138.9; interquartile range -25 to 23.4) in the clinical responders and –19.4 (range -129.6 to 172.2; interquartile range -50.9 to 16.7) in the clinical non-responders. This difference was not statistically significant (MW, p = 0.18). The median change in PCI following chemotherapy was 11.1 (range -34.0 to 88.2; interquartile range -1.7 to 28.6) in the clinical responders and –1.1 (range -33.3 to 37.5; interquartile range -7.5 to 12.2) in the clinical non-responders. This difference tended towards statistical significant (MW, p = 0.052). These results are summarised in **table 3.8** and illustrated using Box and Whisker plots in **figure 3.15**.

3.5.2.2.2 Pathological response

Of the 80 patients with pre- and post-treatment evaluations, there were 24 pathological responders and 56 pathological non-responders. The median change in MVD following chemotherapy was –1.1 (range -163.9 to 113.9; interquartile range -29.9 to 33.1) in the pathological responders and –4.2 (range -393.8 to 172.2; interquartile range -34.0 to 22.2) in the pathological non-responders. This difference was not statistically significant (MW, p = 0.61). The median change in PCI following chemotherapy was 12.9 (range -34.0 to 88.2; interquartile range -0.2 to 35.5) in the pathological responders and 7.9 (range -33.3 to 77.1; interquartile range -6.4 to 22.7) in the pathological non-responders. This difference was not statistically significant (MW, p = 0.14). These results are summarised in **table 3.9** and illustrated using Box and Whisker plots in **figure 3.16**.

3.5.2.3 Changes in VEGF following NAC

Forty-eight paired pre- and post-neoadjuvant FEC chemotherapy breast specimens (diagnostic core biopsy with corresponding surgical resection specimen) were available for assessment of tissue VEGF. The median pre- and

post-treatment VEGF IRS was 6 (range 0 – 12; interquartile range 4 - 9) and 4 (range 0 – 12; interquartile range3 - 6) respectively. This difference between the pre- and post-treatment VEGF IRS was found to be statistically significant (MW, p = 0.002) (**table 3.10** and **figure 3.17**).

3.5.2.4 Change in VEGF according to response

3.5.2.4.1 Clinical Response

Of the 48 patients, there were 39 clinical responders and 9 clinical non-responders. The median change in VEGF IRS following chemotherapy was -2 (range -10 to 6; interquartile range -4 to 0) in the clinical responders and -2 (range -8 to 5; interquartile range -3 to 0) in the clinical non-responders. There was no significant difference in the two groups (p = 0.78) (**table 3.11** and **figure 3.18**).

3.5.2.4.2 Pathological Response

Of the 48 patients, there were 14 pathological responders and 34 pathological non-responders. The median change (range; interquartile range) in VEGF IRS following chemotherapy was -3 (-9 to +1; -5 to 0) in the pathological responders and –1(-10 to +6; -4 to 0) in the pathological non-responders. This difference was not statistically significant (p = 0.32) (**table 3.12** and **figure 3.19**).

3.6 DISCUSSION

Angiogenesis is critical for the growth and metastasis of solid tumours. Novel therapies under investigation for the treatment of cancer have included those that specifically target the tumour vasculature. These have been divided into two main groups: the vascular targeting agents, which work by directly damaging the existing tumour vasculature; and the antiangiogenic agents, which inhibit the process of neovascularisation. These new treatments differ from the conventional cytotoxic chemotherapeutic agents which act directly on the

tumour cells inducing DNA damage and hence cell death. It is anticipated that future anticancer therapies involving antivascular agents will involve a combination of these agents with conventional chemotherapy. As a result, knowledge of the vascular effects of conventional chemotherapeutic agents is important and might help, for example, in the design of rational drug combinations and sequencing.

The treatment of primary breast cancer with neoadjuvant chemotherapy, prior to definitive surgery, provides an ideal in vivo model for assessing the effects of treatment with tumours in situ. Using this treatment model, Makris et al. previously demonstrated a significant reduction in MVD, as assessed by Chalkley point counting, following neoadjuvant chemotherapy [128]. In absolute terms, however, the difference in median scores on the Chalkley count between tumours treated with neoadjuvant chemotherapy and those not treated was only 0.6 (median score 5.7 and 6.3 respectively). This small difference may reflect the fact that MVD can only provide a static quantitative measure of tumour vascularity and fails to provide a qualitative measure of vascular function, that is, the extent of actively proliferating angiogenic vessels. Indeed, it may be that the functional vascular status of a tumour, in terms of the proportion of actively proliferating ("immature") to non-proliferating ("mature") vessels is more important for predicting both response to treatment and long-term outcome than the total number of vessels alone. Bottini et al. also demonstrated a modest but significant reduction in MVD following NAC (pre-treatment median 51.26/mm^2 and post-treatment median 44.27/mm^2) but this change did not correlate with tumour response [129]. In both series, MVD was counted in the area of highest vascular density, the so-called "vascular hotspot".

The aim of this study was to evaluate the effect of neoadjuvant chemotherapy on tumour vascularity in primary breast cancers in a group of women treated uniformly with conventional anthracycline-based chemotherapy (5-fluorouracil, epirubicin and cyclophosphamide [FEC]). In particular, an assessment of the effect on both quantitative and qualitative vascular measures was performed using the parameters MVD and PCI. In physiological angiogenesis, the acquisition of pericyte coverage on endothelial tubes leads to vessel

remodelling, maturation and stabilisation [299]. The relationship between pericytes and endothelial cells in tumour microvessels remains unclear [98], however, pericyte recruitment to tumour vessels does still appear to reflect vessel maturation [133, 137]. Therefore, for this study, the functional vascular status of the breast tumours was assessed using the CD34/α-SMA doublestaining immunohistochemical technique, where mature vessels were defined as those staining with antibodies to both CD34 and α-SMA, and immature vessels as those staining only for CD34. The pericyte coverage index (PCI), defined as the fraction of mature vessels to the total number of vessels (expressed as a percentage), was used as the measure of the functional vascular status. Thus, a low PCI represented a more actively proliferating vascular bed compared with a high PCI. Unlike the previous studies [128, 129], MVD and PCI were calculated from random (or total) fields for each pathological sample rather that from hotspots, in order to inform upon the global effect of NAC on tumour vascularity. The effect of NAC on the expression of the pro-angiogenic factor VEGF was also assessed.

Evaluation of the pre-treatment diagnostic core biopsy specimens revealed that neither MVD, PCI nor VEGF expression predicted for clinico-pathological response to NAC. Further, no correlation was found between MVD and PCI. There was a non-significant trend towards a positive correlation between MVD and VEGF expression ($p=0.06$) which may reflect the significant role VEGF plays in driving tumour angiogenesis within breast tumours. No correlation was found between PCI and VEGF expression.

Following neoadjuvant FEC chemotherapy, no significant change was seen in MVD however, a significant increase in the PCI was observed from 17.3% to 25.5% ($p<0.0001$). This would suggest that despite no apparent alteration in the total number of tumour microvessels following NAC, the quality of the microvessels does change. NAC appears to have a "pruning" effect on immature proliferating vessels resulting in an increase in the proportion of mature, stabilised vessels. Following NAC, a significant reduction in VEGF expression was also observed, with the median VEGF IRS falling from 6 to 4 ($p=0.002$).

The mechanism of action producing this vascular effect is unclear but two possibilities exist:

(1) a direct anti-angiogenic effect of chemotherapy on proliferating microvessels, or

(2) an indirect effect of chemotherapy via tumour cell death, leading to a reduction in the production of the pro-angiogenic cytokines, such a VEGF, that support tumour angiogenesis.

This "pruning" effect on immature proliferating vessels has been observed in studies using antiangiogenic agents, in particular the anti-VEGF agents [300-303], and has been termed vascular "normalisation" [304]. The immature, functionally abnormal tumour blood vessels are cut back through the elimination of endothelial cells, resulting in a more "normal" and hence more efficient vasculature. The "normalised" vasculature remains functionally less effective than its normal counterpart but the change does lead to in an improvement in nutrient and drug delivery to the tumour bed. The changes observed in PCI in this study therefore suggest that anthracycline-based NAC may be inducing a similar effect and that this effect may be mediated through a reduction in VEGF production subsequent to tumour cell death.

When change in MVD and PCI was assessed according to final clinical response to NAC, no difference in MVD was observed, however, a non-significant trend was seen towards an increase in PCI in the clinically responding group compared with the clinically non-responding group (median change in PCI 11.1% and –1.1% respectively, MW, p=0.052). No significant difference was seen when change in either MVD or PCI was assessed according to final pathological response to NAC. Similarly, change in VEGF expression did not correlate with final clinical or pathological response to NAC. These findings suggest that the vascular changes observed in this patient cohort, were not directly contributing to tumour shrinkage with the possible exception of clinical tumour response. This corresponds to the findings from Bottini et al. [129] where the reduction in MVD did not correlate with tumour response but is at odds with findings from Marson et al. [131], where a significant correlation was found between percentage change in MVD and percentage reduction in tumour volume, however, this was in response to tamoxifen therapy.

In summary, therefore, this study demonstrated that neoadjuvant anthracycline-based chemotherapy leads to an alteration in the functional quality of the vascular bed in primary breast cancers with an increase in the proportion of mature microvessels but with no significant effect on the total number of microvessels. An associated reduction in tumour VEGF expression was also observed and may reflect the possible mechanism of action for these vascular changes. No correlation was found between the change in MVD, PCI or VEGF and final clinico-pathological response to NAC suggesting that these vascular changes do not impact directly on tumour shrinkage. In addition, none of the pre-treatment parameter values were able to predict for final clinico-pathological response. The implications of these findings, in particular for combination therapy with antiangiogenic agents are addressed in the final discussion (chapter 5).

Table 3.1. Demographics of the patients with pre-treatment diagnostic core biopsy specimens available for CD34/α-SMA analysis

No. of patients	90	
Median age (range)	48 YEARS (25 – 70)	
Menopausal status	PRE	51
	PERI	12
	POST	27
Stage	II	68
	III	22
GRADE	1	6
	2	33
	3	39
	UNKNOWN	12
ER status	POSITIVE	64
	NEGATIVE	23
	NOT KNOWN	3
PgR status	POSITIVE	45
	NEGATIVE	27
	NOT KNOWN	18
Clinical response	CR	18
	PR	53
	SD	14
	PD	5
Overall clinical response	RESPONDERS	71
	NON-RESPONDERS	19
Pathological response	GRADE 1	1
	GRADE 2	1
	GRADE 3	16
	GRADE 4	9
	GRADE 5	59
	NO SURGERY	4
Overall pathological response (n=86)	RESPONDERS	27
	NON-RESPONDERS	59

Table 3.2. Demographics of the patients with paired pre- and post-treatment specimens available for CD34/α-SMA analysis

No. of patients	**80**	
Median age (range)	**47 YEARS (29 – 70)**	
Menopausal status	**PRE**	**46**
	PERI	**12**
	POST	**22**
Stage	**II**	**59**
	III	**21**
GRADE	**1**	**6**
	2	**29**
	3	**37**
	UNKNOWN	**8**
ER status	**POSITIVE**	**58**
	NEGATIVE	**19**
	NOT KNOWN	**3**
PgR status	**POSITIVE**	**41**
	NEGATIVE	**23**
	NOT KNOWN	**16**
Clinical response	**CR**	**14**
	PR	**48**
	SD	**14**
	PD	**4**
Overall clinical response	**RESPONDERS**	**62**
	NON-RESPONDERS	**18**
Pathological response	**GRADE 1**	**0**
	GRADE 2	**0**
	GRADE 3	**15**
	GRADE 4	**9**
	GRADE 5	**55**
Overall pathological response	**RESPONDERS**	**24**
	NON-RESPONDERS	**56**

Table 3.3. Pre-treatment MVD and PCI according to clinical response

	MVD (interquartile range)	PCI (interquartile range)
Clinical responders (n=71)	75/mm^2 (44.4 – 108.3)	18.3% (6.7 – 31.7)
Clinical non-responders (n=19)	86.1/mm^2 (58.3 – 116.7)	21.5% (3.2 – 33.3)
p-value (Mann-Whitney)	0.49	0.98

Table 3.4. Pre-treatment MVD and PCI according to pathological response

	MVD (interquartile range)	PCI (interquartile range)
Pathological responders (n=27)	77.8/mm^2 (41.7 – 122.8)	13.6% (7.8 – 29.8)
Pathological non-responders (n=59)	75/mm^2 (50 – 105.6)	21.4% (3.2 – 33.3)
p-value (Mann-Whitney)	0.87	0.84

Table 3.5. Pre-treatment tissue VEGF IRS according to clinical response

	Median VEGF IRS (range)
Clinical responders (n=50)	6 (0 – 12)
Clinical non-responders (n=12)	6 (3 – 12)
p-value (Mann-Whitney)	0.87

Table 3.6. Pre-treatment tissue VEGF IRS according to pathological response

	Median VEGF IRS (range)
Pathological responders (n=19)	8 (2 – 12)
Pathological non-responders (n=40)	4 (0 – 12)
p-value (Mann-Whitney)	0.32

Table 3.7. Pre- and post-treatment MVD and PCI

	Median MVD (range)	Median PCI (range)
Pre-treatment (n=80)	76.4/mm^2 (6.25 – 493.8)	17.3% (0 – 66.7)
Post-treatment (n=80)	72.2/mm^2 (25 – 261.1)	25.5% (0 – 100)
p-value (Wilcoxon's signed ranks test)	$p = 0.48$	$p < 0.0001$

Table 3.8. Change in MVD and PCI following neoadjuvant chemotherapy according to clinical response

	Median change in MVD (range)	Median change in PCI (range)
Clinical Responders (n=62)	0 (-393.8 to 138.9)	11.1 (-34.0 to 88.2)
Clinical Non-responders (n=18)	-19.4 (-129.6 to 172.2)	-1.1 (-33.3 to 37.5)
p-value (Mann-Whitney U-test)	0.18	=0.052

Table 3.9. Change in MVD and PCI following neoadjuvant chemotherapy according to pathological response

	Median change in MVD (range)	Median change in PCI (range)
Pathological Responders (n=24)	-1.1 (-163.9 to 113.9)	12.9 (-34.0 to 88.2)
Pathological Non-responders (n=56)	-4.2 (-393.8 to 172.2)	7.9 (-33.3 to 77.1)
p-value (Mann-Whitney U-test)	0.61	0.14

Table 3.10. Pre- and post-treatment VEGF IRS

	Median VEGF IRS (range; interquartile range)
Pre-treatment (n=48)	6 (0 – 12; 4 – 9)
Post-treatment (n=48)	4 (0 – 12; 3 – 6)
p-value (Wilcoxon's signed ranks test)	p = 0.002

Table 3.11. Change in VEGF IRS following neoadjuvant chemotherapy according to clinical response

	Median change in VEGF IRS (range)
Clinical Responders (n=39)	-2 (-10 to 6)
Clinical Non-responders (n=9)	-2 (-8 to 5)
p-value (Mann-Whitney U-test)	0.78

Table 3.12. Change in VEGF IRS following neoadjuvant chemotherapy according to pathological response

	Median change in VEGF IRS (range)
Pathological Responders (n=14)	-3 (-9 to 1)
Pathological Non-responders (n=34)	–1 (-10 to 6)
p-value (Mann-Whitney U-test)	0.32

Figure 3.1.a. Diagram of Avidin-Biotin Complex (ABC) method

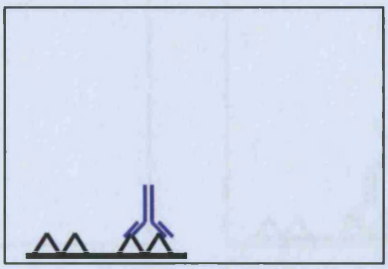

Step 1. Application of primary antibody

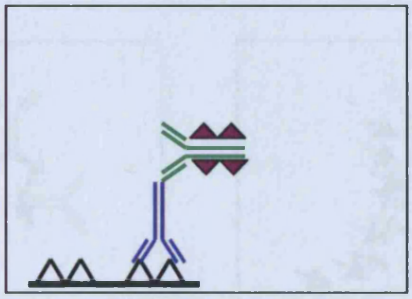

Step 2. Application of biotinylated secondary antibody

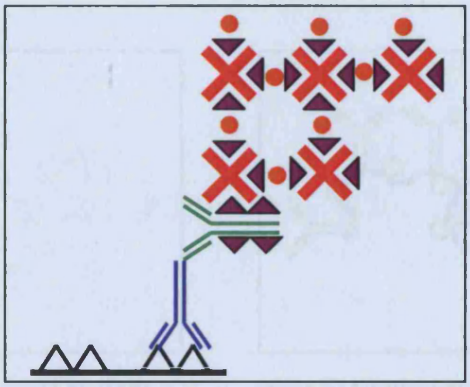

Step 3. Application of pre-formed avidin-biotin enzyme complex (e.g. horseradish peroxidase enzyme)

Figure 3.1.b. Diagram of DAKO EnVision™ Doublestain method

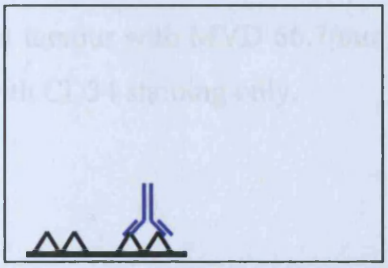

Step 1. Application of primary antibody (anti-CD34)

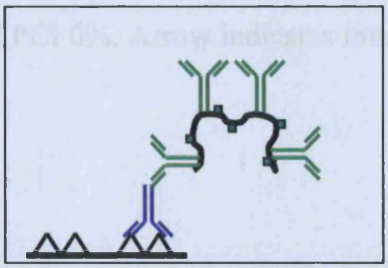

Step 2. Application of HRP labelled polymer (secondary antibody)

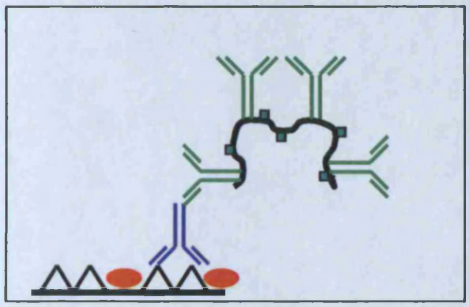

Step 3. Application of DAB chromogen

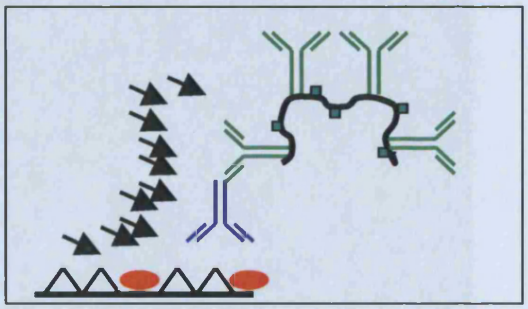

Step 4. Application of Double Stain block

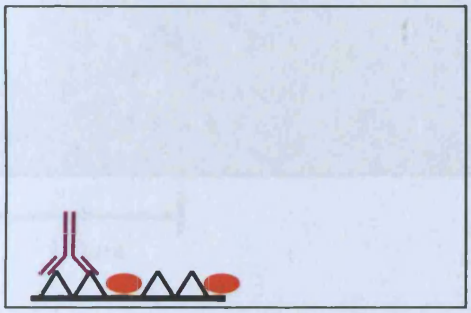

Step 5. Application of (second) primary antibody (α-SMA)

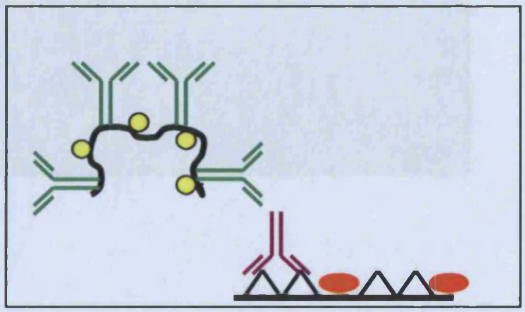

Step 6. Application of AP labelled polymer (secondary antibody)

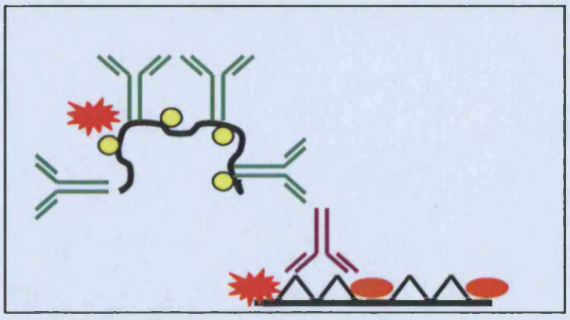

Step 7. Application of Fast Red Chromogen

Figure 3.1 Examples of CD34/α-SMA double staining of breast cancer specimens

(i) Breast tumour with MVD 66.7/mm2 and PCI 0%. Arrow indicates immature vessel with CD34 staining only.

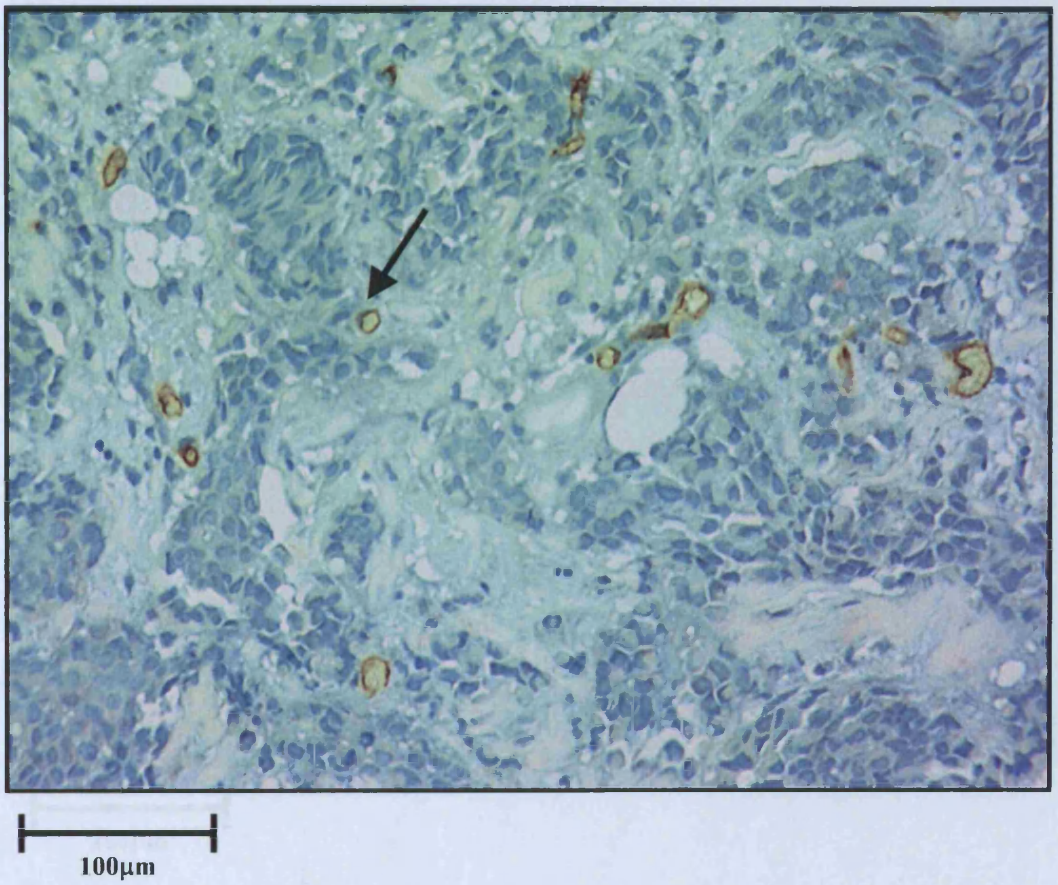

(ii) Breast tumour with MVD 127.8/mm2 and PCI 39%. Arrow indicates mature vessel with CD34 and α-SMA staining .

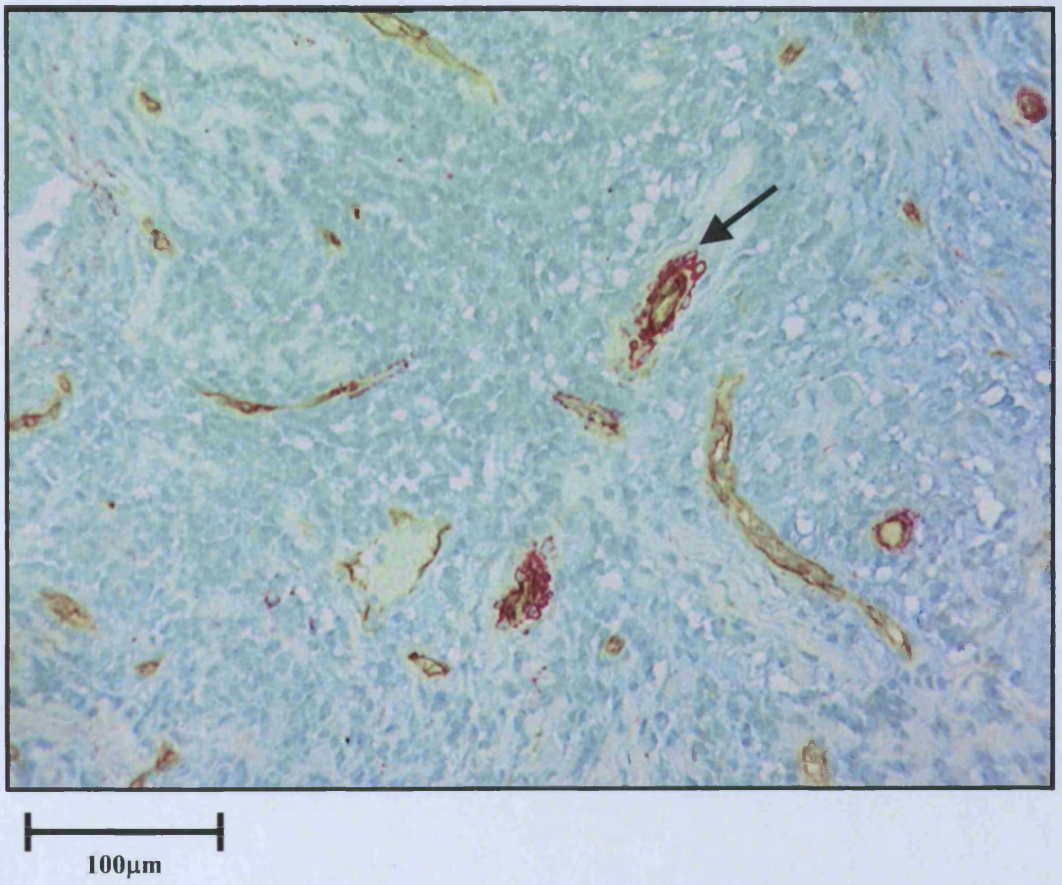

Figure 3.2 VEGF immunoreactive score (VEGF IRS)

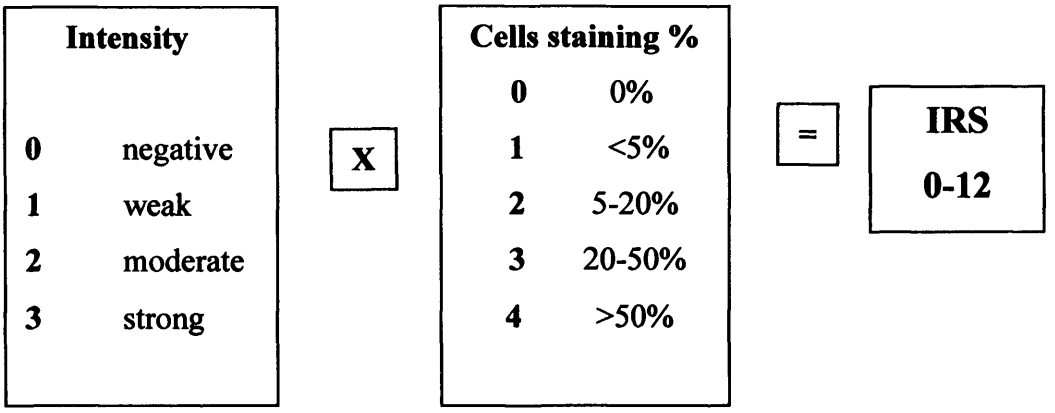

Figure 3.3 Examples of VEGF staining in breast tumour

(i) Breast carcinoma with weak VEGF staining in 20-50% of tumour cells (VEGF IRS 3)

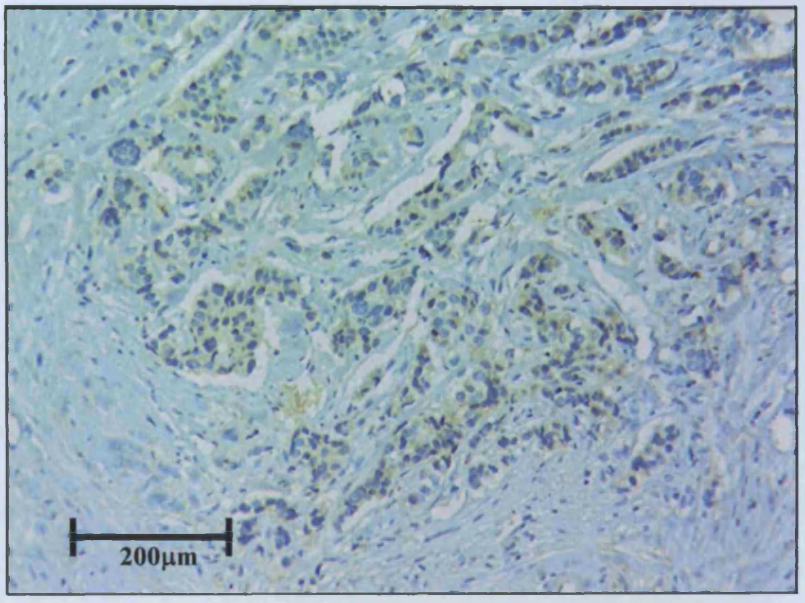

(ii) Breast carcinoma with moderate VEGF staining in >50% of tumour cells (VEGF IRS 8)

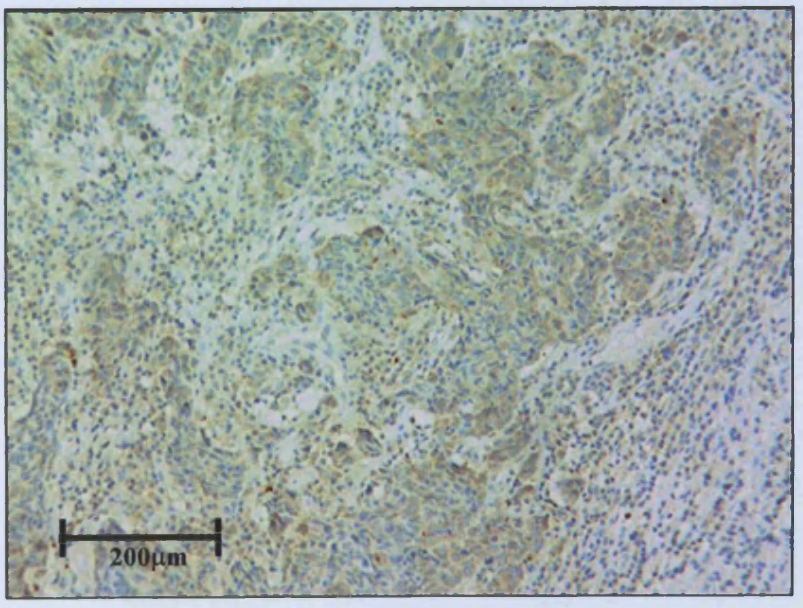

(iii) Breast carcinoma with strong VEGF staining in >50% of tumour cells (VEGF IRS 12)

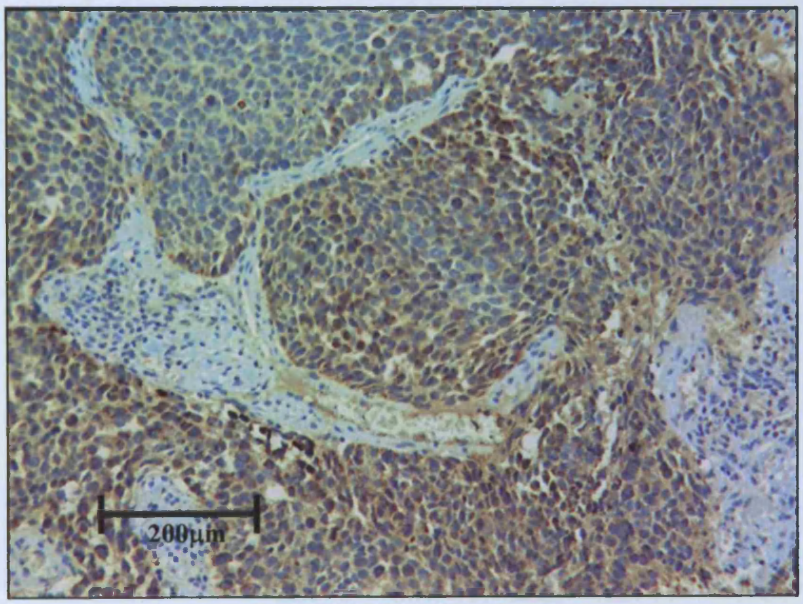

Figure 3.4 Box and Whisker plots of pre-treatment (i) MVD and (ii) PCI according to clinical response

(i)

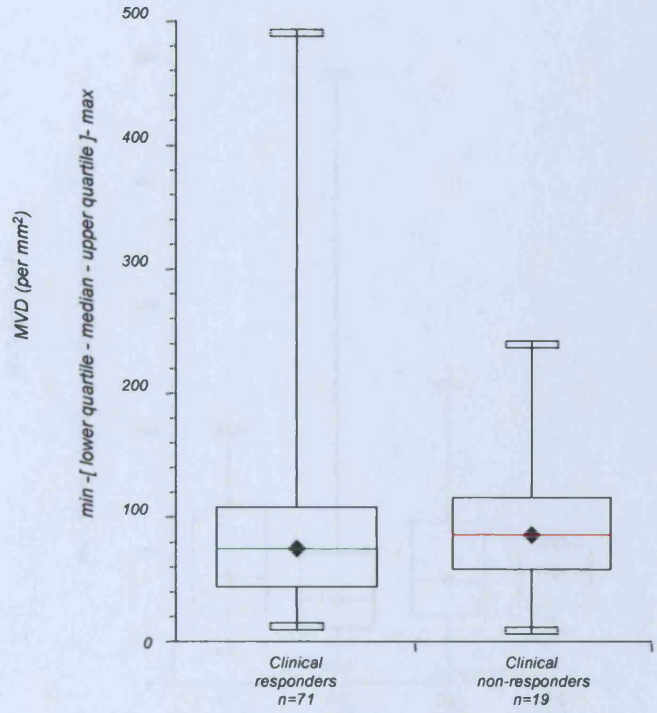

(ii)

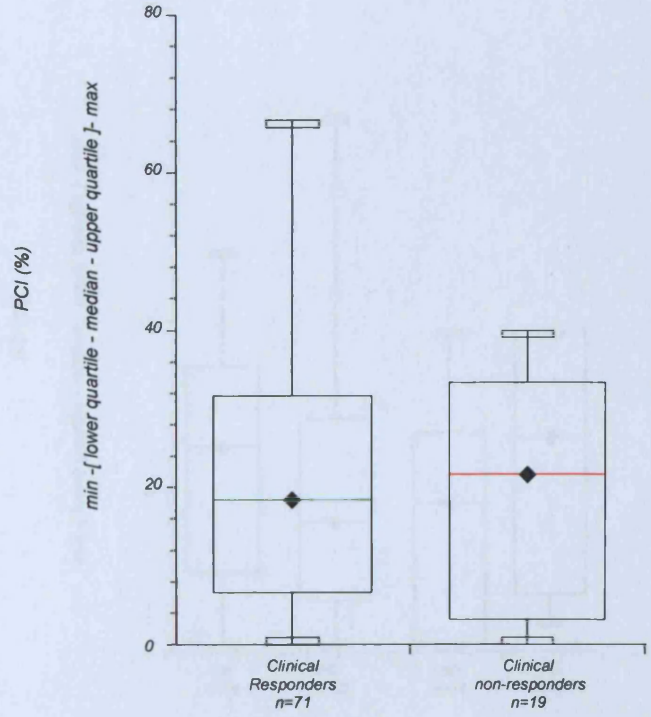

Figure 3.5. Box and Whisker plot of pre-treatment (i) microvessel density and (ii) pericyte coverage index according to clinical response subgroups (CR=complete response, PR=partial response, SD=stable disease, PD=progressive disease)

(i)

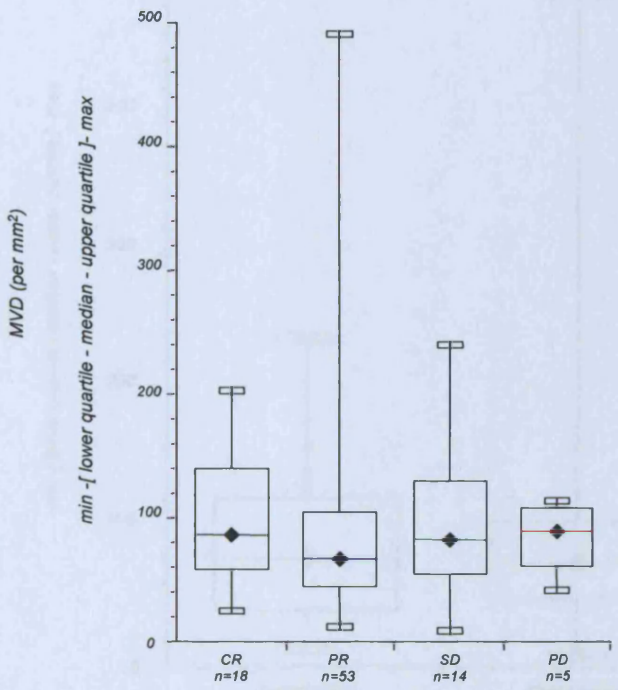

(ii)

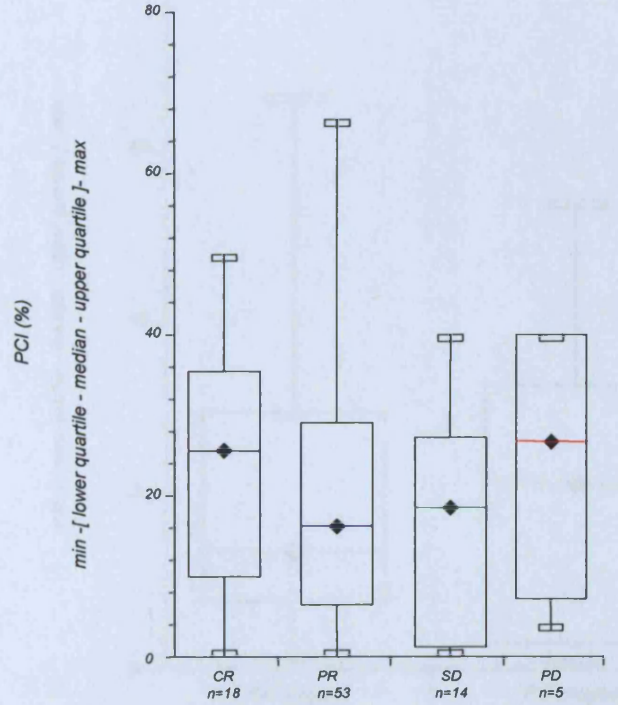

Figure 3.6. Box and Whisker plots of pre-treatment (i) MVD and (ii) PCI according to pathological response

(i)

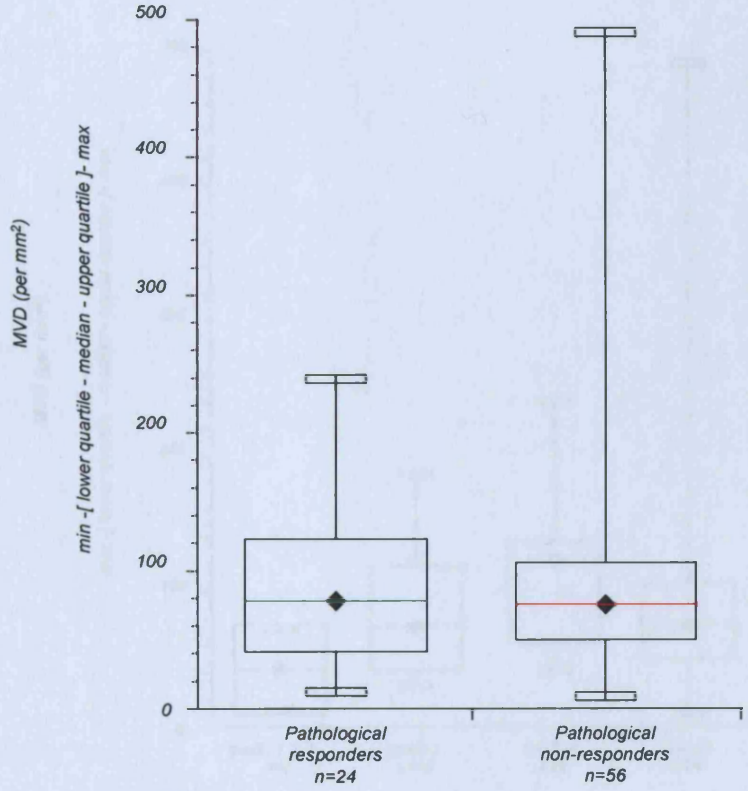

(ii)

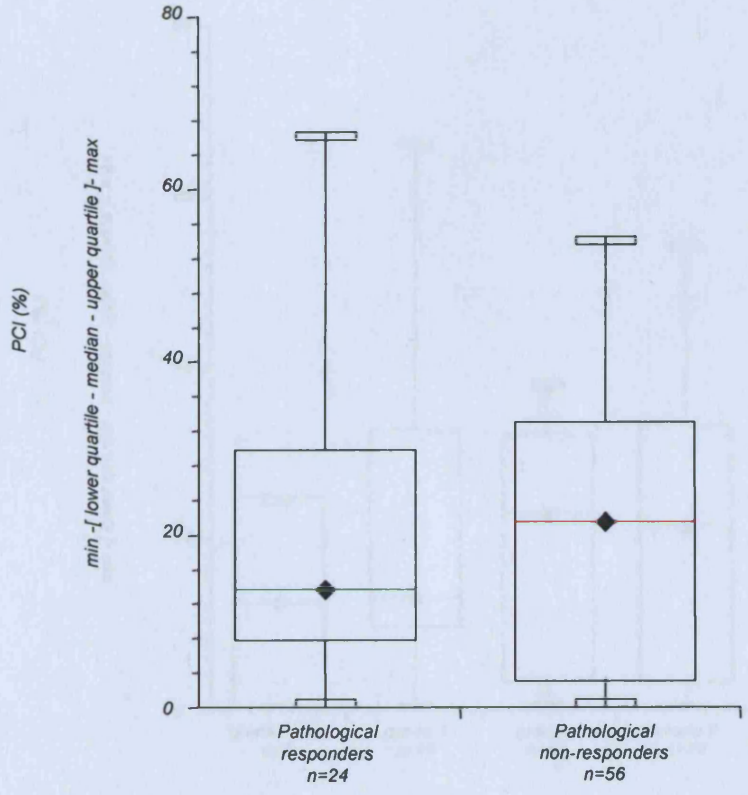

Figure 3.7. Box and Whisker plots of pre-treatment (i) microvessel density (MVD) and (ii) pericyte coverage index (PCI) according to pathological response grade subgroups

(i)

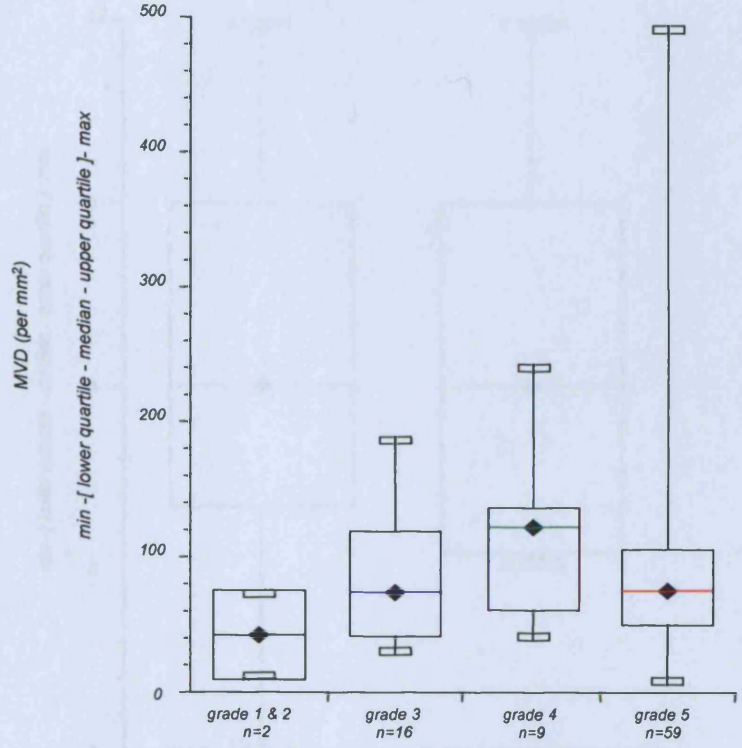

(ii)

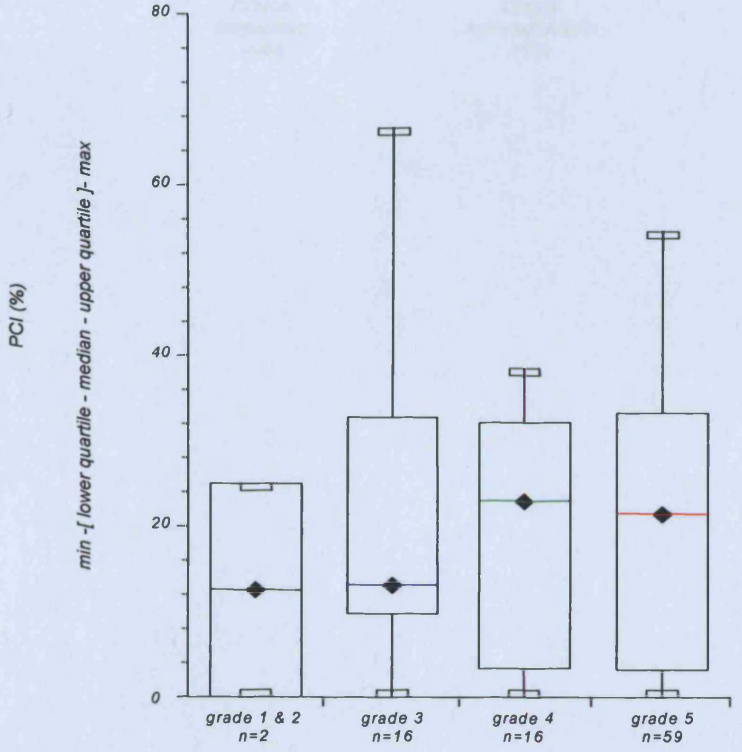

Figure 3.8. Box and Whisker plot of tissue VEGF immunoreactive score (IRS) according to clinical response

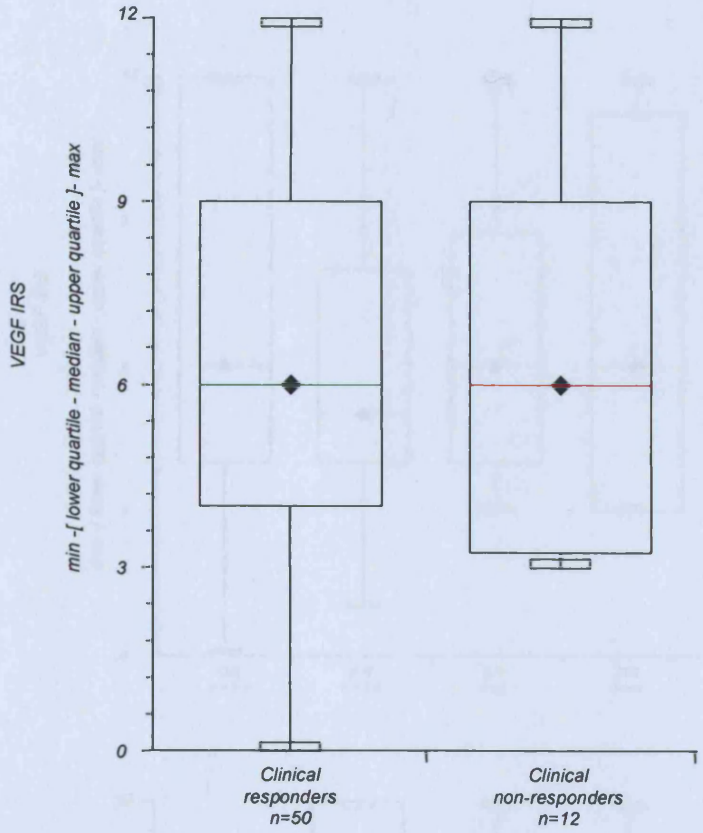

Figure 3.9. Box and Whisker plot of pre-treatment VEGF according to (i) clinical response subgroups (CR=complete response, PR=partial response, SD=stable disease, PD=progressive disease) and (ii) pathological response grade subgroups (grade 1 to 5)

(i)

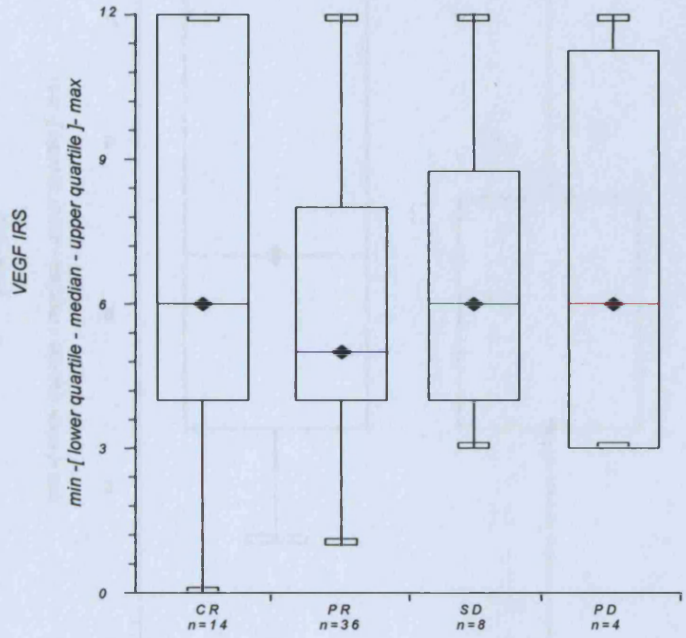

(ii)

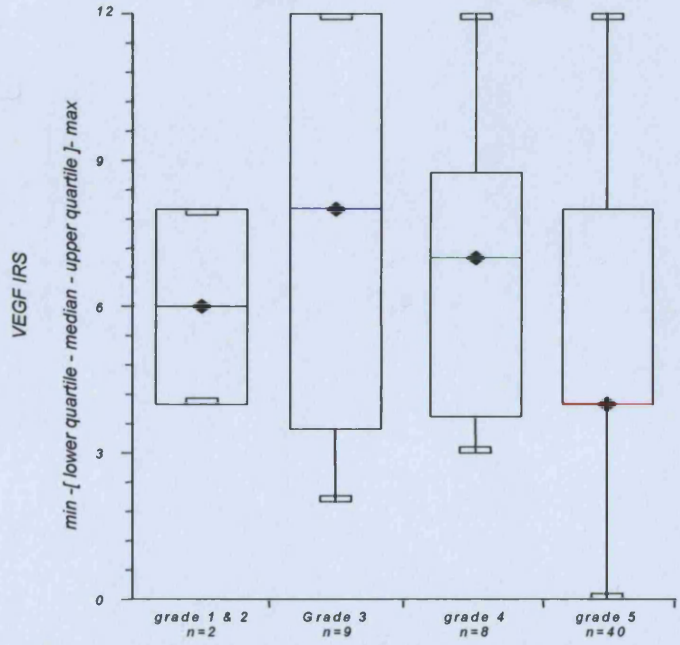

Figure 3.10. Box and Whisker plot of tissue VEGF IRS according to pathological response

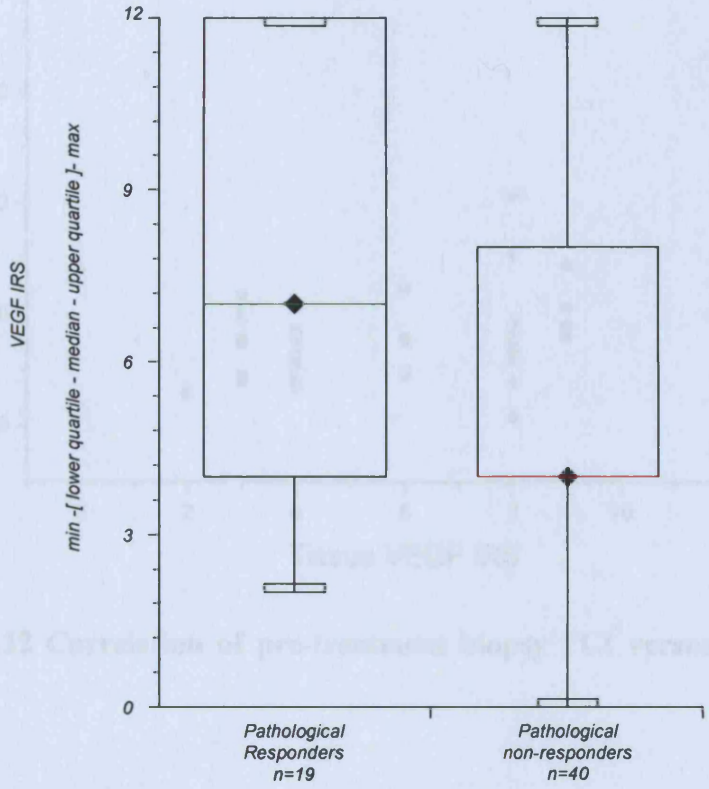

Figure 3.11 Correlation of pre-treatment biopsy MVD versus tissue VEGF IRS

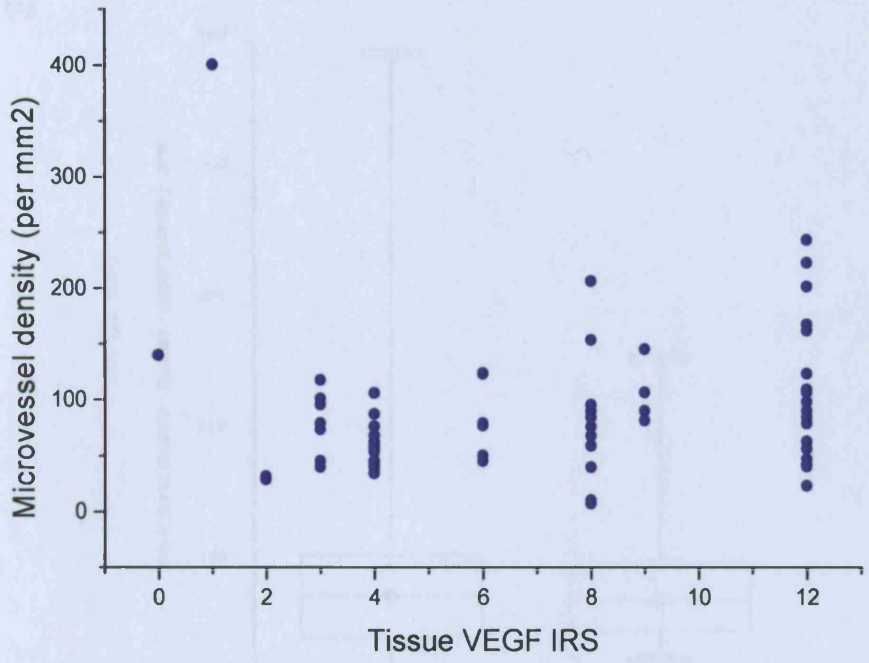

Figure 3.12 Correlation of pre-treatment biopsy PCI versus tissue VEGF IRS

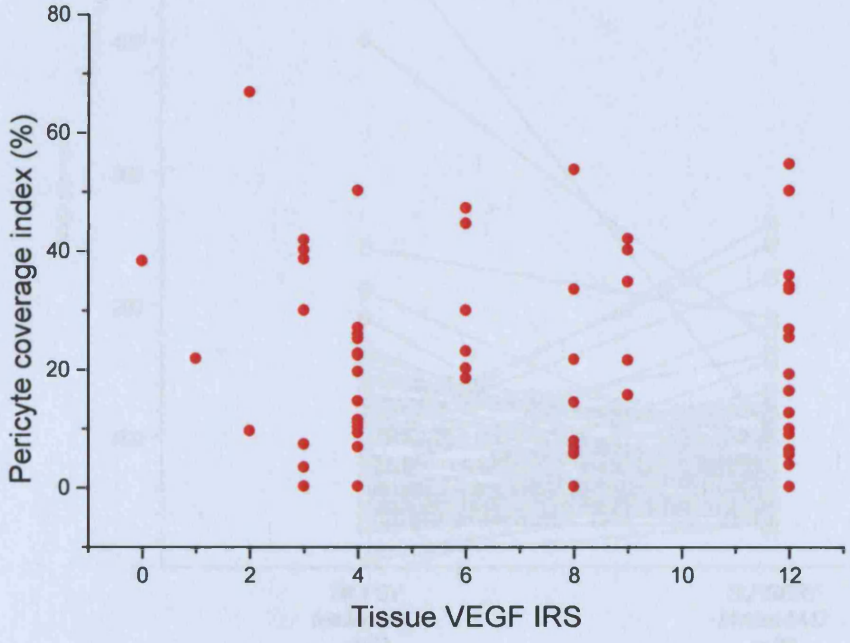

Figure 3.13. Pre- and post-treatment MVD illustrated using (i) Box and Whisker plot and (ii) Ladder plot

(i)

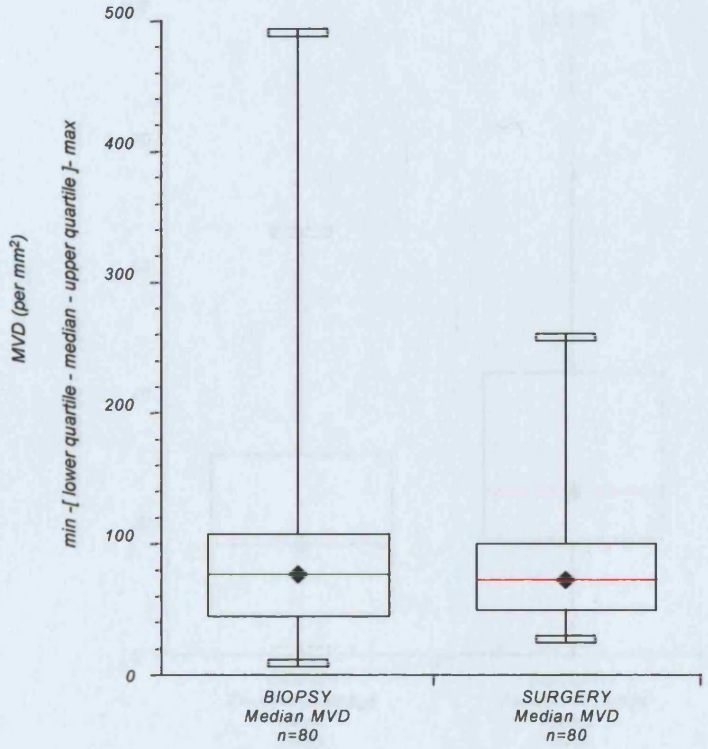

(ii)

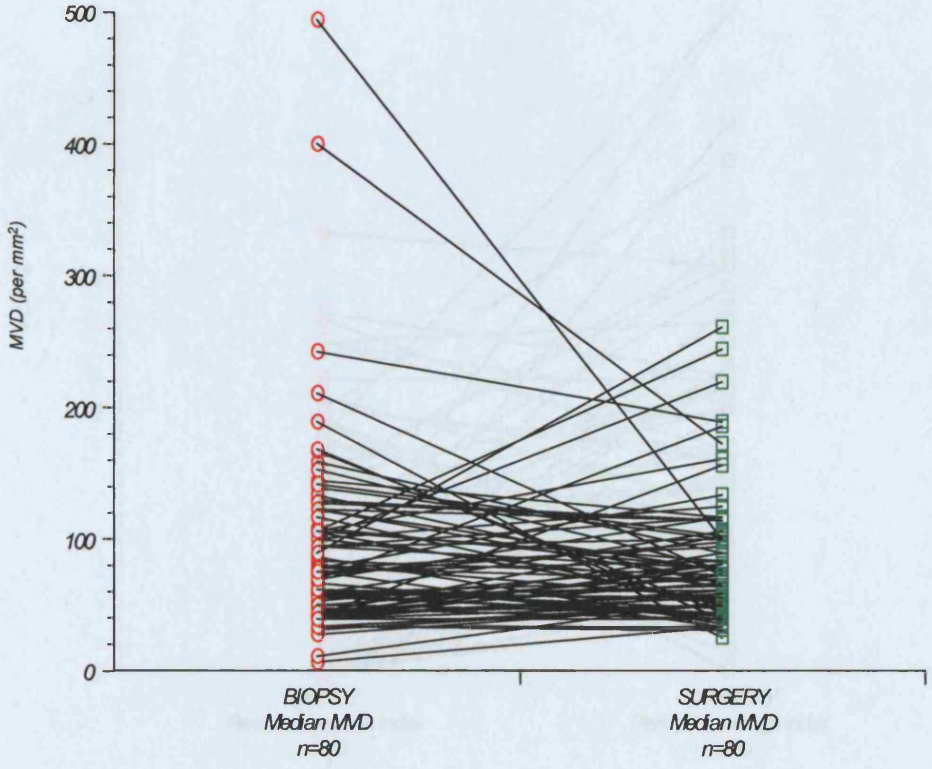

Figure 3.14. Pre- and post-treatment PCI illustrated using (i) Box and Whisker plot and (ii) Ladder plot

(i)

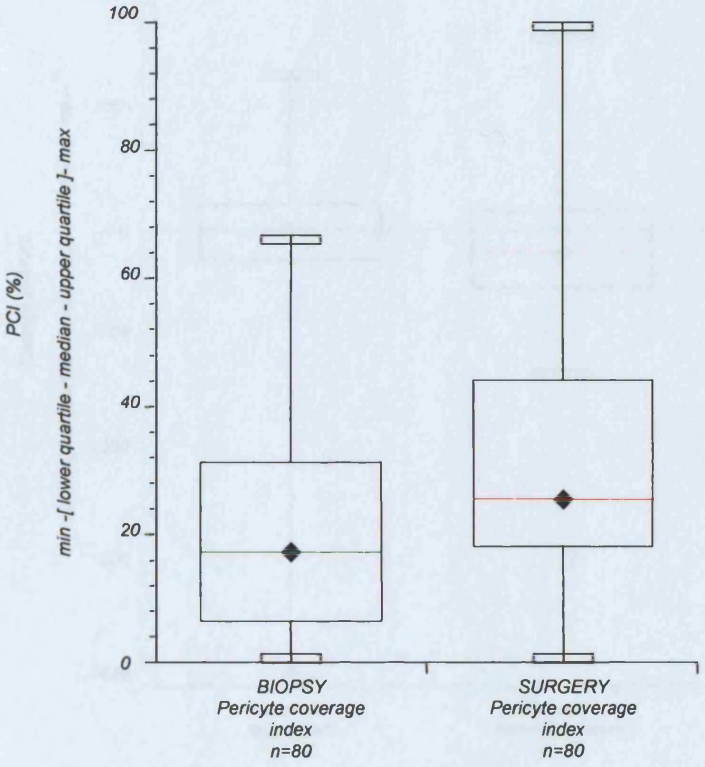

(ii)

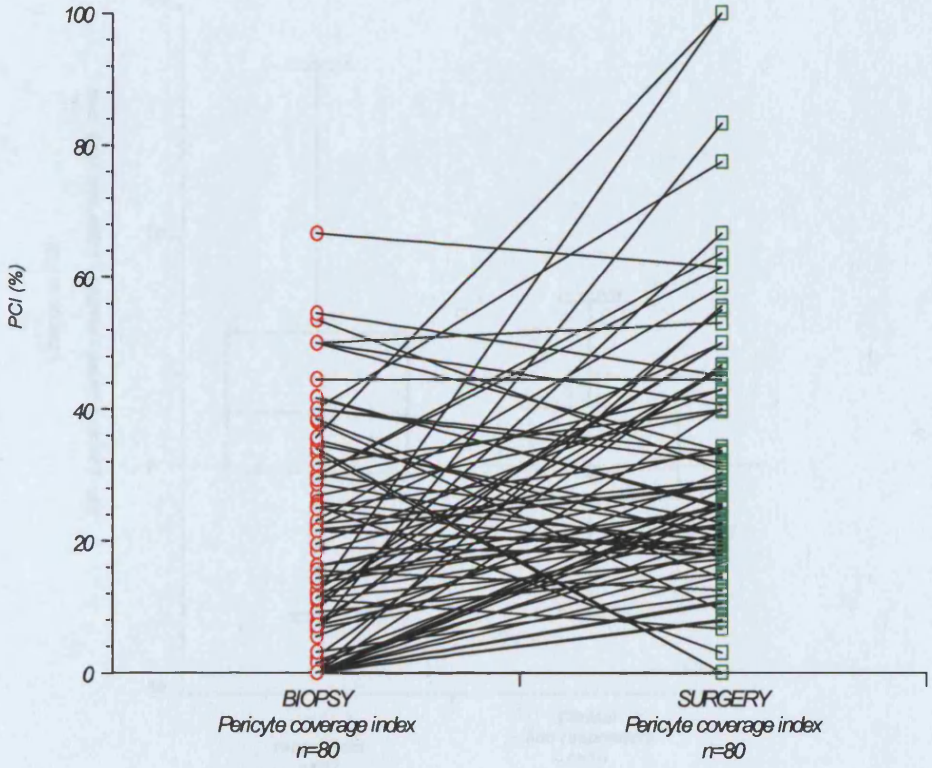

Figure 3.15. Box and Whisker plots of absolute change in (i) MVD and (ii) PCI according to clinical response

(i)

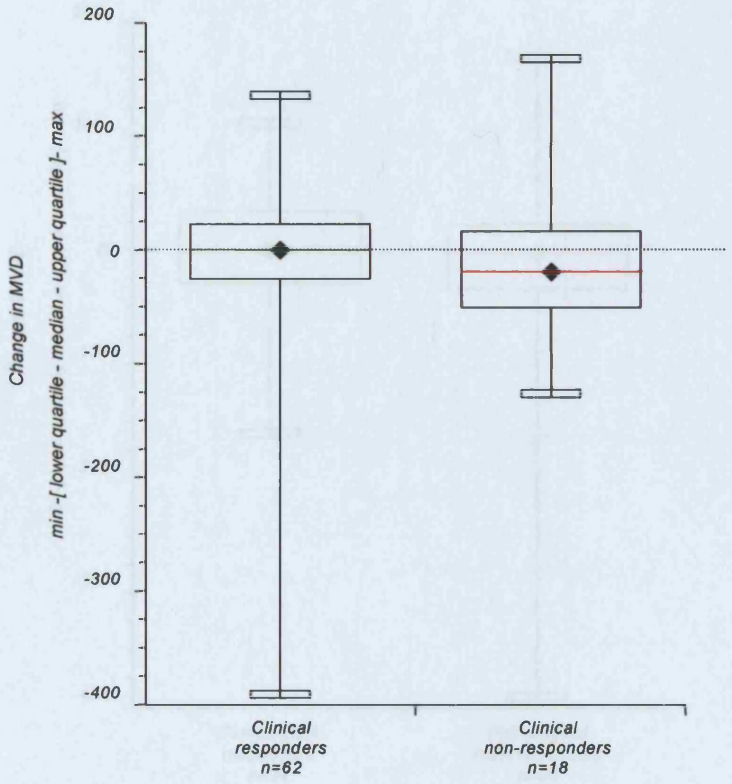

(ii)

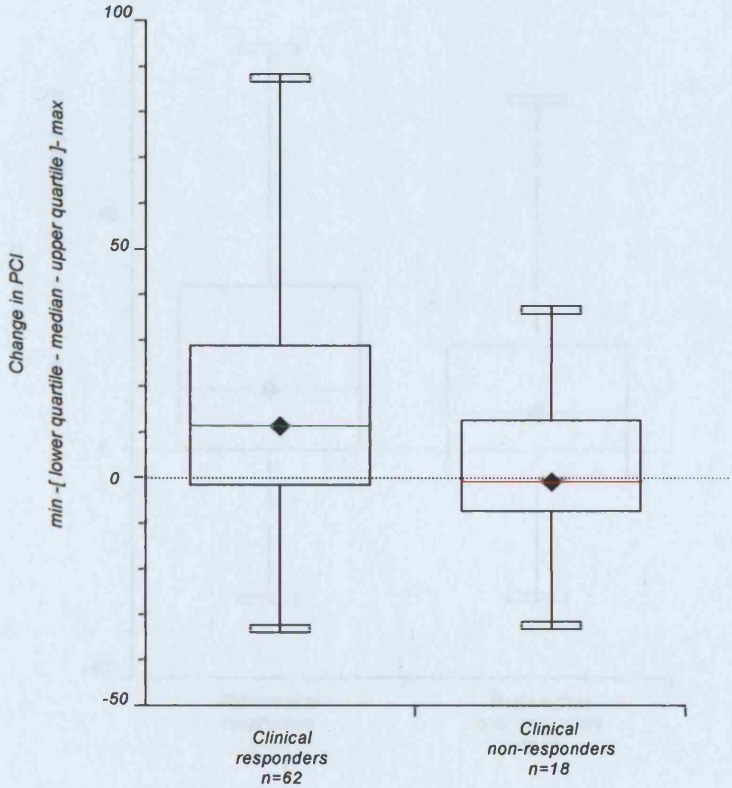

Figure 3.16. Box and Whisker plots of absolute change in (i) MVD and (ii) PCI according to pathological response

(i)

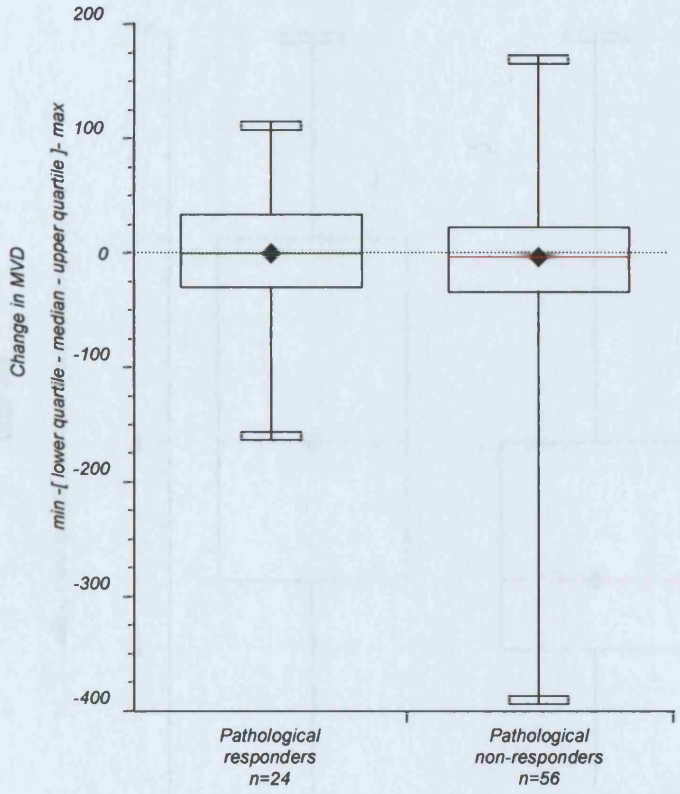

(ii)

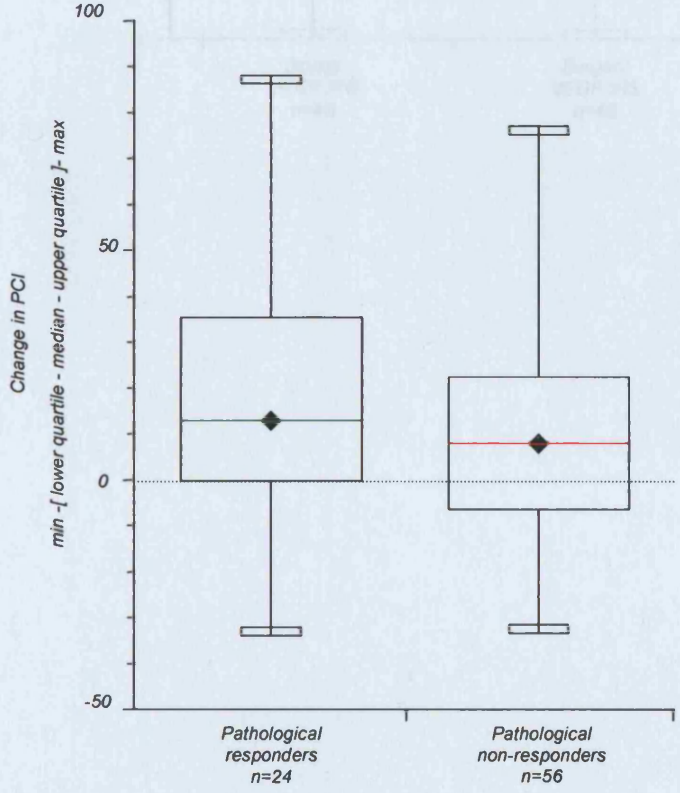

Figure 3.17. Box and Whisker plot of pre- and post-treatment VEGF IRS

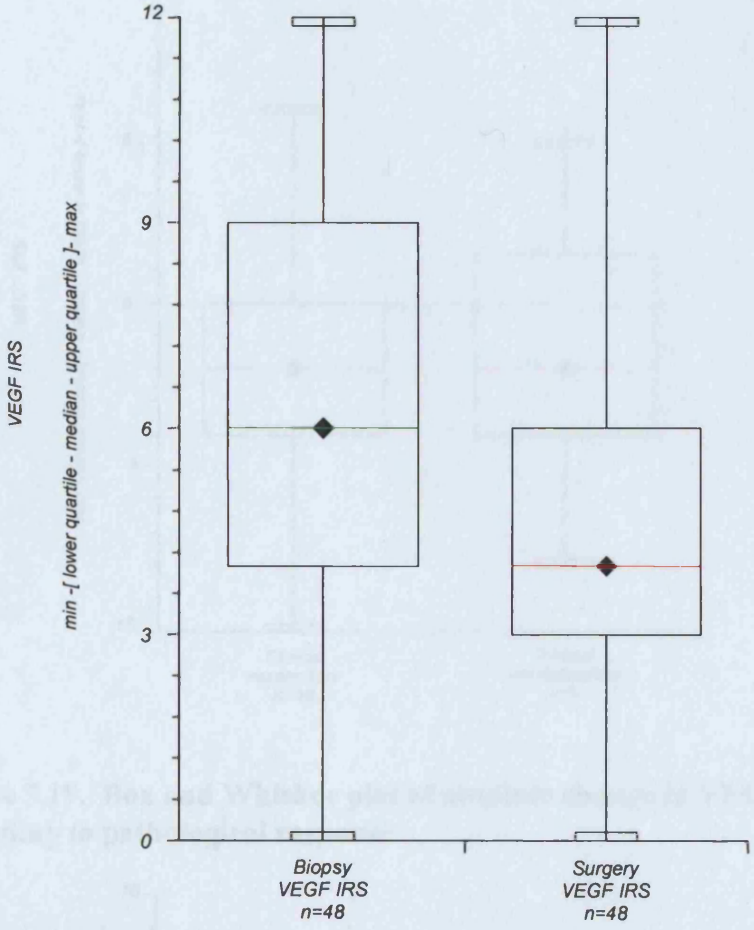

Figure 3.18. Box and Whisker plot of absolutebchange in VEGF IRS according to clinical response

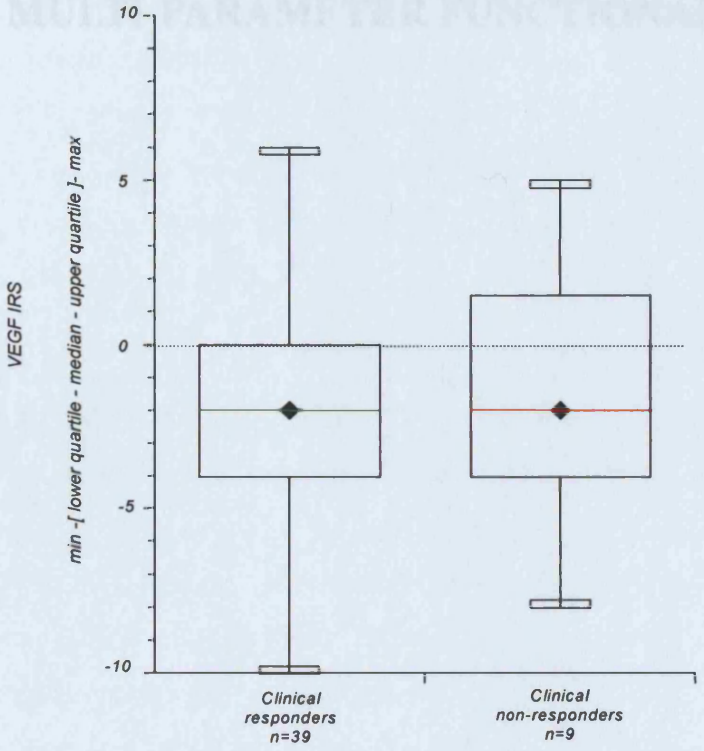

Figure 3.19. Box and Whisker plot of absolute change in VEGF IRS according to pathological response

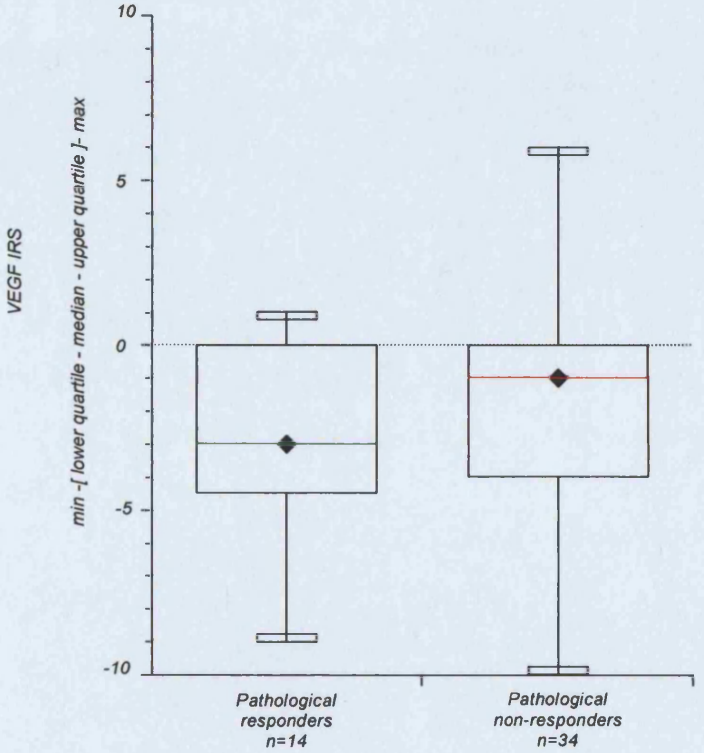

CHAPTER 4: EVALUATION OF THE PATHOPHYSIOLOGICAL CORRELATES OF MULTI-PARAMETER FUNCTIONAL MRI

4.1 INTRODUCTION

In primary breast cancer, the relationship between functional MRI-derived vascular parameters and immunohistochemically-derived measures of tumour angiogenic status remain unclear. Broad correlations between T1-weighted (T1W) kinetic parameters and MVD have been shown by some studies [305-307] while others have found no correlation [174, 308]. Similarly, conflicting results have been found with tumour VEGF expression and tissue enhancement in T1W DCE-MRI [174, 308].

Functional DCE-MRI provides 'real-time' information regarding the functional vascular status of the tumour, however, the underlying pathophysiology of DCE-MRI, in terms of angiogenic activity, is not yet fully understood. A comparison of the DCE-MRI kinetic parameters with immunohistochemical-derived qualitative measures of angiogenic activity, such as pericyte coverage index, rather than the conventional quantitative measure of MVD has not been performed. Further, to date, the histological and immunohistochemical correlates of T2*-weighted (T2*W) DCE-MRI and BOLD MRI have not been assessed and neither have the relationship between the different functional MRI kinetic parameters. Further, BOLD MRI is a non-enhanced MRI techniques that uses deoxyhaemoglobin as an "intrinsic" contrast medium and, as such, provides a potential non-invasive method for assessing the tissue oxygenation. BOLD MRI has not been validated in PBC. Carbonic anhydrase IX (CA IX) is a transmembrane enzyme involved in the regulation of tissue pH and is one of the most strongly hypoxia-inducible proteins. CA IX tissue staining has been shown to correlate with direct measurement of oxygen tension [309]. An assessment of the relationship between tissue CA IX staining and BOLD MRI, together with DCE-MRI, might further our understanding of the effect of hypoxia on the functional MRI parameters

The aims of this study were:

1. To assess the relationship between the T1W DCE-MRI, T2*W DCE-MRI and BOLD MRI kinetic parameters.
2. To assess the relationship between functional MRI kinetic parameters (T1W and T2*W DCE-MRI and BOLD MRI) and histological features of primary breast cancer.
3. To assess the relationship between functional MRI kinetic parameters (T1W and T2*W DCE-MRI and BOLD MRI) and immunohistochemically-derived angiogenesis-related features of primary breast cancer.
4. To assess the relationship between functional MRI kinetic parameters (T1W and T2*W DCE-MRI and BOLD MRI) and the immunohistochemical hypoxia-related parameter, carbonic anhydrase IX (CA IX).
5. To assess the relationship between the hypoxia-related parameter, CA IX, tumour histology and the angiogenesis-related parameters of primary breast cancer.

4.2 PATIENTS AND METHODS

Patients recruited to the " Evaluation of MRI during neoadjuvant chemotherapy in primary breast cancer" (treatment or reproducibility arm) who had successfully undergone a multi-functional dynamic MRI scan prior to treatment (either neoadjuvant chemotherapy or primary surgery) were eligible for this part of the study. Ethical approval was obtained from the local research ethics committee as part of the " Evaluation of MRI during neoadjuvant chemotherapy in primary breast cancer" study (Mount Vernon and Watford Hospitals, protocol number EC2001-26). A pre-treatment formalin-fixed paraffin-embedded diagnostic core biopsy was required for analysis.

A total of 46 patients successfully completed a pre-treatment MRI scan. This included patients from the treatment and the reproducibility arm of the "Evaluation of MRI during neoadjuvant chemotherapy in primary breast cancer" study together with a number of patients who underwent a pre-treatment MRI

scan but then received an alternative chemotherapy regimen to FEC. A pre-treatment diagnostic core biopsy was available on 41 patients. The patient demographics are shown in **table 4.1**. 40 pre-treatment diagnostic core biopsy samples were available for carbonic anhydrase IX analysis; 39 samples were available for CD34/α-SMA analysis; and 38 samples were available for VEGF analysis.

4.2.1 MRI PROTOCOL

All MRI scans were performed at the Paul Strickland Scanner Centre, Mount Vernon Hospital, Northwood, Middlesex, UK. The MRI protocol employed was as described in **sections 2.2.3 and 2.2.4**. For each patient, the median value of each of the following parameters was calculated:

A. Single-slice analysis:

5. T1W semi-quantitative parameters:

(iv) Mean gradient (MeanGrad)(AU)

(v) Maximum signal amplitude (MaxAmp)(%)

(vi) Washout (Wt)(AU)

6. T1W quantitative parameters:

(v) Transfer constant (K^{trans})(min^{-1})

(vi) Leakage space (v_e)(%)

(vii) Rate constant (k_{ep})(min^{-1})

(viii) Maximum Gd-DTPA concentration (MaxGd)(mmol/kg)

7. T2*W quantitative parameters:

(iv) Relative blood volume (rBV)

(v) Relative blood volume (rBF)

(vi) Mean transit time (MTT)(sec)

8. BOLD-MRI quantitative parameter, R_2* (sec^{-1})

B. Three-slice analysis:

T1W quantitative parameters:

(i) Transfer constant (K^{trans})(min^{-1})

(ii) Leakage space (v_e)(%)

(iii) Rate constant (k_{ep})(min^{-1})

(vii) Maximum Gd-DTPA concentration (MaxGd)(mmol/kg)

4.2.2 PRIMARY BREAST CANCER HISTOLOGY

Tumour histological subtype, oestrogen receptor status and tumour grade were assigned according to the pre-treatment diagnostic core-biopsy and/or post-treatment surgical specimen analysis and were obtained from the formal pathological reports. The histological tumour types were: invasive ductal carcinoma (n=35), invasive lobular carcinoma (n=5), mixed invasive ductal and lobular carcinoma (n=4), mucinous carcinoma (n=1) and carcinoma, NOS (not otherwise specified) (n=1).

Oestrogen receptor status was scored as positive or negative. Tumours were scored as oestrogen receptor positive if either the diagnostic core-biopsy or post-treatment surgical specimen demonstrated oestrogen receptor staining.

Tumour grade was assigned according to the Bloom-Richardson system. Where there was a discrepancy between the grade assigned to the pre-treatment diagnostic core biopsy sample and the post-treatment surgical specimen, the highest grade was taken.

Tumour necrosis was scored from the pre-treatment diagnostic core biopsy sample by a single independent pathologist (PIR). Tumour necrosis was scored as present or absent.

4.2.3 IMMUNOHISTOCHEMISTRY

Immunohistochemical staining for CD34/α-SMA (double-staining), VEGF and carbonic anhydrase IX (CA-IX) was performed on pre-treatment diagnostic breast cancer core biopsy specimens. The staining techniques employed for CD34/α-SMA and VEGF are described in **section 3.3.1.4** and **3.3.1.6** respectively. Microvessel density (MVD) and pericyte coverage index (PCI) were quantified as described in **section 3.3.1.5**. MVD was expressed as the number of vessels per mm^2. PCI was the number of CD34 & α-SMA positive vessels (or endothelial cell(s)) per high power field (x 200 magnification) expressed as a percentage of all CD34 positive vessels within that field. VEGF expression was quantified using the VEGF immunoreactive score (VEGF IRS). The VEGF IRS is described in **section 3.3.1.7**.

4.2.3.1 Immunohistochemistry for CA-IX

Paraffin-embedded sections, 4μm thick, were cut from tumour blocks and mounted onto microscope slides (Surgipath Europe Ltd, X-tra slides™). Slides were dewaxed in xylene for 5 minutes prior to rehydration through graded alcohols (100, 90, 70%) to water and then washed in tris buffer saline (50mmol tris-HCL)(TBS). Each section was encircled with a resin pen. The slides were incubated with Dako peroxidase block (DakoCytochromation Ltd, UK, EnVision™ kit, K4006) for 5 minutes to block endogenous peroxidase activity, then washed in water and rinsed in TBS. The slides were then incubated with protein block (DakoCytochromation Ltd, UK, X0909) for 5 minutes to reduce non-specific secondary antibody staining. Carbonic anhydrase-IX (CA-IX) mouse monoclonal antibody (supplied by Professor Adrian Harris, Weatherall Institute of Molecular Medicine, John Radcliffe Hospital, Oxford) diluted 1/50 in antibody diluent (DakoCytochromation Ltd, UK, S3022) was applied and the slides incubated for 1 hour at room temperature. The slides were washed in TBS and then Envision Horseradish peroxidase mouse polymer (DakoCytochromation Ltd, UK, EnVision™ kit, K4006) was applied for 30 minutes. The slides were washed with TBS and then incubated with diaminobenzidine (DAB) substrate (DakoCytochromation Ltd, UK, EnVision™ kit, K4006) for 5 minutes. Slides were rinsed in TBS, washed in water and then

counterstained with Gills haematoxylin (Surgipath Europe Ltd, 01500E). The slides were washed in water, dehydrated in graded alcohols (70, 90, 100%) and mounted in DPX (Surgipath Europe Ltd, 08600E). All runs included a positive control slide (breast carcinoma).

4.2.3.2 Quantification of CA-IX staining

CA-IX immunostaining was quantified in carcinoma cells as positive or negative.

4.3 STATISTICAL ANALYSIS

Statistical analysis was performed using the StatsDirect statistical package. Spearman's rank correlation coefficient, Rho, was used to analyse the relationship between continuous variables. The Mann-Whitney U-test (MW) was used to assess the relationship between two independent subgroups for continuous variables. The Kruskal-Wallis test (KW) was used to assess the relationship between more than two independent subgroups for continuous variables. The Fisher's exact test was used to assess the statistical relationship between two dichotomous variables. A p-value <0.05 was required for statistical significance.

4.4 RESULTS

4.4.1 FUNCTIONAL MRI KINETIC PARAMETERS

Semi-quantitative and quantitative T1W DCE-MRI kinetic parameter data was available on all of the 46 patients who underwent a pre-treatment functional MRI scan of the breasts. Quantitative T2*W DCE-MRI kinetic parameter data was available on 42 patients and the BOLD MRI parameter data, R2*, was available on 44 patients.

4.4.1.1 T1W (single-slice) and T2*W DCE-MRI

A significant positive correlation existed between the median values of the T2*W quantitative kinetic parameters, rBV and rBF, and the median values of the T1W semiquantitative parameters MeanGrad (Rho=0.40, $p<0.01$ and Rho=0.38, $p<0.05$ respectively), MaxAmp (Rho=0.62, $p<0.001$ and Rho=0.66, $p<0.001$ respectively) and Wt (Rho=0.63, $p<0.0001$ and Rho=0.65, $p<0.0001$ respectively). No correlation was found between MTT and the T1W semiquantitative parameters (MeanGrad, Rho=0.08, p=0.69; MaxAmp, Rho=0.30, p=0.06; Wt, Rho=0.01, p=0.93) (**table 4.2**).

A significant positive correlation existed between the median values of the T2*W quantitative kinetic parameters, rBV and rBF, and the median values of the T1W quantitative parameters, K^{trans} (Rho=0.47, p=0.002 and Rho=0.46, p=0.003 respectively) and k_{ep} (Rho=0.47, p=0.002 and Rho=0.48, p<0.002 respectively). There was no correlation between rBV or rBF and the remaining T1W quantitative parameters, v_e (Rho=0.10, p=0.55; Rho=0.12, p=0.46, respectively) or MaxGd (Rho=0.23, p=0.14; Rho=0.28, p=0.07, respectively). A significant correlation existed between MTT and v_e (Rho=0.33, p<0.05) but there was no correlation between MTT and the other T1W quantitative parameters (K^{trans}, Rho=-0.003, p=0.98; k_{ep}, Rho=-0.18, p=0.24; MaxGd, Rho=0.25, p=0.11) (**table 4.2**).

4.4.1.2 T1W (three-slice) and T2*W DCE-MRI

A significant positive correlation existed between the median values of the T2*W quantitative kinetic parameters, rBV and rBF, and the median values of the T1W quantitative parameters (three-slice analysis), K^{trans} (Rho=0.51, p<0.001 and Rho=0.54, p<0.0005 respectively), k_{ep} (Rho=0.49, p=0.001 and Rho=0.51, p<0.001 respectively) (**figure 4.1**) and MaxGd (Rho=0.31, p<0.05 and Rho=0.50, p<0.001 respectively). There was no correlation between v_e and rBV or rBF (Rho=0.16, p=0.32; r=0.18, p=0.27, respectively) but a significant correlation existed with MTT (Rho=0.38, p<0.05). There was no correlation between MTT and K^{trans}, k_{ep} or MaxGd (Rho=-0.10, p=0.52; Rho=-0.23, p=0.15; Rho=0.27, p=0.09, respectively) (**table 4.2**).

4.4.1.3 DCE-MRI and BOLD MRI

There was a significant inverse correlation between the BOLD MRI parameter, R2*, and the T1W semiquantitative parameters MaxAmp (Rho=-0.65, p<0.0001) and Wt (Rho=-0.61, p<0.0001), and the T2*W quantitative parameters rBV (Rho=-0.73, p<0.0001) and rBF (Rho=-0.71, p<0.0001). There was no correlation between R_2* and any of the remaining DCE-MRI kinetic parameters (**table 4.3** and **figure 4.2**)

4.4.2 FUNCTIONAL MRI PARAMETERS AND PRIMARY BREAST CANCER HISTOLOGICAL FEATURES

4.4.2.1 Histological tumour type

The histological tumour types were: invasive ductal carcinoma (n=35); invasive lobular carcinoma (n=5); mixed invasive ductal and lobular carcinoma (n=4); mucinous carcinoma (n=1); and carcinoma, NOS (not otherwise specified)(n=1). Correlations between the functional MRI parameters and the histological tumour type were assessed according to the three commonest histological sub-types only i.e. invasive ductal carcinoma, invasive lobular carcinoma and mixed invasive ductal and lobular carcinoma.

There was a significant difference in the median values for R_2* according to histological subtype (KW, $p<0.04$) with lower median R_2* values seen in the invasive ductal carcinomas (median 32.2sec^{-1}) compared with the invasive lobular (median 38.9sec^{-1}) and mixed invasive ductal and lobular carcinomas (median 39.8sec^{-1}) (**table 4.4** and **figure 4.3**). There was also a significant difference in the median values for Wt according to histological subtype (KW, $p<0.02$) with lower median Wt values seen in the mixed invasive ductal and lobular carcinomas (median -0.60AU) compared with the invasive ductal (median -0.23AU) and invasive lobular carcinomas (median -0.24AU) (**table 4.4** and **figure 4.4**). No significant difference was seen for the remaining MRI parameters according to histological subtype (**table 4.4**).

4.4.2.2 Tumour grade

Tumour grade was assessable in 43 of the 46 patients who underwent a pre-treatment function MRI of the breasts. Where there was a discrepancy between the grade assigned to the pre-treatment diagnostic core biopsy sample and the post-treatment surgical specimen, the highest grade was taken. Thus, three

tumours were graded as grade 1, twenty tumours were graded as grade 2 and twenty tumours were graded as grade 3.

There was a significant difference in the median values for K^{trans}, k_{ep}, rBV, rBF, MeanGrad and Wt according to tumour grade (KW, $p<0.05$ for all groups) with higher median values generally being associated with a higher tumour grade (**table 4.5**). In light of the small number of low grade tumours (n=3), a further analysis was performed with the division of tumour grade into 2 clinically relevant groups: high grade (i.e. grade 3 tumours, n=20) and non-high grade (i.e. grade 1 and 2 tumours, n=23). This demonstrated a significant difference in the median values for rBV, rBF, MaxAmp and MeanGrad according to grade (MW, $P<0.05$ for all groups) with high grade tumours displaying higher kinetic values (**table 4.6**). For the remaining MRI parameters, no difference was found in the median values according to tumour grade (**table 4.5** and **4.6**).

4.4.2.3 Oestrogen-receptor status

Of the 46 patients who underwent a pre-treatment functional MRI of the breasts, 35 had oestrogen-receptor positive tumours and 11 had oestrogen-receptor negative tumours (**table 4.1**). The oestrogen-receptor positive tumours demonstrated a significantly higher median R_2* compared with the oestrogen-receptor negative tumours (median R_2* 37sec^{-1} and 22.2 sec^{-1} respectively; MW, $p<0.0005$) (**table 4.7** and **figure 4.5**). The oestrogen-receptor positive tumours also demonstrated a significantly lower median k_{ep} (three-slice analysis), rBV, rBF and Wt compared with the oestrogen-receptor negative tumours (MW, $p<0.05$ all groups) (**table 4.7** and **figure 4.6**). No significant difference was found for the remaining MRI parameters according to oestrogen-receptor status. These results are shown in **table 4.7**.

4.4.2.4 Tumour necrosis

Tumour necrosis was scored on the pre-treatment diagnostic core-biopsy samples from 40 patients. Tumour necrosis was present in 13 tumour samples and absent in 27 tumour samples. Those tumours with necrosis demonstrated a

significantly lower median R_2* compared with those tumours with no necrosis (median R2* 27.5sec^{-1} and 35.6 sec^{-1} respectively; MW, $p<0.05$) (**figure 4.7**). Those tumours with necrosis also demonstrated a significantly higher median k_{ep} (single-slice and three-slice analysis, MW, $p<0.05$ for both), K^{trans} (single-slice analysis, MW, $p<0.05$) rBV (MW, $p=0.0005$) and rBF (MW, $p<0.001$) compared with those tumours with no necrosis (**figure 4.8**). No significant difference was found for the other remaining MRI parameters according to tumour necrosis. These results are shown in **table 4.8**.

4.4.3 FUNCTIONAL MRI PARAMETERS AND IMMUNOHISTOCHEMICAL ANGIOGENESIS-RELATED PARAMETERS

4.4.3.1 Microvessel density and Pericyte coverage index

Microvessel density (MVD) and pericyte coverage index (PCI) values were available on 39 diagnostic core-biopsy breast tumour samples taken from patients who had undergone a functional MRI scan prior to treatment.

The relationship between MVD and PCI and the T1W semi-quantitative (single-slice) and quantitative DCE-MRI parameters (single-slice and three-slice analysis) were assessable on 39 patients. No significant correlation was found between MVD or PCI and any of the T1W kinetic parameters (Spearman's rank correlation, $p>0.05$ for all). These results are shown in **table 4.9**.

The relationship between MVD and PCI and the T2*W DCE-MRI quantitative parameters (single-slice analysis) was assessable on 36 patients. No significant correlation was found between MVD or PCI and any of the T2*W kinetic parameters (Spearman's rank correlation, $p>0.05$ for all). These results are shown in **table 4.9**.

The relationship between MVD and PCI and the BOLD MRI parameter, R2*, was assessable on 37 patients. A significant positive correlation was found between MVD and R_2* (Rho=0.35, p=0.035). No significant correlation was found between PCI and R_2* (Rho=0.02, p=0.9) **table 4.9**.

4.4.3.2 Vascular endothelial growth factor

The VEGF IRS was available on 38 (diagnostic) core-biopsy breast tumour samples taken from patients who had undergone a functional MRI scan prior to treatment.

The relationship between VEGF IRS and the T1W semi-quantitative (single-slice) and quantitative DCE-MRI parameters (single-slice and three-slice analysis) was assessable on 38 patients. No significant correlation was found between VEGF IRS and any of the T1W kinetic parameters (Spearman's rank correlation, p>0.05 for all groups). These results are shown in **table 4.9**.

The relationship between VEGF IRS and the T2*W DCE-MRI quantitative parameters (single-slice analysis) was assessable on 35 patients. No significant correlation was found between VEGF IRS and any of the T2*W kinetic parameters (Spearman's rank correlation, p>0.05 for all groups). These results are shown in **table 4.9**.

The relationship between VEGF IRS and the BOLD MRI parameter, R_2*, was assessable on 36 patients. No significant correlation was found between VEGF IRS and R_2* (Rho=0.07, p=0.67) **table 4.9**.

4.4.4 FUNCTIONAL MRI PARAMETERS AND THE HYPOXIA-RELATED PARAMETER, CA-IX

Carbonic-anhydrase IX (CA-IX) staining was performed on the pre-treatment diagnostic core-biopsy samples of 40 patients. CA-IX staining was negative in 25 samples and positive in 15 samples.

The relationship between CA-IX staining and the T1W semi-quantitative (single-slice) and quantitative DCE-MRI parameters (single-slice and three-slice analysis) was assessable on 40 patients. CA-IX positive tumours had a significantly higher median Wt compared with CA-IX negative tumours (-0.17AU) and -0.25AU respectively, MW, $p<0.05$) (**figure 4.9**). There was no significant difference between the CA-IX positive or negative tumours for the remaining T1W kinetic parameters (MW, $p>0.05$ for all). These results are shown in **table 4.10**.

The relationship between CA-IX staining and the T2*W quantitative DCE-MRI parameters (single-slice analysis) was assessable on 37 patients. CA-IX positive tumours had significantly higher rBV and rBF values compared with CA-IX negative tumours (rBV 211.6 and 125.2 respectively, MW, $p<0.005$; rBF 8.1 and 5.0 respectively, MW, $p<0.005$) (**figure 4.9**). No significant correlation was found between CA-IX staining and MTT (MW, $p=0.32$). These results are shown in **table 4.10**.

The relationship between CA-IX staining and the BOLD MRI parameter, R_2*, was assessable on 38 patients. CA-IX positive tumours had a significantly lower R_2* compared with CA-IX negative tumour ($28.9sec^{-1}$ and $36.0sec^{-1}$ respectively, MW, $p<0.05$) (**table 4.10** and **figure 4.10**).

4.4.5 CA-IX, HISTOLOGICAL TUMOUR FEATURES AND THE ANGIOGENESIS-RELATED PARAMETERS OF PRIMARY BREAST CANCER

4.4.5.1 Histological tumour features

The relationship between the individual histological tumour features was assessable on up to 45 patients. Tumour grade was divided into two groups for the analysis: high grade (i.e. grade 3 tumours, n=20) and non-high grade (i.e. grade 1 and grade 2 tumours, n=23). There was a significant association between tumour grade and both oestrogen-receptor (ER) status (Fisher's exact, $p<0.005$) and histological tumour type (Fisher's exact, $p<0.0001$), with high grade tumours tending to be ER negative invasive ductal carcinomas (IDC). Further, there was a significant association between ER status and histological tumour type (Fisher's exact, $p<0.05$) with all of the non-IDC tumours being ER positive. ER status was also associated with pathological tumour necrosis (Fisher's exact, $p<0.05$), with no necrosis in the majority of ER positive tumours. These results are shown in **table 4.11**.

4.4.5.2 CA-IX and histological tumour features

The relationship between tumour CA-IX status and tumour grade was assessable in 39 patients. Tumour grade was divided into two groups for the analysis: high grade (i.e. grade 3 tumours, n=18) and non-high grade (i.e. grade 1 and grade 2 tumours, n=21). There was a significant association between tumour grade and CA-IX status (Fisher's exact, $p<0.01$), with negative CA-IX status being associated with non-high grade tumours (**table 4.12**).

The relationship between tumour CA-IX status and oestrogen receptor status was assessable in 40 patients. There was a significant association between oestrogen receptor status and CA-IX status (Fisher's exact, $p<0.05$), with negative CA-IX status being associated with positive oestrogen receptor status (**table 4.12**).

The relationship between tumour CA-IX status and tumour necrosis on the diagnostic core-biopsy samples was assessable in 40 patients. There was a significant association between tumour necrosis and CA-IX status (Fisher's exact, $p<0.001$), with tumour necrosis being associated with positive CA-IX status (**table 4.12**).

4.4.5.3 CA-IX and Angiogenesis-related parameters

The relationship between tumour CA-IX status and MVD and PCI was assessable in 38 patients. There was a non-significant trend towards a lower MVD in CA-IX positive tumours compared with CA-IX negative tumours (55.6/mm^2 and 88.9/mm^2 respectively, MW, $p=0.06$) (**table 4.13** and **figure 4.11**). There was no significant difference in PCI between CA-IX positive and negative tumours (12.5% and 9.8% respectively, MW, $p=0.59$) (**table 4.13**).

The relationship between tumour CA-IX status and VEGF IRS was assessable in 37 patients. There was no significant difference in VEGF IRS between CA-IX positive and negative tumours (9 and 8 respectively, MW, $p=0.58$) (**table 4.13**).

4.4.5.4 Tumour histological features and Angiogenesis-related parameters

The relationships between tumour histology parameters (tumour grade, histological subtype, oestrogen receptor status and tumour necrosis) and the angiogenesis-related parameters (MVD, PCI and VEGF IRS) were assessed. Tumour grade was divided into two groups for the analysis: high grade (n=20) and non-high grade (n=23). No significant correlation was found between any of the individual histological parameters and any of the individual angiogenesis-related parameters. These results are shown in **table 4.14**.

4.5 DISCUSSION

Multi-parameter functional DCE-MRI provides 'real-time' information regarding the tumour microvasculature. The underlying pathophysiological correlates of functional MRI are not yet fully understood. The aim of this study was to assess the relationship between the 3 functional MRI techniques, namely, T1W-DCE-MRI, T2*W DCE-MRI and BOLD, and to assess the relationship between the MRI-derived kinetic parameters and both conventional histological features of breast cancers and immunohistochemically-derived measures of tumour angiogenesis and oxygenation.

Analysis of the T1W and T2*W DCE-MRI kinetic parameters revealed a significant correlation between the T2*W perfusion-related parameters, rBV and rBF, and the T1W semi-quantitative parameters MeanGrad, MaxAmp and Wt, and the T1W quantitative parameters K^{trans}, k_{ep} and MaxGd (MaxGd on three-slice analysis only). While the semi-quantitative parameters describe the tumour signal intensity enhancement following the administration of GdDTPA, the T1W quantitative parameters provide a more accurate measure of the change in contrast medium concentration at the tumour tissue level. Both the T1W semi-quantitative and quantitative parameters are dependant upon microvessel permeability, surface area and tumour blood flow. K^{trans} describes the transendothelial transport of GdDTPA by diffusion from the intravascular space to the extravascular extracellular space (EES) within the tumour (figure 1.10). In tissues where vascular permeability is greater than vascular inflow, the delivery of contrast to the EES becomes dependent on the delivery of the contrast medium to the tissue as a whole, that is the blood perfusion. This is termed a "flow-limited" situation and blood perfusion becomes the dominant factor determining contrast agent kinetics. In a "flow-limited" situation, K^{trans} approximates to tissue blood flow per unit volume. If tissue perfusion is sufficient and transport out of the vasculature does not deplete the intravascular contrast medium concentration, then transport across the vessel wall is the major factor determining contrast medium kinetics. This is termed a "non-flow limited" situation and here K^{trans} approximates to the vessel permeability-surface

area product. In breast tumours, vascular permeability tends to outstrip the vascular in flow (flow-limitation) and hence we would expect the K^{trans} values to be dominated by blood perfusion. The rate constant, k_{ep}, which describes the diffusion of contrast agent back into the vasculature from the EES is similarly affected. Thus, the significant correlation observed between the T1W kinetic parameters, in particular, K^{trans} and k_{ep}, and the T2*W perfusion-related parameters, rBV and rBF, is what would be expected and confirms a "flow-limited" situation in primary breast tumours.

The non-enhanced MRI technique of BOLD MRI uses deoxyhaemoglobin as an "intrinsic" contrast medium and, as such, provides a potential method for assessing tissue oxygenation using the parameter R2*. A high R2* value reflects an increased deoxyhaemoglobin concentration and hence a relatively low tissue oxygenation while a low R2* value reflects a decreased deoxyhaemoglobin level and hence a relatively higher tissue oxygenation. Analysis of the BOLD MRI parameter, R2* with both the T1W and T2*W DCE-MRI parameters, revealed a significant inverse correlation between R2* and the T1W semi-quantitative parameters MaxAmp and Wt, and the T2*W perfusion-related parameters rBV and rBF. These inverse correlations appear to demonstrate what one would expect, that is, tumours with low blood perfusion would exhibit a relatively lower level of oxygenation compared with those with high blood perfusion.

In order to assess the pathophysiological correlates of the functional MRI parameters, the kinetic parameters were analysed according to both conventional histological features of primary breast tumours and immunohistochemically-derived measures of tumour angiogenesis and oxygenation.

Analysis of the functional MRI parameters according to conventional histological tumour features revealed significant differences in kinetic parameter values according to histological tumour type, histological tumour grade, oestrogen-receptor status and pathological tumour necrosis. Invasive ductal carcinomas were found to have significantly lower median R2* values compared with invasive lobular or mixed ductal/lobular carcinomas, however, further

distinction of the invasive ductal carcinoma subgroup was not seen. This may have been a result of the small patient numbers within the two other histological tumour subtypes (lobular carcinomas, n=5; mixed ductal/lobular, n=4).

Histological tumour grade is known to be an important prognostic feature in primary breast cancer, in particular, grade 3 tumours are associated with a worse prognosis [9]. Analysis of the functional MRI parameters according to grade (high grade (i.e. grade 3) versus non-high grade (i.e. grade 1 and 2)) revealed a significant difference in the T1W semi-quantitative parameter values, MaxAmp and MeanGrad, and the T2*W perfusion-related parameters, rBV and rBF according to tumour grade. This suggested a strong relationship between breast cancer blood perfusion/permeability and histological tumour grade, with high grade tumours demonstrating higher perfusion/permeability. This would be in accordance with the finding by others of a positive correlation between tumour grade and angiogenesis [121]. This greater blood perfusion and vessel permeability may result in an increased risk of micrometastic disease and hence, in part, explain the adverse prognostic significance of high tumour grade. In this study, no association was found between the immunohistochemically-derived angiogenesis-related parameters MVD, PCI and VEGF expression and any of the T1W or T2*W DCE-MRI parameters, however, a positive correlation was found between MVD and the BOLD MRI parameter, R2*. This may, in part, reflect hypoxia-driven angiogenesis, however, no association was found between MVD and tumour hypoxia as assessed by CA-IX expression. Further, a paradoxical association was noted between R2* and CA-IX expression, with lower R2* median values associating with CA-IX expression. This is in direct contrast to findings in human prostate cancer, where a significant positive correlation was found between R2* and tumour hypoxia, as assessed by pimonidazole [310]. This would suggest that within primary breast cancers, R2* may not be informing upon the tumour cellular oxygenation state, but rather simply reflecting the oxygenation level within the tumour vessels. This would be supported by the significant inverse correlation seen between R2* and the perfusion-related parameters, rBV and rBF, suggesting that R2* contrast within breast tumours in dominated by blood flow and volume. As such, tumour

cellular hypoxia may be stimulating angiogenesis and this would explain the higher rBV and rBF values associated with CA-IX positive tumours, with low levels of intravascular deoxyhaemoglobin resulting in a low R2* value. This paradox of a large blood volume and concomitant tumour hypoxia has been observed *in vitro* [311]. In a similar fashion, pathological tumour necrosis may be a driving force for angiogenesis, resulting in the higher K^{trans}, k_{ep}, rBV and rBV and lower R2* values that are seen to be associated with tumour necrosis.

Evaluation of the functional MRI parameters according to oestrogen-receptor (ER) status demonstrated significantly lower median k_{ep}, rBV, rBF and Wt in ER positive tumours compared with ER negative tumours, suggesting a lower blood perfusion in ER positive tumours. A significantly higher median R2* was also seen with ER positive tumours. ER status has been shown to be an important prognostic factor in early breast cancer [312, 313], with positive ER status being associated with improved outcome. This may be an indirect effect due to the additional treatment option adjuvant endocrine therapy that is available to patients with ER positive tumours, however, it may also be a direct effect of a biologically less aggressive tumour type. Indeed, as was demonstrated in this study, ER status has been correlated with lower tumour grade [313]. It may be that the biologically less aggressive nature of ER positive tumours may be a result of their lower blood perfusion.

Correlation of CA-IX staining with histological tumour features revealed a significant association between CA-IX staining and tumour grade, ER status and tumour necrosis. Positive CA-IX staining tended to associate with the aggressive tumour features of high grade, ER negative status and necrosis. No association was found between either CA-IX staining or the histological tumour features and any of the immunohistochemically-derived angiogenesis-related parameters.

In summary, therefore, significant positive correlations were found between T1W and T2*W DCE-MRI kinetic parameters suggesting high microvessel permeability within breast tumours and "flow-limited" GdDTPA contrast

kinetics. In addition, a significant inverse correlation was observed between the BOLD MRI parameter, R2*, and the T2*W perfusion-related parameters, rBV and rBF, suggesting the R2* contrast in breast cancers is dominated by blood volume and flow. The apparent paradoxical association between R2* and the immunohistochemically-derived measure of tumour hypoxia (CA-IX staining), suggests that, unlike human prostate cancers, R2* may not reflect the tumour intracellular oxygenation level but rather reflect intravascular oxygenation. Further, the high perfusion-related parameters associated with CA-IX staining may reflect hypoxia driven angiogenesis.

Table 4.1. Demographics of those patients who underwent a pre-treatment multi-parameter functional MRI scan

No. of patients	**46**	
Median age (range)	**48 years (29 – 70)**	
Menopausal status	**Pre**	**26**
	Post	**20**
Stage	**I**	**3**
	II	**31**
	III	**11**
	IV	**1**
Grade	**1**	**3**
	2	**20**
	3	**20**
	Unknown	**3**
ER status	**Positive**	**35**
	Negative	**11**
Histological type	**Invasive ductal**	**35**
	Lobular	**5**
	Mixed	**4**
	Other	**2**
Tumour necrosis (n=40)	**Absent**	**27**
	Present	**13**
CA-IX staining (n=40)	**Negative**	**25**
	Positive	**15**

Table 4.2. Spearman's rank correlation coefficients showing the relationship between the T1W and T2*W DCE-MRI kinetic parameters

T1W MRI sequence	MRI parameter	Spearman's Rank Correlation Coefficient Rho (p-value)		
		T2*W parameters		
		rBV	rBF	MTT
Semi-quantitative	MeanGrad	**0.40 (<0.01)**	**0.38 (<0.05)**	0.08 (0.62)
	MaxAmp	**0.62 (<0.0001)**	**0.66 (<0.0001)**	0.30 (0.06)
	Wt	**0.63 (<0.0001)**	**0.65 (<0.0001)**	0.01 (0.94)
Quantitative (single-slice)	K^{trans}	**0.47 (=0.002)**	**0.46 (<0.005)**	-0.003 (0.98)
	v_e	0.10 (0.55)	0.12 (0.46)	**0.33 (<0.05)**
	k_{ep}	**0.47 (<0.002)**	**0.48 (<0.002)**	-0.18 (0.24)
	MaxGd	0.23 (0.14)	0.28 (0.07)	0.25 (0.11)
Quantitative (three-slice)	K^{trans}	**0.51 (<0.0001)**	**0.54 (<0.0005)**	-0.10 (0.52)
	v_e	0.16 (0.32)	0.18 (0.27)	**0.38 (<0.05)**
	k_{ep}	**0.49 (=0.001)**	**0.51 (<0.001)**	-0.22 (0.16)
	MaxGd	**0.31 (<0.05)**	**0.34 (<0.05)**	0.27 (0.09)

Table 4.3. Spearman Rank correlation coefficients showing the relationship between the T1W and T2*W DCE-MRI kinetic parameters and the BOLD MRI parameter, R2*.

DCE-MRI Sequence	MRI Parameter	Spearman's Rank Correlation Coefficient Rho (p-value)
		BOLD MRI parameter, R2*
T1W semi-quantitative	MeanGrad	-0.14 (0.39)
	MaxAmp	-0.65 (<0.0001)
	Wt	-0.61 (<0.0001)
T1W quantitative (single-slice)	K^{trans}	-0.06 (0.70)
	v_e	0.04 (0.80)
	k_{ep}	-0.15 (0.32)
	MaxGad	-0.02 (0.90)
T1W quantitative (three-slice)	K^{trans}	-0.18 (0.24)
	v_e	-0.11 (0.49)
	k_{ep}	-0.14 (0.36)
	MaxGad	-0.16 (0.29)
T2*W quantitative	rBV	-0.73 (<0.0001)
	rBF	-0.71 (<0.0001)
	MTT	-0.19 (0.24)

Table 4.4. Pre-treatment median functional MRI parameter values according to tumour histological subtype

MRI sequence	MRI parameter (median)	Tumour histology			p-value (Kruskal-Wallis test)
		Invasive ductal (n=35)	Invasive lobular (n=5)	Mixed ductal & lobular (n=4)	
T1W Semi-quantitative	MeanGrad (AU)	39.7	42.6	42.6	0.89
	MaxAmp (%)	92	77	86	0.67
	Wt (AU)	**-0.23**	**-0.24**	**-0.60**	**=0.02**
T1W Quantitative (single-slice)	K^{trans} (min^{-1})	0.58	0.57	0.68	0.60
	v_e (%)	54	50	70	0.07
	k_{ep} (min^{-1})	1.14	0.80	0.97	0.63
	MaxGd (mmol/kg)	0.41	0.37	0.53	0.06
T1W Quantitative (three-slice)	K^{trans} (min^{-1})	0.56	0.55	0.54	1.00
	v_e (%)	49	48	59	0.21
	k_{ep} (min^{-1})	1.05	0.83	0.91	0.55
	MaxGd (mmol/kg)	0.40	0.42	0.45	0.31
T2*W Quantitative	rBV	161.3	95.5	94.0	0.41
	rBF	6.40	4.14	4.23	0.49
	MTT (sec)	23.89	23.20	23.83	0.81
BOLD MRI	R_2* (sec^{-1})	**32.2**	**38.9**	**39.8**	**=0.04**

Table 4.5. Pre-treatment median functional MRI parameter values according to tumour grade

MRI sequence	MRI parameter (median)	Tumour grade			p-value (Kruskal-Wallis test)
		1 (n=3)	2 (n=20)	3 (n=20)	
T1W Semi-quantitative	MeanGrad (AU)	**20.51**	**41.64**	**41.85**	**=0.04**
	MaxAmp (%)	85	86	101	0.11
	Wt (AU)	**-0.24**	**-0.25**	**-0.18**	**=0.04**
T1W Quantitative (single-slice)	K^{trans} (min^{-1})	**0.32**	**0.64**	**0.58**	**=0.04**
	v_e (%)	50	57	51	0.19
	k_{ep} (min^{-1})	**0.60**	**1.05**	**1.14**	**=0.04**
	MaxGd (mmol/kg)	0.37	0.46	0.40	0.10
T1W Quantitative (three-slice)	K^{trans} (min^{-1})	**0.30**	**0.56**	**0.55**	**=0.04**
	v_e (%)	48	53	48	0.23
	k_{ep} (min^{-1})	**0.58**	**0.98**	**1.08**	**=0.02**
	MaxGd (mmol/kg)	0.35	0.42	0.36	0.19
T2*W Quantitative	rBV	**66.3**	**128.1**	**176.6**	**=0.04**
	rBF	**2.69**	**5.21**	**7.13**	**=0.03**
	MTT (sec)	23.8	23.8	23.8	0.81
BOLD MRI	R_2* (sec^{-1})	37.3	33.9	30.5	0.06

Table 4.6. Evaluation of pre-treatment median functional MRI parameter values according to high grade versus non-high grade tumours

MRI sequence	MRI parameter (median)	Tumour grade		p-value (Mann-Whitney U-test)
		High Grade (n=20)	Non-high grade (n=23)	
T1W Semi-quantitative	MeanGrad (AU)	41.8	38.5	0.28
	MaxAmp (%)	**101**	**86**	**<0.05**
	Wt (AU)	**-0.18**	**-0.24**	**<0.05**
T1W Quantitative (single-slice)	K^{trans} (min^{-1})	0.58	0.58	0.60
	v_e (%)	51	55	0.13
	k_{ep} (min^{-1})	1.14	1.00	0.43
	MaxGd (mmol/kg)	0.40	0.43	0.22
T1W Quantitative (three-slice)	K^{trans} (min^{-1})	0.55	0.55	0.93
	v_e (%)	48	53	0.23
	k_{ep} (min^{-1})	1.08	0.90	0.20
	MaxGd (mmol/kg)	0.36	0.42	0.28
T2*W Quantitative	rBV	**176.6**	**127.3**	**<0.05**
	rBF	**7.13**	**5**	**<0.01**
	MTT (sec)	23.8	23.8	0.88
BOLD MRI	R_2^* (sec^{-1})	30.5	34.4	0.06

Table 4.7. Pre-treatment median functional MRI parameter values according to tumour oestrogen-receptor status

MRI sequence	MRI parameter (median)	Oestrogen-receptor positive	Oestrogen-receptor negative	p-value (Mann-Whitney U-test)
T1W Semi-quantitative	MeanGrad (AU)	42.4	39.4	0.86
	MaxAmp (%)	87	100	0.28
	Wt (AU)	**-0.24**	**-0.16**	**=0.03**
T1W Quantitative (single-slice)	K^{trans} (min^{-1})	0.58	0.58	0.60
	v_e (%)	54	54	0.72
	k_{ep} (min^{-1})	0.98	1.21	0.13
	MaxGd (mmol/kg)	0.41	0.45	0.83
T1W Quantitative (three-slice)	K^{trans} (min^{-1})	0.53	0.61	0.11
	v_e (%)	49	50	0.98
	k_{ep} (min^{-1})	**0.93**	**1.22**	**=0.04**
	MaxGd (mmol/kg)	0.40	0.41	0.53
T2*W Quantitative	rBV	**127**	**191**	**=0.01**
	rBF	**5.4**	**8.1**	**=0.007**
	MTT (sec)	24.1	23.6	0.19
BOLD MRI	R_2* (sec^{-1})	**37**	**22.2**	**=0.0004**

Table 4.8. Pre-treatment median parameter values according to tumour necrosis status

MRI sequence	MRI parameter (median)	Tumour necrosis present	Tumour necrosis absent	p-value (Mann-Whitney U-test)
T1W Semi-quantitative	MeanGrad (AU)	40.7	39.7	0.31
	MaxAmp (%)	92	91	0.55
	Wt (AU)	-0.20	-0.25	0.06
T1W Quantitative (single-slice)	K^{trans} (min^{-1})	**0.71**	**0.58**	**=0.02**
	v_e (%)	57	53	0.81
	k_{ep} (min^{-1})	**1.34**	**0.93**	**=0.02**
	MaxGd (mmol/kg)	0.46	0.41	0.20
T1W Quantitative (three-slice)	K^{trans} (min^{-1})	0.62	0.55	0.052
	v_e (%)	54	48	0.98
	k_{ep} (min^{-1})	**0.93**	**1.22**	**=0.035**
	MaxGd (mmol/kg)	0.44	0.40	0.06
T2*W Quantitative	rBV	**218.4**	**126.6**	**=0.0005**
	rBF	**8.5**	**5.4**	**=0.0008**
	MTT (sec)	24.0	23.7	0.51
BOLD MRI	R_2* (sec^{-1})	**27.5**	**35.6**	**=0.02**

Table 4.9. Correlations between the functional MRI parameters and immunohistochemical angiogenesis-related parameters

MRI sequence	MRI parameter	Spearman's Rank Correlation Coefficient, Rho (p-value)		
		MVD	PCI	VEGF IRS
T1W Semi-quantitative	MeanGrad	0.15 (0.37)	0.08 (0.61)	0.10 (0.55)
	MaxAmp	-0.22 (0.18)	0.10 (0.55)	0.12 (0.49)
	Wt	-0.26 (0.11)	-0.15 (0.35)	0.11 (0.50)
T1W Quantitative (single-slice)	K^{trans}	0.07 (0.69)	0.01 (0.96)	0.29 (0.08)
	v_e	0.02 (0.89)	0.14 (0.39)	0.28 (0.09)
	k_{ep}	0.02 (0.91)	0.001 (0.99)	0.15 (0.38)
	MaxGd	-0.02 (0.92)	0.09 (0.60)	0.29 (0.08)
T1W Quantitative (three-slice)	K^{trans}	0.11 (0.51)	0.08 (0.62)	0.12 (0.46)
	v_e	-0.08 (0.64)	0.24 (0.15)	0.19 (0.25)
	k_{ep}	0.03 (0.85)	-0.01 (0.94)	0.07 (0.66)
	MaxGd	-0.17 (0.30)	0.22 (0.19)	0.21 (0.20)
T2*W Quantitative	rBV	-0.21 (0.21)	-0.10 (0.54)	0.14 (0.41)
	rBF	-0.25 (0.14)	-0.06 (0.72)	0.15 (0.39)
	MTT	-0.15 (0.39)	-0.04 (0.81)	0.03 (0.84)
BOLD MRI	R2*	**0.35 (=0.035)**	0.02 (0.90)	0.07 (0.67)

Table 4.10. Pre-treatment median parameter values according to carbonic anhydrase-IX status

MRI sequence	MRI parameter (median)	CA-IX positive	CA-IX negative	p-value (Mann-Whitney U-test)
T1W Semi-quantitative	MeanGrad (AU)	44.7	38.5	0.14
	MaxAmp (%)	102	87	0.08
	Wt (AU)	**-0.17**	**-0.25**	**=0.02**
T1W Quantitative (single-slice)	$K^{trans}(min^{-1})$	0.70	0.58	0.07
	v_e (%)	55	53	0.86
	$k_{ep}(min^{-1})$	1.34	0.98	0.06
	MaxGd (mmol/kg)	0.45	0.41	0.49
T1W Quantitative (three-slice)	$K^{trans}(min^{-1})$	0.60	0.53	0.11
	v_e (%)	54	48	0.29
	$k_{ep}(min^{-1})$	1.25	0.98	0.09
	MaxGd (mmol/kg)	0.44	0.40	0.19
T2*W Quantitative	rBV	**211.6**	**125.2**	**=0.0015**
	rBF	**8.1**	**5.0**	**=0.0011**
	MTT (sec)	24.0	23.4	0.32
BOLD MRI	R_2^* (sec^{-1})	**28.9**	**36.0**	**=0.01**

Table 4.11. Relationship between the individual histological tumour features of primary breast cancer

	p-value (Fisher's exact test)		
	Grade (high vs. non-high)	ER status (positive vs. negative)	Necrosis (present vs. absent)
Histology (IDC vs. non-IDC)	**<0.0001**	**=0.04**	**=0.30**
Grade (high vs. non-high)	-	**=0.003**	**=0.052**
ER status (positive vs. negative)	-	-	**=0.02**

Table 4.12. Relationship between CA-IX status and histological parameters of primary breast cancer

Histological features	CA-IX status (positive vs. negative)
	p-value (Fisher's exact test)
Tumour grade (high grade vs. non-high grade)	<0.001
Oestrogen-receptor status (positive vs. negative)	<0.05
Tumour necrosis (present vs. absent)	<0.001

Table 4.13. Pre-treatment median MVD, PCI and VEGF IRS according to carbonic anhydrase-IX status

Angiogenesis-related parameter	CA-IX positive	CA-IX negative	p-value (Mann-Whitney U-test)
MVD	**55.6/mm2**	**88.9/mm2**	0.06
PCI	**12.5%**	**9.8%**	0.59
VEGF IRS	**9**	**8**	0.58

Table 4.14. Relationship between the pre-treatment angiogenesis-related parameters and tumour histology

Angiogenesis-related parameter	Histological subtype				Tumour grade		
	Invasive ductal	Lobular	Mixed ductal/lobular	p-value (Kruskal-Wallis test)	High grade	Non-high grade	p-value (Mann-Whitney U-test)
MVD	75.0/mm^2	125.0/mm^2	61.1/mm^2	0.14	66.7/mm^2	80.6/mm^2	0.28
PCI	11.6%	20.8%	22.3%	0.90	11.6%	14.9%	0.93
VEGF IRS	8	9	6	0.27	9	8	0.79

Angiogenesis-related parameter	Oestrogen receptor status			Tumour necrosis		
	Positive	Negative	p-value (Mann-Whitney U-test)	Present	Absent	p-value (Mann-Whitney U-test)
MVD	80.6/mm^2	66.7/mm^2	0.25	55.6/mm^2	80.6/mm^2	0.15
PCI	15.5%	10.3%	0.30	12.5%	9.8%	0.83
VEGF IRS	8	10	0.49	9	8	0.41

Figure 4.1 Scatter plot demonstrating correlation between T1W (three-slice) and T2*W DCE-MRI parameters

(i) Plot of rBV against K^{trans}

(ii) Plot of rBF against K^{trans}

(iii) Plot of rBV against k_{ep}

(iv) Plot of rBF against k_{ep}

(i)

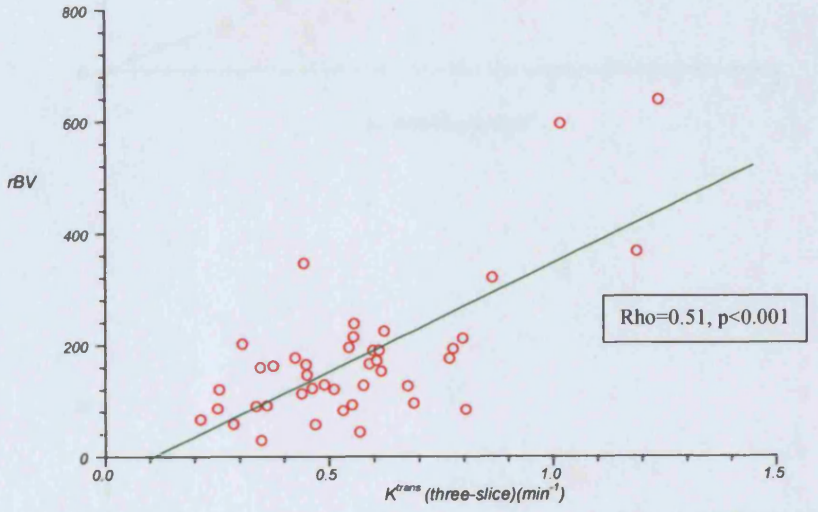

(ii)

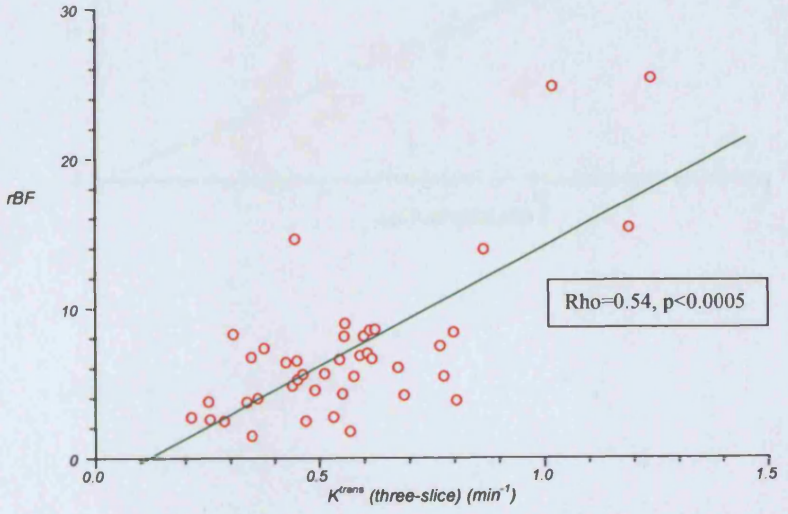

(iii)

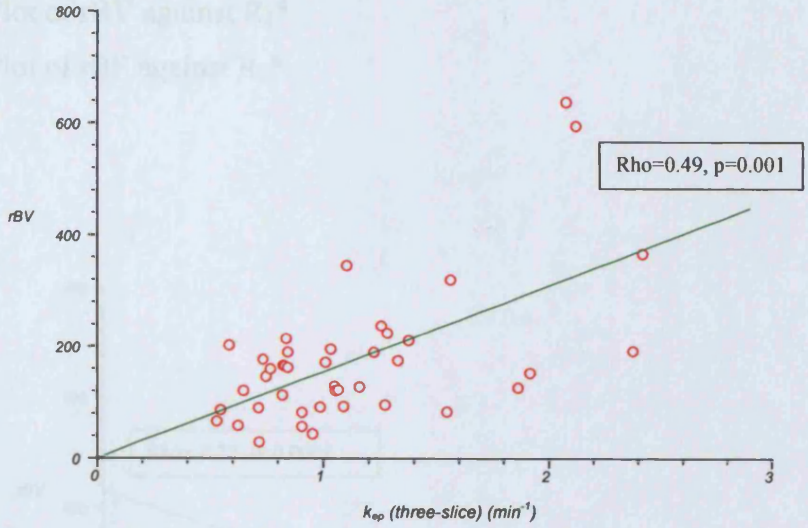
Rho=0.49, p=0.001
rBV
800
600
400
200
0
0
1
2
3
k_{ep} (three-slice) (min^{-1})

(iv)

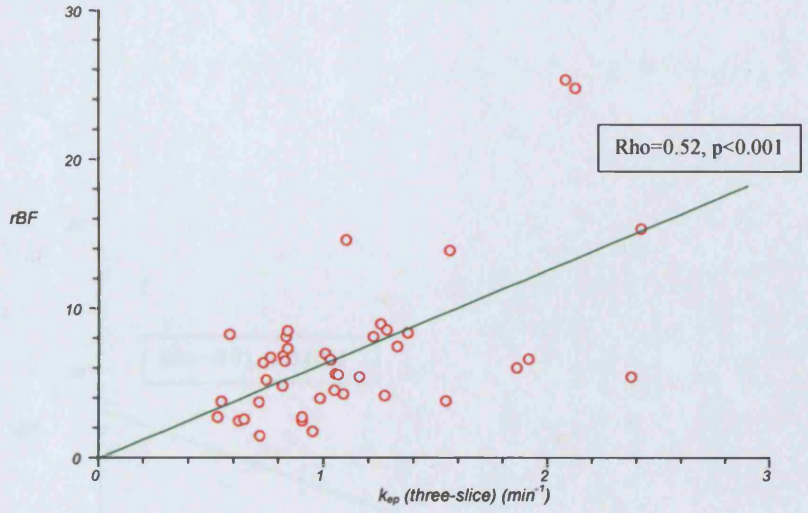
Rho=0.52, p<0.001
rBF
30
20
10
0
0
1
2
3
k_{ep} (three-slice) (min^{-1})

Figure 4.2 Scatter plot demonstrating correlation between BOLD MRI parameter, R_2*, and T2*W DCE-MRI parameters

(i) Plot of rBV against R_2*

(ii) Plot of rBF against R_2*

(i)

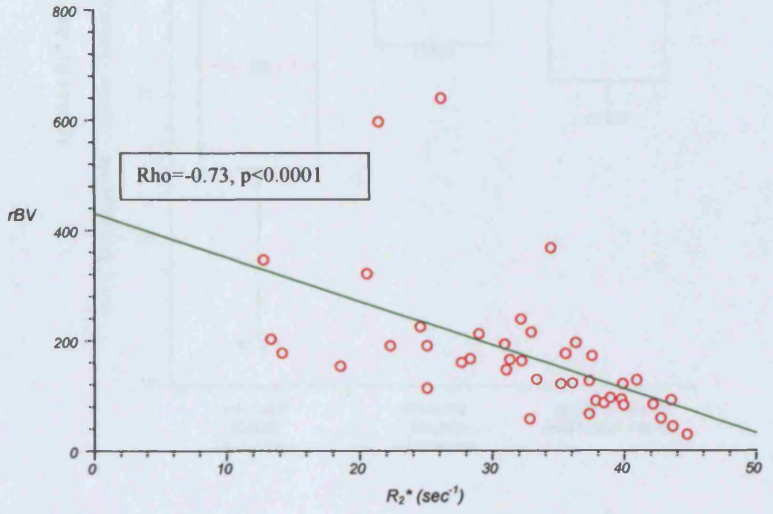

(ii)

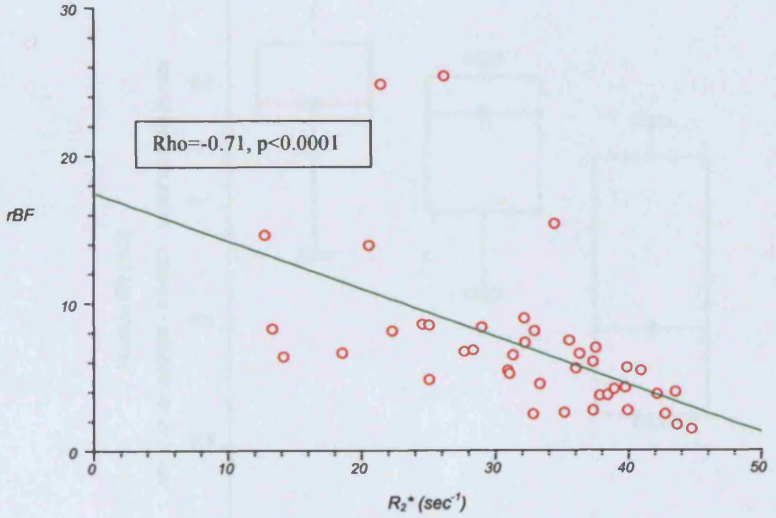

Figure 4.3. Box and Whisker plot of median R_2* according to histological sub-type

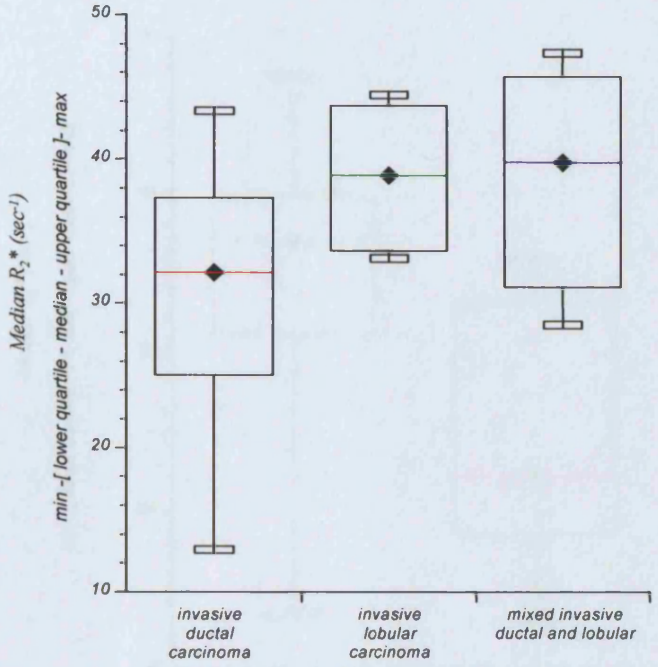

Figure 4.4. Box and Whisker plot of median Wt according to histological sub-type

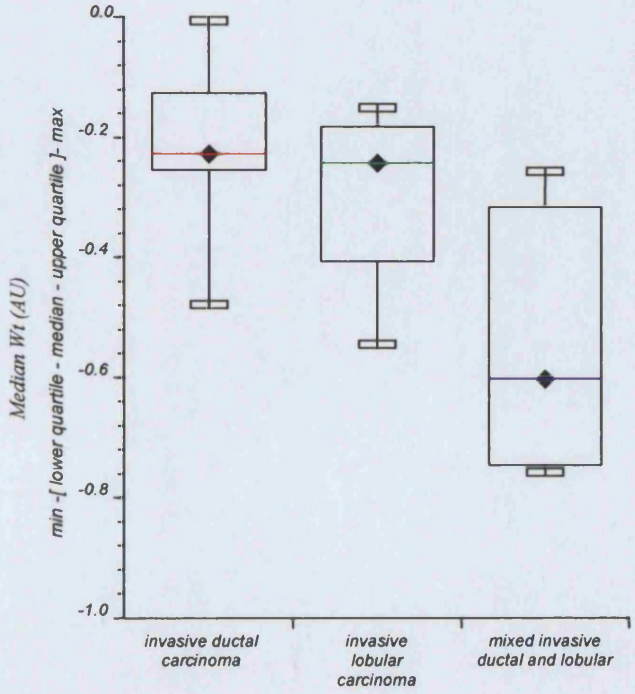

Figure 4.5. Box and Whisker plot of median R_2* according to oestrogen-receptor status

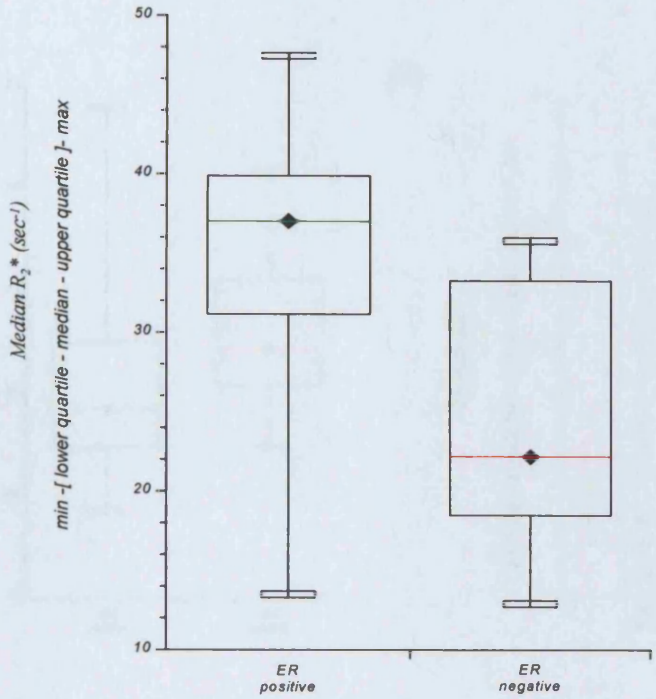

Figure 4.6. Box and Whisker plot of significant DCE-MRI parameters according to oestrogen-receptor status
(i) k_{ep} (ii) rBV (iii) rBF (iv) Wt

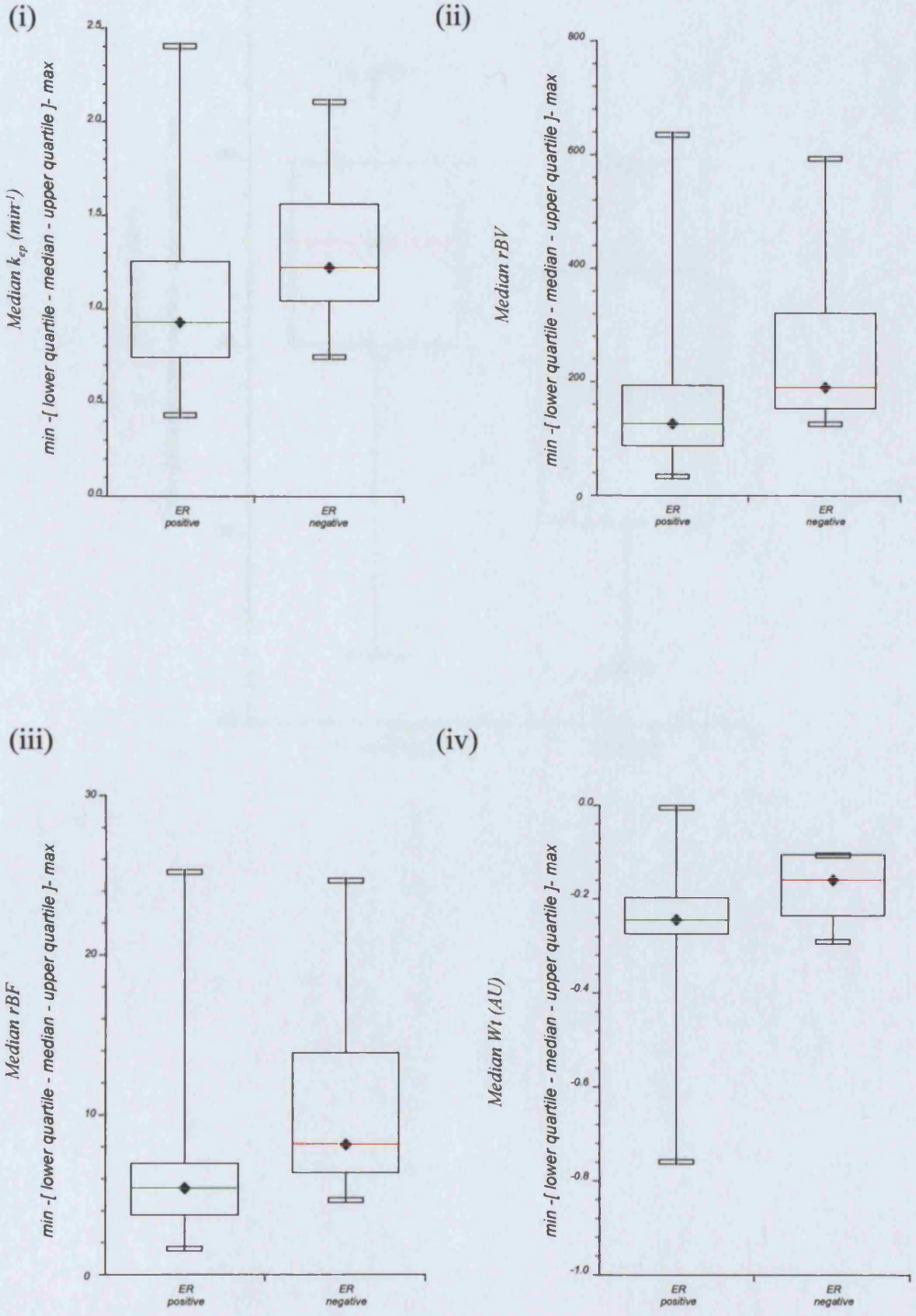

Figure 4.7. Box and Whisker plot of median R_2* according to tumour necrosis

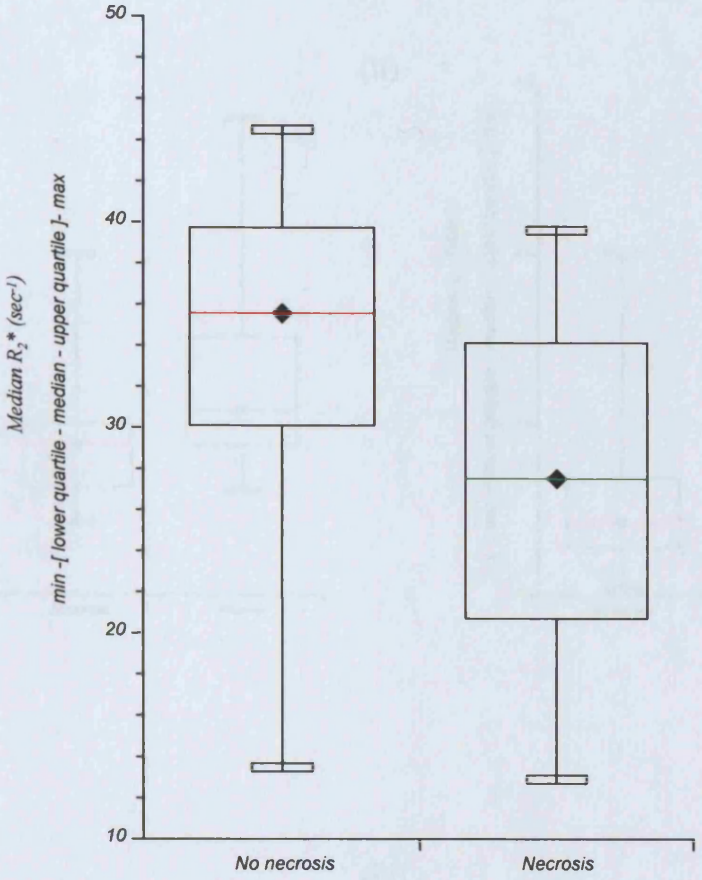

Figure 4.8. Box and Whisker plot of significant DCE-MRI parameters according to tumour necrosis (single-slice data)
(i) K^{trans} (ii) k_{ep} (iii) rBV (iv) rBF

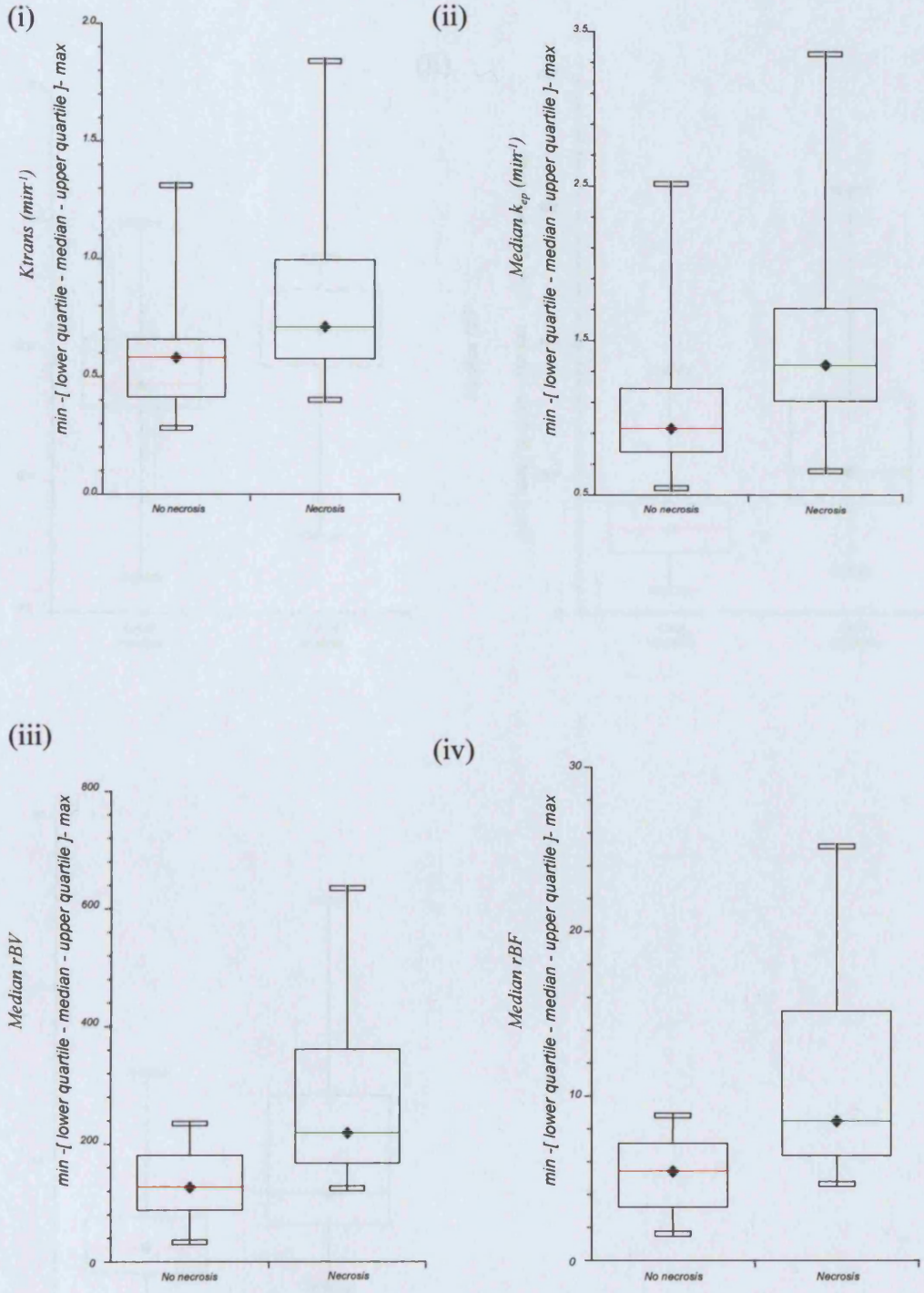

Figure 4.9. Box and Whisker plot of significant DCE-MRI parameters according to CA-IX staining

(i) Wt (ii) rBV (iii) rBF

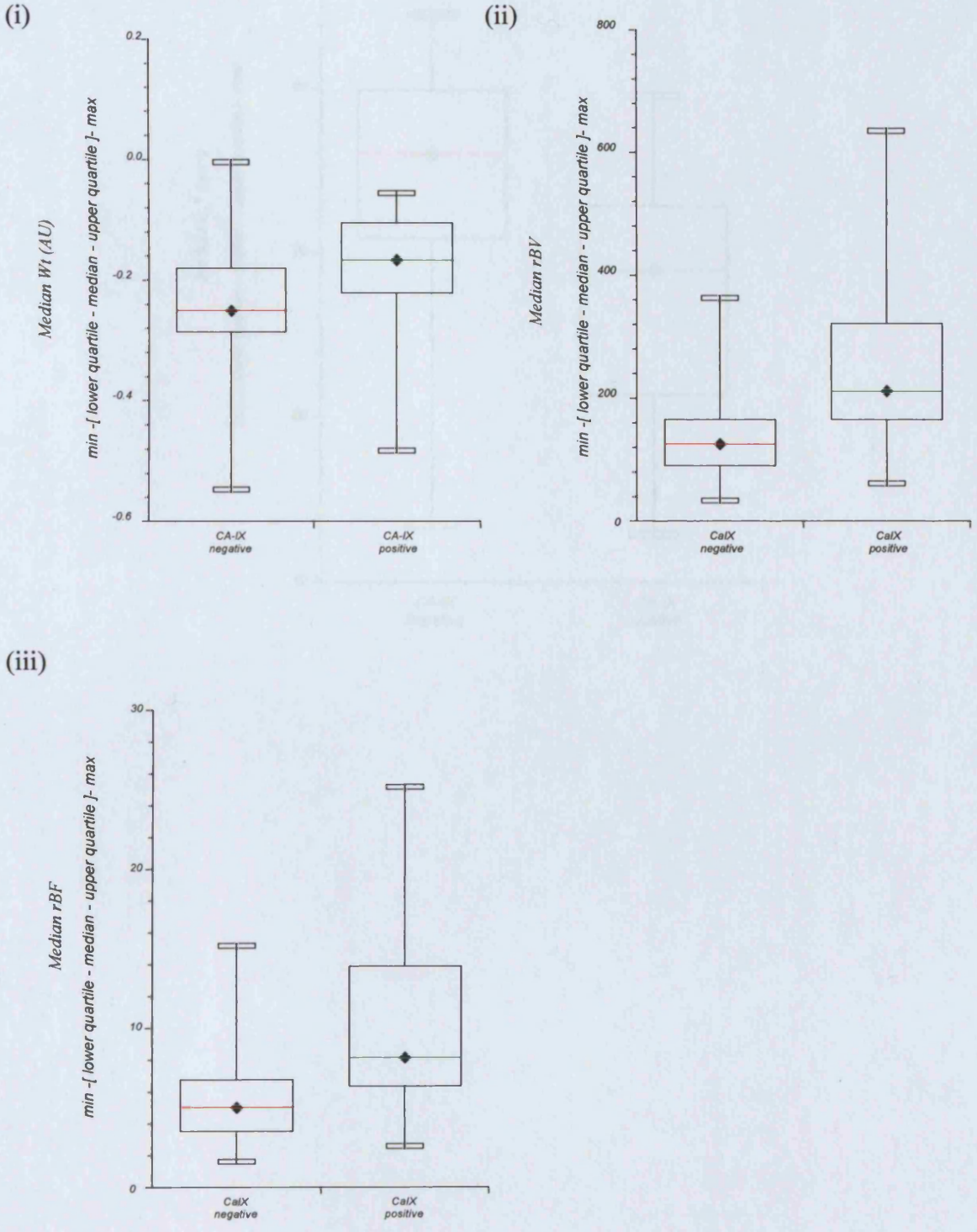

Figure 4.10. Box and Whisker plot of median R_2* according to CA-IX staining

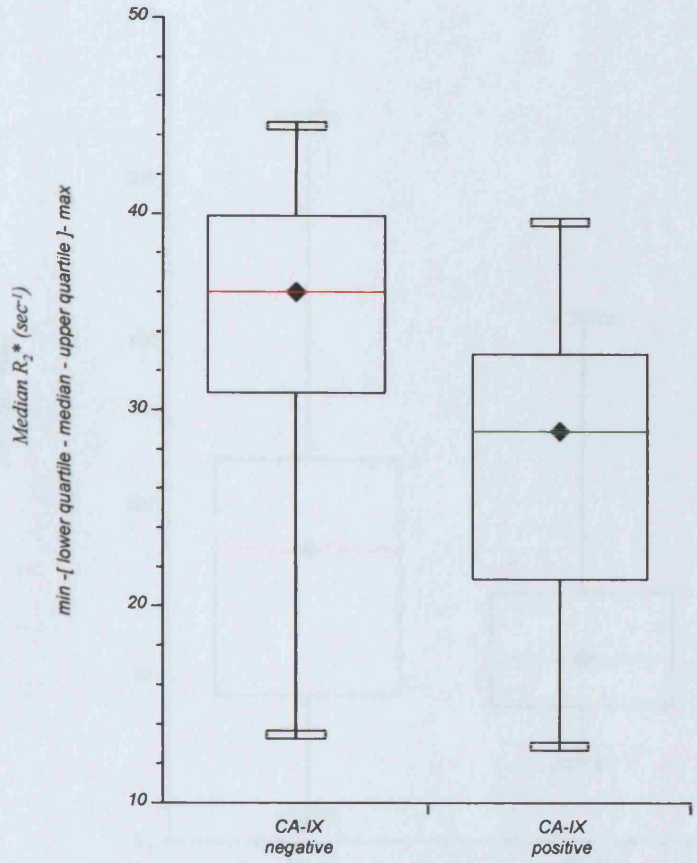

Figure 4.11. Box and Whisker plot of MVD according to CA-IX staining

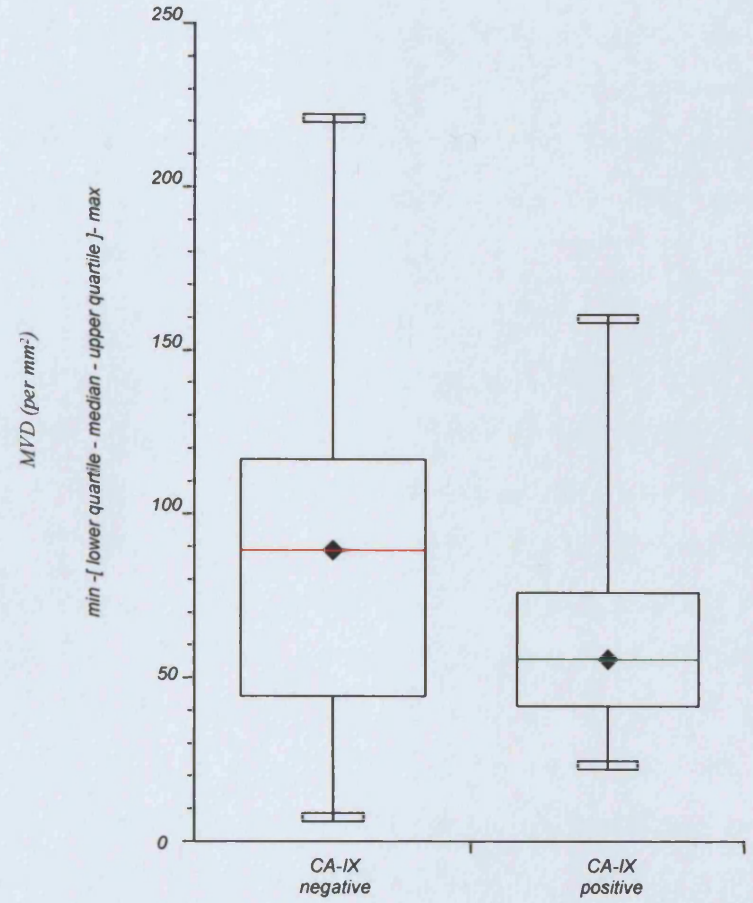

CHAPTER 5: CONCLUDING DISCUSSION

The principal aim of this thesis was to evaluate the vascular response to conventional anthracycline-based cytotoxic chemotherapy in primary breast cancer, using the neoadjuvant treatment setting as an *in vivo* research platform. With the primary tumour *in situ*, the neoadjuvant treatment setting enables a direct assessment of tumour chemo-responsiveness and permits an evaluation of the possible underlying biological mechanisms of response. In addition, response in the primary tumour may act as a surrogate marker of response in occult micrometastatic disease and hence enable the tailoring of treatment according to the individual patient response.

Conventional cytotoxic chemotherapy drugs produce their effect by damaging the reproductive integrity of cancer cells, either through damage to the DNA or damage to the mitotic machinery. With increased understanding of the critical dependence of cancers on angiogenesis for growth and survival, novel therapies that target the tumour vasculature have evolved. These novel treatments can be divided into those that directly damage the tumour vessels (vascular targeting agents) and those that impede the formation of new blood vessels (anti-angiogenic agents). It is proposed that these novel agents will be used in combination with conventional cytotoxic agents, and therefore, it is important to understand the effects of conventional chemotherapy on the tumour vasculature. This may enable the rational design of future treatment regimens.

Advances in radiological technology have lead to the development of functional imaging techniques that provide a non-invasive method for assessing the tumour microvasculature and these techniques have an increasing role in the evaluation of the effects of novel anti-angiogenic and vascular targeting agents. Multi-parameter functional MRI is one such technique and was used to evaluate the vascular response to neoadjuvant FEC chemotherapy in 28 patients with primary breast cancer in the study described in Chapter 2. Vascular kinetic parameters derived from T1W DCE-MRI, T2*W DCE-MRI and BOLD MRI were measured from within primary breast tumours prior to treatment and then again following two cycles of FEC chemotherapy. The whole tumour ROI was assessed rather than the tumour hotspot as this enables an appreciation of the

degree of enhancement heterogeneity across the tumour and removes potential observer bias related to hotspot selection. Further, pixel mapping of the ROI allows spatial matching of the different tumour vascular characteristics. In addition, although Hayes et al. did demonstrate a greater reduction in kinetic parameter values at the tumour hotspot following NAC in PBC, hotspot analysis was not shown to be superior to ROI analysis for predicting response to treatment [314] and a recent consensus guideline has confirmed whole tumour ROI assessment as the technique of choice [315].

In relation to the timing of the second MRI scan, the time-point following two cycles of NAC was selected following data from a pilot study of T1W DCE-MRI in patients receiving a variety of NAC regimens for PBC [316]. This study demonstrated that, although changes in the DCE-MRI kinetic parameter values were seen following a single cycle of NAC, the changes were unable to predict for final clinico-pathological outcome. Following two cycles of NAC, however, changes in the T1W DCE-MRI parameter, K^{trans}, could predict for final pathological response with an accuracy equivalent to change in MRI-derived tumour size. Hence, the baseline parameter values and the changes seen after two cycles of treatment were correlated with final clinical and pathological response to six cycles of treatment in order to determine whether the vascular changes could predict for treatment response.

The UICC/WHO criteria for clinical response [290, 291] was used in this study rather than the RECIST criteria [317] in order to allow a comparison of the results with that of other imaging studies of NAC in primary breast cancer [84, 91, 316]. In addition, the relationship between clinical response and long term outcome has been demonstrated in NAC studies where the UICC/WHO response criteria was used [24] and validation of the RECIST response criteria in this setting remains to be fully assessed [318]. In relation to the pathological tumour response, this was scored by a single experienced pathologist and graded 1 to 5 according to defined criteria as described in chapter 2. Patients with a pathological response grade from 1 to 4 were defined as pathological responders,

while those patients with a grade 5 pathological response were defined as pathological non-responders. This classification was used for a number of reasons. Firstly, although complete pathological response (pCR) has been shown to predict for improved overall survival [24, 30, 83], its clinical usefulness is limited by the small number of patients (5-10%) who achieve such a response following anthracycline-based NAC. Thus, a system that groups patients with a complete or partial pathological response together may be clinically more relevant. Secondly, despite the presence of macroscopic residual tumour following NAC, those patients with a grade 4 pathological response were defined as "pathological responders" as the presence of chemotherapy–induced response features and a reduction in the tumour cell to stromal ratio has been shown to predict for an improved outsome when compared with residual macroscopic disease in the absence of any response features [294, 319, 320]. This may be a reflection of adequate cell kill at the level of systemic tumour micrometastases. Finally, the significance of residual DCIS when there has been a pathological complete response in the invasive cancer component following NAC remains unclear. Some pathological grading systems include residual DCIS within the pCR subgroup [294] while others do not [320]. Although NAC has no effect on DCIS, it remains to be clarified as to whether residual DCIS following NAC has an impact on longterm outcome [321] and hence residual DCIS alone was graded seperately to pCR for the purposes of this study.

Analysis of the data demonstrated that none of the baseline (pre-treatment) MRI-derived kinetic parameters were able to predict for final clinico-pathological response to NAC, however, the early changes in the microvessel permeability and perfusion-related kinetic parameters (MeanGrad, MaxAmp, K^{trans}, k_{ep}, rBV and rBF) following two cycles of treatment did predict for final clinico-pathological response. A reduction in these parameters correlated with treatment response. Using ROC curve analysis, the transfer constant, K^{trans}, a T1W DCE-MRI kinetic parameter that describes the transendothelial diffusion of low molecular weight contrast medium from the intravascular space into the extravascular extracellular space, was shown to be the best predictor of pathological treatment response when evaluated using three-slice imaging data,

with an AUC of 0.93 (sensitivity 94%, specificity 82%). There was, however, a trade-off between the identification of pathological non-responders and the misclassification of pathological responders (3 responding patients misclassified as non-responders). An evaluation of parameter combinations may lead to an improvement in the test specificity. Following the application of repeatability data from a reproducibility cohort of 12 patients, a failure of K^{trans} to drop significantly following two cycles of FEC NAC was able to predict for pathological non-response at an individual patient level with a positive predictive value (PPV) of 84% on the three-slice analysis. The improved accuracy for predicting pathological response with the three-slice data set over the single central-slice data suggests that further improvements in the technique might be possible with greater spatial resolution. This would be at the expense of temporal resolution (a doubling of the tumour slice numbers would require a halving of the data points collected for each slice), however kinetic modelling of the data would still be possible and might lead to an increase in the test's PPV.

Change in K^{trans} was also shown to be superior to change in MRI-derived tumour size for predicting response both on the group analysis and following the application of the reproducibility data. This is important as the conventional imaging techniques, namely X-ray mammography and ultrasonography, principally rely on changes in tumour size for evaluating tumour response to NAC. Calculation of the T1W DCE-MRI quantitative kinetic parameter values, however, relies on the pharmacokinetic modelling technique used to assess the Gd-DTPA concentration-time curve and the assumptions inherent to each model [163]. The Tofts and Kermode model was used in this study [161] and assumes that the vascular volume is negligible and that there is no dilution of contrast medium by the time it reaches the venous end of the capillary bed. Both of these assumptions are probably incorrect for tumours and more sophisticated models that are able to provide insights into tissue comparment behaviour are needed [322]. In general, however, if the contrast agent concentration can be measured accurately and the type, volume and method of administration are consistent, then it is possible to directly compare pharmacokinetic parameters between patients at different scanning sites despite these caveats.

Unfortunately, the effect of chemotherapy on menses and the changes in DCE-MRI kinetic parameter values was not assessed in this study. There is no data on the effects of the menstrual cycle on breast tumour kinetics, however, hormone replacement therapy has been shown to increase normal breast tissue perfusion as assessed by MRI in postmenopausal women [323]. Change in K^{trans} following 2 cycles of NAC, however, did predict for pathological response irrespective of menopausal status. An analysis of the normal breast tissue according to menopausal status may provide further insights into the hormonal effects on breast tissue permeability and perfusion.

Thus, this study demonstrated that conventional anthracycline-based chemotherapy has an effect on the tumour vascularity of primary breast cancers, in particular on microvessel permeability and perfusion, and that the early changes seen in these parameters following two cycles of treatment correlate with final clinico-pathological response. This study also demonstrated that the T1W DCE-MRI parameter, K^{trans}, is able predict for pathological tumour response at the individual patient level with a PPV for non-response of 84%. This might enable the tailoring of treatment according to individual tumour response and as such, prompt a therapy change that would hopefully improve patient outcome. This could be explored in an intervention study where the degree of change in K^{trans} on T1W DCE-MRI following two cycles of FEC NAC would determine whether treatment was continued with FEC chemotherapy or whether a treatment change was instituted, for example, a change to a taxane drug.

What remains unclear from this study is whether FEC chemotherapy is having a direct anti-angiogenic effect on the primary breast cancer microvasulature or whether the chemotherapy is acting indirectly via an effect on the balance of pro-angiogenic and anti-angiogenic factors subsequent to tumour cell death. This could be further explored in vitro, for example, by evaluating the effect of anthracyclines directly on proliferating endothelial cells or by measuring the

changes in angiogenic factor levels and angiogenic activity subsequent to tumour cell death and the effect of angiogenic factor re-exposure. In addition, the changes seen in the MRI-derived kinetic parameters in this study may be specific for FEC chemotherapy and as such, an evaluation of the effects of different chemotherapy agents, such as the taxanes, on the functional MRI parameters warrants investigation.

To further evaluate the vascular response to FEC chemotherapy in primary breast cancer, changes in angiogenesis as assessed at the histological tumour level was assessed and this study was described in Chapter 3. Using immunohistochemical staining techniques, a quantitative and a qualitative (functional) measure of tumour angiogenesis were evaluated in paired pre- and post-NAC pathological tumour specimens. Microvessel density (MVD) is a measure of the total number of microvessels seen within a high power field (x 200 magnification) and informs upon the net effect of tumour angiogenesis and angio-regression. A monoclonal antibody against one of the pan-endothelial cell antigens is used to highlight the tumour vasculature and in this study, the anti-CD34 antibody was used. MVD, however, fails to inform upon the quality, or functional status, of the tumour vasculature. An assessment of the functional status of vessels may provide a better measure of the tumour angiogenic activity and may be more informative in terms of prognosis or predicting response to treatment. Pericyte recriutment to microvessels is thought to reflect vessel maturation, and therefore, pericyte coverage was used as a measure of the functional vascular status in this study. Using immunohistochemical double-staining with the pan-endothelial marker, anti-CD34, and the mural cell marker, alpha-smooth muscle actin (α-SMA), the pericyte coverage index (PCI) was defined as the number of CD-34 and α-SMA positive vessels per high power field, expressed as a percentage of all CD-34 positive vessels within that field. Thus, a low PCI was reflective of an immature, proliferating tumour vasculature, while a high PCI represented a mature, more stabilised vasculature.

Evaluation of the MVD and PCI in the pre-treatment diagnostic core-biopsy breast tumour specimens demonstrated a median MVD of 76.4/mm^2 and a median PCI of 17.3%. Although continuous, the variables did not exhibit a normal distribution and hence non-parameteric statistical testing was used as a more robust method. This demonstrated that neither baseline MVD nor PCI correlated with the clinico-pathological response to treatment. Following 6 cycles of neoadjuvant FEC chemotherapy, the median MVD and PCI values in the definitive surgical specimens were 72.2/mm^2 and 25.5% respectively and the rise in PCI was found to be strongly significant (Wilcoxon's signed ranks test, $p<0.0001$). Thus, despite no apparent change in the total number of tumour microvessels following NAC, the quality or functional status of the vessels does appear to change. NAC appears to have a "pruning" effect on the immature proliferating vessels resulting in an increase in the proportion of mature, stabilised vessels. A similar "pruning" effect on tumour vasculature has been observed in studies using anti-angiogenic agents, in particular the anti-VEGF agents [300-303], and has been termed vascular "normalisation" [304, 324]. This pruning effect results in a more "normal" and hence more efficient vasculature, with improvements in nutrient and drug delivery to the tumour bed. Further, there appears to be a "normalisation window" period during which combination therapy, for example, the anti-angiogenic agents and radiotherapy or cytotoxic chemotherapy, might work best.

The changes observed in PCI in this study would suggest anthracycline-based chemotherapy induces a similar effect. Further, the evaluation of tumour VEGF expression prior to and following NAC within tumour specimens demonstrated a significant reduction in VEGF following chemotherapy. This reduction in VEGF production may, in part, represent the mechanism via which the chemotherapy is mediating its effect and may be a direct response to chemotherapy-induced cell death. The role of other angiogenic factors in this process, however, warrants further evaluation. For example, upregulation of the angiogenic factor, ang-1, has been shown in solid brain tumours following blockage of the VEGF-receptor 2 and is thought to mediate the increase in vessel pericyte coverage and vascular normalisation [302].

The results from the study described in Chapter 3 may assist in the development of rational drug combinations of cytotoxic chemotherapy and novel anti-angiogenic agents in the treatment of breast cancer. For example, if anthracycline-based chemotherapy is inducing a reduction in the immature proliferating vessels but failing to have an impact on the mature, more stabilised tumour vessels, then combination therapy with a novel agent that preferentially targets the mature blood vessels would be most appropriate. Further, if anthracycline-based chemotherapy is having its effect via a reduction in VEGF expression then further VEGF blockage may not necessarily improve tumour response, and the targeting alternative angiogenic factors might be more appropriate.

Change in MVD, PCI and VEGF expression failed to predict for clinico-pathological response to NAC, although a non-significant trend was observed towards an increase in PCI in the clinically responding group compared with the clinically non-responding. Failure of the baseline and changes in MVD to predict for response to NAC has been demonstrated by others [128-130] and Hlatky et al. have proposed that MVD cannot be used as a marker of response to treatment as it does not provide a direct measure of the angiogenic activity or the angiogenic dependence of a tumour [132]. PCI was assessed as a measure of "functional" vascular status, however, also failed to predict for response and it may be that more specific measures of activated endothelium need to be measured to predict for treatment response, for example, endoglin (CD105) [142]. The evaluation of other markers reflecting endothelial actvitiy and functional vascular status is suggested. An alternative explanation for these negative results may be sampling error. Breast tumours are known to be heterogenous and the pre-treatment diagnostic core biopsy may not provide an accurate representation of the whole tumour. Indeed, consistency in terms of the tumour histological grade between the diagnostic core biopsy and the subsequent whole breast tumour following primary surgery varies between 76-90% [325, 326].

The apparent vascular "normalisation" observed following NAC might in part explain the reduction in the permeability and perfusion-related DCE-MRI parameters observed in responding patients following two cycles of neoadjuvant chemotherapy. An assessment of the tumour MVD and PCI at this time-point might have determined whether this was the case or not. To further explore the pathophysiological correlates of the functional MRI kinetic parameters, the relationship between the MRI parameters and primary breast cancer features was evaluated and this study was described in Chapter 4.

The relationship between the functional MRI parameters and the conventional tumour histological features was assessed, as was the relationship with tumour MVD, PCI, VEGF expression and CA-IX staining (hypoxia-related marker) as evaluated from the pre-treatment diagnostic core biopsy specimens. Again non-parameteric statistical testing was used as a more robust method in the absence of a normal distribution of the data. This revealed a significant correlation between the permeability and perfusion-related DCE-MRI parameters and the aggressive tumour features of high grade and ER negative status. The increased vascularity of these tumours might explain, in part, their aggressive nature via an increased route of access for micrometastases into the peripheral circulation. No correlation was found, however, between the anigogenesis-related parameters (MVD, PCI and VEGF) and tumour grade or ER status, or any of the T1W or T2*W DCE-MRI parameters. A positive correlation was found between MVD and the BOLD MRI parameter, R2*, possibly reflecting hypoxia-driven angiogenesis, however, given the multiple testing this positive correltation may have occurred by chance. Doubt was cast over the role of R2* as a potential measure of the intra-tumour oxygenation level when CA-IX expression (hypoxia-related marker) within the tumour was found to be associated with a lower median R2*. A low R2* is thought to reflect low deoxyhaemoglobin and high oxygen levels, while a high R2* reflects the reverse and, as such, a positive association between CA IX staining and high R2* had been expected. It would appear, however, that R2* does not inform upon the tumour cellular oxygenation status in PBC but rather reflects the oxygenation level within the tumour vessels.

Thus, a high R2* might be the result of high oxygen extraction by active tumour cells leading to a high intravascular deoxyhaemoglobin level in the absence of tumour hypoxia. The dominant effect of tumour blood flow and volume on R2* was further supported by the significant inverse correlation between R2* and both rBV and rBF. CA-IX staining was found to associate with higher rBV and rBF values and this may reflect hypoxia-induced angiogenesis. In addition, CA-IX was associated with the aggressive tumour features of high grade, ER negative status and necrosis.

Failure to demonstrate a positive correlation between the angiogenesis-related parameters and the functional MRI parameters measuring microvascular permeability and perfusion may reflect sampling differences between the MRI-defined tumour regions of interest (ROI) and the pathological specimens. The functional MRI parameter values were the median values measured from the whole tumour ROI, whereas MVD, PCI, VEGF and CA-IX were evaluated from a single random core-biopsy sample. However, others have attempted to make a comparison between T1W DCE-MRI kinetic parameters and tumour MVD ("hotspot" counting) using larger primary surgical breast cancer specimens with mixed results [174, 305, 307, 308]. It may be that failure to consistently demonstrate a correlation between these measures is a reflection of the disparity between the visible microvasculature as evaluated from a single "snap-shot" in time (i.e. pathological specimen) & the "real-time" functional microvasculature as measured by functional imaging.

In summary, this research has demonstrated a vascular response to neoadjuvant conventional anthracycline-based chemotherapy in primary breast cancer as assessed both by functional MRI and by immunohistochemical evaluation of pathological tumour specimens. The early vascular changes observed on DCE-MRI during treatment are able to predict for final clinico-pathological response and may enable more accurate tailoring of treatment to the individual with the aim of improving outcome. The pathophysiological correlates of functional MRI have also been explored. Further, FEC neoadjuvant chemotherapy appears to

cause vascular "normalisation" and this process may be mediated through a reduction in VEGF expression. These findings should help in the rational design of future cytotoxic and anti-angiogenic combination therapies.

REFERENCES

1. *National Statistics, Health, breast cancer.* 2004, www.statistics.gov.uk.
2. Fisher, B., et al., *Twenty-year follow-up of a randomized trial comparing total mastectomy, lumpectomy, and lumpectomy plus irradiation for the treatment of invasive breast cancer.* N Engl J Med, 2002. **347**(16): p. 1233-41.
3. EBCTCG, *Polychemotherapy for early breast cancer: an overview of the randomised trials. Early Breast Cancer Trialists' Collaborative Group.* Lancet, 1998. **352**(9132): p. 930-42.
4. EBCTCG, *Tamoxifen for early breast cancer: an overview of the randomised trials. Early Breast Cancer Trialists' Collaborative Group.* Lancet, 1998. **351**(9114): p. 1451-67.
5. EBCTCG, *Effects of chemotherapy and hormonal therapy for early breast cancer on recurrence and 15-year survival: an overview of the randomised trials.* Lancet, 2005. **365**(9472): p. 1687-717.
6. Kaufmann, M., et al., *International expert panel on the use of primary (preoperative) systemic treatment of operable breast cancer: review and recommendations.* J Clin Oncol, 2003. **21**(13): p. 2600-8.
7. Carter, C.L., C. Allen, and D.E. Henson, *Relation of tumor size, lymph node status, and survival in 24,740 breast cancer cases.* Cancer, 1989. **63**(1): p. 181-7.
8. Hopton, D.S., et al., *Histological grading of breast cancer; significance of grade on recurrence and mortality.* Eur J Surg Oncol, 1989. **15**(1): p. 25-31.
9. Elston, C.W. and I.O. Ellis, *Pathological prognostic factors in breast cancer. I. The value of histological grade in breast cancer: experience from a large study with long-term follow-up.* Histopathology, 1991. **19**(5): p. 403-10.
10. Ellis, I.O., et al., *Pathological prognostic factors in breast cancer. II. Histological type. Relationship with survival in a large study with long-term follow-up.* Histopathology, 1992. **20**(6): p. 479-89.
11. Collett, K., R. Skjaerven, and B.O. Maehle, *The prognostic contribution of estrogen and progesterone receptor status to a modified version of the Nottingham Prognostic Index.* Breast Cancer Res Treat, 1998. **48**(1): p. 1-9.
12. Haybittle, J.L., et al., *A prognostic index in primary breast cancer.* Br J Cancer, 1982. **45**(3): p. 361-6.
13. Galea, M.H., et al., *The Nottingham Prognostic Index in primary breast cancer.* Breast Cancer Res Treat, 1992. **22**(3): p. 207-19.
14. Gunduz, N., B. Fisher, and E.A. Saffer, *Effect of surgical removal on the growth and kinetics of residual tumor.* Cancer Res, 1979. **39**(10): p. 3861-5.
15. Fisher, B., et al., *Presence of a growth-stimulating factor in serum following primary tumor removal in mice.* Cancer Res, 1989. **49**(8): p. 1996-2001.
16. Fisher, B., et al., *Effect of local or systemic treatment prior to primary tumor removal on the production and response to a serum growth-stimulating factor in mice.* Cancer Res, 1989. **49**(8): p. 2002-4.
17. Bonadonna, G., et al., *Primary chemotherapy to avoid mastectomy in tumors with diameters of three centimeters or more.* J Natl Cancer Inst, 1990. **82**(19): p. 1539-45.
18. Hortobagyi, G.N., et al., *Management of stage III primary breast cancer with primary chemotherapy, surgery, and radiation therapy.* Cancer, 1988. **62**(12): p. 2507-16.
19. Gardin, G., et al., *Locally advanced non-metastatic breast cancer: analysis of prognostic factors in 125 patients homogeneously treated with a combined modality approach.* Eur J Cancer, 1995. **31A**(9): p. 1428-33.
20. Smith, I.E., et al., *High complete remission rates with primary neoadjuvant infusional chemotherapy for large early breast cancer.* J Clin Oncol, 1995. **13**(2): p. 424-9.
21. Chollet, P., et al., *Clinical and pathological response to primary chemotherapy in operable breast cancer.* Eur J Cancer, 1997. **33**(6): p. 862-6.
22. Kuerer, H.M., et al., *Pathologic tumor response in the breast following neoadjuvant chemotherapy predicts axillary lymph node status.* Cancer J Sci Am, 1998. **4**(4): p. 230-6.
23. Fisher, B., et al., *Effect of preoperative chemotherapy on the outcome of women with operable breast cancer.* J Clin Oncol, 1998. **16**(8): p. 2672-85.

24. Wolmark, N., et al., *Preoperative chemotherapy in patients with operable breast cancer: nine-year results from National Surgical Adjuvant Breast and Bowel Project B-18.* J Natl Cancer Inst Monogr, 2001(30): p. 96-102.
25. Mauriac, L., et al., *Neoadjuvant chemotherapy for operable breast carcinoma larger than 3 cm: a unicentre randomized trial with a 124-month median follow-up. Institut Bergonie Bordeaux Groupe Sein (IBBGS).* Ann Oncol, 1999. **10**(1): p. 47-52.
26. Semiglazov, V.F., et al., *Primary (neoadjuvant) chemotherapy and radiotherapy compared with primary radiotherapy alone in stage IIb-IIIa breast cancer.* Ann Oncol, 1994. **5**(7): p. 591-5.
27. Scholl, S.M., et al., *Neoadjuvant versus adjuvant chemotherapy in premenopausal patients with tumours considered too large for breast conserving surgery: preliminary results of a randomised trial: S6.* Eur J Cancer, 1994. **30A**(5): p. 645-52.
28. Powles, T.J., et al., *Randomized trial of chemoendocrine therapy started before or after surgery for treatment of primary breast cancer.* J Clin Oncol, 1995. **13**(3): p. 547-52.
29. Makris, A., et al., *A reduction in the requirements for mastectomy in a randomized trial of neoadjuvant chemoendocrine therapy in primary breast cancer.* Ann Oncol, 1998. **9**(11): p. 1179-84.
30. van der Hage, J.A., et al., *Preoperative chemotherapy in primary operable breast cancer: results from the European Organization for Research and Treatment of Cancer trial 10902.* J Clin Oncol, 2001. **19**(22): p. 4224-37.
31. Reichman, B.S., et al., *Taxol and recombinant human granulocyte colony-stimulating factor, an active regimen as initial therapy for metastatic breast cancer. A preliminary report.* Ann N Y Acad Sci, 1993. **698**: p. 398-402.
32. Holmes, F.A., et al., *Phase II trial of taxol, an active drug in the treatment of metastatic breast cancer.* J Natl Cancer Inst, 1991. **83**(24): p. 1797-805.
33. Chan, S., et al., *Prospective randomized trial of docetaxel versus doxorubicin in patients with metastatic breast cancer.* J Clin Oncol, 1999. **17**(8): p. 2341-54.
34. Seidman, A.D., et al., *Paclitaxel as second and subsequent therapy for metastatic breast cancer: activity independent of prior anthracycline response.* J Clin Oncol, 1995. **13**(5): p. 1152-9.
35. Nabholtz, J.M., et al., *Prospective randomized trial of docetaxel versus mitomycin plus vinblastine in patients with metastatic breast cancer progressing despite previous anthracycline-containing chemotherapy. 304 Study Group.* J Clin Oncol, 1999. **17**(5): p. 1413-24.
36. Smith, I.C., et al., *Neoadjuvant chemotherapy in breast cancer: significantly enhanced response with docetaxel.* J Clin Oncol, 2002. **20**(6): p. 1456-66.
37. Hutcheon, A.W., Heys, S.W., Sarkar, T.K., Eremin, O., Walker, L.G., Miller, I.D., *Docetaxel primary chemotherapy in breast cancer: a five year update of the Aberdeen trial.* Breast Cancer Res Treat, 2003. **82**: p. S9 (supplement 1, abstract 11).
38. Bear, H.D., et al., *The effect on tumor response of adding sequential preoperative docetaxel to preoperative doxorubicin and cyclophosphamide: preliminary results from National Surgical Adjuvant Breast and Bowel Project Protocol B-27.* J Clin Oncol, 2003. **21**(22): p. 4165-74.
39. Bear, H.D. *A randomized trial comparing preooperative (preop) doxorubicin/cyclophosphamide (AC) to preop AC followed by preop docetaxel (T) and to preop AC followed by postoperative (postop) T in patients (pts) with operable carcinoma of the breast: results of the NSABP B-27.* in *San Antonio Breast Cancer Symposium.* 2004. San Antonio, Texas, USA.
40. Buzdar, A.U., et al., *Prospective evaluation of paclitaxel versus combination chemotherapy with fluorouracil, doxorubicin, and cyclophosphamide as neoadjuvant therapy in patients with operable breast cancer.* J Clin Oncol, 1999. **17**(11): p. 3412-7.
41. Gianni, L., Baselga, J., Eiermann, N. et al., *First report of the European Cooperative Trial in operable breast cancer (ECTO): Effects of primary systemic therapy (PST) on locoregional disease.* Proc Am Soc Clin Oncol, 2002. **21**: p. 34a (abstract 132).
42. Green, M.C., Budzar, A.U., Smith, T., Ibrahim, N.K., Valero, V., Rosales, M., Crostofanilli, M., Booser, D.J., Pusztai, L., Rivera, E., Theriault, R., Carter, C., Singletary, S.E., Kuerer, H.M., Hunt, K., Strom, E., Hortobagyi, G.N., *Weekly paclitaxel followed by FAC as primary systemic chemotherapy of operable breast cancer improves pathologic complete remission rates when compared to every 3 week*

paclitaxel therapy followed by FAC - final results of a prospective randomised trial. Proc Am Soc Clin Oncol, 2002. **21**: p. 35a (abstract 135).
43. Jackisch, C., et al., *Dose-dense biweekly doxorubicin/docetaxel versus sequential neoadjuvant chemotherapy with doxorubicin/cyclophosphamide/docetaxel in operable breast cancer: second interim analysis.* Clin Breast Cancer, 2002. **3**(4): p. 276-80.
44. Budzar, A.U., et al., *Significantly higher pathological complete remission (PCR) rate following neoadjuvant therapy with trastuzumab (H), paclitaxel (P), and anthracycline-containing chemotherapy (CT): initial results of a randomized trial in operable breast cancer (BC) with HER/2 positive disease.* Meeting Proceedings of American Society of Clinical Oncology, 2004. **Vol. 23**.
45. von Minckwitz, G., et al., *In vivo chemosensitivity-adapted preoperative chemotherapy in patients with early-stage breast cancer: the GEPARTRIO pilot study.* Ann Oncol, 2005. **16**(1): p. 56-63.
46. Gusterson, B.A., et al., *Prognostic importance of c-erbB-2 expression in breast cancer. International (Ludwig) Breast Cancer Study Group.* J Clin Oncol, 1992. **10**(7): p. 1049-56.
47. Paik, S., et al., *erbB-2 and response to doxorubicin in patients with axillary lymph node-positive, hormone receptor-negative breast cancer.* J Natl Cancer Inst, 1998. **90**(18): p. 1361-70.
48. Yamauchi, H., V. Stearns, and D.F. Hayes, *When Is a Tumor Marker Ready for Prime Time? A Case Study of c-erbB-2 as a Predictive Factor in Breast Cancer.* J Clin Oncol, 2001. **19**(8): p. 2334-2356.
49. Allred, D.C., et al., *Prognostic and predictive factors in breast cancer by immunohistochemical analysis.* Mod Pathol, 1998. **11**(2): p. 155-68.
50. Lippman, M.E. and J.C. Allegra, *Quantitative estrogen receptor analyses: the response to endocrine and cytotoxic chemotherapy in human breast cancer and the disease-free interval.* Cancer, 1980. **46**(12 Suppl): p. 2829-34.
51. Bardou, V.J., et al., *Progesterone receptor status significantly improves outcome prediction over estrogen receptor status alone for adjuvant endocrine therapy in two large breast cancer databases.* J Clin Oncol, 2003. **21**(10): p. 1973-9.
52. Mortimer, J., et al., *Influence of estrogen receptor status on response to combination chemotherapy for recurrent breast cancer.* Cancer Treat Rep, 1981. **65**(9-10): p. 763-6.
53. Lippman, M.E. and J.C. Allegra, *Lack of estrogen receptor associated with an increased response rate to cytotoxic chemotherapy in metastatic breast cancer?* Recent Results Cancer Res, 1980. **71**: p. 155-61.
54. Young, P.C., C.E. Ehrlich, and L.H. Einhorn, *Relationship between steroid receptors and response to endocrine therapy and cytotoxic chemotherapy in metastatic breast cancer.* Cancer, 1980. **46**(12 Suppl): p. 2961-3.
55. Kiang, D.T., et al., *Estrogen receptors and responses to chemotherapy and hormonal therapy in advanced breast cancer.* N Engl J Med, 1978. **299**(24): p. 1330-4.
56. Makris, A., et al., *Prediction of response to neoadjuvant chemoendocrine therapy in primary breast carcinomas.* Clin Cancer Res, 1997. **3**(4): p. 593-600.
57. Chang, J., et al., *Biologic markers as predictors of clinical outcome from systemic therapy for primary operable breast cancer.* J Clin Oncol, 1999. **17**(10): p. 3058-63.
58. Cleator, S.J., et al., *Good clinical response of breast cancers to neoadjuvant chemoendocrine therapy is associated with improved overall survival.* Ann Oncol, 2005. **16**(2): p. 267-72.
59. Penault-Llorca, F., et al., *Induction chemotherapy for breast carcinoma: predictive markers and relation with outcome.* Int J Oncol, 2003. **22**(6): p. 1319-25.
60. Bottini, A., et al., *Effect of neoadjuvant chemotherapy on Ki67 labelling index, c-erbB-2 expression and steroid hormone receptor status in human breast tumours.* Anticancer Res, 1996. **16**(5B): p. 3105-10.
61. Burcombe, R.J., et al., *Evaluation of ER, PgR, HER-2 and Ki-67 as predictors of response to neoadjuvant anthracycline chemotherapy for operable breast cancer.* Br J Cancer, 2005. **92**(1): p. 147-55.
62. Colleoni, M., et al., *Response to primary chemotherapy in breast cancer patients with tumors not expressing estrogen and progesterone receptors.* Ann Oncol, 2000. **11**(8): p. 1057-9.
63. Faneyte, I.F., et al., *Breast cancer response to neoadjuvant chemotherapy: predictive markers and relation with outcome.* Br J Cancer, 2003. **88**(3): p. 406-12.

64. Assersohn, L., et al., *Studies of the potential utility of Ki67 as a predictive molecular marker of clinical response in primary breast cancer.* Breast Cancer Res Treat, 2003. **82**(2): p. 113-23.
65. Bottini, A., et al., *Relationship between tumour shrinkage and reduction in Ki67 expression after primary chemotherapy in human breast cancer.* Br J Cancer, 2001. **85**(8): p. 1106-12.
66. Vincent-Salomon, A., et al., *Proliferation markers predictive of the pathological response and disease outcome of patients with breast carcinomas treated by anthracycline-based preoperative chemotherapy.* Eur J Cancer, 2004. **40**(10): p. 1502-8.
67. Collecchi, P., et al., *Primary chemotherapy in locally advanced breast cancer (LABC): effects on tumour proliferative activity, bcl-2 expression and the relationship between tumour regression and biological markers.* Eur J Cancer, 1998. **34**(11): p. 1701-4.
68. Stearns, V., et al., *A prospective randomized pilot study to evaluate predictors of response in serial core biopsies to single agent neoadjuvant doxorubicin or paclitaxel for patients with locally advanced breast cancer.* Clin Cancer Res, 2003. **9**(1): p. 124-33.
69. Archer, C.D., et al., *Early changes in apoptosis and proliferation following primary chemotherapy for breast cancer.* Br J Cancer, 2003. **89**(6): p. 1035-41.
70. Chang, J., et al., *Apoptosis and proliferation as predictors of chemotherapy response in patients with breast carcinoma.* Cancer, 2000. **89**(11): p. 2145-52.
71. Kallab, A.M., et al., *Immunohistochemical tumour markers do not predict response to neoadjuvant doxorubicin and doctaxel in breast cancer.* Meeting Proceedings of American Society of Clinical Oncology, 2004. **Vol. 23**: p. Abstract 794.
72. Perou, C.M., et al., *Molecular portraits of human breast tumours.* Nature, 2000. **406**(6797): p. 747-52.
73. Chang, J.C., et al., *Gene expression profiling for the prediction of therapeutic response to docetaxel in patients with breast cancer.* Lancet, 2003. **362**(9381): p. 362-9.
74. Pierga, J.Y., et al., *Prognostic factors for survival after neoadjuvant chemotherapy in operable breast cancer. the role of clinical response.* Eur J Cancer, 2003. **39**(8): p. 1089-96.
75. Bonadonna, G., et al., *Primary chemotherapy in operable breast cancer: eight-year experience at the Milan Cancer Institute.* J Clin Oncol, 1998. **16**(1): p. 93-100.
76. Gajdos, C., et al., *Relationship of clinical and pathologic response to neoadjuvant chemotherapy and outcome of locally advanced breast cancer.* J Surg Oncol, 2002. **80**(1): p. 4-11.
77. Allen, S.A., et al., *Pre-operative estimation of primary breast cancer size: a comparison of clinical assessment, mammography and ultrasound.* Breast, 2001. **10**(4): p. 299-305.
78. Meden, H., et al., *A clinical, mammographic, sonographic and histologic evaluation of breast cancer.* Int J Gynaecol Obstet, 1995. **48**(2): p. 193-9.
79. Forouhi, P., et al., *Ultrasonography as a method of measuring breast tumour size and monitoring response to primary systemic treatment.* Br J Surg, 1994. **81**(2): p. 223-5.
80. Pain, J.A., et al., *Assessment of breast cancer size: a comparison of methods.* Eur J Surg Oncol, 1992. **18**(1): p. 44-8.
81. Fornage, B.D., O. Toubas, and M. Morel, *Clinical, mammographic, and sonographic determination of preoperative breast cancer size.* Cancer, 1987. **60**(4): p. 765-71.
82. Herrada, J., et al., *Relative value of physical examination, mammography, and breast sonography in evaluating the size of the primary tumor and regional lymph node metastases in women receiving neoadjuvant chemotherapy for locally advanced breast carcinoma.* Clin Cancer Res, 1997. **3**(9): p. 1565-9.
83. Feldman, L.D., et al., *Pathological assessment of response to induction chemotherapy in breast cancer.* Cancer Res, 1986. **46**(5): p. 2578-81.
84. Smith, I.C., et al., *Positron emission tomography using [(18)F]-fluorodeoxy-D-glucose to predict the pathologic response of breast cancer to primary chemotherapy.* J Clin Oncol, 2000. **18**(8): p. 1676-88.
85. Delille, J.P., et al., *Invasive ductal breast carcinoma response to neoadjuvant chemotherapy: noninvasive monitoring with functional MR imaging pilot study.* Radiology, 2003. **228**(1): p. 63-9.

86. Drew, P.J., et al., *Evaluation of response to neoadjuvant chemoradiotherapy for locally advanced breast cancer with dynamic contrast-enhanced MRI of the breast.* Eur J Surg Oncol, 2001. **27**(7): p. 617-20.
87. Abraham, D.C., et al., *Evaluation of neoadjuvant chemotherapeutic response of locally advanced breast cancer by magnetic resonance imaging.* Cancer, 1996. **78**(1): p. 91-100.
88. Rieber, A., et al., *Breast MRI for monitoring response of primary breast cancer to neo-adjuvant chemotherapy.* Eur Radiol, 2002. **12**(7): p. 1711-9.
89. Esserman, L., et al., *Utility of magnetic resonance imaging in the management of breast cancer: evidence for improved preoperative staging.* J Clin Oncol, 1999. **17**(1): p. 110-9.
90. Harms, S.E., et al., *MR imaging of the breast with rotating delivery of excitation off resonance: clinical experience with pathologic correlation.* Radiology, 1993. **187**(2): p. 493-501.
91. Martincich, L., et al., *Monitoring response to primary chemotherapy in breast cancer using dynamic contrast-enhanced magnetic resonance imaging.* Breast Cancer Res Treat, 2004. **83**(1): p. 67-76.
92. Folkman, J., *New perspectives in clinical oncology from angiogenesis research,* in *Eur J Cancer.* 1996. p. 2534–2539.
93. Folkman, J., *The role of angiogenesis in tumor growth.* Semin Cancer Biol, 1992. **3**(2): p. 65-71.
94. Senger, D.R., et al., *Tumor cells secrete a vascular permeability factor that promotes accumulation of ascites fluid.* Science, 1983. **219**(4587): p. 983-5.
95. Ferrara, N., *Role of vascular endothelial growth factor in physiologic and pathologic angiogenesis: therapeutic implications.* Semin Oncol, 2002. **29**(6 Suppl 16): p. 10-4.
96. Rak, J., et al., *Oncogenes and tumor angiogenesis: differential modes of vascular endothelial growth factor up-regulation in ras-transformed epithelial cells and fibroblasts.* Cancer Res, 2000. **60**(2): p. 490-8.
97. Toi, M., T. Matsumoto, and H. Bando, *Vascular endothelial growth factor: its prognostic, predictive, and therapeutic implications.* Lancet Oncol, 2001. **2**(11): p. 667-73.
98. Jain, R.K., *Molecular regulation of vessel maturation.* Nat Med, 2003. **9**(6): p. 685-93.
99. Liu, W., et al., *Antiangiogenic therapy targeting factors that enhance endothelial cell survival.* Semin Oncol, 2002. **29**(3 Suppl 11): p. 96-103.
100. Gasparini, G., et al., *Prognostic significance of vascular endothelial growth factor protein in node-negative breast carcinoma.* J Natl Cancer Inst, 1997. **89**(2): p. 139-47.
101. Linderholm, B., et al., *p53 and vascular-endothelial-growth-factor (VEGF) expression predicts outcome in 833 patients with primary breast carcinoma.* Int J Cancer, 2000. **89**(1): p. 51-62.
102. Toi, M., et al., *Tumor angiogenesis in breast cancer: its importance as a prognostic indicator and the association with vascular endothelial growth factor expression.* Breast Cancer Res Treat, 1995. **36**(2): p. 193-204.
103. Ragaz, J., Miller, K., Badve, S., Dayachko, Y., Dunn, S., Nielsen, T., Brodie, A., Huntsman, D., Bajdik, C., Sledge, G.,, *Adverse association of expression of vascular endothelial growth factor(VEGF) with long-term outcome of stage I-III breast cancer, with co-expression data of VEGF and HER2, Cox2, uPA and ER. Results from the British Columbia Tissue Microarray project.* Proc Am Soc Clin Oncol, 2004. **22**(14S): p. 8S (abstract 524).
104. Adams, J., et al., *Vascular endothelial growth factor (VEGF) in breast cancer: comparison of plasma, serum, and tissue VEGF and microvessel density and effects of tamoxifen.* Cancer Res, 2000. **60**(11): p. 2898-905.
105. Lissoni, P., et al., *Chemotherapy and angiogenesis in advanced cancer: vascular endothelial growth factor (VEGF) decline as predictor of disease control during taxol therapy in metastatic breast cancer.* Int J Biol Markers, 2000. **15**(4): p. 308-11.
106. Lantzsch, T., et al., *The correlation between immunohistochemically-detected markers of angiogenesis and serum vascular endothelial growth factor in patients with breast cancer.* Anticancer Res, 2002. **22**(3): p. 1925-8.
107. Mulcahy, M.F. and A.B. Benson, 3rd, *Bevacizumab in the treatment of colorectal cancer.* Expert Opin Biol Ther, 2005. **5**(7): p. 997-1005.

108. Konner, J. and J. Dupont, *Use of soluble recombinant decoy receptor vascular endothelial growth factor trap (VEGF Trap) to inhibit vascular endothelial growth factor activity.* Clin Colorectal Cancer, 2004. **4 Suppl 2**: p. S81-5.
109. Klement, G., et al., *Continuous low-dose therapy with vinblastine and VEGF receptor-2 antibody induces sustained tumor regression without overt toxicity.* J Clin Invest, 2000. **105(8)**: p. R15-24.
110. Ciardiello, F., et al., *Antitumor effects of ZD6474, a small molecule vascular endothelial growth factor receptor tyrosine kinase inhibitor, with additional activity against epidermal growth factor receptor tyrosine kinase.* Clin Cancer Res, 2003. **9(4)**: p. 1546-56.
111. Thomas, A.L., et al., *Vascular endothelial growth factor receptor tyrosine kinase inhibitors: PTK787/ZK 222584.* Semin Oncol, 2003. **30(3 Suppl 6)**: p. 32-8.
112. Miller, K.D., et al., *Phase III trial of capecitabine plus bevacizumab versus capecitabine alone in women with metastatic breast cancer previously treated with an anthracycline and a taxane.* Breast Cancer Res Treat, 2002. **71(Supplement 1)**.
113. Vermeulen, P.B., et al., *Quantification of angiogenesis in solid human tumours: an international consensus on the methodology and criteria of evaluation.* Eur J Cancer, 1996. **32A(14)**: p. 2474-84.
114. Lee, A.H.S., Happerfield, L.C., Bobrow, L.G., *Comparison of four endothelial markers for asessing angiogenesis in carcinoma of the breast.* Journal of Cellular Pathology, 1997. **2(2)**: p. 67-73.
115. Yamazaki, K., Eyden, B.P., *Ultrastructural and immunohistochemical observations in intralobular fibroblasts of human breast, with pbservation on the CD34 antigen.* J Submicrosc Cytol Pathol, 1995. **27**: p. 309 - 323.
116. Martin, L., et al., *Examining the technique of angiogenesis assessment in invasive breast cancer.* Br J Cancer, 1997. **76(8)**: p. 1046-54.
117. Weidner, N., et al., *Tumor angiogenesis and metastasis--correlation in invasive breast carcinoma.* N Engl J Med, 1991. **324(1)**: p. 1-8.
118. Weidner, N., et al., *Tumor angiogenesis: a new significant and independent prognostic indicator in early-stage breast carcinoma.* J Natl Cancer Inst, 1992. **84(24)**: p. 1875-87.
119. Folkman, J., *Angiogenesis and breast cancer.* J Clin Oncol, 1994. **12(3)**: p. 441-3.
120. Fox, S.B., et al., *Tumor angiogenesis in node-negative breast carcinomas--relationship with epidermal growth factor receptor, estrogen receptor, and survival.* Breast Cancer Res Treat, 1994. **29(1)**: p. 109-16.
121. Hansen, S., et al., *The prognostic value of angiogenesis by Chalkley counting in a confirmatory study design on 836 breast cancer patients.* Clin Cancer Res, 2000. **6(1)**: p. 139-46.
122. Fox, S.B., *Tumour angiogenesis and prognosis.* Histopathology, 1997. **30(3)**: p. 294-301.
123. Hasan, J., R. Byers, and G.C. Jayson, *Intra-tumoural microvessel density in human solid tumours.* Br J Cancer, 2002. **86(10)**: p. 1566-77.
124. Fitzgibbons, P.L., et al., *Prognostic factors in breast cancer. College of American Pathologists Consensus Statement 1999.* Arch Pathol Lab Med, 2000. **124(7)**: p. 966-78.
125. Vermeulen, P.B., et al., *Second international consensus on the methodology and criteria of evaluation of angiogenesis quantification in solid human tumours.* Eur J Cancer, 2002. **38(12)**: p. 1564-79.
126. Colpaert, C., et al., *Intratumoral hypoxia resulting in the presence of a fibrotic focus is an independent predictor of early distant relapse in lymph node-negative breast cancer patients.* Histopathology, 2001. **39(4)**: p. 416-25.
127. Guidi, A.J., et al., *Association of angiogenesis and disease outcome in node-positive breast cancer patients treated with adjuvant cyclophosphamide, doxorubicin, and fluorouracil: a Cancer and Leukemia Group B correlative science study from protocols 8541/8869.* J Clin Oncol, 2002. **20(3)**: p. 732-42.
128. Makris, A., et al., *Reduction in angiogenesis after neoadjuvant chemoendocrine therapy in patients with operable breast carcinoma.* Cancer, 1999. **85(9)**: p. 1996-2000.
129. Bottini, A., et al., *Changes in microvessel density as assessed by CD34 antibodies after primary chemotherapy in human breast cancer.* Clin Cancer Res, 2002. **8(6)**: p. 1816-21.

130. Tynninen, O., et al., *Tumour microvessel density as predictor of chemotherapy response in breast cancer patients.* Br J Cancer, 2002. **86**(12): p. 1905-8.
131. Marson, L.P., et al., *The effect of tamoxifen on breast tumour vascularity.* Breast Cancer Res Treat, 2001. **66**(1): p. 9-15.
132. Hlatky, L., P. Hahnfeldt, and J. Folkman, *Clinical application of antiangiogenic therapy: microvessel density, what it does and doesn't tell us.* J Natl Cancer Inst, 2002. **94**(12): p. 883-93.
133. Eberhard, A., et al., *Heterogeneity of angiogenesis and blood vessel maturation in human tumors: implications for antiangiogenic tumor therapies.* Cancer Res, 2000. **60**(5): p. 1388-93.
134. Beecken, W.D., et al., *Effect of antiangiogenic therapy on slowly growing, poorly vascularized tumors in mice.* J Natl Cancer Inst, 2001. **93**(5): p. 382-7.
135. Lindahl, P., et al., *Pericyte loss and microaneurysm formation in PDGF-B-deficient mice.* Science, 1997. **277**(5323): p. 242-5.
136. Benjamin, L.E., et al., *Selective ablation of immature blood vessels in established human tumors follows vascular endothelial growth factor withdrawal.* J Clin Invest, 1999. **103**(2): p. 159-65.
137. Gee, M.S., et al., *Tumor vessel development and maturation impose limits on the effectiveness of anti-vascular therapy.* Am J Pathol, 2003. **162**(1): p. 183-93.
138. Kakolyris, S., et al., *Relationship of vascular maturation in breast cancer blood vessels to vascular density and metastasis, assessed by expression of a novel basement membrane component, LH39.* Br J Cancer, 2000. **82**(4): p. 844-51.
139. Kakolyris, S., et al., *Assessment of vascular maturation in lung and breast carcinomas using a novel basement membrane component, LH39.* Anticancer Res, 2001. **21**(6B): p. 4311-6.
140. Almeida, B.M., et al., *A novel lamina lucida component of epithelial and endothelial basement membranes detected by LH39 monoclonal antibody.* J Pathol, 1992. **166**(3): p. 243-53.
141. Almeida, B.M., et al., *The distribution of LH39 basement membrane epitope in the tumour stroma of oral squamous cell carcinomas.* J Pathol, 1992. **166**(4): p. 369-74.
142. Kumar, S., et al., *Breast carcinoma: vascular density determined using CD105 antibody correlates with tumor prognosis.* Cancer Res, 1999. **59**(4): p. 856-61.
143. Wang, J.M., et al., *A monoclonal antibody detects heterogeneity in vascular endothelium of tumours and normal tissues.* Int J Cancer, 1993. **54**(3): p. 363-70.
144. Kaiser, W.A. and E. Zeitler, *MR imaging of the breast: fast imaging sequences with and without Gd-DTPA. Preliminary observations.* Radiology, 1989. **170**(3 Pt 1): p. 681-6.
145. Heywang, S.H., et al., *MR imaging of the breast with Gd-DTPA: use and limitations.* Radiology, 1989. **171**(1): p. 95-103.
146. Fobben, E.S., et al., *Breast MR imaging with commercially available techniques: radiologic-pathologic correlation.* Radiology, 1995. **196**(1): p. 143-52.
147. Stomper, P.C., et al., *Suspect breast lesions: findings at dynamic gadolinium-enhanced MR imaging correlated with mammographic and pathologic features.* Radiology, 1995. **197**(2): p. 387-95.
148. Orel, S.G., et al., *Suspicious breast lesions: MR imaging with radiologic-pathologic correlation.* Radiology, 1994. **190**(2): p. 485-93.
149. Padhani, A.R. and A. Dzik-Jurasz, *Perfusion MR imaging of extracranial tumor angiogenesis.* Top Magn Reson Imaging, 2004. **15**(1): p. 41-57.
150. Boetes, C., et al., *MR characterization of suspicious breast lesions with a gadolinium-enhanced TurboFLASH subtraction technique.* Radiology, 1994. **193**(3): p. 777-81.
151. Flickinger, F.W., et al., *Differentiation of benign from malignant breast masses by time-intensity evaluation of contrast enhanced MRI.* Magn Reson Imaging, 1993. **11**(5): p. 617-20.
152. Gilles, R., et al., *Assessment of breast cancer recurrence with contrast-enhanced subtraction MR imaging: preliminary results in 26 patients.* Radiology, 1993. **188**(2): p. 473-8.
153. Roberts, T.P., *Physiologic measurements by contrast-enhanced MR imaging: expectations and limitations.* J Magn Reson Imaging, 1997. **7**(1): p. 82-90.
154. Kuhl, C.K., et al., *Dynamic breast MR imaging: are signal intensity time course data useful for differential diagnosis of enhancing lesions?* Radiology, 1999. **211**(1): p. 101-10.

155. Liu, P.F., et al., *Improved diagnostic accuracy in dynamic contrast enhanced MRI of the breast by combined quantitative and qualitative analysis.* Br J Radiol, 1998. **71**(845): p. 501-9.
156. Denton, E.R., et al., *Comparison and evaluation of rigid, affine, and nonrigid registration of breast MR images.* J Comput Assist Tomogr, 1999. **23**(5): p. 800-5.
157. Ikeda, D.M., et al., *Development, standardization, and testing of a lexicon for reporting contrast-enhanced breast magnetic resonance imaging studies.* J Magn Reson Imaging, 2001. **13**(6): p. 889-95.
158. Gribbestad, I.S., et al., *Comparative signal intensity measurements in dynamic gadolinium-enhanced MR mammography.* J Magn Reson Imaging, 1994. **4**(3): p. 477-80.
159. Evelhoch, J.L., *Key factors in the acquisition of contrast kinetic data for oncology.* J Magn Reson Imaging, 1999. **10**(3): p. 254-9.
160. Parker, G.J., et al., *Probing tumor microvascularity by measurement, analysis and display of contrast agent uptake kinetics.* J Magn Reson Imaging, 1997. **7**(3): p. 564-74.
161. Tofts, P.S. and A.G. Kermode, *Measurement of the blood-brain barrier permeability and leakage space using dynamic MR imaging. 1. Fundamental concepts.* Magn Reson Med, 1991. **17**(2): p. 357-67.
162. Tofts, P.S., et al., *Estimating kinetic parameters from dynamic contrast-enhanced T(1)-weighted MRI of a diffusable tracer: standardized quantities and symbols.* J Magn Reson Imaging, 1999. **10**(3): p. 223-32.
163. Tofts, P.S., *Modeling tracer kinetics in dynamic Gd-DTPA MR imaging.* J Magn Reson Imaging, 1997. **7**(1): p. 91-101.
164. Tofts, P.S., B. Berkowitz, and M.D. Schnall, *Quantitative analysis of dynamic Gd-DTPA enhancement in breast tumors using a permeability model.* Magn Reson Med, 1995. **33**(4): p. 564-8.
165. den Boer, J.A., et al., *Pharmacokinetic analysis of Gd-DTPA enhancement in dynamic three-dimensional MRI of breast lesions.* J Magn Reson Imaging, 1997. **7**(4): p. 702-15.
166. Knopp, M.V., et al., *Pathophysiologic basis of contrast enhancement in breast tumors*, in *J Magn Reson Imaging*. 1999. p. 260-6.
167. Buadu, L.D., et al., *Breast lesions: correlation of contrast medium enhancement patterns on MR images with histopathologic findings and tumor angiogenesis*, in *Radiology*. 1996. p. 639-49.
168. Matsubayashi, R., et al., *Breast masses with peripheral rim enhancement on dynamic contrast-enhanced MR images: correlation of MR findings with histologic features and expression of growth factors*, in *Radiology*. 2000. p. 841-8.
169. Weidner, N., *Tumoural vascularity as a prognostic factor in cancer patients: the evidence continues to grow*, in *J Pathol*. 1998. p. 119-22.
170. Stomper, P.C., et al., *Angiogenesis and dynamic MR imaging gadolinium enhancement of malignant and benign breast lesions*, in *Breast Cancer Res Treat*. 1997. p. 39-46.
171. Buckley, D.L., et al., *Microvessel density of invasive breast cancer assessed by dynamic Gd-DTPA enhanced MRI*, in *J Magn Reson Imaging*. 1997. p. 461-4.
172. Hulka, C.A., et al., *Dynamic echo-planar imaging of the breast: experience in diagnosing breast carcinoma and correlation with tumor angiogenesis*, in *Radiology*. 1997. p. 837-42.
173. Su, M.Y., et al., *Correlation of dynamic contrast enhancement MRI parameters with microvessel density and VEGF for assessment of angiogenesis in breast cancer*, in *J Magn Reson Imaging*. 2003. p. 467-77.
174. Su, M.Y., et al., *Correlation of dynamic contrast enhancement MRI parameters with microvessel density and VEGF for assessment of angiogenesis in breast cancer.* J Magn Reson Imaging, 2003. **18**(4): p. 467-77.
175. Hartmann, L.C., et al., *Efficacy of bilateral prophylactic mastectomy in women with a family history of breast cancer.* N Engl J Med, 1999. **340**(2): p. 77-84.
176. Rebbeck, T.R., et al., *Bilateral prophylactic mastectomy reduces breast cancer risk in BRCA1 and BRCA2 mutation carriers: the PROSE Study Group.* J Clin Oncol, 2004. **22**(6): p. 1055-62.
177. Rebbeck, T.R., et al., *Breast cancer risk after bilateral prophylactic oophorectomy in BRCA1 mutation carriers.* J Natl Cancer Inst, 1999. **91**(17): p. 1475-9.

178. Fisher, B., et al., *Tamoxifen for prevention of breast cancer: report of the National Surgical Adjuvant Breast and Bowel Project P-1 Study.* J Natl Cancer Inst, 1998. **90**(18): p. 1371-88.
179. King, M.C., et al., *Tamoxifen and breast cancer incidence among women with inherited mutations in BRCA1 and BRCA2: National Surgical Adjuvant Breast and Bowel Project (NSABP-P1) Breast Cancer Prevention Trial.* Jama, 2001. **286**(18): p. 2251-6.
180. Thurfjell, E.L. and J.A. Lindgren, *Breast cancer survival rates with mammographic screening: similar favorable survival rates for women younger and those older than 50 years.* Radiology, 1996. **201**(2): p. 421-6.
181. Bjurstam, N., et al., *The Gothenburg Breast Screening Trial.* Cancer, 2003. **97**(10): p. 2387-96.
182. Brekelmans, C.T., et al., *Effectiveness of breast cancer surveillance in BRCA1/2 gene mutation carriers and women with high familial risk.* J Clin Oncol, 2001. **19**(4): p. 924-30.
183. Deniz, K., et al., *Breast cancer in women after treatment for Hodgkin's disease.* Lancet Oncol, 2003. **4**(4): p. 207-14.
184. Fourquet, A., A. De La Rochefordiere, and F. Campana, *Occult primary cancer with axillary metastases*, in *Diseases of the breast*, L.M. Harris JR, Morrow M, Hellman S (Eds), Editor. 1996, Lippincott-Raven: Philadelphia, Pa. p. 892-896.
185. Rosen, P.P. and M. Kimmel, *Occult breast carcinoma presenting with axillary lymph node metastases: a follow-up study of 48 patients.* Hum Pathol, 1990. **21**(5): p. 518-23.
186. Fortunato, L., et al., *Occult breast cancer. A case report and review of the literature.* N Y State J Med, 1992. **92**(12): p. 555-7.
187. Ellerbroek, N., et al., *Treatment of patients with isolated axillary nodal metastases from an occult primary carcinoma consistent with breast origin.* Cancer, 1990. **66**(7): p. 1461-7.
188. Orel, S.G., et al., *Breast MR imaging in patients with axillary node metastases and unknown primary malignancy.* Radiology, 1999. **212**(2): p. 543-9.
189. Olson, J.A., Jr., et al., *Magnetic resonance imaging facilitates breast conservation for occult breast cancer.* Ann Surg Oncol, 2000. **7**(6): p. 411-5.
190. Tilanus-Linthorst, M.M., et al., *MRI in patients with axillary metastases of occult breast carcinoma.* Breast Cancer Res Treat, 1997. **44**(2): p. 179-82.
191. Schorn, C., et al., *MRI of the breast in patients with metastatic disease of unknown primary.* Eur Radiol, 1999. **9**(3): p. 470-3.
192. Knapper, W.H., *Management of occult breast cancer presenting as an axillary metastasis.* Semin Surg Oncol, 1991. **7**(5): p. 311-3.
193. Takehara, M., et al., *Examination of breast conserving therapy in lobular carcinoma.* Breast Cancer, 2004. **11**(1): p. 69-72.
194. Diekmann, F., et al., *[Preoperative MRT of the breast in invasive lobular carcinoma in comparison with invasive ductal carcinoma].* Rofo Fortschr Geb Rontgenstr Neuen Bildgeb Verfahr, 2004. **176**(4): p. 544-9.
195. Qayyum, A., et al., *MR imaging features of infiltrating lobular carcinoma of the breast: histopathologic correlation.* AJR Am J Roentgenol, 2002. **178**(5): p. 1227-32.
196. Yeh, E.D., et al., *Invasive lobular carcinoma: spectrum of enhancement and morphology on magnetic resonance imaging.* Breast J, 2003. **9**(1): p. 13-8.
197. Ringberg, A., B. Palmer, and F. Linell, *The contralateral breast at reconstructive surgery after breast cancer operation--a histopathological study.* Breast Cancer Res Treat, 1982. **2**(2): p. 151-61.
198. Rosen, P.P., et al., *Noninvasive breast carcinoma: frequency of unsuspected invasion and implications for treatment.* Ann Surg, 1979. **189**(3): p. 377-82.
199. Ciatto, S., et al., *In situ ductal carcinoma of the breast--analysis of clinical presentation and outcome in 156 consecutive cases.* Eur J Surg Oncol, 1990. **16**(3): p. 220-4.
200. Holland, R., et al., *Extent, distribution, and mammographic/histological correlations of breast ductal carcinoma in situ.* Lancet, 1990. **335**(8688): p. 519-22.
201. Neubauer, H., et al., *High grade and non-high grade ductal carcinoma in situ on dynamic MR mammography: characteristic findings for signal increase and morphological pattern of enhancement.* Br J Radiol, 2003. **76**(901): p. 3-12.
202. Gilles, R., et al., *Ductal carcinoma in situ: MR imaging-histopathologic correlation.* Radiology, 1995. **196**(2): p. 415-9.

203. Liberman, L., et al., *Ductal enhancement on MR imaging of the breast.* AJR Am J Roentgenol, 2003. **181**(2): p. 519-25.
204. Snelling, J.D., et al., *Measurement of tumour size in case selection for breast cancer therapy by clinical assessment and ultrasound.* Eur J Surg Oncol, 2004. **30**(1): p. 5-9.
205. Pritt, B., et al., *Influence of breast cancer histology on the relationship between ultrasound and pathology tumor size measurements.* Mod Pathol, 2004.
206. Davis, P.L., et al., *Breast cancer measurements with magnetic resonance imaging, ultrasonography, and mammography.* Breast Cancer Res Treat, 1996. **37**(1): p. 1-9.
207. Boetes, C., et al., *Breast tumors: comparative accuracy of MR imaging relative to mammography and US for demonstrating extent.* Radiology, 1995. **197**(3): p. 743-7.
208. Yang, W.T., et al., *Sonographic, magnetic resonance imaging, and mammographic assessments of preoperative size of breast cancer.* J Ultrasound Med, 1997. **16**(12): p. 791-7.
209. Fischer, U., L. Kopka, and E. Grabbe, *Breast carcinoma: effect of preoperative contrast-enhanced MR imaging on the therapeutic approach.* Radiology, 1999. **213**(3): p. 881-8.
210. Slanetz, P.J., et al., *Occult contralateral breast carcinoma incidentally detected by breast magnetic resonance imaging.* Breast J, 2002. **8**(3): p. 145-8.
211. Lee, S.G., et al., *MR imaging screening of the contralateral breast in patients with newly diagnosed breast cancer: preliminary results.* Radiology, 2003. **226**(3): p. 773-8.
212. Liberman, L., et al., *MR imaging findings in the contralateral breast of women with recently diagnosed breast cancer.* AJR Am J Roentgenol, 2003. **180**(2): p. 333-41.
213. Orel, S.G., et al., *Staging of suspected breast cancer: effect of MR imaging and MR-guided biopsy.* Radiology, 1995. **196**(1): p. 115-22.
214. Drew, P.J., et al., *Dynamic contrast enhanced magnetic resonance imaging of the breast is superior to triple assessment for the pre-operative detection of multifocal breast cancer.* Ann Surg Oncol, 1999. **6**(6): p. 599-603.
215. Mumtaz, H., et al., *Staging of symptomatic primary breast cancer with MR imaging.* AJR Am J Roentgenol, 1997. **169**(2): p. 417-24.
216. Liberman, L., et al., *MR imaging of the ipsilateral breast in women with percutaneously proven breast cancer.* AJR Am J Roentgenol, 2003. **180**(4): p. 901-10.
217. Bedrosian, I., et al., *Magnetic resonance imaging-guided biopsy of mammographically and clinically occult breast lesions.* Ann Surg Oncol, 2002. **9**(5): p. 457-61.
218. Kramer, S., et al., *Magnetic resonance imaging and its role in the diagnosis of multicentric breast cancer.* Anticancer Res, 1998. **18**(3C): p. 2163-4.
219. Esserman, L., et al., *Utility of magnetic resonance imaging in the management of breast cancer: evidence for improved preoperative staging*, in *J Clin Oncol.* 1999. p. 110-9.
220. Drew, P.J., et al., eds. *Dynamic contrast enhanced magnetic resonance imaging of the breast is superior to triple assessment for the pre-operative detection of multifocal breast cancer.* Ann Surg Oncol. Vol. 6. 1999. 599-603.
221. Tan, J.E., et al., *Role of magnetic resonance imaging and magnetic resonance imaging--guided surgery in the evaluation of patients with early-stage breast cancer for breast conservation treatment.* Am J Clin Oncol, 1999. **22**(4): p. 414-8.
222. Knopp, M.V., et al., *MR mammography with pharmacokinetic mapping for monitoring of breast cancer treatment during neoadjuvant therapy*, in *Magn Reson Imaging Clin N Am.* 1994. p. 633-58.
223. Hayes, C., A.R. Padhani, and M.O. Leach, *Assessing changes in tumour vascular function using dynamic contrast-enhanced magnetic resonance imaging*, in *NMR Biomed.* 2002. p. 154-63.
224. Esserman, L., et al., *MRI phenotype is associated with response to doxorubicin and cyclophosphamide neoadjuvant chemotherapy in stage III breast cancer*, in *Ann Surg Oncol.* 2001. p. 549-59.
225. Fiorentino, C., et al., *Accuracy of mammography and echography versus clinical palpation in the assessment of response to primary chemotherapy in breast cancer patients with operable disease*, in *Breast Cancer Res Treat.* 2001. p. 143-51.
226. Feldman, L.D., et al., *Pathological assessment of response to induction chemotherapy in breast cancer*, in *Cancer Res.* 1986. p. 2578-81.
227. Vinnicombe, S.J., et al., *Primary breast cancer: mammographic changes after neoadjuvant chemotherapy, with pathologic correlation.* Radiology, 1996. **198**(2): p. 333-40.

228. Helvie, M.A., et al., *Locally advanced breast carcinoma: accuracy of mammography versus clinical examination in the prediction of residual disease after chemotherapy*, in *Radiology*. 1996. p. 327-32.
229. Herrada, J., et al., *Relative value of physical examination, mammography, and breast sonography in evaluating the size of the primary tumor and regional lymph node metastases in women receiving neoadjuvant chemotherapy for locally advanced breast carcinoma*, in *Clin Cancer Res*. 1997. p. 1565-9.
230. Sever, A.R., et al. *Coil insertion prior to neoadjuvant chemotherapy in patients with breast cancer*. in *26th Annual San Antonio Breast Cancer Symposium*. 2004. San Antonio, Texas, U.S.A.: Kluwer Academic Publishers.
231. Delille, J.P., et al., *Invasive ductal breast carcinoma response to neoadjuvant chemotherapy: noninvasive monitoring with functional MR imaging pilot study*, in *Radiology*. 2003. p. 63-9.
232. Drew, P.J., et al., *Evaluation of response to neoadjuvant chemoradiotherapy for locally advanced breast cancer with dynamic contrast-enhanced MRI of the breast*, in *Eur J Surg Oncol*. 2001. p. 617-20.
233. Abraham, D.C., et al., *Evaluation of neoadjuvant chemotherapeutic response of locally advanced breast cancer by magnetic resonance imaging*, in *Cancer*. 1996. p. 91-100.
234. Rieber, A., et al., *Breast MRI for monitoring response of primary breast cancer to neo-adjuvant chemotherapy*, in *Eur Radiol*. 2002. p. 1711-9.
235. Gilles, R., et al., *Locally advanced breast cancer: contrast-enhanced subtraction MR imaging of response to preoperative chemotherapy*, in *Radiology*. 1994. p. 633-8.
236. Weatherall, P.T., et al., *MRI vs. histologic measurement of breast cancer following chemotherapy: comparison with x-ray mammography and palpation*, in *J Magn Reson Imaging*. 2001. p. 868-75.
237. Esserman, L., et al., *Utility of magnetic resonance imaging in the management of breast cancer: evidence for improved preoperative staging*, in *J Clin Oncol*. 1999. p. 110-9.
238. Harms, S.E., et al., *MR imaging of the breast with rotating delivery of excitation off resonance: clinical experience with pathologic correlation*, in *Radiology*. 1993. p. 493-501.
239. Bonadonna, G., et al., *Primary chemotherapy to avoid mastectomy in tumors with diameters of three centimeters or more*, in *J Natl Cancer Inst*. 1990. p. 1539-45.
240. Pierce, W.B., et al., *Three-dimensional gadolinium-enhanced MR imaging of the breast: pulse sequence with fat suppression and magnetization transfer contrast. Work in progress*, in *Radiology*. 1991. p. 757-63.
241. Davis, P.L., et al., *Breast cancer measurements with magnetic resonance imaging, ultrasonography, and mammography*, in *Breast Cancer Res Treat*. 1996. p. 1-9.
242. Veronesi, U., et al., *Twenty-year follow-up of a randomized study comparing breast-conserving surgery with radical mastectomy for early breast cancer*. N Engl J Med, 2002. **347**(16): p. 1227-32.
243. van Dongen, J.A., et al., *Long-term results of a randomized trial comparing breast-conserving therapy with mastectomy: European Organization for Research and Treatment of Cancer 10801 trial*. J Natl Cancer Inst, 2000. **92**(14): p. 1143-50.
244. Kurtz, J.M., et al., *Results of salvage surgery for mammary recurrence following breast-conserving therapy*. Ann Surg, 1988. **207**(3): p. 347-51.
245. Osborne, M.P., et al., *Salvage mastectomy for local and regional recurrence after breast-conserving operation and radiation therapy*. Surg Gynecol Obstet, 1992. **174**(3): p. 189-94.
246. Boccardo, F., et al., *Appropriateness of the use of clinical and radiologic examinations and laboratory tests in the follow-up of surgically-treated breast cancer patients. Results of the Working Group on the Clinical Aspects of Follow-up*. Ann Oncol, 1995. **6 Suppl 2**: p. 57-9.
247. RCR, *The use of imaging in the follow-up of patients with breast cancer*. London: Royal College of Radiologists, 1995.
248. Sickles, E.A. and K.A. Herzog, *Mammography of the postsurgical breast*. AJR Am J Roentgenol, 1981. **136**(3): p. 585-8.
249. Paulus, D.D., *Conservative treatment of breast cancer: mammography in patient selection and follow-up*. AJR Am J Roentgenol, 1984. **143**(3): p. 483-7.
250. Krishnamurthy, R., et al., *Mammographic findings after breast conservation therapy*. Radiographics, 1999. **19 Spec No**: p. S53-62; quiz S262-3.

251. Stomper, P.C., et al., *Mammographic detection of recurrent cancer in the irradiated breast.* AJR Am J Roentgenol, 1987. **148**(1): p. 39-43.
252. Orel, S.G., et al., *Breast cancer recurrence after lumpectomy and irradiation: role of mammography in detection.* Radiology, 1992. **183**(1): p. 201-6.
253. Homer, M.J., *Mammographic interpretation: a practical approach.* New York, NY: McGraw-Hill 4-5., 1991.
254. Revel, D., et al., *Gd-DTPA contrast enhancement and tissue differentiation in MR imaging of experimental breast carcinoma.* Radiology, 1986. **158**(2): p. 319-23.
255. Lewis-Jones, H.G., G.H. Whitehouse, and S.J. Leinster, *The role of magnetic resonance imaging in the assessment of local recurrent breast carcinoma.* Clin Radiol, 1991. **43**(3): p. 197-204.
256. Dao, T.H., et al., *Tumor recurrence versus fibrosis in the irradiated breast: differentiation with dynamic gadolinium-enhanced MR imaging.* Radiology, 1993. **187**(3): p. 751-5.
257. Kerslake, R.W., et al., *Dynamic contrast-enhanced and fat suppressed magnetic resonance imaging in suspected recurrent carcinoma of the breast: preliminary experience.* Br J Radiol, 1994. **67**(804): p. 1158-68.
258. Whitehouse, G.H. and N.R. Moore, *MR imaging of the breast after surgery for breast cancer.* Magn Reson Imaging Clin N Am, 1994. **2**(4): p. 591-603.
259. Murray, A.D., et al., *Dynamic magnetic resonance mammography of both breasts following local excision and radiotherapy for breast carcinoma.* Br J Radiol, 1996. **69**(823): p. 594-600.
260. Mussurakis, S., et al., *Dynamic contrast-enhanced magnetic resonance imaging of the breast combined with pharmacokinetic analysis of gadolinium-DTPA uptake in the diagnosis of local recurrence of early stage breast carcinoma.* Invest Radiol, 1995. **30**(11): p. 650-62.
261. Viehweg, P., et al., *Retrospective analysis for evaluation of the value of contrast-enhanced MRI in patients treated with breast conservative therapy.* Magma, 1998. **7**(3): p. 141-52.
262. Heywang, S.H., et al., *Gd-DTPA enhanced MR imaging of the breast in patients with postoperative scarring and silicon implants.* J Comput Assist Tomogr, 1990. **14**(3): p. 348-56.
263. Heywang-Kobrunner, S.H., et al., *Contrast-enhanced MRI of the breast after limited surgery and radiation therapy.* J Comput Assist Tomogr, 1993. **17**(6): p. 891-900.
264. Muuller, R.D., et al., *Assessment of local recurrence after breast-conserving therapy with MRI.* J Comput Assist Tomogr, 1998. **22**(3): p. 408-12.
265. Drew, P.J., et al., *Routine screening for local recurrence following breast-conserving therapy for cancer with dynamic contrast-enhanced magnetic resonance imaging of the breast.* Ann Surg Oncol, 1998. **5**(3): p. 265-70.
266. Belli, P., et al., *Magnetic resonance imaging in breast cancer recurrence.* Breast Cancer Res Treat, 2002. **73**(3): p. 223-35.
267. Mumtaz, H., et al., *Comparison of magnetic resonance imaging and conventional triple assessment in locally recurrent breast cancer.* Br J Surg, 1997. **84**(8): p. 1147-51.
268. Barbier, E.L., L. Lamalle, and M. Decorps, *Methodology of brain perfusion imaging*, in *J Magn Reson Imaging*. 2001. p. 496-520.
269. Sorensen, A.G., et al., *Contrast agents in functional MR imaging*, in *J Magn Reson Imaging*. 1997. p. 47-55.
270. Dennie, J., et al., *NMR imaging of changes in vascular morphology due to tumor angiogenesis*, in *Magn Reson Med*. 1998. p. 793-9.
271. Bruening, R., et al., *Effects of three different doses of a bolus injection of gadodiamide: assessment of regional cerebral blood volume maps in a blinded reader study*, in *AJNR Am J Neuroradiol*. 2000. p. 1603-10.
272. Rosen, B.R., et al., *Contrast agents and cerebral hemodynamics*, in *Magn Reson Med*. 1991. p. 285-92.
273. Ostergaard, L., et al., *High resolution measurement of cerebral blood flow using intravascular tracer bolus passages. Part II: Experimental comparison and preliminary results*, in *Magn Reson Med*. 1996. p. 726-36.
274. Liu, Y.J., et al., *A reinvestigation of maximal signal drop in dynamic susceptibility contrast magnetic resonance imaging*, in *J Neuroimaging*. 2002. p. 330-8.

275. Taylor, N.J., et al., *Pre- and post-chemotherapy comparisons of calculated rBV and rBF with signal intensity drop on T2* dynamic contrast-enhanced MRI of breast cancers.* Proc. I.S.M.R.M., 2005. **13th Annual Meeting**: p. Abstract 91.
276. Kuhl, C.K., et al., *Breast neoplasms: T2* susceptibility-contrast, first-pass perfusion MR imaging*, in *Radiology*. 1997. p. 87-95.
277. Kvistad, K.A., et al., *Differentiating benign and malignant breast lesions with T2*-weighted first pass perfusion imaging*, in *Acta Radiol.* 1999. p. 45-51.
278. Weind, K.L., et al., *Invasive carcinomas and fibroadenomas of the breast: comparison of microvessel distributions--implications for imaging modalities*, in *Radiology*. 1998. p. 477-83.
279. Jitsuiki, Y., et al. *Optimizing microvessel counts according to tumor zone in invasive ductal carcinoma of the breast.* in *Mod Pathol.* 1999.
280. Howe, F.A., et al., *Issues in flow and oxygenation dependent contrast (FLOOD) imaging of tumours.* NMR Biomed, 2001. **14**(7-8): p. 497-506.
281. Taylor, N.J., et al., *BOLD MRI of human tumor oxygenation during carbogen breathing.* J Magn Reson Imaging, 2001. **14**(2): p. 156-63.
282. Warner, E., et al., *Comparison of breast magnetic resonance imaging, mammography, and ultrasound for surveillance of women at high risk for hereditary breast cancer.* J Clin Oncol, 2001. **19**(15): p. 3524-31.
283. Kuhl, C.K., et al., *Breast MR imaging screening in 192 women proved or suspected to be carriers of a breast cancer susceptibility gene: preliminary results.* Radiology, 2000. **215**(1): p. 267-79.
284. Podo, F., et al., *The Italian multi-centre project on evaluation of MRI and other imaging modalities in early detection of breast cancer in subjects at high genetic risk.* J Exp Clin Cancer Res, 2002. **21**(3 Suppl): p. 115-24.
285. Stoutjesdijk, M.J., et al., *Magnetic resonance imaging and mammography in women with a hereditary risk of breast cancer.* J Natl Cancer Inst, 2001. **93**(14): p. 1095-102.
286. Tilanus-Linthorst, M.M., et al., *First experiences in screening women at high risk for breast cancer with MR imaging.* Breast Cancer Res Treat, 2000. **63**(1): p. 53-60.
287. Kriege, M., et al., *Efficacy of MRI and mammography for breast-cancer screening in women with a familial or genetic predisposition.* N Engl J Med, 2004. **351**(5): p. 427-37.
288. Schnall, M.D. and D.M. Ikeda, *Lesion Diagnosis Working Group report.* J Magn Reson Imaging, 1999. **10**(6): p. 982-90.
289. Oken, M.M., et al., *Toxicity and response criteria of the Eastern Cooperative Oncology Group.* Am J Clin Oncol, 1982. **5**(6): p. 649-55.
290. Hayward, J.L., et al., *Assessment of response to therapy in advanced breast cancer. A project of the programme on clinical oncology of the International Union against Cancer, Geneva, Switzerland.* Eur J Cancer, 1978. **14**(11): p. 1291-2.
291. Miller, A.B., et al., *Reporting results of cancer treatment.* Cancer, 1981. **47**(1): p. 207-14.
292. Sharkey, F.E., et al., *Effects of preoperative chemotherapy on the morphology of resectable breast carcinoma.* Mod Pathol, 1996. **9**(9): p. 893-900.
293. Aktepe, F., N. Kapucuoglu, and I. Pak, *The effects of chemotherapy on breast cancer tissue in locally advanced breast cancer.* Histopathology, 1996. **29**(1): p. 63-7.
294. Ogston, K.N., et al., *A new histological grading system to assess response of breast cancers to primary chemotherapy: prognostic significance and survival.* Breast, 2003. **12**(5): p. 320-7.
295. D'Arcy, J., et al., *Magnetic Resonance Imaging Workbench (MRIW): Dynamic contrast enhanced MRI data analysis and visualisation.* Radiographics - submitted, 2004.
296. Galbraith, S.M., et al., *Reproducibility of dynamic contrast-enhanced MRI in human muscle and tumours: comparison of quantitative and semi-quantitative analysis.* NMR Biomed, 2002. **15**(2): p. 132-42.
297. Bland, J.M. and D.G. Altman, *Measurement error.* Bmj, 1996. **312**(7047): p. 1654.
298. Toi, M., J. Kashitani, and T. Tominaga, *Tumor angiogenesis is an independent prognostic indicator in primary breast carcinoma.* Int J Cancer, 1993. **55**(3): p. 371-4.
299. Gerhardt, H. and C. Betsholtz, *Endothelial-pericyte interactions in angiogenesis.* Cell Tissue Res, 2003. **314**(1): p. 15-23.

300. Kadambi, A., et al., *Vascular endothelial growth factor (VEGF)-C differentially affects tumor vascular function and leukocyte recruitment: role of VEGF-receptor 2 and host VEGF-A.* Cancer Res, 2001. **61**(6): p. 2404-8.
301. Willett, C.G., et al., *Direct evidence that the VEGF-specific antibody bevacizumab has antivascular effects in human rectal cancer.* Nat Med, 2004. **10**(2): p. 145-7.
302. Winkler, F., et al., *Kinetics of vascular normalization by VEGFR2 blockade governs brain tumor response to radiation: role of oxygenation, angiopoietin-1, and matrix metalloproteinases.* Cancer Cell, 2004. **6**(6): p. 553-63.
303. Tong, R.T., et al., *Vascular normalization by vascular endothelial growth factor receptor 2 blockade induces a pressure gradient across the vasculature and improves drug penetration in tumors.* Cancer Res, 2004. **64**(11): p. 3731-6.
304. Jain, R.K., *Normalizing tumor vasculature with anti-angiogenic therapy: a new paradigm for combination therapy.* Nat Med, 2001. **7**(9): p. 987-9.
305. Buckley, D.L., et al., *Microvessel density of invasive breast cancer assessed by dynamic Gd-DTPA enhanced MRI.* J Magn Reson Imaging, 1997. **7**(3): p. 461-4.
306. Hulka, C.A., et al., *Dynamic echo-planar imaging of the breast: experience in diagnosing breast carcinoma and correlation with tumor angiogenesis.* Radiology, 1997. **205**(3): p. 837-42.
307. Stomper, P.C., et al., *Angiogenesis and dynamic MR imaging gadolinium enhancement of malignant and benign breast lesions.* Breast Cancer Res Treat, 1997. **45**(1): p. 39-46.
308. Knopp, M.V., et al., *Pathophysiologic basis of contrast enhancement in breast tumors.* J Magn Reson Imaging, 1999. **10**(3): p. 260-6.
309. Loncaster, J.A., et al., *Carbonic anhydrase (CA IX) expression, a potential new intrinsic marker of hypoxia: correlations with tumor oxygen measurements and prognosis in locally advanced carcinoma of the cervix.* Cancer Res, 2001. **61**(17): p. 6394-9.
310. Taylor, N.J. in *ISMRM.* 2003.
311. Kostourou, V., et al., *Overexpression of dimethylarginine dimethylaminohydrolase enhances tumor hypoxia: an insight into the relationship of hypoxia and angiogenesis in vivo.* Neoplasia, 2004. **6**(4): p. 401-11.
312. Hawkins, R.A., et al., *Prospective evaluation of prognostic factors in operable breast cancer.* Br J Cancer, 1996. **74**(9): p. 1469-78.
313. Horita, K., et al., *Prognostic factors affecting disease-free survival rate following surgical resection of primary breast cancer.* Eur J Histochem, 2001. **45**(1): p. 73-84.
314. Hayes, C., A.R. Padhani, and M.O. Leach, *Assessing changes in tumour vascular function using dynamic contrast-enhanced magnetic resonance imaging.* NMR Biomed, 2002. **15**(2): p. 154-63.
315. Leach, M.O., et al., *The assessment of antiangiogenic and antivascular therapies in early-stage clinical trials using magnetic resonance imaging: issues and recommendations.* Br J Cancer, 2005. **92**(9): p. 1599-610.
316. Padhani, A.R., et al., *Prediction of clinicopathologic response of breast cancer to primary chemotherapy at contrast-enhanced MR imaging: initial clinical results.* Radiology, 2006. **239**(2): p. 361-74.
317. Therasse, P., et al., *New guidelines to evaluate the response to treatment in solid tumors. European Organization for Research and Treatment of Cancer, National Cancer Institute of the United States, National Cancer Institute of Canada.* J Natl Cancer Inst, 2000. **92**(3): p. 205-16.
318. Therasse, P., E.A. Eisenhauer, and J. Verweij, *RECIST revisited: A review of validation studies on tumour assessment.* Eur J Cancer, 2006. **42**(8): p. 1031-9.
319. Sataloff, D.M., et al., *Pathologic response to induction chemotherapy in locally advanced carcinoma of the breast: a determinant of outcome.* J Am Coll Surg, 1995. **180**(3): p. 297-306.
320. Chevallier, B., et al., *Inflammatory breast cancer. Pilot study of intensive induction chemotherapy (FEC-HD) results in a high histologic response rate.* Am J Clin Oncol, 1993. **16**(3): p. 223-8.
321. Jones, R.L., et al., *Pathological complete response and residual DCIS following neoadjuvant chemotherapy for breast carcinoma.* Br J Cancer, 2006. **94**(3): p. 358-62.
322. Port, R.E., et al., *Multicompartment analysis of gadolinium chelate kinetics: blood-tissue exchange in mammary tumors as monitored by dynamic MR imaging.* J Magn Reson Imaging, 1999. **10**(3): p. 233-41.

323. Delille, J.P., et al., *Hormone replacement therapy in postmenopausal women: breast tissue perfusion determined with MR imaging--initial observations.* Radiology, 2005. **235**(1): p. 36-41.
324. Jain, R.K., *Normalization of tumor vasculature: an emerging concept in antiangiogenic therapy.* Science, 2005. **307**(5706): p. 58-62.
325. Crowe, J.P., Jr., et al., *Does ultrasound core breast biopsy predict histologic finding on excisional biopsy?* Am J Surg, 2003. **186**(4): p. 397-9.
326. Monticciolo, D.L., *Histologic grading at breast core needle biopsy: comparison with results from the excised breast specimen.* Breast J, 2005. **11**(1): p. 9-14.
327. (UICC), I.U.A.C., *TNM Classification of Malignant Tumours.* Sixth edition ed. 2002, New York: Wiley-Liss.

Appendices

Appendix 1: International Union Against Cancer (UICC)/World Health Organisation (WHO) criteria for clinical response to therapy

Complete Response (cCR)	Disappearance of all known disease
Partial Response (cPR)	Decrease by at least 50% of the sum of the products of the largest perpendicular diameters of measurable lesions
Stable disease (cSD)	Less than 50% decrease and less than 25% increase in the sum of the products of the largest perpendicular diameters of measurable lesions
Progressive disease (cPD)	Increase of more than 25% in the size of a measurable lesion or appearance of a new lesion

Appendix 2: WHO performance status scale

Grade	Performance scale
0	Able to carry out all normal activity without restriction
1	Restricted in physically strenuous activity but ambulatory and able to carry out light work.
2	Ambulatory and capable of all self-care but unable to carry out any work; up and about more than 50% of waking hours.
3	Capable of only limited self-care; confined to bed or chair more than 50% of waking hours
4	Completely disabled; cannot carry on any self-care; totally confined to bed or chair.

Appendix 3: Exclusions for MRI scan

- Central nervous system aneurysm clips
- Implanted neural stimulator
- Implanted cardiac pacemaker of defibrillator
- Certain cardiac valve replacements
- Cochlear implant
- Ocular foreign body eg. metal fragments
- Metal shrapnel or bullet injuries
- Recent surgery requiring clips insertion
- Other implanted medical devices

Appendix 4: International Union Against Cancer (UICC) TNM classification of Primary Breast Cancer [327]

(i) Clinical

PRIMARY TUMOUR (T)	TX	Primary tumour cannot be assessed	
	T0	No evidence of primary tumour	
	Tis	Carcinoma in situ	
	T1	Tumour 2.0cm or less in greatest dimension	
		T1mic	Microinvasion 0.1cm or less
		T1a	More than 0.1cm but no more than 0.5cm
		T1b	More than 0.5cm but no more than 1.0cm
		T1c	More than 1.0cm but no more than 2.0cm
	T2	Tumour more than 2.0cm but not more than 5.0cm in greatest dimension	
	T3	Tumour more than 5.0cm in greatest dimension	
	T4	Tumour of any size with direct extension to (a) chest wall or (b) skin, only as described below	
		T4a	Extension to chest wall, not including pectoralis muscle
		T4b	Oedema (including peau d'orange) or ulceration of the skin of the breast, or satellite skin nodules confined to the same breast
		T4c	Both T4a and T4b
		T4d	Inflammatory carcinoma
REGIONAL LYMPH NODES (N)	NX	Regional lymph nodes (LN) cannot be assessed (e.g. previously removed)	
	N0	No regional LN metastasis	
	N1	Metastasis to moveable ipsilateral axillary LN(s)	
	N2	Metastasis to ipsilateral axillary LN(s) fixed or matted, or in clinically apparent* ipsilateral internal mammary nodes in the absence of clinically evident LN metastasis	
		N2a	Metastasis in ipsilateral axillary LNs fixed to one another (matted) or to other structures
		N2b	Metastasis only in clinically apparent* ipsilateral internal mammary nodes and in the absence of clinically evident LN metastasis
	N3	Metastasis in ipsilateral infraclavicular LN(s) with or without axillary LN involvement, or in clinically apparent* ipsilateral internal mammary LN(s) and in the presence of clinically evident axillary LN metastasis; or metastasis in the ipsilateral supraclavicular LN(s) with or without axillary or internal mammary LN involvement	
		N3a	Metastasis in ipsilateral infraclavicular LN(s)
		N3b	Metastasis in ipsilateral internal mammary LN(s) and axillary LN(s)
		N3c	Metastasis in ipsilateral supraclavicular LN(s)
DISTANT METASTASIS (M)	MX	Presence of distant metastasis cannot be assessed	
	M0	No distant metastasis	
	M1	Distant metastasis	

*clinically apparent is defined as detected by imaging studies (excluding lymphoscintigraphy) or by clinical examination or grossly visible pathologically

(ii) Pathological

PRIMARY TUMOUR (pT)	pT categories correspond to the T categories. Requires the examination of primary carcinoma with no gross tumour at the margins of resection. Can be classifed pT if only microscopic tumour in a margin		
REGIONAL LYMPH NODES (pN)*	pNX	Regional LNs cannot be assessed	
	pN0	No regional LN metastasis histologically, no additional examination for isolated tumour cells (ITC) [Note: ITC are defined as single tumour cells or small cell clusters not greater than 0.2mm, usually detected only by immunohistochemistry (IHC) or molecular methods but which may be verifed on H&E stains. ITCs do not usually show evidence of malignant activity e.g. proliferation or stromal reaction]	
	pN0(I-)	No regional LN metastasis histologically, negative IHC	
	pN0(I+)	No regional LN metastasis histologically, positive IHC, no IHC cluster greater than 0.2mm	
	pN0(mol-)	No regional LN metastasis histologically, negative molecular findings (RT-PCR)**	
	pN0(mol+)	No regional LN metastasis histologically, positive molecular findings (RT-PCR)**	
	pN1	Metastasis in 1 to 3 axillary LN(s), and/or in internal mammary nodes with microscopic disease detected by sentinel LN dissection but not clinically apparent***	
		pN1mi	Micrometastasis (greater than 0.2mm but not greater than 2.0mm)
		pN1a	Metastasis in 1 to 3 axillary LN(s)
		pN1b	Metastasis in internal mammary nodes with microscopic disease detected by sentinel LN dissection but not clinically apparent**
		pN1c	Metastasis in 1 to 3 axillary LN(s), and in internal mammary nodes with microscopic disease detected by sentinel LN dissection but not clinically apparent**
	pN2	Metastasis in 4 to 9 axillary LNs, or in clinically apparent*** internal mammary LN(s) in the absence of axillary LN metastasis to ipsilateral axillary LN(s) fixed to each other or to other structures	
		pN2a	Metastasis in 4 to 9 axillary LNs (at least one tumour deposit greater than 2.0mm)
		pN2b	Metastasis in clinically apparent*** internal mammary LN(s) in the absence of axillary LN metastasis
	pN3	Metastasis in 10 or more axillary LNs, or in infraclavicular LNs, or in clinically apparent*** ipsilateral internal mammary LN(s) in the presence of 1 or more positive axillary LN(s); or in more than 3 axillary LNs with clinically negative microscopic metastasis in internal mammary LNs; or in ipsilateral supraclavicular LNs	
		pN3a	Metastasis in 10 or more axillary LNs (at least one tumour deposit greater than 2.0mm), or metastasis to the infraclavicular LNs
		pN3b	Metastasis in clinically apparent*** ipsilateral internal mammary LN(s) in the presence of 1 or more positive axillary LN(s); or in more than 3 axillary LNs and in internal mammary LNs with microscopic disease detected by sentinel lymph node dissection but not clinically apparent
		PN3c	Metastasis in ipsilateral supraclavicular LNs
DISTANT METASTASIS (pM)	pM categories correspond to the M categories.		

*Classification based on axillary LN dissection(ALND) with or without sentinel LN dissection (SLND). Classification based solely on SLND without subsequent ALND is designated (sn) for "sentinel node";

**RT-PCR: reverse transcriptase/polymerase chain reaction;

***Clinically apparent is defined as detected by imaging studies (excluding lymphoscintigraphy) or by clinical examination.

Appendix 5: Patient information sheet

PATIENT INFORMATION SHEET

Evaluation of MRI during neoadjuvant chemotherapy in primary breast cancer

You are being invited to take part in a research study. Before you decide it is important for you to understand why the research is being done and what it will involve. Please take time to read the following information carefully and discuss it with friends, relatives and your GP if you wish. Ask us if there is anything that is not clear or if you would like more information. Take time to decide whether or not you wish to take part.

What is the purpose of this study?

This study is being done to evaluate the changes in blood flow, as measured by a special scanning method called Magnetic Resonance Imaging (MRI), during chemotherapy in patients with breast cancer. These changes help us to understand how cancers react to chemotherapy and additionally may help us in the future to identify those patients who will respond to treatment early in its course.

Why I have been chosen?

A total of 40 patients will be studied. You have been selected for this study because you are receiving chemotherapy prior to surgery.

Do I have to take part?

No. It is up to you to decide whether or not to take part. If you decide to take part you will be given this information sheet to keep and be asked to sign a consent form. You may still decide to withdraw at any time without having to give a reason.

If you decide not to take part, or if you withdraw, this will not affect the standard of care you receive, nor will your legal rights be affected by agreeing or refusing to take part.

What will happen to me if I take part?

You will receive chemotherapy every three weeks. You will be asked to have an MRI scan prior to commencing chemotherapy and another prior to the third cycle of chemotherapy. A maximum of two extra visits may be required for the MRI scans.

At the same time you will be asked to give a blood sample, which will help us to measure substances in the blood which may be related to the blood flow which is measured by the MRI. In addition to the blood samples taken on the occasions you are having the MRI scans, we will ask you to have a repeat blood test with the last cycle of chemotherapy and another after your surgery. The amount of blood taken on each of these occasions will be 9mls (approximately two teaspoons). We will also ask for permission to review and perform special tests on part of the biopsy specimen and post-chemotherapy operation specimen that are taken as part of your treatment.

What are the risks of taking part?

MRI is considered to be a very safe technique as it does not use radiation. However, you will be exposed to a large magnetic field and radiowaves. International guidelines have been set up to prevent you receiving an excessive exposure. Because the scanner uses a magnetic field it may be unsafe for you to be scanned if you have a cardiac pacemaker, implanted metallic material such as surgical clips or possibly if you have had major surgery. You should also not be scanned if there is any possibility that you are pregnant. You will be asked to complete a safety questionnaire before the examination.

What are the possible benefits of taking part?

Information from this study may help us to treat future patients with breast cancer. Additionally, the repeat scan may show evidence that your disease is not responding to the chemotherapy in which case alternative chemotherapy may be offered to you.

What if new information becomes available?

Sometimes during the course of a research project, new information becomes available about the treatment/drug that is being studied. If this happens, your research doctor will tell you about it and discuss with you whether you want to continue in this study. If you decide to withdraw, your research doctor will make arrangements for your care to continue. If you decide to continue in the study, you will be asked to sign an updated consent form. Also on receiving new information, your research doctor might consider it to be in your best interests to withdraw you from the study. He/she will explain the reasons, and arrange for your care to continue.

Will my taking part in this study be kept confidential?

All information which is collected about you, during the course of this research, will be kept strictly confidential. Any information about you which leaves the hospital/surgery will have your name and address removed so that you cannot be recognised from it. Your GP will be informed that you have agreed to take part in this study.

What will happen to the results of the research study?

At the end of the research study, the results will be analysed and presented at scientific meetings as well as being published in a medical journal.

Who is organising and funding the research?

This research study is being conducted by clinicians at Mount Vernon Hospital and the scans are funded by the Paul Strickland Scanner Centre.

How can I make a complaint if something goes wrong?

There are no special compensation arrangements for taking part in this study but the normal NHS complaints mechanism is available to you if you wish to complain about any aspect of the way you are approached or treated. Formal complaints should be addressed to the Quality Assurance Office, Administration Block, Watford General Hospital, Watford, WD1 2AA (Tel: 01923 245285). Should you require independent advice, you may wish to contact the South West Herts Community Health Council, Abbey House (3rd Floor), 26 The Parade, High Street, Watford, WD1 2AA (Tel: 01923 245285).

Who can I contact if I want any more information about this study?

If you have any further questions please contact Linda Culver or James Stirling at the Scanner Centre on 01923 844353.

This study has been reviewed by the Local Research Ethics Committee for Mount Vernon and Watford Hospitals.

A copy of the information sheet can be kept by the patient.

We very much appreciate your taking time to read this information sheet.

Appendix 6: MRI study patient consent form

Patient Identification Number for this trial:

CONSENT FORM

Title of Project: Evaluation of MRI during neoadjuvant chemotherapy in primary breast cancer

Name of Researchers: Dr. A Makris, Dr. A Padhani, Dr. M Ah-See

I (name) _____

of (address) _____

_____

Please initial box

1. I confirm that I have read and understand the patient information sheet dated _____ for the above study and have had the opportunity to ask questions. ☐
2. I understand that my participation is voluntary and that I am free to withdraw at any time, without giving any reason, without my medical care or legal rights being affected. ☐
3. I understand that sections of any of my medical notes may be looked at by responsible individuals or from regulatory authorities where it is relevant to my taking part in research. ☐
4. I give permission for these individuals to have access to my records. ☐
5. I grant permission for samples from pathological specimens taken during my treatment (diagnostic or operation specimens) to be collected, stored and then analysed as part of a research study. ☐
6. I agree to take part in the above study. ☐

_____	_____	
Name of Patient	Signature	Date
_____	_____	
Name of Person taking consent (if different from researcher)	Signature	Date
_____	_____	
Researcher	Signature	Date

1 for patient; 1 for researcher; 1 to be kept with hospital notes